Fate and Transport of Particulate Matter in Geotextile Tube Dewatering of Dioxin and Furans Contaminated Sediments

by

Masoumeh Alimohammadi

Submitted in partial fulfilment of the requirements
for the degree of Doctor of Philosophy

at

Dalhousie University
Halifax, Nova Scotia
November 2020

TABLE OF CONTENTS

LIST OF TABLES

LIST OF FIGURES

ABSTRACT

Geotextile tube dewatering is a pre-treatment method frequently utilized in the remediation of high-water content materials. Given the association that some contaminants (e.g. dioxins and furans) have with the particulate matter in contaminated sediments, understanding the fate and transport of this particle matter during the dewatering process is essential. This thesis attempts to provide a novel examination of the fate and transport of particle matter during geotextile dewatering. A sediment known to contain dioxin and furans was used to investigate this problem.

To show the prevalence of dioxins and furans (PCDD/F) in the Boat Harbour (BH) sediment used in this thesis, organic sediment contaminants were assessed using secondary monitoring data collected between 1992-2015. Historical secondary monitoring data showed that sediment PCDD/F concentrations exceeded highest effect thresholds posing severe ecological health risks.

A field sampling program was undertaken to assess the variability of the physical characteristics of BH contaminated sediment. It was demonstrated that by understanding sediment variability, composite samples can be shown to be an efficient method of obtaining representative samples.

For this sediment, geotextile tube dewatering was compared to more conventional dewatering methods (i.e. centrifuge, sedimentation) in the context of how geotextile dewatering performs at reducing particulate matter in dewatering effluent. Filtrate quality of suspended solids was examined for differences based on three dewatering techniques assessed. All methods provided effective removal of particulate matter during dewatering, but geotextile dewatering could be a more cost-effective and practical solution for dewatering of these sediments.

Pressure filtration tests as well as transport tests were conducted to investigate the effect of pressure and filter cake formation on particle transport during the geotextile dewatering. Also, a HYDRUS 1-dimensional model was employed to simulate experimental particle transport results. Modeling outputs suggest that both attachment and detachment mechanisms are involved in a given particles fate and transport during geotextile dewatering. It was also shown that different parameters such as confining pressure and filter cake properties influence the particle transport. Furthermore, HYDRUS was used to predict the particles transport during the geotextile tube dewatering under different circumstances, the findings of which are presented in this thesis.

LIST OF ABBREVIATIONS USED

AB	Aeration basin
ABS	Acrylonitrile butadiene styrene (plastic)
An	Anthracene
ANOVA	one-way analysis of variance
AOS	Apparent opening size
ASB	Aeration stabilization basin
ASTM	American Society for Testing and Materials
Br^-	Bromide
BH	Boat Harbour
BHSL	Boat Harbour stabilization Lagoon
BHTF	Boat Harbour Treatment Facility
BHVP	Boat Harbour vacuum pump sample
BTEX	Benzene, Toluene, Ethylbenzene and Xylenes
C_c	Colloid concentration in liquid phase
CCME	Canadian Council of Ministers of the Environment
CEC	Cation exchange capacity
cm	Centimeter
CWRS	Centre for Water Resources Studies
D_{85}	85 % of the mass is smaller than the given value
DL	Detection limit
D_L	longitudinal dispersivity

ER-L	Effects range low
ER-M	Effects range median
FHT	Falling head test
Fl	Fluoranthene
g/cm^3	gram per cubic centimeter
GDT	Geotube Dewatering Test
GIS	Geographic information system
GT-500	Geotextile #500
h	Hour
ha	Hectare (10,000 m^2)
HBT	Hanging bag test
HDPE	High density polyethylene
ICP-MS	Inductively coupled plasma mass spectrometry
ISQG	Interim sediment quality guideline
K_{ac}	Colloid attachment coefficient
K_{dc}	Colloid detachment coefficient
kg	Kilogram
kPa	Kilo pascal
L	Liter
$l/min/m^2$	Liter per minute per square meter
L/s	Liter per second
m^3	Cubic meter
MFI	Micro flow imaging

mg	Milligram
mg/L	Milligram per liter
min	Minute
mL	Milliliter
mS/cm	millisiemens per centimeter
mV	Millivolt
n.d.	Not detected
nm	Nanometer
NP	Northern Pulp
NPRI	National Pollution Release Inventory
NTU	Turbidity
PAH	Polycyclic aromatic hydrocarbon
PCB	Polychlorinated biphenyl
PCDD/F	polychlorinated dibenzo-p-dioxins, polychlorinated dibenzofuran
PCOC	Potential contaminants of concern
PEL	Probable effect level
PFT	Pressure filtration test
Ph	Phenanthrene
PLFN	Pictou Landing First Nation
PPER	Pulp and Paper Effluent Regulations
PVC	Polyvinyl chloride (plastic)
Py	Pyrene
ppm	Part per million

ppt	Part per trillion
RDT	Rapid dewatering test
rpm	Revolutions per minute
s	Second
S_C	Colloid concentration in solid phase
SC	Solid content
SEM	Scanning electron microscope
SQG	Sediment quality guideline
SQGHH	Soil quality guideline for human health
TCDD	Tetrachlorodibezodioxin
TEQ	Toxic equivalent
TEF	Toxic equivalency factor
TOC	Total organic carbon
TPH	Total petroleum hydrocarbons
TSS	Total suspended solids
VOC	Volatile organic compound
WC	Water content
WHO	World health organization
WWTF	Wastewater treatment facility
±	Plus or minus a given measurement
µg	Microgram
µm	Micrometer
#/mL	Number per milliliter

#/mg	Number per milligram
θ	Volumetric water content

ACKNOWLEDGEMENTS

First and foremost, I would like to thank my supervisor, Dr. Craig Lake for his endless support and guidance for the past five years during the course of my study at Dalhousie University. I am, and will forever be, grateful for the encouragement you continuously provided me. You were always willing and enthusiastic to assist me in any way you could throughout this research. Thank you for giving me the opportunity to join your research group and making my journey at Dalhousie joyful and unforgettable. Simply, I say you are the BEST advisor and mentor that I could have ever asked for. I hope we can continue to do research together in the future. I would like to express my gratitude to my advisory committee Dr. Tony Walker and Dr. Rob Jamieson for their insightful comments and assistance during different stages of this work. Moreover, I am sincerely grateful to Dr. Ian Spooner for providing guidance and also sampling equipment during the field work.

I have been lucky to work with great friends at our research team. Thank you: Hun Choi, Chris Song, Kirklyn Davidson, and Baillie Holmes for helping me. But special thanks goes to my friend Hayden Tackley, without him I would not have been able to complete this research. Hayden, thank you for being such a smart, funny, kind, patient, helpful, and handy lab mate who made all the lab and field works enjoyable.

I would like to acknowledge the financial support from the Natural Sciences and Engineering Research Council (NSERC), Nova Scotia Lands, Faculty of Graduate Studies at Dalhousie University, and most of all Mr. Abdul Majid Bader who created the graduate scholarship for Iranian students at Dalhousie. Without their support this research would not have been possible.

I am thankful to the staff of the Civil and Resource Engineering Department of Dalhousie University and also Centre for Water Resources Studies (CWRS) for their kindness and support. Blair Nickerson, Brian Kennedy, June Ferguson, Terra Chartrand, and Heather Daurie helped me in different ways through this work.

To conclude, I must thank my parents and siblings for all their spiritual support during my many years as a student and my life in general. Mom and dad, thank you for believing in me and supporting my fearless, yet sometimes crazy decisions. Finally, I would like to

thank my best friend forever, the only and one love of my life, Reza. Without your unconditional love and support I wouldn't be where I am today, and I would not have made it through my PhD degree. Thank you for understanding me, being by my side through all ups and downs in past ten years.

CHAPTER 1: INTRODUCTION

1.1 Introduction

Over the past few decades, geotextile tubes have been utilized as a simple and low cost technology for dewatering high water content solid materials such as dredged sediment, industrial process waste, agricultural process waste, pulp and paper mill sludge, fly ash, and mining and drilling waste (Khachan and Bhatia, 2017). Geotextiles tubes (i.e. trade name Geotubes©) are constructed from geotextiles sewn together to create long hollow tubes as well as influent port(s) for receiving slurry material. In a dewatering operation, the slurry is pumped into the geotextile tube with the geotextile acting as a filter for separation of solids and liquids. Due to pressure buildup inside the tube from the pumping operation, the filtering of solids occurs such that solids are retained inside the geotube and the liquid (i.e. filtrate) is expelled through the pores of geotextile. In this process, a filter cake of the dewatering material forms adjacent to the geotextile. After the majority of the filtrate is expelled, the geotextile tube is then refilled, and the cycle is repeated several times until the amount of filtrate is insignificant (Lawson, 2008). Synthetic polymers are typically used as a liquid conditioner in geotextile tube dewatering applications, to enhance the dewatering rate and retention of fine particles by aggregation.

1.1.1 Geotextile-Tube (Geotube) Dewatering

Dewatering efficiency of geotextile tubes under different conditions has been studied by numerous researchers using both laboratory and field scale testing. Factors that have been investigated include the effects of slurry properties (e.g. initial water content, particle size distribution), geotextile characteristics (e.g. pore size distribution, manufacture), additive conditioning (e.g. flocculant, coagulant), and applying pressure on dewatering rate and final solids content (e.g. Gaffney et al. 1999; Moo-Young and Ochola, 1999a, b; Moo-Young et al., 2002; Mori et al., 2002; Bhatia and Liao, 2004; Gaffney et al., 2004; Kutay and Aydilek, 2004; Huang and Koerner, 2005; Koerner and Koerner, 2006; Liao and Bhatia, 2005; Liao and Bhatia, 2006; Muthukumaran and Ilamparuthi, 2006; Liao, 2007; Huang and Luo, 2007; Satyamurthy, 2008; Segre, 2011; Bhatia et al., 2013; Khachan et al., 2014). Gastaud et al. (2014) conducted pressure filtration tests on different nonwoven

geotextiles used to filter high-clay-content sludges and showed that only during the early stages of dewatering did the geotextile properties influence the filtering process. Upon forming the filter cake, particle retention is predominantly controlled by the filter cake characteristics. Liao et al. (2004) showed that a high water content appears to decrease the filtration efficiency and hence dewatering efficiency. The study also indicated that addition of the polymer is very important to accelerate the dewatering process and increase the stable flow rate of the fine-grained materials. Although it was found that slurry and geotextile characteristics could influence the filtration process, it was also shown that no single criterion accurately predicts the filtration performance of the geotextiles (Moo-Young et al., 2002; Kutay, 2002; and Aydilek and Edil, 2002). Muthukumaran et al. (2006) found that filtration efficiency is less affected by water content, apparent opening size, and gradation of sludge. The filtration efficiency was found to be greatly reduced if the apparent opening size of greater than 0.425mm was present for the sludges tested in their study.

In addition to laboratory research, many successful field applications of geotextile tubes in dewatering of high water content materials have been reported. Highly contaminated sediment with heavy metals, polyaromatic hydrocarbons (PAHs), and volatile organic compounds (VOCs) was collected from the Indiana Harbor Canal-located on the southwest shore of Lake Michigan- and mechanically mixed with an organic cationic flocculant and then transferred onto a geotextile pillow for dewatering (Pianto et al., 2011). In other study by Yee et al. (2012), large volumes of contaminated sediments at the Tianjin Eco-City site in China were dewatered using a geotextile and then deposited in a specially constructed secured landfill. Generally speaking, research and practice has shown geotextile tubes to be an effective technique to dewater high water content sediment.

1.1.2 Boat Harbour

The general motivation for this research originated from the Boat Harbour (BH) remediation project in Pictou, Nova Scotia, Canada. At the time of this thesis, it is an ongoing remediation project and is anticipated to involve removal of approximately 577,000 m^3 of unconsolidated contaminated sediment from the former wastewater stabilization lagoon followed by storage in a secure containment cell (GHD, 2018; Alimohammadi et al., 2019). The contaminated sediment within Boat Harbour sediments

generally consist of a thin layer of black anthropogenic freshwater organic particulate (referred to as "black sediment" in this research), underlain by a grey organic silt, glacial till and sedimentary bedrock (Spooner and Dunnington, 2016; Stantec, 2016). Since different contributors (primarily a pulp and paper mill) have been discharging their wastewater into the BH over past 60 years (1960-2020), BH sediments are impacted by various inorganic and organic contaminants (heavy metals, PAHs, dioxin and furans [PCDD/Fs], volatile organic compounds [VOCs], Benzene, Toluene, Ethylbenzene and Xylenes [BTEX], total petroleum hydrocarbons [TPHs], polychlorinated biphenyls [PCBs]). However, among all these contaminants, PCDD/Fs are of a primary concern, because they are highly persistent, bioaccumulative, and can be acutely toxic to biota and humans (Norstrom, 2006; Hites, 2011). Despite regulatory efforts aimed at reducing dioxins and furans during the past decade (i.e. implementation of Pulp and Paper Mill Effluent Chlorinated Dioxins and Furans Regulations in 1992), the high sediment PCDD/F concentrations have persisted in Boat Harbour (as will be discussed in chapter 2). The large volume (577,000 m^3) and high water content (~1000%) of these contaminated sediments have suggested that dewatering is one of the main challenges in the BH remediation project. However, concentrations of dioxin and furan transport via particulate matter in expelled water from sediments must be controlled and, if necessary, treated. It is therefore important to understand particulate matter (i.e. PCCD/Fs) fate and transport through the geo-textile tube dewatering process.

1.1.3 Dioxin and Furans

Dioxins are a class of structurally and chemically related polyhalogenated aromatic hydrocarbons that mainly includes polychlorinated dibenzo-p-dioxins (PCDDs or dioxins), dibenzofurans (PCDFs or furans) and the 'dioxin-like' biphenyls (PCBs). They constitute a group of persistent environmental chemicals and usually occur as a mixture of congeners. Only 7 of the 75 possible PCDD congeners, and 10 of the 135 possible PCDF congeners, those with chlorine substitution in the 2,3,7,8 positions, have dioxin-like toxicity (USEPA, 1994a, b). Primary sources of dioxins to the environment include, but are not limit to, hospital waste, diesel vehicles, cement kilns, coal fired utilities, pulp and paper mills, forest fires (Kulkarni et al., 2008). There are several important physical and chemical properties of PCDD/Fs controlling their fate and transport in the environment and particularly in

aquatic systems. These properties include water solubility, vapor pressure, octanol-water partition coefficient, and soil-water partition coefficient (Wente, 1991). Table 1.1 shows some of the properties of the most harmful dioxin congener (2,3,7,8-tetrachlorodibezodioxin-TCDD) were compared to Phenanthrene as a PAHs compound and Benzene as a VOCs compound.

Table 1.1 Comparing of 2,3,7,8-TCDD properties to Phenanthrene (selected PAHs compound) and Benzene (selected VOCs compound)

	2,3,7,8-TCDD	**Phenanthrene**	**Benzene**
Water Solubility (mg/L)	**2×10^{-4}** at 25°C (NIOSH, 1984)	**1.2** at 25°C (ATSDR, 1995)	**1790** at 15°C (Arnold et al. 1958)
Octanol/Water Partition Coefficient, log K_{ow}	**6.8-7.58** (ATSDR, 1998)	**4.45** (ATSDR, 1995)	**2.13** (ATSDR, 2007)
Vapor Pressure (mm Hg)	**1.7×10^{-6}** (NIOSH, 1984)	**6.8×10^{-4}** (ATSDR, 1995)	**75** (ATSDR, 2007)
Sorption Partition Coefficient, log K_{oc}	**7.25-7.59** (Lodge and Cook, 1989)	**4.15** (ATSDR, 1995)	**1.8-1.9** (ATSDR, 2007)

Very low water solubility and high partition coefficients of highly lipophilic PCDD/Fs result in high affinity of these compounds for the organic matter in the soil/sediment and also a tendency to bioaccumulate in fish and benthic invertebrates (Persson et al., 2007). Mobility and bioavailability of these persistent compounds in the environment has been a subject of considerable concern. Chalmers et al. (2019) examined the partitioning of PCDD/Fs in sediments adjacent to the Woodfibre Pulp and Paper Mill, in a core retrieved from an area exposed to effluent discharge by the mill. Results showed that both dioxin and furan concentrations were related to organic matter concentration, molecular chlorination, and sediment surface area. In another study by Louchouarn et al. (2018), dioxin and furans concentration of the San Jacinto Superfund site (waste pit) in the Houston Ship Channel (HSC) were compared with those from sediments of the HSC and a control site. Results suggested that the remobilization of contaminated particles did not occur beyond the close vicinity of the pit itself. They also concluded that diffusive transport of dioxins is very unlikely from these sediments and that the only potentially significant export mechanism from the waste pit is advective transport of particulate or colloid-sorbed dioxins.

In the literature there appears to be only several works related to dewatering of polychlorinated dibenzo-p-dioxins (PCDD/Fs generically referred to as dioxins and furans) contaminated sediments with geotextile tubes. Mori et al. (2002) studied the applicability of geotextile tubes as a containment method for dioxin-contaminated sediment. Soil samples were taken from a dioxin-contaminated site in Japan while two types of woven and non-woven polyester were chosen as a geotextile. The results showed that greater than 99.8% of dioxin concentration were successfully trapped in the geo-tube. Also, the dioxins leached from the geo-tube is scarcely observed. Suspended solids and turbidity of filtrate were measured and a strong correlation (R^2>0.98) between measured suspended solids (SS) and dioxin concentration in the drainage was also observed. Mori at al. (2002) suggested that suspended solids can be an alternative measured value for concentration of dioxins. Another study by Moo-Young et al. (1999) investigated the migration of particles and contaminants through geosynthetic fabric containers (GFCs). Thirty pressure filtration tests were conducted using four different fabrics on contaminated dredged sediments from New York Harbour. Filtrate quality in terms of TSS showed that more than 99% of initial TSS was removed by different geotextile. They also conducted laboratory barge simulation tests to estimate the release of contaminants (e.g. heavy metals, PAHs, PCBs, dioxin and furans) through the GFC when the sediment is reworked. Results showed low concentration of dioxin and furans ($\times 10^{-7}$ mg/L) in water column, while initial concentration of dioxin and furans were ($\times 10^{-2}$ mg/kg) in the sediments.

1.1.4 Research Questions

Based on the literature, the fate and transport of particulate matter contaminated with PCDD/Fs during geotextile dewatering is not well understood. The known presence of PCDD/Fs in the high water content sediments of BH provide a unique opportunity to assess the particle transport of PCDD/Fs during geotextile dewatering (i.e. with an actual sediment planning to be dewatered with geotextile tubes). Numerous studies have investigated the geotextile-tube dewatering efficiency, but there is no work related to likely mechanisms of particle transport during the geotube dewatering process. The Boat Harbour sediment, known to contain elevated levels of PCDD/Fs, represent an opportunity to investigate the lack of research related fate and transport of particulate matter associated

with these contaminants during geotube dewatering. To address this research gap, the following research questions have been identified:

I. What are the levels of PCDD/Fs from a historical perspective in the study site and what are their spatial distribution?
II. What are the sediment characteristics that influence geotube dewatering efficiency in terms of filtrate quality (particle concentration)?
III. What is the variability of the sediment's characteristics throughout the study site and how different sediment sampling techniques affect that?
IV. What is the role of filter cake and pressure in particle concentrations in geotextile dewatering?
V. What are the likely mechanisms responsible for particle transport through the filter cake during dewatering?
VI. Can fate and transport of particles in the filter cake/geotextile system during the dewatering be predicted using conventional reactive transport models?

1.1.5 Research Objectives

The research questions were addressed with the following research objectives:

1. Assess the BH sediment anthropogenic contaminant characteristics (e.g., depth, spatiotemporal extent and magnitude of impacts);
2. Evaluate the variability of physical and chemical properties of BH sediments;
3. Determine whether different sampling methods have an effect on the sediment's physical characteristics;
4. Evaluate the filtrate quality (i.e. particle concentration) of conventional dewatering techniques (i.e. centrifuge, sedimentation) and compare them to that of geotextile dewatering;
5. Examine the parameters affecting the filtrate quality (i.e. particle concentration) of the geo-textile tube dewatering at the laboratory and field scale;
6. Apply numerical modeling to simulate particle transport during the geotextile dewatering process in order to better understand particle transport mechanisms.

1.1.6 Thesis Organization

The thesis presented herein is organized with the following structure:

CHAPTER 1 provides a background for the state of the research on particles transport during geo-textile tube dewatering, outlines the knowledge gaps at the time of this thesis, and identifies the research questions and objectives.

CHAPTER 2 addresses research objective 1. This work conducts a comprehensive sediment characterization examining a group of organic contaminants, focusing on PCDD/Fs and PAHs, using a long-term secondary data between 1992-2015. A version of this research was published in Environmental Monitoring and Assessment.

CHAPTER 3 addresses research objectives 2 and 3. This work was focused on comparing different sampling methods (i.e. discrete and composite) to evaluate sediment physical properties (water/solids content, bulk density, and particle size). A version of this research was published in Environmental Geotechnics.

CHAPTER 4 addresses research objectives 4. This work was examined the filtrate quality of suspended solids (concentration, particle size distribution) for differences based on three dewatering techniques (centrifuge, sedimentation, geo-textile tube) assessed. A version of this research was published in Canadian Journal of Civil Engineering.

CHAPTER 5 addresses research objectives 5. This work evaluates the filtrate quality (particle concentration) of a field scale geotube dewatering.

CHAPTER 6 addresses research objectives 5 and 6. This work investigates the role of filter cake and pressure in particle matters concentration in the effluent after geotextile dewatering and also applies the numerical HYDRUS model for simulation of fate and transport of particle matters during geotextile dewatering.

CHAPTER 7 provides the overall conclusions and recommendations from the thesis research.

CHAPTER 2: CHARACTERIZATION AND SPATIAL DISTRIBUTION OF ORGANIC CONTAMINATED SEDIMENT DERIVED FROM HISTORICAL INDUSTRIAL EFFLUENTS

Abstract[1]

Organic sediment contaminants (polychlorinated dibenzo-p-dioxins, polychlorinated dibenzofurans [PCDD/Fs] and polycyclic aromatic hydrocarbons [PAHs]) were assessed using secondary monitoring data from a former tidal estuary (Boat Harbour) impacted by historical industrial effluents. Spatiotemporal characterization of PCDD/Fs and PAHs in sediments was conducted to inform a sediment remediation program designed to return this contaminated aquatic site back to a tidal lagoon. Spatiotemporal variation of sediment PCDD/Fs and PAHs concentrations across Boat Harbour and off-site reference locations, were assessed using secondary monitoring data collected between 1992-2015. Sediment PCDD/F toxic equivalent (TEQ) and PAH concentrations were compared to sediment quality guidelines. Sediment PCDD/F concentrations exceeded highest effect thresholds posing severe ecological health risks. High sediment PCDD/F concentrations have persisted in Boat Harbour despite implementation of Pulp and Paper Mill Effluent Chlorinated Dioxins and Furans Regulations in 1992. PAH concentrations varied greatly. Five individual PAH compounds frequently exceeded severe effect thresholds, in contrast to total PAHs, which were below severe effect thresholds. Forensic analysis using PAH diagnostic ratios suggest pyrogenic PAHs derived from wood processes or coal combustion were likely sources. Twenty-five years of monitoring data revealed large data gaps in our understanding of sediment characteristics in Boat Harbour. Gaps included spatial (vertical and horizontal) and temporal variation, presenting challenges for remediation to accurately

[1] Note: A version of this chapter is published in Environmental Monitoring and Assessment.

Hoffman, E., Alimohammadi, M., Lyons, J., Davis, E., Walker, T. R., & Lake, C. B. (2019). Characterization and spatial distribution of organic contaminated sediment derived from historical industrial effluents. *Environmental Monitoring and Assessment, 191(9):590*.

delineate sediment contaminants. Deeper horizons were poorly characterized compared to shallow sediments (0-15 cm). Historical secondary monitoring data showed that spatial coverage across Boat Harbour was inadequate. Due to severe ecological health risks associated with high sediment PCDD/F concentrations, remediation of the entire sediment inventory is recommended. Detailed vertical and horizontal sampling within Boat Harbour, establishment of local baseline concentrations and additional sampling in down-gradient receiving environments for a suite of contaminants are required to better characterize sediments prior to remediation.

2.1 Introduction

Pulp mill effluents can deleteriously impact aquatic ecosystems (Sunito et al. 1988; Colodey and Wells 1992; Ali and Sreekrishnan 2001) caused by inorganic and organic loadings (Pokhrel and Viraraghavan 2004; Hewitt et al. 2006; Soskolne and Sieswerda 2010; Munkittrick et al. 2013; Hoffman et al. 2015, 2017a,b). Deleterious releases to aquatic ecosystems from pulp mills in Canada are governed under Pulp and Paper Effluent Regulations (PPER) pursuant to the Fisheries Act (1985) (PPER 1992; Roach and Walker 2017). In Canada, Pulp and Paper Mill Effluent Chlorinated Dioxins and Furans Regulations, issued under the Canadian Environmental Protection Act (1999), requires mills using chlorine for bleaching to discharge effluent with dioxin and furans below measurable levels (EC 2013, 2014).

A bleached kraft pulp mill and chlor-alkali facility in Pictou County, Nova Scotia has discharged wastewater effluent into the Boat Harbour Treatment Facility (BHTF) and subsequently into a 140-hectare former tidal lagoon (Boat Harbour) since 1967. Boat Harbour lies within the Mi'kmaq Pictou Landing First Nation (PLFN) community (Fig. 2.1). The chlor-alkali facility used the BHTF and Boat Harbour to treat effluent from 1971-1992. The mill has undergone several ownership changes since 1967, as well as several changes to the pulping process. Previous owners used elemental chlorine in the bleaching process which was changed to chlorine dioxide in 1997 (Northern Pulp 2017) to meet PPER requirements for dioxins and furans (PPER 1992). Effluent treatment has been previously described in greater detail by Hoffman et al. (2017a). The treatment process has

undergone several upgrades in aeration capacity since original inception of the plant. Currently, effluent is pumped to settling ponds, then to an aerated stabilization basin (ASB) for treatment prior to discharge into Boat Harbour and subsequent discharge through a dam at the mouth of the former estuary (JWEL and Beak Consultants 1992; Fig. 2.2, top). Residence time (~20-30 d) of treated effluent in Boat Harbour has deposited large volumes of unconsolidated sediments, impacted with inorganic and organic contaminants, raising concerns for the PLFN and nearby local communities (Hoffman et al. 2015; Pictou Landing Native Women's Group et al. 2016). The province of Nova Scotia owned and operated the BHTF from 1967 to 1995, after which the mill owners took over operation.

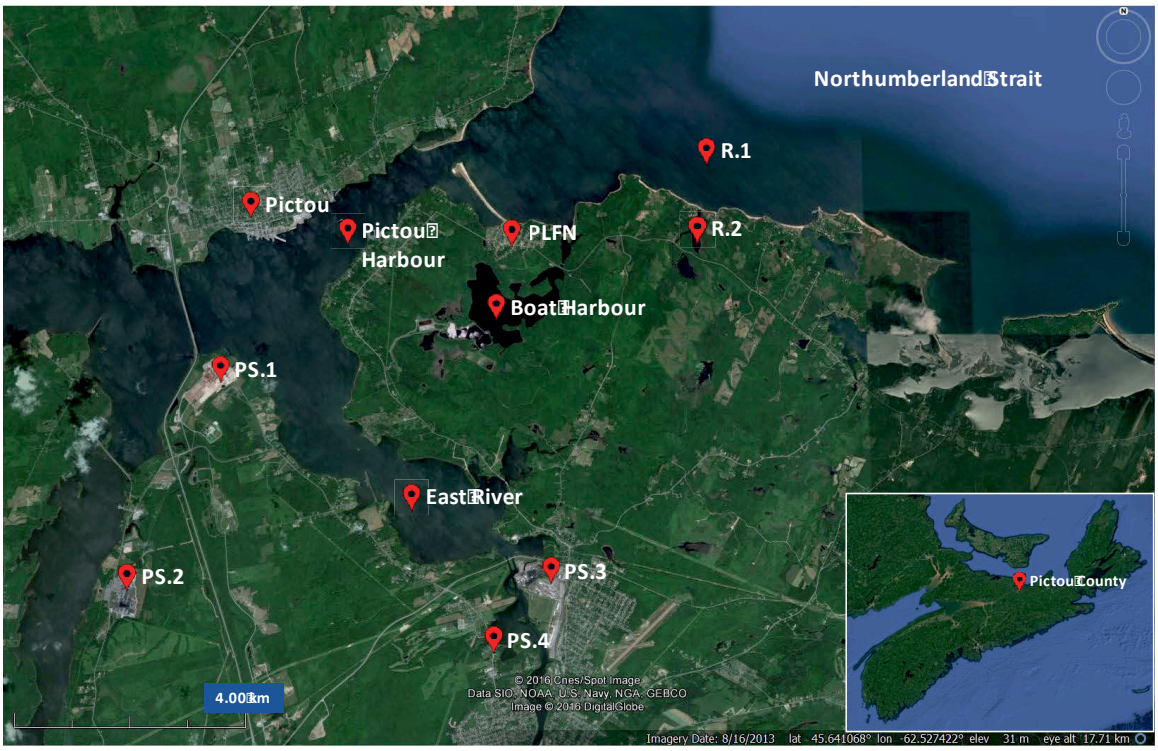

Figure 2.1 Location of Boat Harbour in Pictou County, Nova Scotia relative to communities (e.g., Pictou, and Pictou Landing First Nation [PLFN]), two previously studied reference sediment sampling sites (i.e., offshore [R.1], and Fergusons Pond [R.2]), and local point source emitters (e.g., pulp and paper mill [PS.1], tire manufacturing facility [PS.2], coal-fired thermal electrical generating station [PS.3], former chlor-alkali facility [PS.4]) (©Google Earth).

The province of Nova Scotia committed to ceasing use of Boat Harbour as an effluent receiving lagoon by January 30, 2020 to enable remediation of contaminated sediments under the Boat Harbour Act (2015). However, before remediation can begin, detailed

undergone several upgrades in aeration capacity since original inception of the plant. Currently, effluent is pumped to settling ponds, then to an aerated stabilization basin (ASB) for treatment prior to discharge into Boat Harbour and subsequent discharge through a dam at the mouth of the former estuary (JWEL and Beak Consultants 1992; Fig. 2.2, top). Residence time (~20-30 d) of treated effluent in Boat Harbour has deposited large volumes of unconsolidated sediments, impacted with inorganic and organic contaminants, raising concerns for the PLFN and nearby local communities (Hoffman et al. 2015; Pictou Landing Native Women's Group et al. 2016). The province of Nova Scotia owned and operated the BHTF from 1967 to 1995, after which the mill owners took over operation.

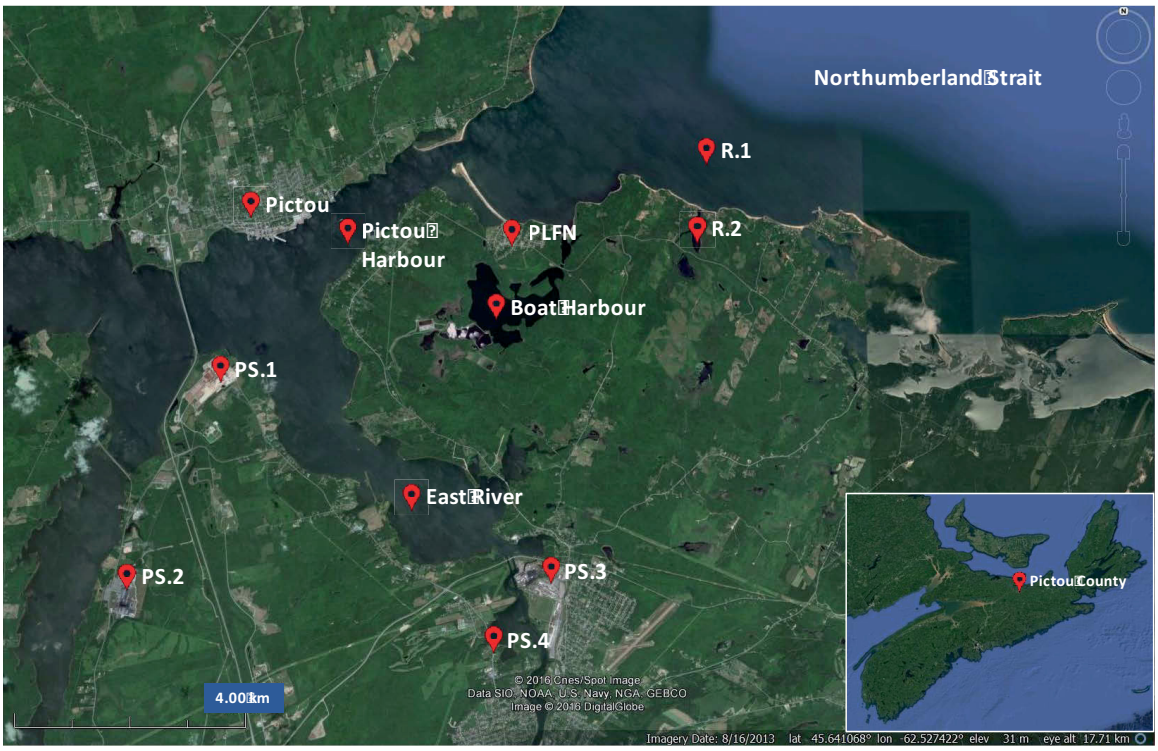

Figure 2.1 Location of Boat Harbour in Pictou County, Nova Scotia relative to communities (e.g., Pictou, and Pictou Landing First Nation [PLFN]), two previously studied reference sediment sampling sites (i.e., offshore [R.1], and Fergusons Pond [R.2]), and local point source emitters (e.g., pulp and paper mill [PS.1], tire manufacturing facility [PS.2], coal-fired thermal electrical generating station [PS.3], former chlor-alkali facility [PS.4]) (©Google Earth).

The province of Nova Scotia committed to ceasing use of Boat Harbour as an effluent receiving lagoon by January 30, 2020 to enable remediation of contaminated sediments under the Boat Harbour Act (2015). However, before remediation can begin, detailed

undergone several upgrades in aeration capacity since original inception of the plant. Currently, effluent is pumped to settling ponds, then to an aerated stabilization basin (ASB) for treatment prior to discharge into Boat Harbour and subsequent discharge through a dam at the mouth of the former estuary (JWEL and Beak Consultants 1992; Fig. 2.2, top). Residence time (~20-30 d) of treated effluent in Boat Harbour has deposited large volumes of unconsolidated sediments, impacted with inorganic and organic contaminants, raising concerns for the PLFN and nearby local communities (Hoffman et al. 2015; Pictou Landing Native Women's Group et al. 2016). The province of Nova Scotia owned and operated the BHTF from 1967 to 1995, after which the mill owners took over operation.

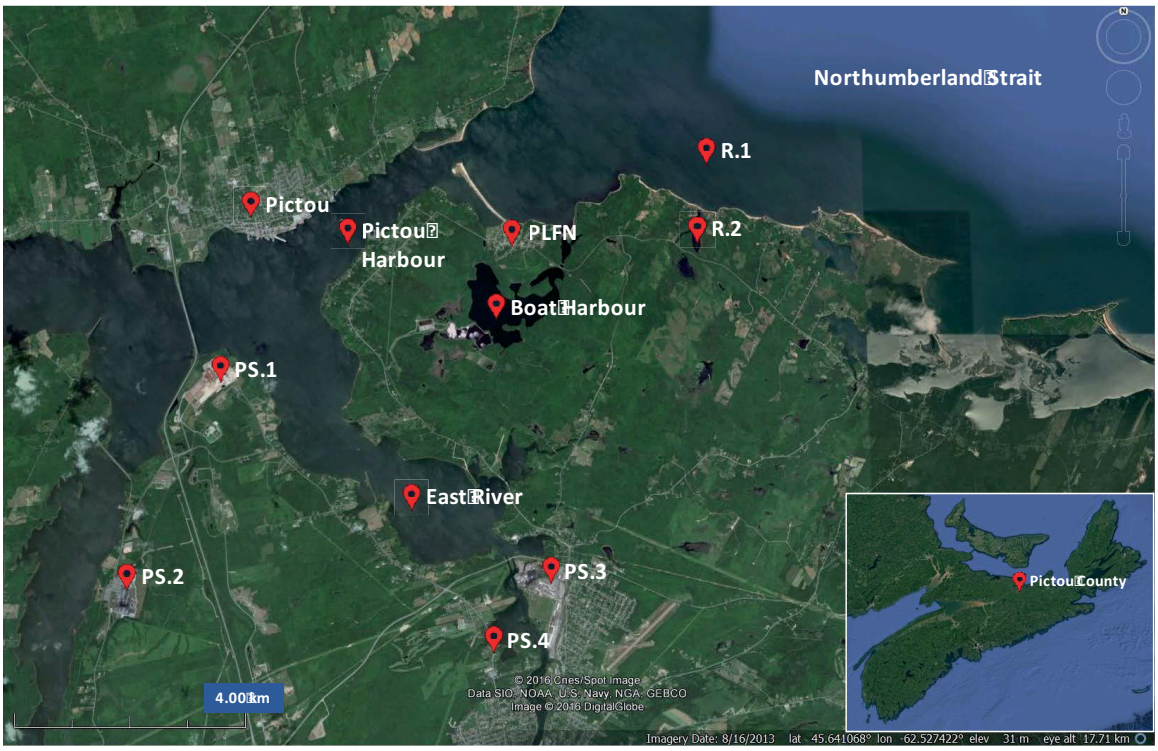

Figure 2.1 Location of Boat Harbour in Pictou County, Nova Scotia relative to communities (e.g., Pictou, and Pictou Landing First Nation [PLFN]), two previously studied reference sediment sampling sites (i.e., offshore [R.1], and Fergusons Pond [R.2]), and local point source emitters (e.g., pulp and paper mill [PS.1], tire manufacturing facility [PS.2], coal-fired thermal electrical generating station [PS.3], former chlor-alkali facility [PS.4]) (©Google Earth).

The province of Nova Scotia committed to ceasing use of Boat Harbour as an effluent receiving lagoon by January 30, 2020 to enable remediation of contaminated sediments under the Boat Harbour Act (2015). However, before remediation can begin, detailed

characterization of sediments is required to inform remedial decisions. Despite dozens of ad hoc historical studies conducted in and around Boat Harbour, the only holistic characterization of sediment contaminants has been performed by Hoffman et al. (2017a) who reported widespread metal(loid) sediment contamination. No comparable study exists for organic contaminants which is the focus of this study. Previous studies (e.g., JWEL 1997, 1999, 2001, 2005; JWEL and Beak Consultants 1992, 1993; Stantec 2013, 2016) reported a suite of polychlorinated dibenzo-p-dioxins and polychlorinated dibenzofurans (PCDD/Fs) along with polycyclic aromatic hydrocarbons (PAHs) distributed throughout Boat Harbour sediments. PCDD/Fs are unintentional by-products of combustion processes and various industrial activities (Sunito et al. 1988). Industrial chlorinated organic chemical processes that produce PCDD/Fs include effluent wastewater from pulp mills (McLeay 1987; Richman et al. 2016) and chlor-alkali facilities (Svensson et al. 1993; Kannan et al. 1998; Yamamoto et al. 2018). Although naturally occurring, PAH contamination largely originates from anthropogenic activities, including combustion processes (MacAskill et al. 2016; Walker et al. 2017; Davis et al. 2019) and pulp processing, especially those involving elemental chlorine (Hoffman et al. 2017a, b).

Sediments impacted by industrial activity can accumulate organic contaminants and pose unacceptable ecological risks to aquatic biota (Hope 2006; El-Shahawi et al. 2010; Walker and MacAskill 2014). Although some PAHs are carcinogenic, they generally have lower risk of acute toxicity to humans (CCME 2008; ATSDR, 2009). However, PCDD/Fs are of a primary concern, because they are highly persistent, lipophilic, bioaccumulative, and can be acutely toxic and carcinogenic to biota and humans (Norstrom 2006; Hites 2011). Long-term sediment contamination exceeding sediment quality guidelines (SQGs) often requires intensive remediation and site-specific disposal procedures (Walker et al. 2013a; 2015a,b).

A comprehensive assessment of organic contamination has not been conducted for Boat Harbour but is essential prior to remediation to accurately delineate sediment contaminant characteristics (e.g., depth, spatiotemporal extent and magnitude of impacts). This paper expands on previous work by Hoffman et al. (2017a) to conduct a comprehensive sediment characterization examining a suite of organic contaminants, focusing on PCDD/Fs and PAHs, using secondary monitoring data. Specifically, this study examines long-term

sediment monitoring data between 1992-2015, using geographic information system (GIS) techniques. Distribution of organic sediment concentrations was examined spatiotemporally. A discussion of findings in relation to potential contamination sources and gaps in long-term monitoring data is provided to better inform future remedial action plans for Boat Harbour.

2.2 Material and Methods

2.2.1 Review of Secondary Monitoring Data

Relevant sediment organic chemistry secondary monitoring data related to Boat Harbour was obtained from government reports and peer-reviewed articles based on approaches reported by Hoffman et al. (2017a). Organic sediment concentrations (including PAHs, PCDD/Fs, volatile organic compounds [VOCs], benzene, toluene, ethylbenzene and xylenes [BTEX], total petroleum hydrocarbons [TPHs], polychlorinated biphenyls [PCBs], and total organic carbon [TOC]) using standardized laboratory analytical methods were relevant for this study. Sample locations had to be georeferenced. Details about sediment sampling methods and depth was also a requirement. This resulted in only eight relevant studies used for this review (JWEL 1997, 1999, 2001, 2005; JWEL and Beak Consultants 1992, 1993; Stantec 2013, 2016).

2.2.2 Sediment Sampling

Sediments were collected using cores or grabs between 1992 and 2015. Assumptions made regarding georeferencing sampling locations (entered in ©ArcMap) and sampling techniques can be found in Hoffman et al. (2017a). Relevant criteria included: PCDD/F and PAH concentrations; location of sample (decimal degrees x, y coordinates), sample identification, date, depth (cm), and characteristics such as marine sediment, unconsolidated sediment/deposits. Sample location coordinates were generated by overlaying report maps in ©Google Earth to attain a unified coordinate system (Hoffman et al. 2017a).

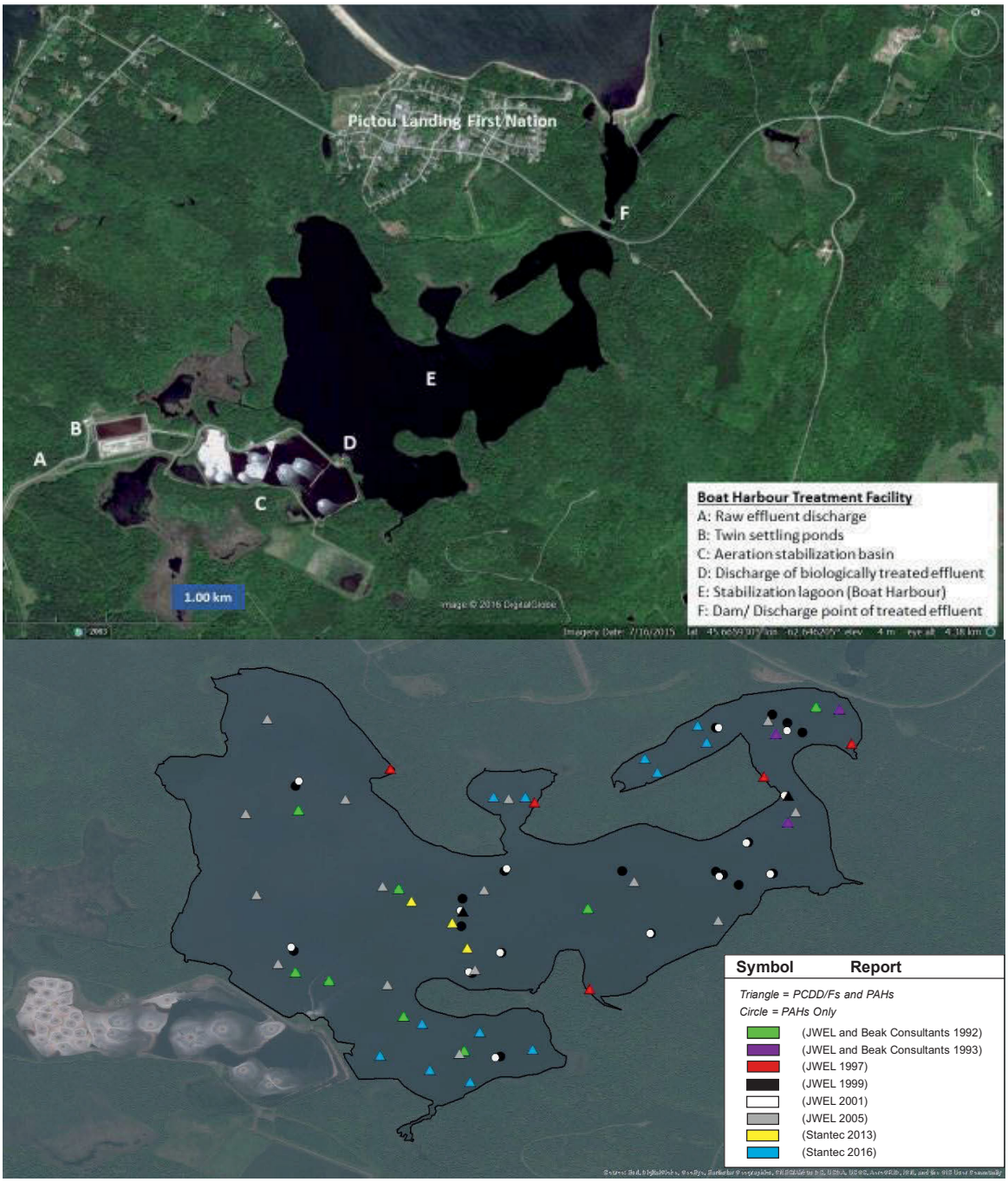

Figure 2.2 Components of the Boat Harbor Treatment Facility (BHTF) and Pictou Landing First Nation (PLFN) community (top). Spatiotemporal coverage (1992-2015) of sediment sampling stations in Boat Harbour (bottom). Coloured triangles indicate sampling and analysis of PCCD/Fs and PAHs, coloured circles indicate sampling and analysis of PAHs only (©Google Earth; from Hoffman et al. 2017a).

2.2.3 Quality Control

Individual reports are cited where use of method blanks, spike blanks, matrix spikes, duplicate samples varied (Hoffman et al. 2017a). As reported by Hoffman et al. (2017a), commercial laboratories accredited by Standards Council of Canada, were used for analysis of samples using Environment Canada EPS 1/RM/19 standard methods (Trudel 1991; Environment Canada. 1992). Unless otherwise indicated, samples and field duplicates, were analyzed on a dry weight (dw) basis. Detection limits (DLs) for PCDD/Fs varied between 0.0987 to 46 pg/g and 0.005 to 0.06 mg/kg for PAHs. Recovery rates for PCDD/Fs varied between 30 to 120%. Censored data (½DL) were used for all <DL data (MacAskill et al. 2016; Davis et al. 2018). Total PAH values were derived by using summed concentrations plus ½DL values for all <DL. Boat Harbour sediment PCDD/F and PAH data were compared to two reference sites in the down-gradient receiving marine environment (R.1) (JWEL 1994) and Fergusons Pond (R.2) (Fig. 2.1) (JWEL 1997; 1999; 2001).

2.2.4 Data Analysis

Currently Boat Harbour is a freshwater habitat but will be returned to tidal conditions post-remediation (Hoffman et al. 2017a). For this study, similar approaches were used as Hoffman et al. (2017a). For example, PAH concentrations of 103 samples from 85 stations were compared to both current freshwater and marine Canadian Council of Ministers of the Environment (CCME) SQGs (CCME 2016). Contaminant concentrations below low effect level CCME interim sediment quality guidelines (ISQGs) have little chronic or acute effect on aquatic biota, whereas contaminant concentrations above severe effect level CCME probable effect levels (PELs) are highly likely to negatively impair aquatic biota (Walker et al. 2015a,b). In this study, sediment concentrations were assessed as severely contaminated if PELs were exceeded, moderately contaminated between ISQGs and PELs, and uncontaminated if sediment concentrations <ISQGs (Walker et al. 2015a). No CCME guidelines for total PAHs exist, so total PAH sediment concentrations were compared to effects range low (ER-L) (4.02 mg/kg) and effects range median (ER-M) (44.8 mg/kg) (Long et al. 1998; NOAA 1999).

Toxic equivalency (TEQ) concentrations of 60 PCDD/F samples from 48 stations, were calculated by multiplying PCDD/F concentrations with associated toxic equivalency factors (TEFs), representing a weighted quantity measure based on the toxicity of each PCDD/F congener. Boat Harbour PCDD/F TEQ concentrations were determined using WHO-established TEFs applying to fish, birds and humans/mammals (van den Berg et al. 1998) and then compared to related CCME guidelines (CCME 2001a, 2001b, 2002). Temporal PCDD/F congener patterns and percent contributions (∑17PCDD/Fs) in sampled Boat Harbour sediment were illustrated using stacked bars. In the down-gradient receiving marine environment, PCDD/F congener concentration data was limited to a single sample at R.1 (JWEL 1994) (Fig. 2.1).

PAH diagnostic ratios were used to determine source apportionment for PAH compounds, as PAH mixtures maintain their proportional integrity (ratio of compounds present) following release, regardless of changes in PAH bulk concentration (Tobiszewski and Namiesnik 2012). PAH ratios are particularly useful for determination of PAH source apportionment using historical datasets (MacAskill et al. 2016; Walker et al. 2017; Davis et al. 2019). PAH ratios were applied using anthracene (An), fluoranthene (Fl), phenanthrene (Ph), and pyrene (Py), due to high levels of detection: Fl/Py to Ph/An (adopted from Maxxam 2016) and Fl/Fl+Py to An/An+Ph (Yunker et al. 2002). Box and scatter plots were used to display temporal (1992-2015) and spatial (vertical) variation, respectively of PCDD/F and PAH sediment concentrations. Significant temporal differences ($p<0.05$ level) were determined by one-way analysis of variance (ANOVA) followed by a Tukey's test using Minitab.

Organic sediment concentrations from reports were presented unmodified (except censored data). Statistical analysis of independent temporal differences in organic contaminant concentrations used ANOVA. Inter-annual data independence was assumed because of variation in sampling techniques (abiotic variation) and bioturbation (biotic variation) conditions. Mid-range sample depths were used to assess vertical variation of PCDD/F and PAH concentrations. Like Hoffman et al. (2017a) spatiotemporal variation of PAH and PCDD/F concentrations and sampling locations were assessed using ©ArcMap over three

periods (1992-1996; 1998-2003; and 2004-2016) against which future studies post remediation can compare against (Hoffman et al. 2017a).

2.3 Results and Discussion

Hoffman et al. (2017a) reported that secondary monitoring data varied widely in sampling techniques (e.g., using grabs, cores, discrete or composite sampling) and sample depth (e.g., shallow vs. deep). For this study, approximately 17% and 38% of PCDD/F and PAH samples respectively, were grab samples, while 83% and 62% of PCDD/F and PAH samples were cores. This variability created challenges for inter-annual comparisons. Overall, sediments were highly organic (4-27% mean TOC). Generally, the highest PCDD/F and PAH concentrations corresponded with high TOC contents and is an important factor governing occurrence of persistent organic contaminants (Alimohammadi et al. 2017). Although TOC data is not presented herein, it has previously been reported in greater detail by Hoffman et al. (2017a). Review of previous sediment sampling programs in Boat Harbour showed that subsurface conditions consisted of anthropogenic black freshwater organic sediment (12-26 cm deep), underlain by marine clay (Spooner and Dunnington 2016; Stantec 2016). Temporal georeference analysis of sampling locations revealed that overall spatial coverage was lacking (Fig. 2.2, bottom), corroborating Hoffman et al. (2017a), who reported a lack of spatial coverage for metal(loid)s. Half of (54%) Boat Harbour sediment samples analyzed for PCDD/F concentrations (from 60 samples and 49 locations) and PAH concentrations (69%) (from 103 samples and 81 locations), were from shallow horizons (0-15 cm), leaving deeper horizons under characterized. This presents challenges for accurate horizontal and vertical delineation of impacted sediment for future remedy decisions (Fig. 2.3; Supplemental Fig. A1 and Supplemental Table B1 and B2).

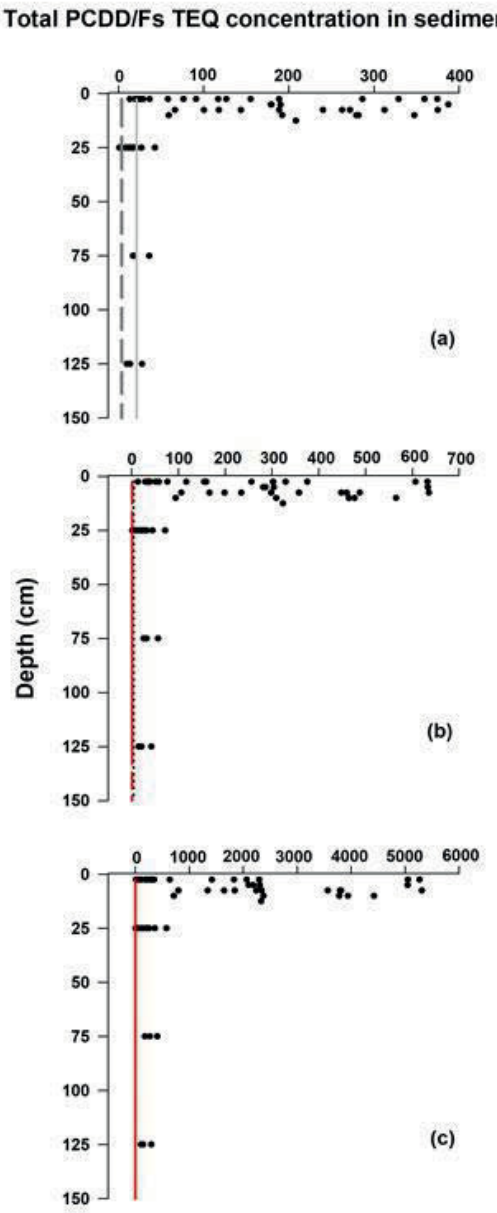

Figure 2.3 Vertical variation of total PCCD/F TEQs sediment concentrations (n=60) with depth (cm) for different receptors: (a) fish, (b) human/mammals, and (c) birds. CCME freshwater and marine sediment quality guidelines are same for fish category and indicated using solid vertical line for PEL (21.50 pg/g) and dashed line for ISQG (0.85 pg/g) values (CCME 2001a). Soil quality guideline for the protection of environmental and human health for all land uses is shown using black dotted vertical line (4.00 pg/g) (CCME 2002). CCME tissue residue guidelines for the protection of wildlife consumers of aquatic biota are indicated using red dashed line for mammals (0.71 pg/g) and red solid line (4.75 pg/g) for birds (CCME 2001b).

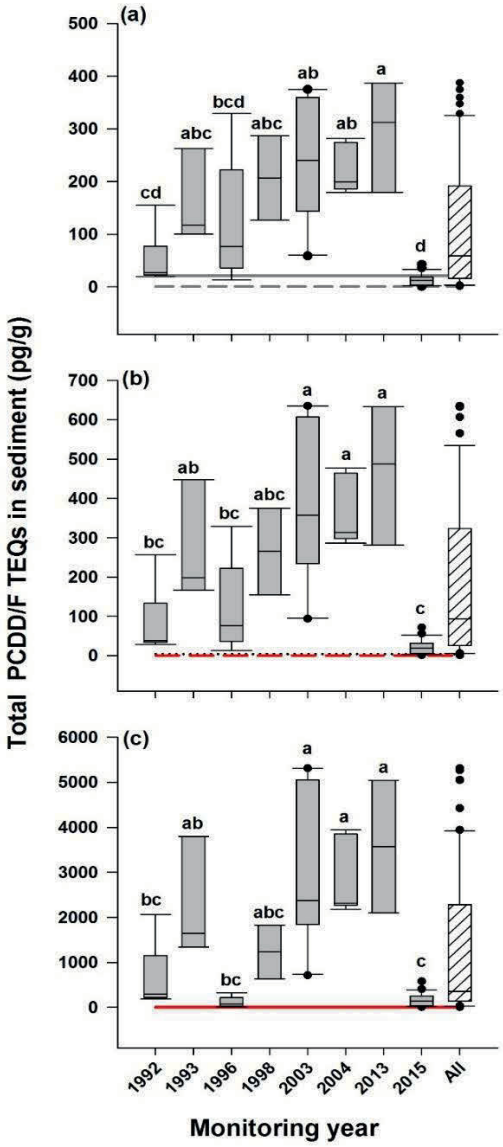

Figure 2.4 Temporal variation (~25 years) of total PCCD/F TEQs sediment concentrations (n=60) in Boat Harbour for different receptors: (a) fish, (b) human/mammals, and (c) birds. CCME freshwater and marine sediment quality guidelines are same for fish category and indicated using solid horizontal line for PEL (21.50 pg/g) and dashed line for ISQG (0.85 pg/g) values (CCME 2001a). Soil quality guideline for the protection of environmental and human health for all land uses is shown using black dotted horizontal line (4.00 pg/g) (CCME 2002). CCME tissue residue guidelines for the protection of wildlife consumers of aquatic biota are indicated using red dashed line for mammals (0.71 pg/g) and red solid line for birds (4.75 pg/g) (CCME 2001b). Significant temporal differences were determined by one-way ANOVA followed by Tukey's test; years attributed with same letters were not significant and those with different letters were significantly different ($p<0.05$ level).

Despite wide variation in sampling methods, there was widespread PCDD/F sediment contamination reported across Boat Harbour for the entire period (Fig. 2.4). Temporal analysis of PCDD/F TEQs differed from PAHs. Temporal sediment PAH concentrations peaked around 1998 and mirrored peaks in sediment metal(loid) concentrations reported by Hoffman et al. (2017a). In contrast, PCDD/F TEQs did not peak in 1998, although concentrations were significantly higher compared to 1996 in all TEF categories during this year. PCDD/F patterns were consistent across sampling years, except for 1998, when a substantial spike in 2,3,7,8-Tetra CDD concentrations occurred. The change in pattern of PCDD/F in 1998 suggests that previous ASB improvements or dredging caused a change of chemical composition in Boat Harbour sediments. PCDD/F TEQs peaked between 2003-2013, declining significantly in 2015 to concentrations below those reported in the 1990s. However, the number of samples collected in 2015 was limited and included composite samples which presumably attenuated overall concentrations. Despite this significant decline, all (n=60) PCDD/F TEQs exceeded low effect CCME fish ISQGs and 66.6% (n=40) exceeded severe effect CCME fish PELs and 93.3% (n=56) exceeded soil quality guideline for human health (SQGHH), indicating severe contamination and risk to biota (Table 1). Results were replicated in the spatiotemporal analysis displaying discrete locations and relative PCDD/F TEQ concentrations (Fig. 2.5). Of the samples detected below upper effect PELs (33.4%; n=20) and SQGHH (6.7%; n=4), most were from isolated coves (Stantec 2016; Fig. 2.5).

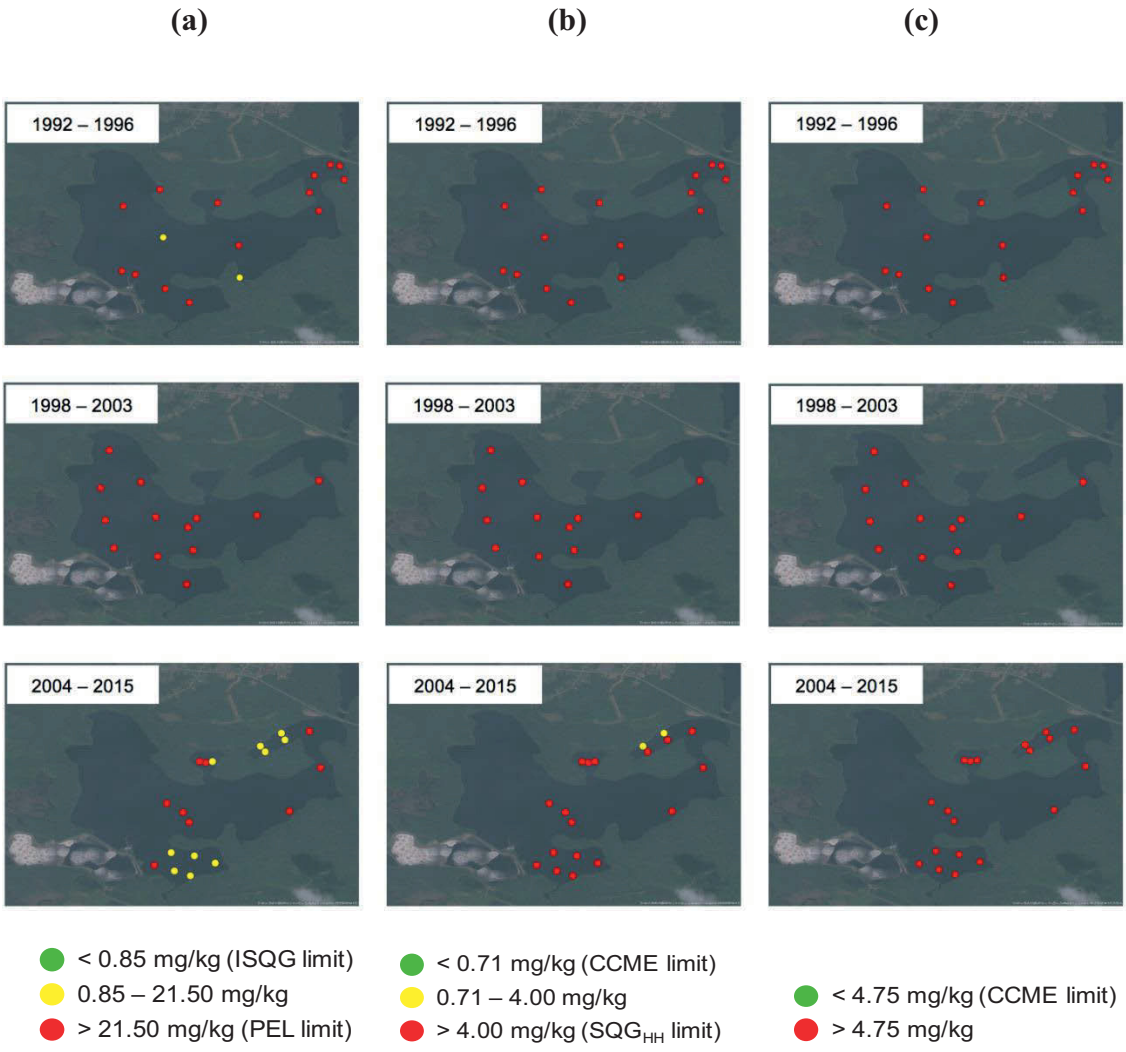

Figure 2.5 Spatiotemporal variation of PCCD/F TEQs sediment concentrations (n=60) for different receptors: (a) fish compared to CCME freshwater and marine sediment quality guidelines (green, <0.85 [ISQG]; yellow, 0.85-21.50; red, >21.50 [PEL] pg/g); (b) human/ mammals compared to CCME tissue residue guidelines for the protection of wildlife consumers of aquatic biota and soil quality guideline (SQG) for the protection of environmental and human health for all land uses (green, <0.71 pg/g [CCME]; yellow, 0.71-4.00; red, >4.00 [SQGHH] pg/g); (c) birds compared to CCME tissue residue guidelines for the protection of wildlife consumers of aquatic biota (green, <4.75; red >4.75) over three periods: top 1992-1996; middle 1998-2003; bottom 2004-2015.

Percent contributions of PCDD/F congeners indicate higher proportions of 2,3,7,8-Tetra CDF (68.6-97.3%), and 2,3,7,8-Tetra CDD (10.7-63.8%) in Boat Harbour sediment for all TEF categories. Congener patterns in Boat Harbour sediment differ to R.1 reference samples, where higher proportions of 1,2,3,7,8-Penta CDD (20-33%) and 2,3,4,7,8-Penta CDF (17-24%) were present (Supplemental Fig. A3). Additionally, there were no SQG exceedance of PCDD/F concentrations at R.1. However, PCDD/F chemistry data in down-gradient receiving waters was limited to a single sampling event (JWEL 1994); thus, may not represent current conditions. Findings suggest inputs of PCDD/Fs result from sorption to organic rich Boat Harbour sediments and are not released in appreciable amounts to down-gradient marine receiving waters. This is consistent with the original design objectives of utilizing Boat Harbour as a sedimentation lagoon. Furthermore, differences in congener signatures, may suggest different inputs of PCDD/Fs in the marine environment from anthropogenic sources. Further investigation both within Boat Harbour sediments and down-gradient receiving environments within marine sediments and biota is required to adequately characterize local PCDD/F contamination and to address uncertainty regarding offsite migration of PCDD/F contaminated sediment (Romo et al. 2019).

High sediment PCDD/F concentrations, with limited inter-annual variation, have persisted in Boat Harbour over the entire period (25 years). This is despite implementation of Pulp and Paper Mill Effluent Chlorinated Dioxins and Furans Regulations in 1992, which prohibits the release of measurable PCDD/Fs in effluent wastewater (EC 2013, 2014). This was supported by data reported under the National Pollution Release Inventory (NPRI) program. According to recent substance reports submitted to NPRI from 2011-2016, no on-site releases of dioxins and furans (total) to water were reported by the mill (EC 2017). High PCDD/Fs concentrations measured in Boat Harbour sediments after 1992, reflect highly persistent properties of these bioaccumulative, acutely toxic organic compounds, which were presumably present before sediments were collected and reported in studies reviewed herein. Sediment PCDD/Fs concentrations were presumably derived from nearby historical pulp mill effluents, prior to 1997 when the bleaching process was changed to meet PPER requirements, or from a former chlor-alkali facility, between 1971-1992 when the BHTF and Boat Harbour were used to treat effluents. Pulp mill effluent wastewater has

long been associated with legacy PCDD/F sediment contamination (Norstrom 2006; Hites 2011; Richman et al. 2016), but chlor-alkali facilities, normally associated with mercury releases (Walker 2016), are well known point sources for PCDD/Fs in effluent wastewater (Svensson et al. 1993; Kannan et al. 1998; Yamamoto et al. 2018).

Although most individual PAHs were <DLs, five individual PAHs (anthracene, fluoranthene, fluorene, phenanthrene, pyrene) frequently exceeded low effect freshwater and marine ISQGs and PELs (Table 2.1; Figs. 2.6 and 2.7). Again, SQG exceedances for PAHs were mostly measured in surface (0-15 cm) horizons, leaving deeper horizons under characterized. Total PAHs frequently exceeded ER-L (45%), but due to the relatively large quantity of individual PAH compounds <DLs, total PAH concentrations did not exceed ER-M. However, total PAH concentrations were still higher than those reported by Davis et al. (2018), who characterized total PAH concentrations in nine small craft harbours along the Northumberland Strait covering roughly the same temporal period (2001-2017). Total PAH concentrations varied widely between 0.10-15.4 mg/kg over 25 years (Fig. 2.7). Significantly higher total PAH concentrations were measured in 1998 compared to those measured before or after; consistent with temporal trends found with metal(loid) concentrations (Hoffman et al. 2017a). There appears to have been a gradual decline of individual PAH compounds and total PAH concentrations after 1998, presumably due to weathering or degradation of PAHs associated with increased oxygen concentrations following ASB improvements in 1996 (JWEL 1999). Results were also mirrored spatiotemporally for some individual PAH sediment concentrations. For example, there were higher frequencies of both freshwater and marine PEL exceedances for phenanthrene between 1998 and 2003 (Fig. 2.8). To a lesser extent this spatiotemporal pattern was observed in fluoranthene and total PAH sediment concentrations (Figs. A2 and A4 in Appendix A). However, decreasing PAH concentrations after 1998 may not indicate improving conditions. Apparent decreases in PAH concentrations since 1998 may also be attributable to bioturbation (Nedwell and Walker 1995); burial from less contaminated sediment (Walker et al. 2013b,c); under-sampling; more stringent provincial industrial approvals (NSE 2015); improvements to effluent wastewater treatment combined with increased federal regulatory oversight (EC 2013, 2014); or changes to deposition rates. These factors may have attenuated PAH concentrations temporally (Hoffman et al. 2017a).

Ratios of Fl/Py to Ph/An indicates coarse clustering suggesting a common source (Supplemental Fig. A5a). Furthermore, double PAH diagnostic ratios of Fl/Fl+Py to An/An+Ph suggest ~67% of PAH samples were derived from pyrogenic PAH sources (e.g., wood and coal combustion processes), based on transition values proposed by Yunker et al. (2002) (Supplemental Fig. A5b). Less than 20% of samples suggest petroleum combustion, while only a small fraction (13.6%) suggest direct petroleum sourcing. Similar ratio values (>0.5) for the ratio of Fl/Fl+Py were observed from pulp mill effluent samples and surrounding sediment samples in Kitimat Harbour, BC, a harbour site in proximity to a pulp mill (Yunker et al. 2011). Likely sources for pyrogenic PAHs could be derived from local industrial combustion point source emitters (e.g. pulp and paper mill, a tire manufacturing facility and a coal-fired thermal electrical generating station) (Hoffman et al. 2015, 2017a,b) or long-range atmospheric transport. Nova Scotia is known as the tail pipe of North America, due to being within the trajectory of long-range transport of emissions from transboundary sources along the Eastern Seaboard, plus central and eastern Canada (NSE 2014). Despite the pyrogenic PAH signature observed, it is suggested that plant-derived PAHs (terpenes and other hydrocarbon constituents) may be dominant in pulp mill effluent, while parent and alkylated PAHs may not be emitted in as large of proportions, and that plant-derived PAHs emitted by pulp mill effluent may pose a large risk to biota as they demonstrated increased bioavailability and toxicity in biological assessments at Kitimat Harbour (Yunker et al., 2011).

Table 2.1 Sediment quality guideline (SQG) exceedances for select PAH compounds, total PAHs and PCDD/F TEQs in Boat Harbour between 1992-2015. Total sediment samples (*n*) are indicated under each parameter and include sediment collected from all depth horizons.

Parameter	Freshwater				Marine			
	ISQG		PEL		ISQG		PEL	
	SQG Limit	Number of exceedances (%)	SQG Limit	Number of exceedances (%)	SQG Limit	Number of exceedances (%)	SQG Limit	Number of exceedances (%)
Anthracene mg/kg (*n* = 103)	0.047	52(50.5)	0.245	31(30.1)	0.047	52(50.5)	0.245	31(30.1)
Fluoranthene mg/kg (*n* = 103)	0.111	77(74.8)	2.355	8(7.8)	0.113	77(74.8)	1.494	29(28.2)
Fluorene mg/kg (*n* = 103)	0.021	76(73.8)	0.144	7(6.8)	0.021	76(73.8)	0.144	7(6.8)
Phenanthrene mg/kg (*n* = 103)	0.042	86(83.5)	0.515	60(58.3)	0.087	77(74.8)	0.544	59(57.3)
Pyrene mg/kg (*n* = 103)	0.053	81(78.6)	0.875	42(40.8)	0.153	72(69.9)	1.398	29(28.2)

Total PAHs mg/kg (n = 103)	ER-L		ER-M	
	SQG Limit	Number of exceedances (%)	SQG Limit	Number of exceedances (%)
	4.02	46(44.7)	44.80	0(0)

PCDD/Fs pg/g (n = 60)	Freshwater and Marine (Fish)				Canadian Tissue Residue Guidelines				Canadian Soil Quality Guidelines for the Protection of Environmental and Human Health	
	ISQG		PEL		Mammals		Birds		Human	
	0.85	60(100)	21.50	40(66.6)	0.71	60(100)	4.75	60(100)	4.00	56(93.3)

ISQG indicates CCME interim sediment quality guidelines and PEL indicates CCME probable effect levels (CCME 2016). There are no CCME guidelines for total PAHs, so these were compared to effects range low (ER-L) and effects range median (ER-M) (Long et al. 1998; NOAA 1999).

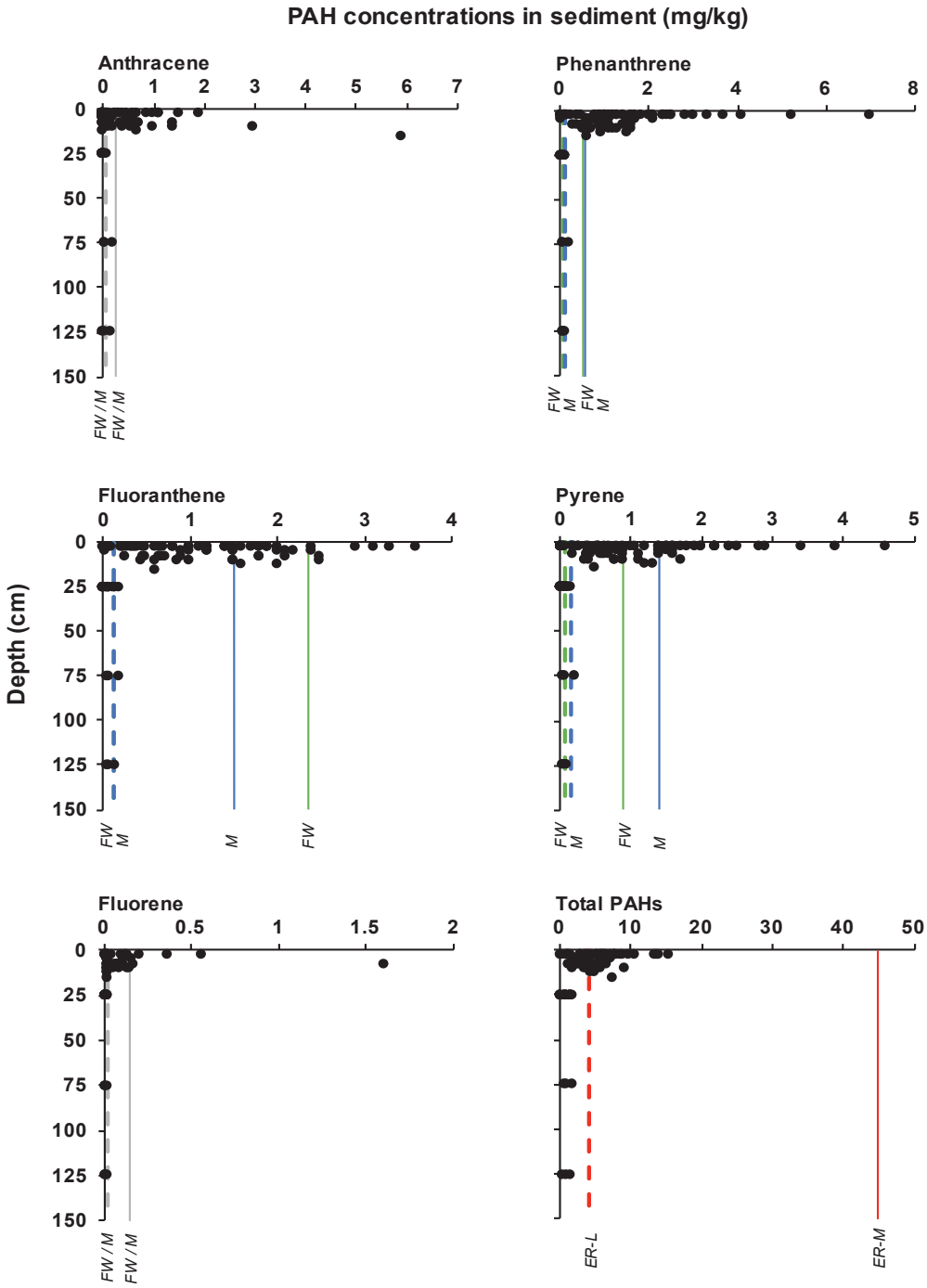

Figure 2.6 Vertical variation of select individual PAH compounds and total PAH sediment concentrations (n=103) with depth (cm). For individual PAH compounds CCME freshwater (dark green) and marine (blue) sediment quality guidelines (SQGs) are indicated using solid vertical lines for PEL and dashed lines for ISQG values. Grey represents when marine and freshwater SQGs are equal (CCME 2016). For total PAH concentrations, dashed line indicates the ER-L (4.02 mg/kg) and solid line indicates ER-M (44.80 mg/kg) (Long et al. 1998; NOAA 1999).

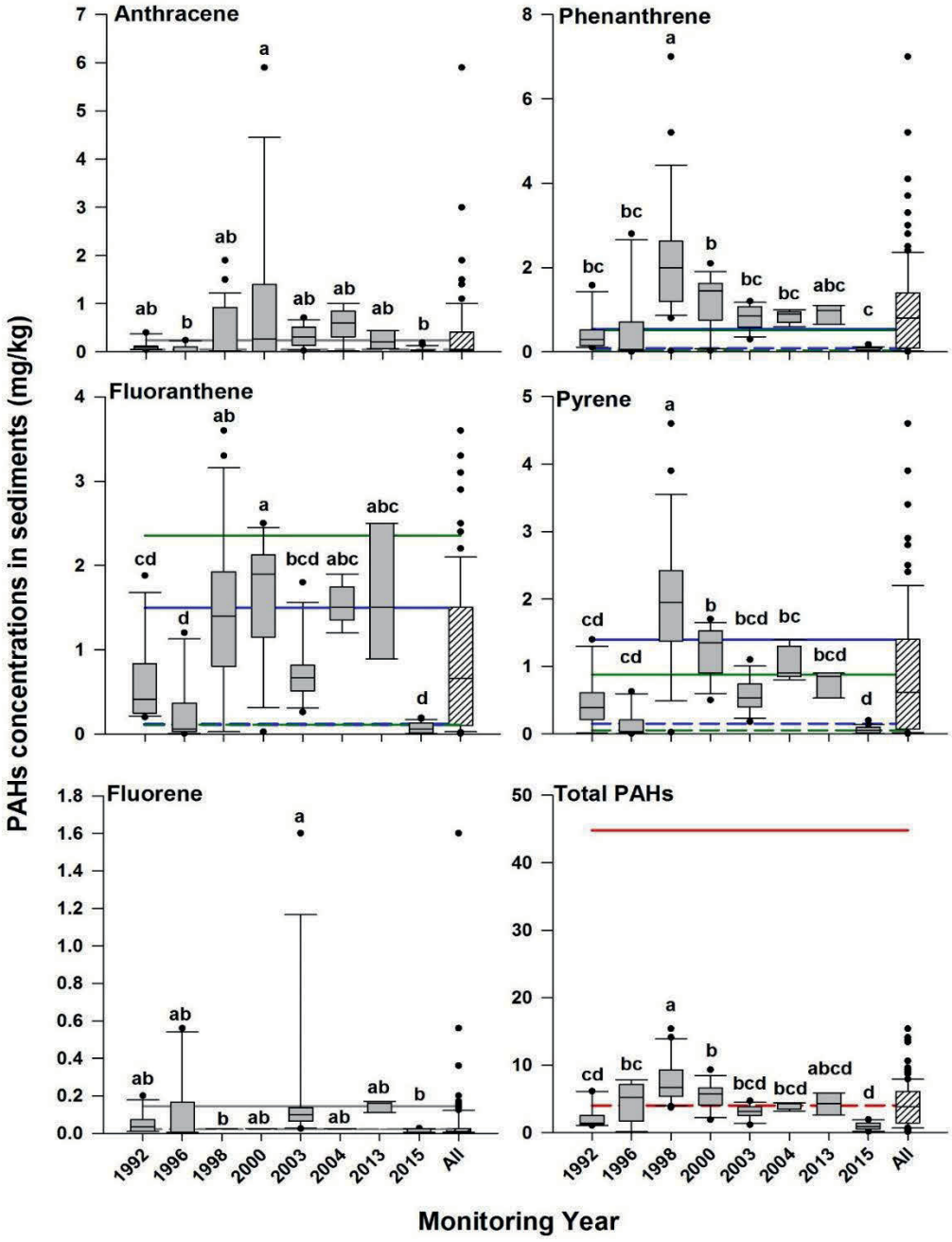

Figure 2.7 Temporal variation (~25 years) of select individual PAH compounds and total PAH sediment concentrations (n=103) in Boat Harbour. For individual PAH compounds CCME freshwater (dark green) and marine (blue) sediment quality guidelines are indicated using solid horizontal lines for PEL and dashed lines for ISQG values. Grey represents when marine and freshwater SQGs are equal (CCME 2016). For total PAH concentrations, solid horizontal red lines indicate ER-M (44.80 mg/kg) and dashed lines indicate ER-L (4.02 mg/kg) (Long et al. 1998; NOAA 1999). Significant temporal differences were determined by one-way ANOVA followed by Tukey's test; years attributed with same letters were not significant and those with different letters were significantly different ($p<0.05$ level).

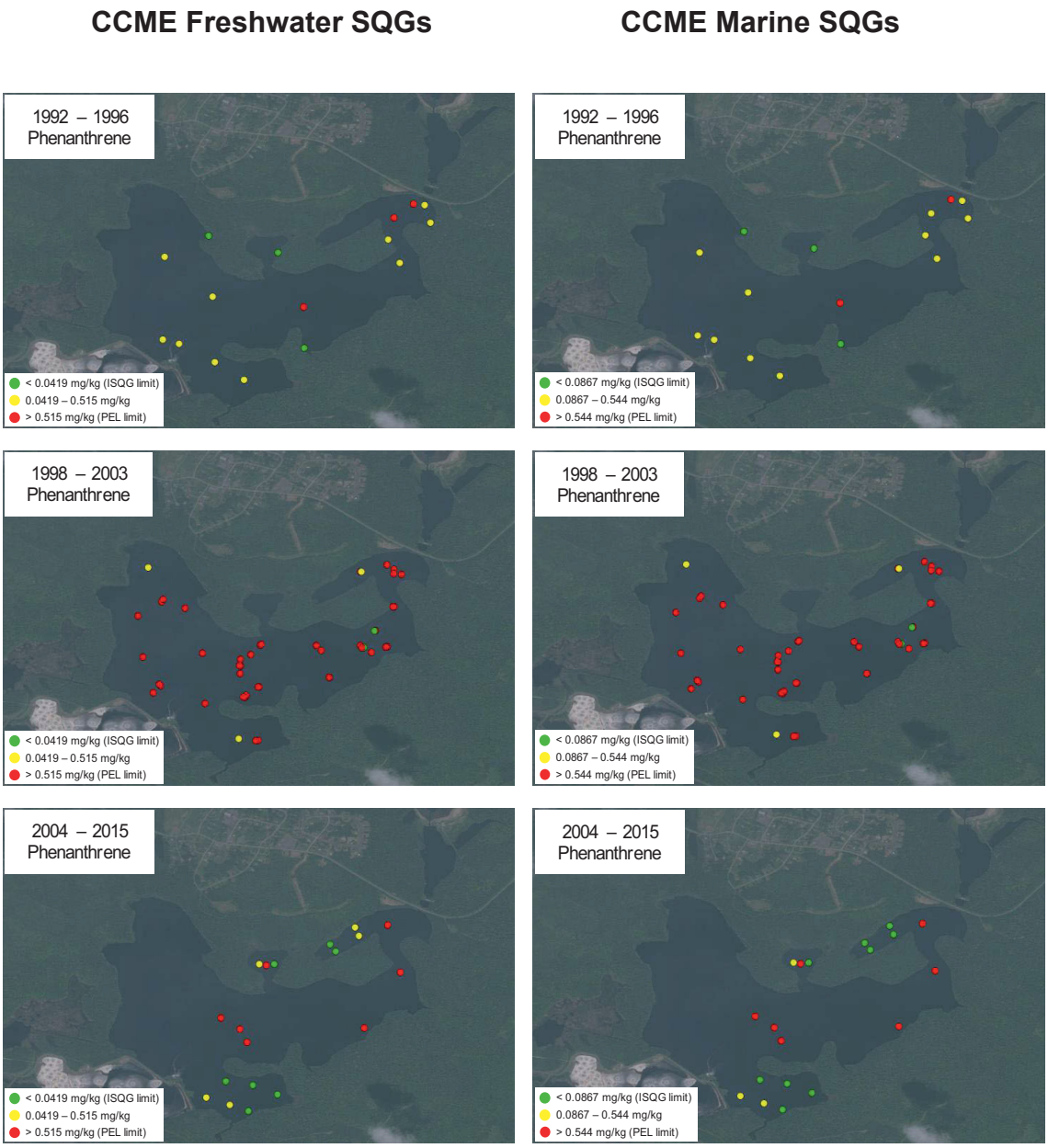

Figure 2.8 Spatiotemporal variation of sediment phenanthrene concentrations (n=103) compared to CCME freshwater (green, <0.0419 [ISQG]; yellow, 0.0419-0.515; red, >0.515 [PEL] mg/kg) and marine (green, <0.0867 [ISQG]; yellow, 0.0867-0.544; red, >0.544 [PEL] mg/kg) SQGs in Boat Harbour sediment over three periods: top 1992-1996; middle 1998-2003; bottom 2004-2015.

VOCs and BTEX were other organic contaminant classes reported in two reports (JWEL and Beak Consultants 1992; Stantec 2016). All VOC (n=27; DL= 0.01-0.05 mg/kg) and BTEX (n=16; DL=0.01-0.05 mg/kg) concentrations were <DL. Modified TPH concentrations (resembling lube oil) in all Stantec (2016) samples (n=9) collected from the cove south of point D exceeded Nova Scotia Tier 1 Standards for sediment of 43 mg/kg for protection of freshwater and marine aquatic life (Atlantic RBCA 2012). Highest concentrations of 3,800 mg/kg and 1,400 mg/kg were detected at 0.5-1.0 m and 1.0-1.5 m, respectively. Samples with the highest concentrations were rerun for TPH with silica gel to assess whether naturally occurring hydrocarbons were present, but no significant difference between samples were detected, suggesting hydrocarbons were likely from anthropogenic sources. Additionally, from two Boat Harbour reports analyzing PCBs (n=10; DL=0.05 mg/kg), all concentrations were <DL (JWEL and Beak Consultants 1992; JWEL 1999). However, due to limited spatiotemporal sediment sampling, VOCs, BTEX, TPHs, and PCBs were historically under-assessed and lack adequate characterization.

Although the mill effluents are likely the primary source of organic contaminant loadings in Boat Harbour, other local sources may have contributed to the organic contaminant burden. In addition to the former chlor-alkali plant, a nearby coal-fired thermal generating station reported releases of atmospheric emissions of PCDD/Fs, ranging from 0.273 g TEQ in 2002 to 0.012 g TEQ in 2015, under the NPRI program (EC 2016). Atmospheric emissions of PCDD/Fs from mill smoke stacks ranged from 0.011 TEQ g in 2002 to 0.008 g TEQ in 2015 (EC 2016). This is supported by PAH ratios in the sediment, which suggests wood or coal combustion as primary sources, but warrants further investigation for other possible sources. PCDD/F and PAH concentrations in sediment using various sampling techniques and subsequent sub-sampling techniques showed wide spatiotemporal variation between 1992 and 2015. One of the key findings showed that although PAH concentrations varied greatly (likely due to inconsistent sampling techniques), PCDD/F sediment concentrations did not follow this trend and exceeded the highest effect thresholds for 25 years; hence, remain contaminants of concern for future remediation.

Exceedances of organic contaminants indicate potential ecological risk to biota. A recent fish survey by Oakes (2016) found Mummichog and Ninespine sticklebacks in Boat

Harbour. Other than several cycles of pulp and paper environmental effects monitoring events (see Hoffman et al. 2015), there have been few studies conducted in the down-gradient receiving marine environment to determine potential ecological impacts (St-Jean et al. 2003; Romo et al. 2019). For example, Fergusons Pond (located 2.5 km NE of Boat Harbour on the Northumberland Strait), was previously used as a reference site (i.e., JWEL 1997; 1999; 2001), and considered a priori unimpacted by industrial activities (R.2) (Fig. 2.1). All individual PAHs were <ISQGs in Fergusons Pond (n=4). Over the past 25 years, Boat Harbour sediment total PAH concentrations were up to 12 times higher than samples collected from Fergusons Pond, assuming total PAH values summed concentrations plus ½DL values for <DL (0.01 and 0.05 mg/kg). Of the five priority individual PAHs, phenanthrene concentrations were up to 1,400 and 280 times higher than samples collected in Fergusons Pond for 0.01 and 0.05 mg/kg DL, respectively. Coastal sediments near industrial facilities around Nova Scotia have been widely reported as sinks for organic contaminants (King and Chou 2003; Walker et al. 2013a,bc,d; 2015a,b), but limited background data exist. Therefore, Fergusons Pond and other suitable estuaries nearby, require further investigation to better understand local baseline conditions and to help guide remedial objectives.

More sediment characterization is required to predict ecological risks associated with contaminated organic sediments in Boat Harbour and down-gradient receiving marine environments prior to implementing costly remediation activities (Walker et al. 2013a,b; Walker 2014; Alimohammadi et al. 2017; Hoffman et al 2017a; Romo et al. 2019). Assessment of contaminated aquatic sites in Canada follows federal and provincial ecological risk frameworks to guide remediation decisions (e.g. Chapman 2011; Contaminated Sites Regulations 2013; Hoffman et al 2017a). Engineering considerations and stakeholder engagement (e.g. with knowledge holders and elders in the Mi'kmaq PLFN community) will be key to help establish local historical pre-mill conditions (Bennett 2013). According to Hoffman et al. (2017a) to return Boat Harbour to pre-mill tidal conditions, collection and measurement of local baseline data, combined with stakeholder engagement are required to establish remediation end-point goals. Remediation will require ex-situ or in-situ sediment treatment to attain concentrations

comparable to local or regional baseline conditions or below low effect levels (Hoffman et al. 2017a).

Gaps in vertical and spatial sediment characteristics were revealed by this review and were consistent with findings by Hoffman et al. (2017a) related to metal concentrations. This study and those by Alimohammadi et al. (2017) and Hoffman et al. (2017a) suggest detailed vertical sediment core sampling is required, and greater spatial coverage to accurately determine depth and volumes of unconsolidated sediment prior to remediation. Adequate vertical and horizontal coverage is required for spatial analysis of hotspots vs. depth (Hoffman et al. 2017a). Accurate delineation of impacted sediments would allow for treatment or removal and proper disposal of sediments (Walker et al. 2013a). As reported by Hoffman et al. 2017a, sampling by Spooner and Dunnington (2016) using 14 cores reported that effluent impacted organic sediments reached <30 cm across all stations helping to establish pre-mill background conditions. Confirmatory sampling of underlying marine clay sediments in Boat Harbour is required prior to remediation.

Baseline monitoring using multiple reference sites is crucial to establish background conditions and for comparing contaminated sediment sites to pre- and post-remediation (Walker 2014). Hoffman et al. (2017a) indicated that few studies have assessed Fergusons Pond or comparable reference sites in any detail (JWEL 1997; 2001) but warrants further study for comparison. Because of the extent and magnitude of PCDD/F TEQ concentrations in Boat Harbour sediments and potential ecological and human health effects associated with PCDD/Fs (Svensson et al. 1991, 1993; Hites 2011; Richman et al. 2016), treatment of all sediments and an ecological risk assessment across different media and trophic levels in the area is recommended. Sediment and water quality along with biota (lobster, rock crab and mussel tissue chemistry) in the Northumberland Strait is required to understand potential ecological risks associated with contaminated sediments transported from Boat Harbour (Walker et al. 2013d; Walker and MacAskill 2014; Roach and Walker 2017). According to Hoffman et al. 2017a, follow up studies beyond the physical boundaries of Boat Harbour prior to and post remediation are also recommended with several studies already completed or underway. These ongoing and future studies will allow local PLFN community members, engineers and environmental managers to

document this unique Canadian cleanup and remediation of this impacted wastewater treatment lagoon, as it is restored to a tidal estuary for future use by the PLFN.

2.4 Conclusions

Previous pulp mill (from 1967 to present) and chlor-alkali (from 1971 to 1992) effluent discharge into Boat Harbour has deposited large quantities of unconsolidated sediment requiring remediation. Despite wide variation in sampling techniques, PCDD/F sediment concentrations consistently exceeded highest effect thresholds for CCME SQGs, posing ecological risk, making them the main contaminant of concern. Conversely, total PAH concentrations showed wide temporal variation between 1992-2015, apparently peaking between 1998-2000, but did not exceed severe effect thresholds. However, some individual PAH compounds (anthracene, fluoranthene, fluorene, phenanthrene, pyrene) frequently exceeded low effect thresholds. PAH diagnostic ratios suggest pyrogenic PAH sources (wood/coal combustion), are the primary source of PAH loadings. Review of secondary data revealed gaps in sediment characteristics (vertical and spatial coverage). The Mi'kmaq PLFN communities desire to return Boat Harbour to a pre-mill tidal estuary supported by the Boat Harbour Act requires remediation of sediments to concentrations comparable to local baseline conditions or below low effect levels. The following studies are recommended: (i) detailed sediment sampling in and around Boat Harbour including vertical and horizontal delineation of contaminants; (ii) establishment of local baseline concentrations for a suite of organic and inorganic contaminants, which should also be complimented by discussions with local knowledge holders to elucidate pre-1967 conditions within Boat Harbour; and (iii) additional sampling of organic and inorganic contaminants, particularly PCDD/Fs, in up-gradient and down-gradient receiving environments to better characterize these sediments prior to remediation.

CHAPTER 3: CHARACTERIZING SEDIMENT PHYSICAL PROPERTY VARIABILITY FOR BENCH SCALE DEWATERING PURPOSES

Abstract[2]

A field sampling program was undertaken to assess the variability of physical characteristics of contaminated sediments in a large (160 ha) effluent stabilization lagoon. The objective of this paper is to use this "field lab" as a basis for comparing different sampling techniques (i.e. discrete and composite) for remediation-based evaluations (i.e. sediment volume estimates and bench scale dewatering studies). The distribution of sediment thickness measured throughout the lagoon by gravity core sampling is presented for context. Selected gravity core sediment samples are evaluated with respect to physical property (water/solids content, bulk density, and particle size) variability in both the vertical (i.e. within a single gravity core) and spatial directions (among gravity cores). Composite samples created via homogenization of a single entire gravity core is performed to compare to the discrete and average physical properties of a nearby gravity core. Vacuum-based samples are also compared to gravity core samples in terms of particle size. It is demonstrated that by understanding sediment variability, composite samples can be shown to be an efficient method of obtaining representative samples. When large samples for dewatering trials are required, vacuum sampling can produce samples with similar mean particles size to discrete and composite samples.

[2] Note: A version of this chapter is published in Environmental Geotechnics.

Alimohammadi, M., Tackley, H. A., Holmes, B., Davidson, K., Lake, C. B., Spooner, I. S., Jamieson, R. C., & Walker, T. R. (2020). Characterizing Sediment Physical Property Variability for Bench Scale Dewatering Purposes. Environmental Geotechnics

3.1 Introduction

The Boat Harbour Stabilization Lagoon (BHSL) is part of an industrial wastewater treatment facility (160 ha in plan area, Tackley, 2019) located in Pictou County, Nova Scotia, Canada. This lagoon was originally a tidal estuary until it was separated from the Atlantic Ocean (i.e. Northumberland Strait) via modifications introduced by the provincial government in 1967 (Hoffman et al., 2019). These modifications were completed in order to transition the estuary into a wastewater treatment facility for predominately pulp and paper process effluent, although other industrial operations are also known to have contributed to the wastewater effluent since 1967 (Hoffman et al., 2019). During operation, up to 75,000 m^3 of wastewater was discharged to the treatment facility daily (GHD, 2018). Over 50 years of operation have resulted in the accumulation of a thin layer of organic-rich, black sediment in the BHSL (GHD, 2018). This black sediment, which is underlain by a native grey marine sediment, contains a mix of inorganic and organic contaminants (i.e. metal[loid]s, polycyclic aromatic hydrocarbons [PAHs], dioxins and furans) present above regulatory limits (Hoffman et al., 2017; Hoffman et al., 2019). BHSL has been effectively closed since January 2020; remediation to its pre-industrial state is underway (i.e. a tidally influenced estuary). It is anticipated that dredging of the BHSL will result in the dewatering of greater than 577,000 m^3 of unconsolidated sediment followed by storage in a secure containment cell (GHD, 2018). This site serves as an opportunity to compare different sediment sampling methodologies for remediation purposes, such as those explored in this paper.

Given that sediment properties are site and location specific, it is critical before establishing a dewatering/remediation approach that effective sampling protocols be developed to ensure representative samples are obtained. This is true for bench scale dewatering trials as well as estimating required volumes for future sediment containment structures. Sediment characteristics such as solids content, particle size distribution, and density must be established to prepare a basis for an effective sediment management plan (Reis et al., 2007). Past studies have also identified the need for assessing sediment properties prior to remediation efforts (e.g. Mao, 1997; Ya, 2017) as physical and chemical properties of sediment deposits in aquatic ecosystems may vary spatially (Reis et al., 2007).

Understanding the variability in sediment composition is particularly important when considering bench scale dewatering studies and sediment volume estimations, as these studies often require the use of large sample volumes from a given depth and location to represent the contaminated sediment throughout a large sampling area. The BHSL is an excellent "field lab" to assess how different sampling methods influence the determination of sediment physical characteristics; the large areal extent and potentially highly variable characteristics with depth at BHSL are typical of other contaminated waste ponds. The objectives of this paper are: 1) to present a method of comparing time-consuming discrete sampling techniques to more time-efficient composite sample techniques. This is particularly relevant for volume estimates of contaminated sediments, and, 2) to present a method of comparing composite sampling techniques to a vacuum sampling technique developed for this project. The vacuum sampling method produces large volumes of sediment for bench scale dewatering purposes but involves significant physical disturbance of the sample. To investigate these objectives, the distribution of sediment thickness measured throughout the lagoon by gravity core sampling is presented; extrusion of these gravity core samples are then performed to evaluate sediment physical properties in both the vertical (i.e. within a single gravity core) and spatial directions (between gravity cores) and provide context for the sediment's variability. Composite samples are created by homogenization of single entire gravity cores to compare to the discrete subsamples and average discrete subsample physical properties (i.e. water/solids content, bulk density, and particle size) of a nearby gravity core and also provide some comparison to vacuum samples. Vacuum-based samples are compared to gravity core samples (both discrete and composite) in terms of particle size (i.e. a key physical parameter for dewatering).

3.2 Experimental Work

3.2.1 Sediment Sampling

Figure 3.1 shows sampling locations (i.e. gravity core and vacuum samples) throughout the BHSL, taken over a four-year period (i.e. 2016-2019). Area A was isolated from the remainder of the BHSL in March 2017 by an earthen berm (shown in Figure 3.1) for pilot dewatering studies (GHD, 2018). The rest of the lagoon, which was receiving effluent at

the time of sampling, has been subdivided into three regions (Area B, C, and D) in this study to assess the variability of sediment characteristics throughout the BHSL.

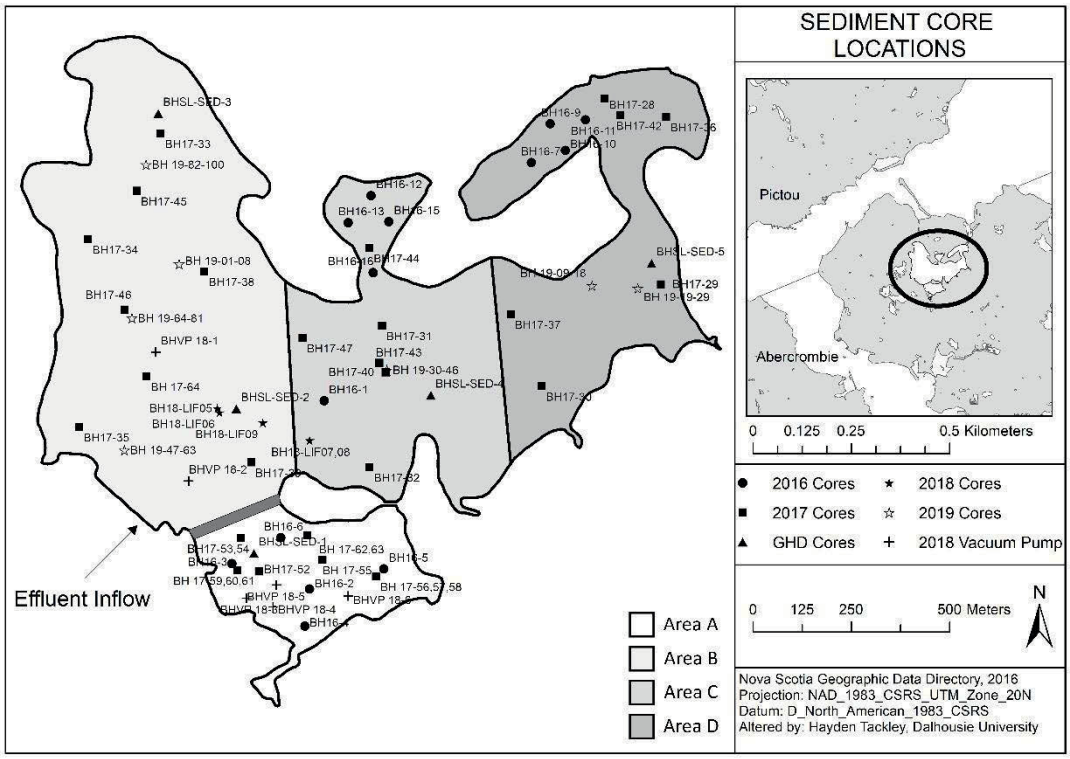

Figure 3.1 Spatial coverage of sediment sampling locations in Boat Harbour ("BH 19" symbols identify multiple samples taken within a 1 m distance from each other at a specific location).

The majority of samples (151 cores in total) were obtained using a gravity corer (60 cm in length and 6.5 cm in diameter) (Glew et al., 2001). The device was ideal for this site, as much of the contaminated sediment was shallower than the core length. This coring method has been shown to be reliable for taking core samples sufficient for precise paleolimnology work (Dunnington et al., 2017). The device consisted of a collar, which secured the core barrel, and a spring release mechanism. The weight of the device, when secured to the core barrel, allowed it to easily penetrate the sediment (see Figure A6). During the core penetration, the top of the core barrel remained open until a weighted messenger was lowered to trigger the device. At this time, the spring mechanism was activated, and suction

was maintained in the core barrel with a rubber stopper until the sample was brought to the surface. Upon recovery, the sample was then sealed at each end for transport. The method is simple, inexpensive, and does not require supplementary mechanical assistance (i.e. a winch).

151 cores were used for thickness determination to assess variability throughout BHSL. A spatial analysis of the thickness distribution in the BHSL was conducted using the ArcGIS (10.5) "Topo to Raster" interpolation method for "lake polygons". This method is specifically designed to analyze contour and elevation inputs (Esri, 2019) and can be constrained to the limit of a given polygon (BHSL in this case). The interpolation used a 1 m x 1 m cell length (resolution), with contour lines representing each 5 cm change in thickness. The map presents a realistic interpretation of the sediment thickness, based on the data which was available at the time of publication (additional data points may alter this interpolation). This information is presented to provide an indication of the distribution of sediment throughout the BSHL.

In addition, 30 of the 151 sediment cores were selected for detailed physical testing (i.e. beyond sediment thickness determination) and were transported to Dalhousie University laboratories for analysis. Nineteen (19) of these cores were used to obtain vertically discrete samples (described in detail below), and the remaining 11 were used for depth integrated composite samples. Variability in physical properties (i.e. particle size, water / solids content) at different depths (vertically) were investigated using discrete vertical samples. Sample BH 19-01 was selected for discrete particle size analyses. To obtain these discrete samples, sediment in the core was sampled at 5cm intervals using an extruder (Glew et al., 2001). As can be seen in Figure A7, the extruder apparatus consisted of an aluminum rod (shaft) connected to a base and situated vertically. An extruding disk that was slightly smaller than the core barrel diameter was placed at the top of the rod. A core holder (collar) was situated below the extruding disk, which allowed for an accurate and controlled descent of the core barrel. After carefully removing the rubber stopper at the bottom of core barrel, the core barrel was mounted on top of the extruding disk. The top rubber stopper was then removed from the core barrel and a sampling stage was attached to the top of the barrel. The core barrel was moved downward to remove the top water until

the top of the sediment was even with the sampling stage. A series of spacer plates (5cm aluminum cuboids) were placed on the adjuster disc, which was situated on the shaft, below the collar. The adjuster disc was carefully moved upward until the top of the aluminum cubes touched the bottom of the core holder, then was secured in place. At this time, one of the aluminum cuboids was removed, and the core barrel gently pulled downward to extrude 5 cm of sediment from the barrel. Each extruded sample was then removed from the sampling stage into pre-labeled sample bags (showing core ID, depth, and date), weighed, and refrigerated at 4°C until further analysis. Although each increment was 5 cm, smaller increments were used to section the 5 cm increment near the black / grey sediment interface. After weighing each 5 cm sediment interval, the center portion of each interval was isolated for further analysis, while the surrounding sediment was trimmed and discarded to avoid portions which may have been smeared due to the sampling tube penetration.

In addition to discrete samples, 11 individual cores were homogenized to create a composite sample that simulates the mixing of the sediment that will occur during a dredging process. Composite samples were also used to compare to sediment properties at each discrete sampling location (spatially) throughout the BHSL. For each composite sample, the total thickness of sediment in one core was mixed, weighed, and then stored in sterile containers at 4°C. At the time of analysis of the composite specimens, sediments in the container were mixed thoroughly, homogenized, and a representative sample from each composite sample was selected for water / solids content, and particle size analyses. All 11 composite samples were then evaluated for mean and variation range values of each of these physical properties.

A vacuum sampling method was used to simulate sediment sampling conditions which could arise during a dredging procedure. A barge of 4.5 m × 2 m was constructed from high density polyethylene (HDPE) pipe (sealed) to form the support for the wooden platform decking. The barge and sampling gear were then towed by a boat to the desired sampling location. Anchors were used to fix barge in position while sampling was performed. A gas-powered generator was used to power an electric submersible vacuum pump (560-watt stainless steel sewage pump), which in turn was used to recover the

sediment. The pump was hand-lowered into the water, to the surface of the sediment, via a rope secured to the pump. Upon engagement of the pump, the sediment was drawn through a 50 mm diameter tube, 3 m in length, to the surface of the barge and placed in a 20L container (see Figure A8). The pump was situated at various locations on the basin bottom in order to obtain eight 20 L containers of the sediment, which were then transported to Dalhousie University in Halifax, Canada for characterization tests. Vacuum sampling results in a significantly disturbed sample with added water being entrained in the vacuum process.

3.2.2 Physical Analysis

Physical characteristics of the black sediment were evaluated at Dalhousie University laboratories. The water / solids content (relevant ASTM standard D2216, last revised 2019), bulk density, specific gravity (ASTM D854, 2014), organic material (ASTM D2974, 2020), and particle size were measured for selected samples (i.e. discrete and composite cores). Each measurement was repeated three times for all experiments. Water / solids content and density measurements are important for remediation projects utilizing containment approaches for volume estimates of remediation projects while particle size analyses are useful when developing dewatering approaches. Specific gravity and organic carbon determinations were used for characterization purposes only.

Particle size distributions of the sediment were evaluated using a micro flow imaging technique (MFI-DPA4100/4200-Series B) (Mackie, 2010), which counts particle sizes from 2 to 400 μm. In this technique, 1 ml of sample fluid (1% dilution by volume was used for all of the samples in this study) was captured in successive image frames as the sample stream passed through a flow cell. Frame images displayed during operation provided immediate visual feedback on the nature of the particle population in the sample. Images were also digitally analyzed using the software to compile a database containing count, size, and concentration, and to produce parameter distributions using histograms and scatter plots (Sharma et al., 2010).

3.2.3 Statistical Analysis

A statistical analysis was performed for the physical test date collected. The mean physical properties obtained for discrete, composite, vacuum samples as well as area groupings were compared using Tukey's comparison test of one-way analysis of variance (ANOVA) in Minitab. ANOVA is used to determine whether the mean of two or more groups differ, and Tukey's method is used to formally test whether the difference between a pair of groups is statistically significant. Tukey's method also provides a range of values showing the confidence interval for the difference between the means for each pair of groups. If this range does not include zero, it means that the difference between these means is significant (Minitab express support, 2019).

3.3 Results and Discussion

As previously mentioned, the black sediment layer in the BHSL consisted mostly of solids accumulated from predominantly pulp and paper treated wastewater since the 1960s. Results from organic material testing showed the solid portion of black sediment contained 25% - 31% organic carbon with a specific gravity of 1.71 (± 0.13 SD).

For context of the distribution of sediment thickness throughout the BHSL, Figure 3.2 presents the frequency distribution of black sediment thicknesses measured in the 151 gravity core samples. For example, a 35 cm thickness of black sediment was measured in 16 samples. An average thickness of 26.6 cm (±12.2 SD) was measured in black sediment. The maximum thickness of approximately 45 cm for the black sediment was identified in core samples of BH 17-34, BH 17-33, and BH 19-82-100.

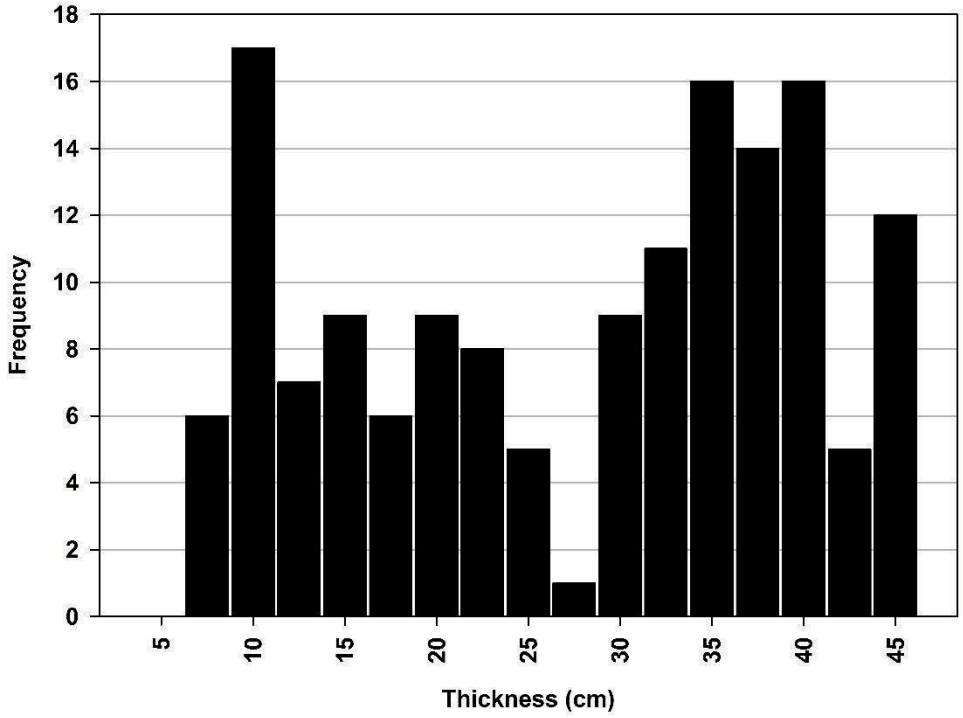

Figure 3.2 Histogram of black sediment thickness for 151 gravity cores.

A contour map of the spatial distribution of sediment thickness determined using the methods previously described is presented in Figure 3.3. The results show the black sediment was not evenly distributed across the BHSL; sediment thickness is greatest in Area B (west side of BHSL, near the location of cores BH 17-34 and BH 17-33). A bathymetric survey indicates that this location is the deepest part of the basin (Spooner and Dunnington 2016). The thicker sediment in this location is likely due to its proximity to the effluent inflow point (Figure 3.3), and with increasing distance from that point (notably in Areas C and D), the thickness decreases.

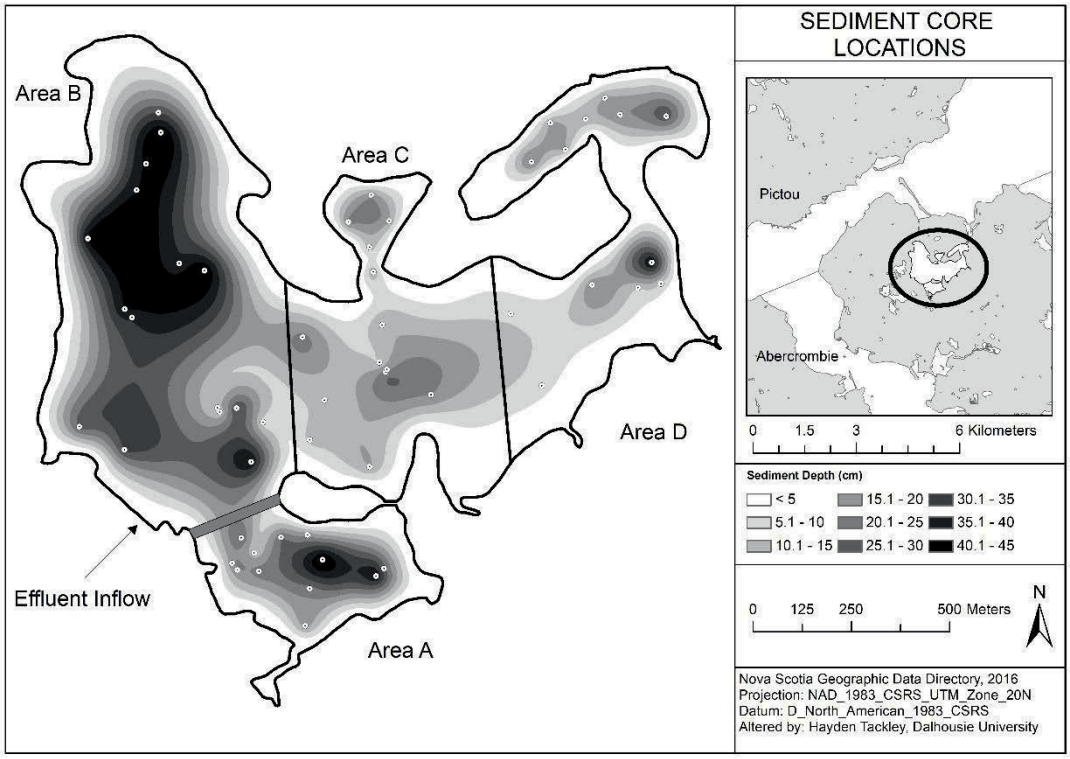

Figure 3.3 Isopach map of black sediment thickness based on 151 samples presented in this study.

To examine the influence of this varying distribution of sediment on its physical properties, Figure 3.4 shows both water and solids content, versus depth for the 19 discrete gravity core samples. Results are plotted relative to distance from the black / grey interface (dotted line). Due the large amount of data (shown in Figure A9), data has been presented in term of mean and one standard deviation from the mean for each depth. The focus of this study was the black sediment characterization, however, grey sediment properties (water / solids content) were also evaluated in selected cores and are shown for reference. Results show that discrete samples, regardless of location, show a similar water / solids content trend. As expected, water content decreased with depth (Figure 3.4), as self-weight consolidation of settled particles occurred. In this study, the black sediment exhibited high water contents (max 3200%) near the surface (0-5 cm) which decreased to around 500% at the black / grey sediment interface.

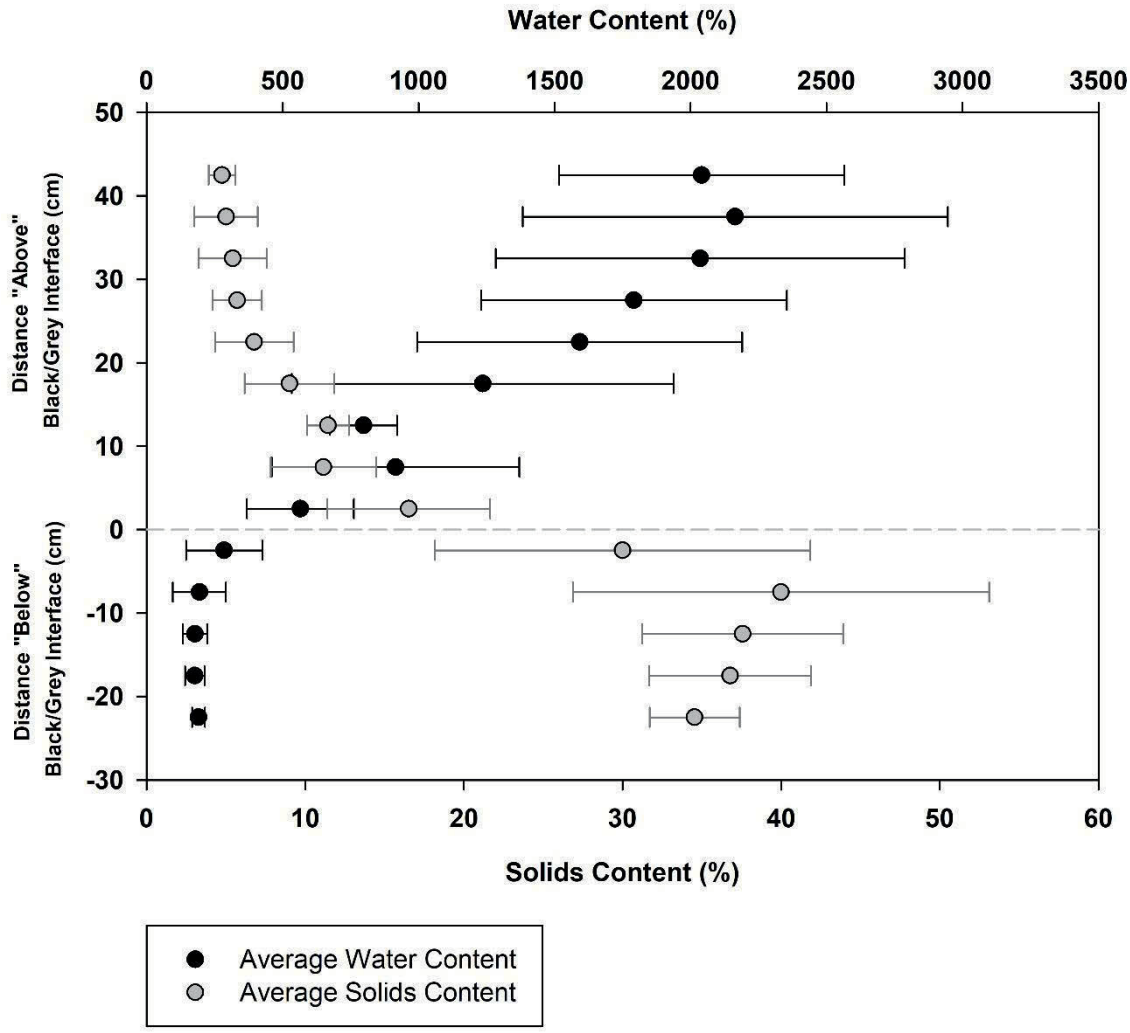

Figure 3.4 Water and solid contents at various depths taken via discrete sampling of selected cores (dashed grey line shows interface between black and grey sediments, distances expressed from this interface). The symbols represent the mean values, the error bars represent one standard deviation from the mean.

Water /solid content and density are key parameters to understand for remediation projects involving containment cells of dredged sediments. The self-weight consolidation process also resulted in the solids content increasing with depth from an average of 2% at the water / black sediment interface to around 12% at the black / grey sediment interface (Figure A9b). Likewise, the density of the black sediment increased with depth, increasing from 1.01 g/cm^3 near the surface (0-5cm) to 1.17 g/cm^3 at 45 cm below the black sediment-water contact (as presented in Table 3.1 and Figure A10). The density of composite samples, however, was 1.07 g/cm^3, which was close to the average density of discrete samples (1.10 g/cm^3).

Table 3.1 Density values of discrete and composite samples.

Depth (cm)	Density (g/cm^3) Mean + SD
0-5	1.01 ± 0.13
5-10	1.06 ± 0.03
10-15	1.08 ± 0.04
15-20	1.07 ± 0.04
20-25	1.18 ± 0.21
25-30	1.13 ± 0.08
30-35	1.10 ± 0.02
35-40	1.11 ± 0.02
40-45	1.17 ± 0.07
Average of discrete samples	1.10 ± 0.05
Composite samples	1.07 ± 0.05

Box-whisker plots (Figure 3.5a & 3.5b) present the range of water / solids content of black sediments for the cores used to create discrete and composite samples, as well as samples taken using the vacuum pump. For individual discrete samples, the plot represents data taken vertically in the core, while for composite samples, the plot represents the data analysis of a combination of all composite samples. For comparison, the data analysis of all discrete samples for each of the four areas (A, B, C, and D) are also shown. The box-whisker plot is a standard technique for presenting a 5-number summary of a dataset which consists of the minimum and maximum range values, the upper and lower quartiles, and the median (the line that divides the box into two parts). In the box plot, an outlier is an observation that is numerically distant from the rest of the data and is defined as a data point that is located outside the whiskers of the box plot. This collection of values is an effective way to summarize the distribution of a dataset (Williamson et al., 1989). In Figure 3.5, boxes with the same pattern show the cores taken from the same area, while grey colored boxes represent the data analysis for the collection of discrete samples from the given area. The solid black boxes represent the vacuum samples taken from Area A and B, and the solid white box shows the dataset of composite samples.

One-way ANOVA test results (using the Tukey method with 95% confidence) indicated that there was no significant difference between water / solids content of different cores representing discrete samples throughout the BHSL. In this study, Tukey's results are

shown with the letters on the graphs. In Figure 3.5, samples attributed with identical letters are not significantly different.

As presented in Figure 3.5, an average water content and solids content of 957% and 9% respectively was obtained for the composite samples (over the entire depth of black sediment in a given core). These values are statistically similar to the average water / solids content of discrete samples, suggesting that composite sampling can be an acceptable method of identifying the properties of discrete samples for this site. This result is important for sediment volume estimates, as composite samples can yield higher volumes and are more readily gathered when compared to discrete samples; as a result composite samples were used for other dewatering studies by the authors (e.g. Alimohammadi et al. 2019). The locations from which the gravity core samples were taken were thought to effectively represent the entire basin. Average percent water content (corresponding solids contents are shown in brackets) were measured for Areas A, B, C, and D respectively, as follows: 1052%(11.5%), 1150%(10.3%), 1188%(8.9%), and 1153%(11.9%).Statistical analysis of this data showed no significant difference between discrete, composite or area samples. These results suggest that all black sediment samples are consistent in terms of water / solids content despite the location from which they were taken. It can be concluded that this sediment maintained spatial consistency throughout the BHSL (spatial direction), and therefore sediment gathered through composite sampling should be representative of the average found throughout the basin.

The solids contents obtained from Area A and B (sampling locations are shown in Figure 3.1) using the vacuum sampling technique were 0.5% and 2.8%, respectively. The solids content of vacuum samples was significantly lower than that obtained by gravity coring (discrete and composite), because of water mixing with the sediments during the procedure (Figure 3.5b). Even though the same sampling procedure was used for both Areas A and B, a lower water content and a higher solids content was measured in Area B, which can be explained by the fact that thickness of black sediment is greater at the location of sampling in Area B, allowing the intake to be more immersed in the sediment at the time of sampling. This confirms that water / solids content measurements are not comparable to gravity core methods due to the high level of disturbance in the samples.

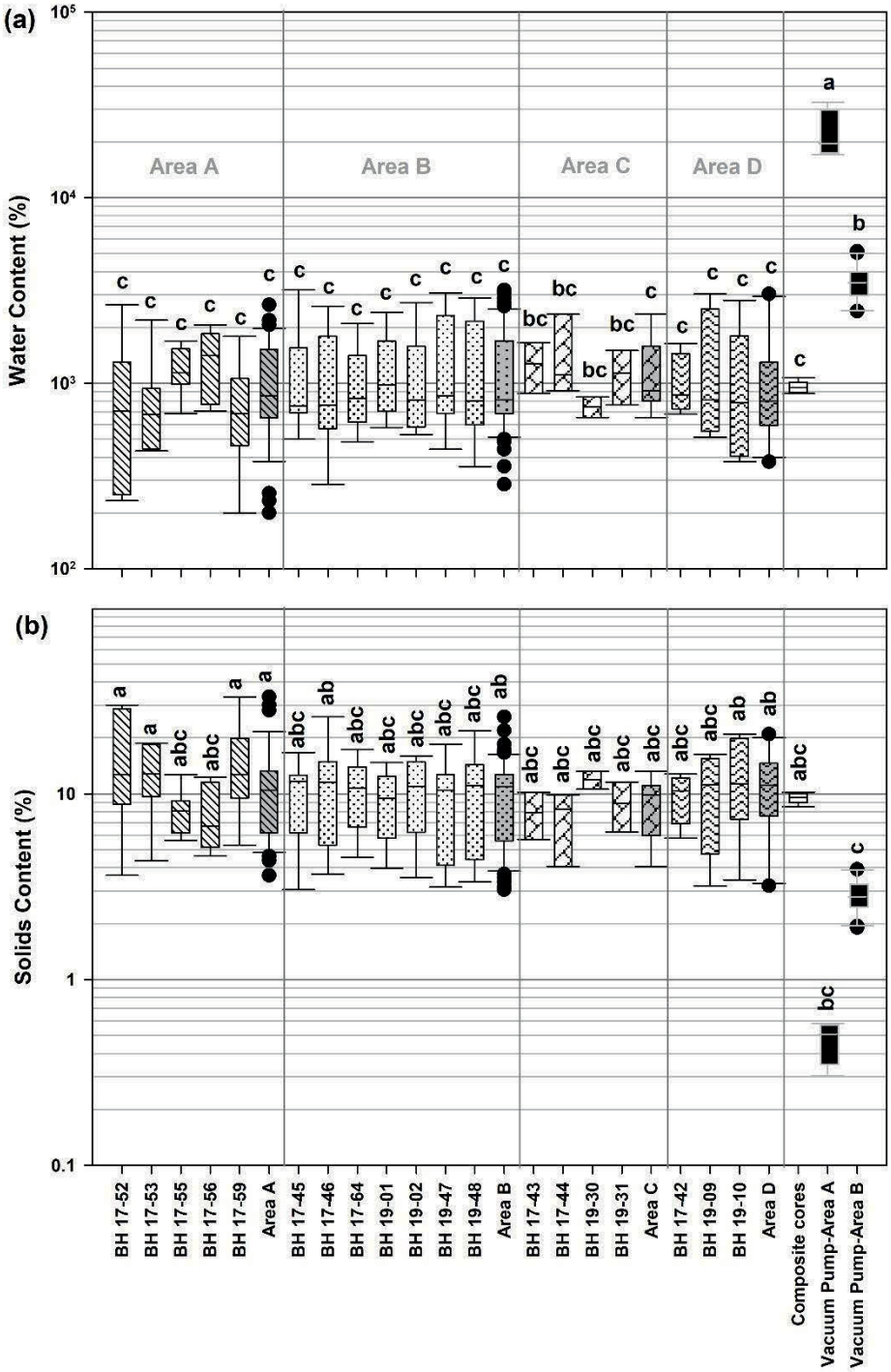

Figure 3.5 (a) Water and (b) solids content variation of black sediment in discrete and bulk samples. Samples labelled with identical letters (i.e. a, b, or c,) were not significantly different from each other (p <0.05 level). Samples labelled with different letters are significantly different from each other (p<0.05 level). Vertical lines denote areas from which samples were obtained (i.e. Area A, B, C or D).

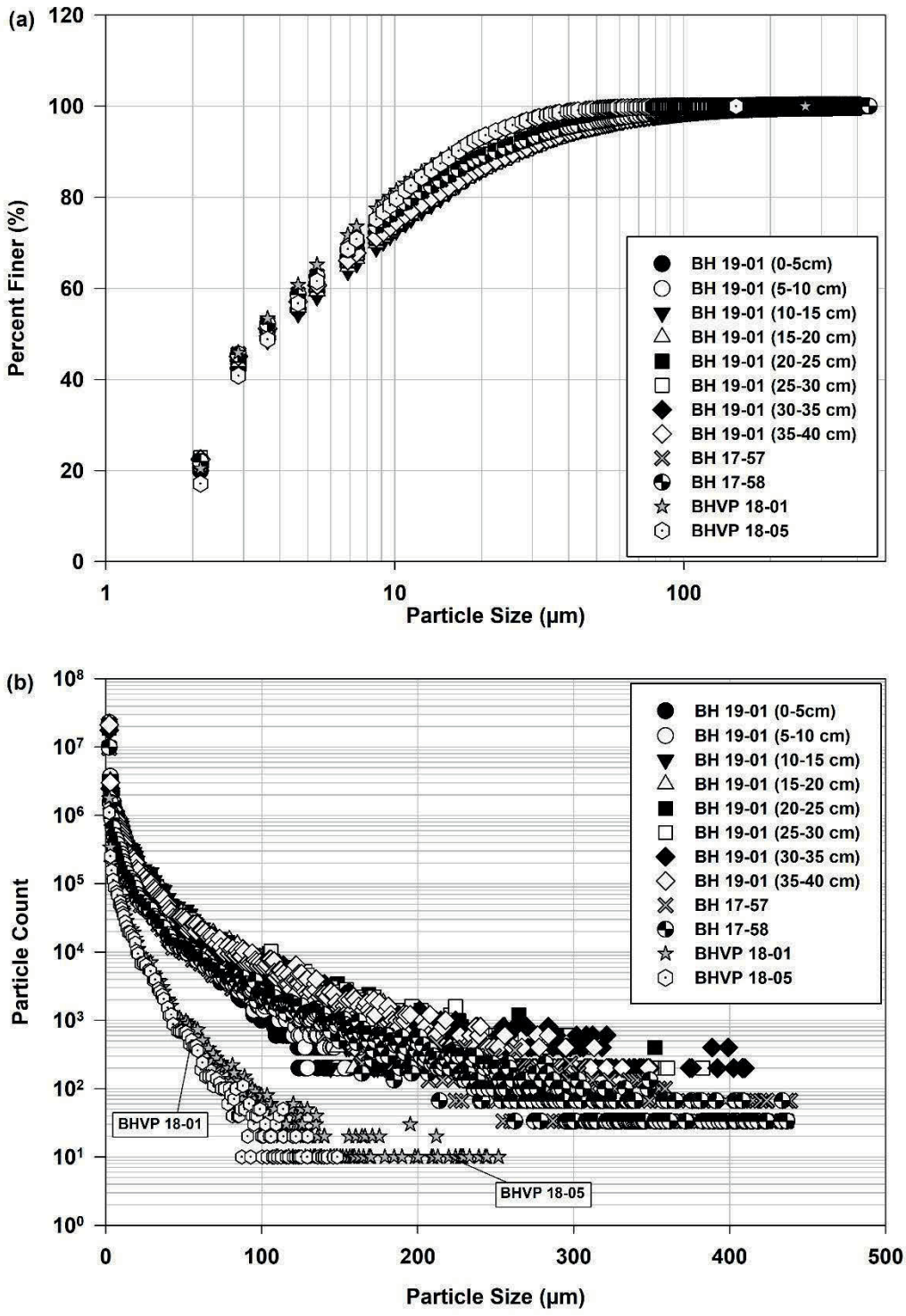

Figure 3.6 (a) Particle size, and (b) count distribution of discrete samples of (BH 19-01), composite core samples of (BH17-57 and BH17-58), and Vacuum samples of (BHVP 18-01 and BHVP 18-05)

Particle size distributions of discrete sample BH 19-01 and vacuum sample BHVP 18-01 (taken from Area B), two composite samples BH17-57, BH17-58, and vacuum sample of BHVP 18-05 (taken from Area A) are presented in Figure 3.6a. Results show that the black sediment had a similar particle size distribution at various depths and locations, regardless of the sampling method. The results (Figure 3.6a) indicate that 85% of sediment particles (discrete or composite) are finer than 11 μm (D_{85} = 11 μm). However, a D_{85} value of vacuum sampling was slightly less than 11 μm as shown in this figure, indicating that sediment particles obtained by vacuum sampling were slightly finer compared to coring samples. The majority (>80%) of particles (~10^7) range between 2 μm-10 μm, in the case of gravity coring (Figure 3.6b). As the particle size increased from 10 μm to 100 μm, the number of particles decreased from ~10^6 to ~2×10^3. When obtained by vacuum sampling, however, the black sediment contains fewer particles at each certain size compared to sampling by gravity coring. For instance, the number of particles at 100 μm and 200 μm is 100 and 10, respectively, in BHVP samples, while results show almost 20 times more in coring samples (discrete and composite). These findings show that sediment / water mixing during the vacuum sampling results in dilution (a decrease in the number of particles), and perhaps a reduction in aggregation of particles during the process.

Geotextile dewatering is one feasible option for recovering and processing these sediments prior to containment based on studies related to developing remediation options for the BHSL (GHD, 2018). An understanding of particle size becomes important as it influences dewatering. Figure 3.7 compares the range of average (mean) size of the black sediment particles at different depths to that of the composite and vacuum samples. The average particles size ranged between approximately 6 μm and 12 μm. One-way ANOVA test (Tukey method) results indicate that there was no significant difference in particle size at various depths. Tukey's results are shown with the letters on the graph 3.7, and samples attributed with identical letters are not significantly different.

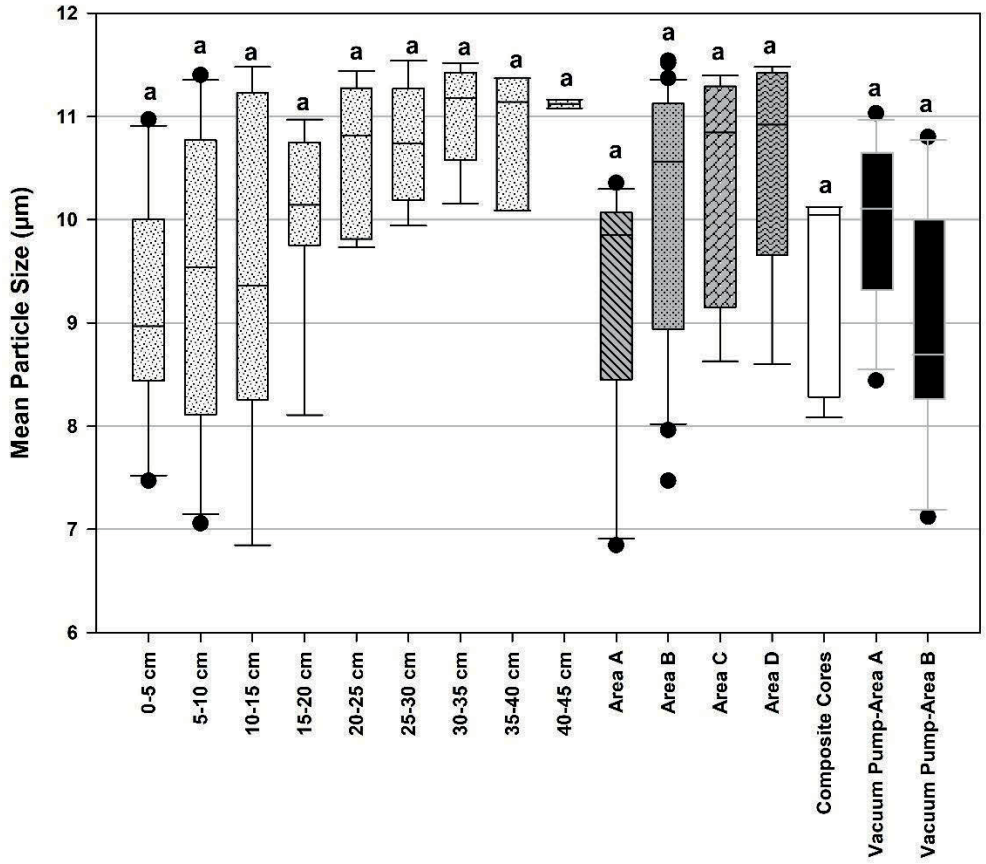

Figure 3.7 Variation in mean particle size versus depth and location. Samples labelled with identical letters (i.e. a) were not significantly different from each other ($p < 0.05$ level).

In addition, the average particle size of composite samples was statistically similar to discrete samples at various depths, and at different locations in the BHSL (9.3 µm, 10.0 µm, 10.4 µm, and 10.5 µm for Area A, B, C, and D respectively). The vacuum sampling method resulted in similar particle sizes distribution (slightly larger for Area A (9.9 µm) and finer for Area B (8.9 µm)) to other composite and discrete samples, indicating that sediments throughout the BHSL are consistent in terms of particle size.

3.4 Conclusions

This paper presents results of a field sampling program performed to assess the impact of various sampling methods (i.e. discrete versus composite versus vacuum) on the physical characteristics of contaminated sediments obtained from a large effluent stabilization

lagoon. The overall objective of this paper was to use this "field lab" as the basis for assessing how different sampling techniques can be relied upon for representative samples for remediation-based evaluations (i.e. sediment volume estimates and bench scale dewatering studies). A method of comparing time-consuming discrete sampling techniques to more time-efficient composite sample techniques was presented as well as a method of comparing composite sampling techniques to a vacuum sampling technique developed for this project.

The distribution of sediment thickness measured throughout the lagoon by gravity core sampling was shown to vary substantially throughout the 160 ha site. Extrusions of these gravity core samples to obtain discrete and composite samples indicate that there was no significant difference between physical characteristics (water / solids content, density, particle size) of composite samples taken from different areas within the BHSL when compared to discrete samples. For this particular site, it appears that composite sampling would provide reasonable physical parameters when compared to more time-consuming discrete sampling methods (i.e. should reflect the overall physical characteristics of the black sediment throughout the basin for practical purposes).

The physical characteristics of vacuum-obtained samples were compared to gravity core samples (both discrete and composite). This sampling method resulted in more water entrained in the samples, lower solids content (~0.5–2.8%) and slightly finer particles in the samples. However, the mean particle size for the vacuum sampling was not statistically different than that of discrete and composite samples.

The sampling evaluation process investigated in this study provides evidence that more expeditious methods can be used to characterize sediments over large-scale, both in spatial and stratigraphic extent. The results may also provide guidance on how to choose sampling techniques for obtaining representative samples for aquatic sediment projects.

3.5 Acknowledgements

The authors wish to acknowledge the financial support of Nova Scotia Lands and Government of Nova Scotia. Partial funding was also provided by NSERC (RGPIN-2018-

04049) awarded to Dr. Lake. The authors thank the reviewers of this paper for the thoughtful and constructive comments which improved the overall focus and readability of the paper.

CHAPTER 4: EFFECT OF DIFFERENT SEDIMENT DEWATERING TECHNIQUES ON SUBSEQUENT PARTICLE SIZES IN INDUSTRIAL DERIVED EFFLUENT

Abstract[3]

A paucity of literature has compared geotextile dewatering methods to more conventional dewatering methods (i.e. centrifuge, sedimentation) in the context of how geotextile dewatering performs at reducing particulate matter in dewatering effluent. Particulate matter is the primary source of inorganic and organic contaminants (i.e. dioxins and furans) in an unconsolidated sediment (estimated 577,000 m^3) that has accumulated in a wastewater stabilization basin in Nova Scotia, Canada. Physical and chemical properties of contaminated sediment were initially characterized, and subsequent laboratory experiments were carried out for three common dewatering methods: sedimentation, centrifugation, and geotextile filtration. Filtrate quality of suspended solids (number, particle size distribution of particles) was examined for differences based on three dewatering techniques assessed. All three methods provided effective removal of particulate matter during dewatering, but geotextile dewatering could be a more cost-effective and practical solution for dewatering of these sediments.

[3] Note: A version of this chapter is published in Canadian Journal of Civil Engineering.

Alimohammadi, M., Tackley, H. A., Lake, C. B., Spooner, I. S., Walker, T. R., Jamieson, R. C., Gan, C., Bossy, K. (2020). Effect of different sediment dewatering techniques on subsequent particle sizes in industrial derived effluent. Canadian Journal of Civil Engineering, 191(9):590.

4.1 Introduction

The Boat Harbour Treatment Facility (BHTF) in Pictou County, Nova Scotia, Canada was constructed in the 1960s by damming a 140-hectare former tidal estuary to receive industrial wastewater from various facilities (Ogden III 1972). A description of the facility is provided by Hoffman et al. (2017). The facility is slated for closure in 2020 and a remediation project of the estimated 577,000 m^3 of contaminated sediments (i.e. metal[loid]s, polycyclic aromatic hydrocarbons [PAHs], and dioxins and furans) will commence (GHD 2018a). The current estimated cost of this remediation project is $217 million (CAD) (CBC News 2019) with the goal to return Boat Harbour (BH) to its previous ecological form (i.e. restore to a tidal estuary). Physical characteristics of BH contaminated sediment suggests that dredging, dewatering and subsequent disposal/treatment processes will be required for remediation (GHD 2018b). There is a need to understand and manage this type of contaminated sediment and water during the dewatering process, given that various contaminants, such as dioxins and furans, are present at concentrations exceeding regulatory guidelines (Hoffman et al. 2019).

A known risk of dioxin and furan mobilization in soil and water systems relates to transport via particulate matter, predominately organic matter (Mackay et al. 1992), due to their low solubility and high partitioning coefficients to organic matter. In this paper, "particulate matter" will refer to particles ranging from 0.45 μm to 80 μm and which are composed of suspended and colloidal material (Faust and Aly 1999). The presence of dioxins and furans in organic-rich sediments can pose challenges during dewatering projects, resulting in increased costs for water treatment processes. For dewatering remediation applications involving metal and hydrocarbon contaminated sediments, concentrations of contaminant discharge permitted during dewatering operations via particulate matter is relatively low (i.e. in the order of μg/g) while for dioxins and furans, regulatory standards are up to six orders of magnitude lower (van den Berg et al. 1998, CCME 2002). For this reason, when dewatering dioxin and furan contaminated sediment, concentrations of dioxin and furan transport via particulate matter in expelled water from sediments must be controlled and, if necessary, treated.

The use of geotextile bags for dewatering purposes and control of solids in the effluent is relatively new compared to sedimentation and centrifuge techniques of dewatering and has been shown by Fowler et al. (1997) to retain almost 100% of the fine-grained materials. Stephens et al. (2011) reported that 2,000,000 m^3 of dredged sediments in Brazil were successfully dewatered and contained by geotextile tubes in six months and achieved required effluent standards. In another successful project, 1,650,000 m^3 contaminated sediments of Onondaga Lake, in the State of New York were hydraulically dredged and transported to the sediment management area including ~1000 geotextile tubes (76,200 meters) for dewatering and containment (Parsons and Geosyntec. 2010). Even though researchers such as Rupakheti (2016), Segré (2013), and Satyamurthy (2008) have looked at water quality from geotextile tubes, there is a paucity of literature that has compared geotextile dewatering to more conventional dewatering methods (i.e. centrifuge, sedimentation) in the context of how geotextile dewatering will perform at reducing particulate matter in the dewatering effluent. Few studies have investigated small scale centrifuges for dewatering testing (e.g., Segré 2013, Khachan et al. 2017). As discussed by Mori et al. (2002), by monitoring particulate matter in the dewatering effluent, one a priori assesses the quality of dewatering effluent in terms of dioxins and furans. Mori et al. (2002) found that when particulate matter was sufficiently removed during geotextile dewatering, the dioxins and furans were essentially contained in the solids retained by the geotextile. Another study by Moo-Young et al. (1999) investigated the effluent quality from geotextile dewatering in terms of dioxin and furan concentrations, albeit at field scale and for limited conditions.

In this paper, the main objective was to investigate factors influencing size and quantity of particles obtained in dewatering filtrate of BH sediments. Initially, basic physical and chemical properties of the sediment were characterized to plan for dewatering tests. Laboratory experiments were then carried out for three common dewatering approaches: sedimentation, centrifugation, and filtration using a geotextile. Considering that dioxin and furan fate during dewatering is related to particulate matter in the sediment, filtrate quality (i.e. in terms of number, particle size distribution of particles) was examined for differences based on the three dewatering techniques assessed.

4.1.1 Study area

Sediment samples for this work were collected from BH at two locations. Location A is within an area of BH that has been isolated from the remainder of the stabilization basin via an earthen berm constructed in March 2017. Location M is within the main stabilization lagoon that was receiving effluent at the time of sampling. Although sediments were physically similar at these two locations, the water quality at these two locations at the time of sampling proved to be different. The isolation of location A has resulted in no effluent being supplied to the partitioned area since the time of construction (and sampling). The berm was created to prepare for a pilot dredging program carried out by the owners of the facility in late 2018/early 2019. As a result of this isolation, freshwater inputs to location A have resulted in lower salinity than location M (0.13 ppt vs. 0.68 ppt). Consequently, the two sampling locations represent two areas of potentially comparable sediment characteristics but different water quality conditions. Sediment samples (near surface) were taken at these two locations via a vacuum pump on a barge. The in-situ solids content of the sediment from Boat Harbour ranges from 2% at the surface to 10% at depth (average thickness of ~25 cm) (Alimohammadi et al. 2019). A solids content of 0.3% was obtained by this sampling method due to entrapment of basin water during sampling. Water samples were taken at these same locations.

4.2 Materials and Methods for Dewatering Tests

4.2.1 Water Quality Test Methods

Various water quality characterization tests were performed at the two sample locations; electrical conductivity, pH, and salinity testing was performed (see Table 4.1 for the various standard methods used). For dewatering testing described in this paper, total suspended solids of the filtrate/supernatant samples were analyzed using a HACH DR 5000 bench-top spectrophotometer (Hach Company 2014). Size distribution of the solids remaining in the supernatant/filtrate was evaluated using a micro flow imaging technique (MFI-DPA4100/4200-Series B) (Mackie 2010). With the exception of particle size analyses, these water quality measurements serve as useful benchmarks to compare to other dewatering studies.

Table 4.1 Summary of BH water and sediment characteristics.

	Unit	Sediment		Water		Reference
		Location A	Location M	Location A	Location M	
Solid content	%	0.3-1	2-4			ASTM D2216
Specific gravity		1.71	1.71	-	-	ASTM D854
Organic Matter	%	27-30	28.5-31.6	-	-	ASTM D2974
Zeta Potential	mV	-27	-28	-14	-24	APHA et al. (2005)
Cation Exchange Capacity (CEC)	Cmol/kg	95.8	62	-	-	ASTM D7503
Electrical conductivity	ms/cm	-	-	0.3	1.5	APHA et al. (2005)
pH		-	-	6.6	7.3	ASTM D4972
Salinity	Ppt	-	-	0.13	0.68	APHA et al. (2005)
Total suspended solids (TSS)	mg/L	-	-	9	25	Hach Company/Hach Lange GmbH (2014)
Total suspended solids (TSS) of sediment diluted to 0.3% solids content	mg/L	2650	3490	-	-	Hach Company/Hach Lange GmbH (2014)
D_{85}	μm	11	10.8	-	-	Mackie (2010)

4.2.2 Sediment Characteristics

For initial characterization of sediment used in the dewatering studies, the following tests were performed: solids content, specific gravity, organic matter, zeta potential, cation exchange capacity (CEC). Table 1 lists standard methods used for these tests.

Solids and water content of the filter cake/settled material after dewatering by geotextile, centrifuge, or sedimentation were measured according to ASTM D2216. Results presented in this study are the average of three measurements.

4.2.3 Jar Testing and Rapid Dewatering Test (RDT)

Application of various additives for use as a polymer/coagulant to enhance dewatering efficiency through flocculation/coagulation is typically performed via trial and error (i.e. type and dose). For this research, BH sediment samples taken from location A were sent to Bishop Water Technologies (Renfrew, Ontario, Canada) to investigate the effectiveness of

different polymer/coagulant doses. Hand mixing was used for the samples with different types and doses of polymers in glass jars. Based on these initial trials, an appropriate polymer (Solve 9244) was identified for further jar testing at the Centre for Water Resources Studies (CWRS) laboratory located at Dalhousie University. Solve 9244 is a cationic polymer, soluble in water, with density of 1.03 g/cm^3, boiling point of 103 °C, and melting point of < -15°C. For this study, the polymer was diluted with distilled water (i.e. "made down") to 0.5% concentration for use as recommended by the manufacturer.

At the time of sampling and testing, it was assumed that water quality differences between locations A and M would be minor and hence polymer doses were based on location A. However, this minor difference in water quality resulted in differing polymer performance between the two locations, as discussed later in the paper.

Table 4.2 Summary of polymer doses for each test.

Amount of polymer solution added (ml)	Polymer dose (ppm)	Jar test	RDT		Centrifuge		Sedimentation	
Sediment sample's location		A	A	M	A	M	A	M
0	0	×[4]	×	×	×	×	×	×
0.5	12.3	×						
1	24.6	×						
1.5	36.9	×						
2	49.5	×	×					
2.5	61.5	×	×					
3	73.8	×	×	×	×	×	×	×
3.5	86	×	×					
4	98.4	×	×					
4.5	110.7	×						
5	123	×						
5.5	135.3	×						
6	147.6	×						
Initial solids content		0.3%						
Amount of sediment sample		200 ml	200 ml		200 ml		5 litre	

For jar testing, sediment samples were diluted using the water from each location to a consistent solids content of 0.3% for jar testing. Jar testing was performed using a Phipps and Bird PB 700TM jar tester to establish an optimum polymer dose (ASTM 2035-13). A

[4] × denotes test performed at the given dose

set of 6 standard jars (500 ml glass beaker) and stirring mechanism was used to mix the sediment and the polymer additive. In each test, different polymer doses were added to 200 ml of sediment solution (Table 4.2) at 0.3% solids content, then stirred in the jars at a constant rate of 270 rpm (rapid mixing) for 1 min, followed by 50 rpm (slow mixing) for 10 min. This procedure was conducted to ensure thorough mixing. After mixing, the sediment was allowed to settle in the jars for 5 min. A 10 ml representative sample of supernatant from each jar was then taken using a pipette, from a depth of 2 to 3 cm from the top level of the treated sediment to measure total suspended solid (TSS). This sampling was repeated at 5, 30, and 60 min of settling time. These time intervals were based on visual observations in the laboratory related to rates of sedimentation. TSS was measured for all sediment/polymer combinations at each dosing increment.

A rapid dewatering test (RDT) (Tencate 2017) was then performed for the five polymer doses which exhibited the lowest TSS results and best visual evidence of flocculation (see Table 4.2). For comparison, untreated (i.e. no polymer) sediment was also subjected to RDT testing. The RDT apparatus consisted of a funnel (15 cm diameter) covered by a circular (15 cm diameter) geotextile fabric (GT500-Bishop). GT500 is polypropylene geotextile. Based on the data sheet provided by the manufacturer (Tencate 2015) the apparent opening size (AOS) of GT500 is 0.43 mm. The funnel was placed in a clean 250 ml Erlenmeyer flask to collect filtrate during the test. For each test, 200 ml of untreated or treated sediment was slowly poured into the RDT funnel. During the experiment, the volume of filtrate at cumulative times of 60 seconds and 60 min was measured to examine the dewatering rate. After 60 min, the geotextile fabric was removed from the funnel and the retained sediment was collected to measure the solid content of the remaining “filter cake”. Total suspended solids (TSS) measurements and particle size analysis were then conducted on the filtrate to determine the most efficient polymer dose. This polymer dose was then used for subsequent centrifuge and sedimentation tests as described below.

4.2.4 Laboratory Centrifuge Testing

Prior to each test, the optimum polymer dose (which was identified by jar and rapid dewatering tests) was added to 200 ml of BH sediments at 0.3% solids content and then

mixed using the method described for the jar test mixing procedure. For each test, 3 identical centrifuge tubes of polymer-sediment mixture (results were averaged), as well as one tube containing untreated sediment were used. Samples were then rotated in an IEC CENTRA GP8R temperature-controlled centrifuge at both 2500 rpm (1279 g) or 4500 rpm (4143 g) for 1 h to allow comparison of different centrifugal forces on the settling characteristics of sediment. The centrifuge was stopped at 5, 30, and 60 min time intervals during the course of the experiment to take 10 ml samples of the supernatant. This sample was then analyzed for TSS and particle size. Solids content of the retained sediment at the bottom of each tube was determined at the end of 60 min of centrifugation.

4.2.5 Sedimentation Testing

Two plexiglass cylinders (height of 92 cm and internal diameter of 9.2 cm) with five nozzles installed at different elevations relative to the bottom of the cylinder (nozzle 1 at 5 cm; nozzle 2 at 25 cm; nozzle 3 at 45 cm; nozzle 4 at 65 cm; nozzle 5 at 85 cm) were used to conduct sedimentation tests. For these tests, ~5 L (initial height of 80 cm) of homogeneous treated (i.e. prepared by adding the optimum polymer doses identified in the RDT and jar tests) sediment was placed in one cylinder and the untreated sediment placed in the other. Cylinders were then placed on a level surface and the sediment allowed to settle via gravity. Samples of 10 ml of supernatant was taken from sampling nozzles 2, 3, and 4 at predetermined time intervals (e.g. 15, 30, 60, 120 min). TSS and particle size were then measured using the same technique as RDT and centrifuge tests. Upon culmination of the test, overlying supernatant was removed via suction, to avoid disturbing sediment. Solids content of settled material was then measured.

4.3 Results and Discussion

For data presented in this section, results represent mean values of three measurements in which the coefficient of variation was <1 for each result presented.

4.3.1 Initial Sediment and Water Column Characterization

Several physical and chemical properties of BH sediments and water taken from two locations are presented in Table 4.1. Results listed in Table 4.1 show that the BH sediment

has similar zeta potential values of -27 mV for location A and -28 mV for the location M. As a result of the separation of location A from the rest of the basin by the construction of an embankment, the water column quality above the location A sediments varied from that of the location M (which is still being utilized as an active settling lagoon). TSS measurements performed on the water from both locations returned values of 9 and 25 mg/L for location A, and location M respectively. Several other parameters were also determined regarding the water, including the zeta potential, where a value of -14 mV was revealed for location A compared to -24 mV for location M. This is important given that dredging of the sediment will likely recover some of the water column, which could cause differences in flocculation trials if used for dilution purposes (Table 4.1). Location A also generated lower values for electrical conductivity (0.3 vs. 1.5 mV), pH (6.6 vs. 7.3), and salinity (0.13 vs. 0.68 ppt) compared to location M (as shown, respectively).

4.3.2 Jar and Rapid Dewatering Testing (RDT)

A preliminary dose range between 49.2 to 98.4 ppm of polymer solution, which corresponded to the lowest TSS range during jar testing, was selected to be examined for rapid dewatering testing (RDT). Jar test results showed TSS of 43 mg/L, 18 mg/L, 16 mg/L, 27 mg/L, and 37 mg/L at polymer doses of 49.2 ppm, 61.5 ppm, 73.8 ppm, 86.1 ppm, and 98.4 ppm, respectively, after 60 min of settlement. As the polymer dose increased from 49.2 ppm to 73.8 ppm, the TSS decreased from 43 mg/L to 16 mg/L; further increasing the polymer dose to 98. 4 ppm resulted in TSS values increasing to 37 mg/L. The trend from the experiments suggests that an optimum polymer dose is approximately 74 ppm. Figure 4.1 shows cumulative volume of filtrate after 1 and 60 min of filtration. TSS and particle size distribution tests were conducted on collected filtrate after 60 min. In addition to treated sediments, an untreated sample (0 ppm) was filtered using the RDT method as a control.

Figure 4.1 shows that as polymer dose increased to 73.8 ppm, the volume of filtrate also increased (up to 195 ml). In other words, as the system approaches optimum polymer conditioning, more water becomes free for removal. It was found however, that at lower doses, flocs failed to form, and aggregated particulates clogged the geotextile, resulting in

a higher moisture content of the filter cake and lower filtrate volume collected. At doses lower than 73.8 ppm, time also played a significant role in the volume of released water. At doses equal to or greater than 73.8 ppm, dewatering occurred at a faster rate and most of the volume of filtrate was obtained after 1 min; 60 min did not result in any additional filtrate.

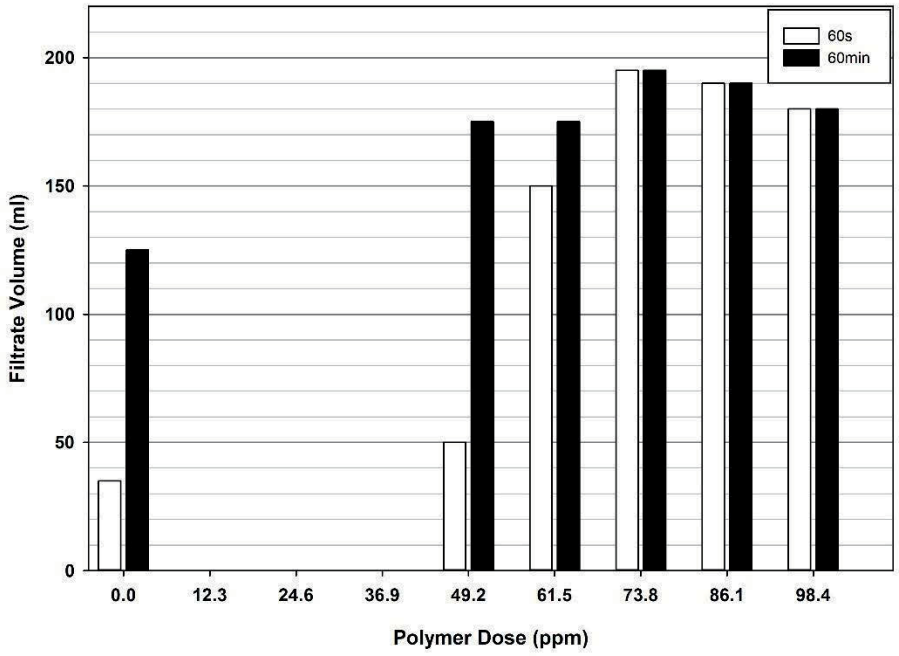

Figure 4.1 RDT filtrate volume results for location A sediments.

Filter cake formation due to the addition of polymer, also affected the filtrate volume. A thin layer of filter cake was formed at the end of dewatering of the control (0 ppm) sample and the addition of 49.2 ppm did not visually appear to change the cake structure. At a polymer dose of 73.8 ppm, the cake appeared to be comprised of sediment flocs which tended to cluster together forming a structurally weak but porous structure. This structure allowed liquid to flow through the filter cake without significant resistance (Satyamurthy 2008). Further increase in polymer dose, up to 98.4 ppm, resulted in a similar filter cake, but with an increased cake height. However, overdosing up to 98.4 ppm seemed to decrease filtrate volume (Figure 4.1).

TSS analysis of the filtrate showed a decrease to 1220 mg/L from an initial value of 2650 mg/L for the untreated control sample after 1 h of geotextile filtering. For treated sediments, a minimum TSS of 31 mg/L was obtained using the 73.8 ppm polymer dose, which is consistent with jar test results in terms of optimum dose (Figure 4.2a). As the polymer dose increased up to 98.4 ppm, the filtrate became visibly cloudy (associated with overdosing) and TSS increased.

MFI analysis for the filtrate of RDT (Figure 4.2b) showed that particle diameters remaining in the filtrate in which 85% of the sample is smaller (i.e. D_{85}) were approximately 10, 8, 5, 4, 6, and 6 μm at 0, 49.2, 61.5, 73.8, 86.1, and 98.4 ppm of polymer dose, respectively. A noticeable difference in particle size distribution was not observed before and after geotextile filtration with the untreated sediment (0 ppm). However, at the 49.2 ppm polymer dose, D_{85} decreased to 8 μm from 11 μm (original). Figure 4.2c shows that the number of particles remaining after geotextile filtration decreased, as the dose increased from 0 to 73.8 ppm. By increasing the dose to 86.1 and 98.4 ppm, the number of particles in the filtrate increased, which agrees with the increase in TSS discussed above.

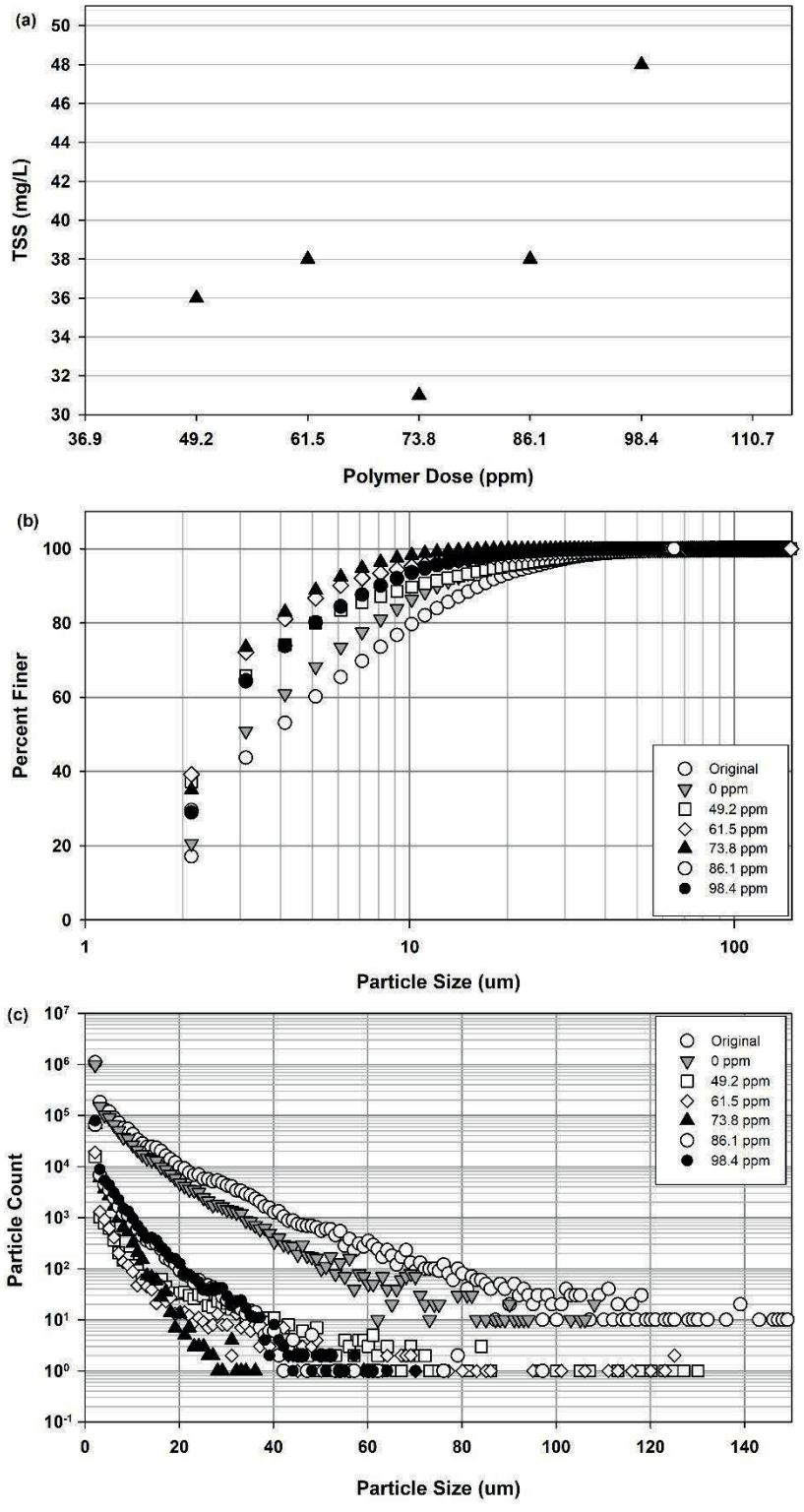

Figure 4.2 RDT filtrate (a) TSS (b) particle size distribution (c) particle count for location A sediments.

Results of the RDT and jar tests performed in this study suggest that the optimum polymer dose for dewatering of location A sediments is 73.8 ppm or 24.6 kg/bone dry ton. As sediments from location M revealed similar physical properties (Table 4.1) to location A sediments, it was assumed that a similar optimum dose would be identified for location M sediments, if jar test and RDT were conducted. Therefore, an optimum polymer dose of 73.8 ppm was used for all dewatering techniques performed (i.e. centrifuge, RDT, sedimentation) on sediments from both locations. It should be noted that to keep initial solids content constant (0.3%) for all the tests, when required, sediments were diluted with water taken from the location from which the sediment originated.

RDT was then performed with treated sediments from location M (73.8 ppm polymer) and untreated samples used for control. Table 4.3 shows TSS of filtrate, volume of filtrate, and solids content of filter cake for both locations after the RDT. Dewatering of location M sediments at, optimum dose via RDT, did not reveal similar results to those observed for location A sediments. As shown in Table 4.3, the filtrate volume following the dewatering test (60 min) on treated sediments was 120 ml, which was less than the filtrate volume of the location A control sample. Dewatering of this treated location M sediment was not rapid (observed with location A sediments), rather it occurred over a much longer time period. Filtrate of location M dewatering was observed to be cloudy with visible fine suspended solids, and the filter cake appeared saturated after one hour of filtering. This amount of water can explain the low solids content of 0.81% compared to 7.37% obtained from treated location A sediments.

Table 4.3 RDT filtrate and filter cake characteristics for BH sediment.

	Polymer Dose (ppm)	TSS (mg/L)	Filtrate volume (ml)		Solids content %
			1 min	60 min	
Location A	0	1220	35	125	0.65
	73.8	31	195	195	7.37
Location M	0	1550	5	21	0.40
	73.8	686	25	120	0.81

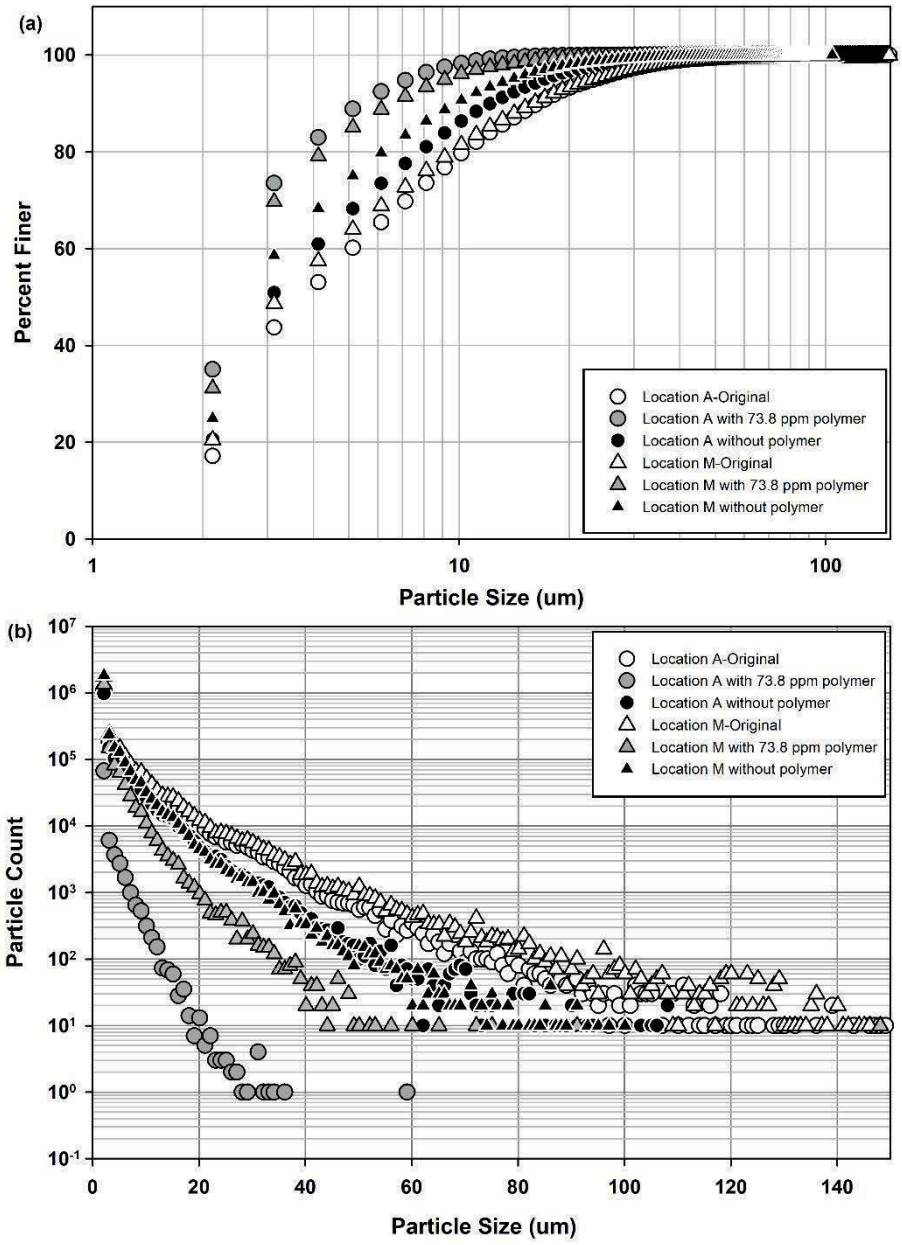

Figure 4.3 RDT filtrate (a) particle size distribution (b) particle count for BH sediments.

The particle size distribution graph from the MFI in Figure 4.3a also shows that particles remaining after dewatering of location A with 73.8 ppm polymer are slightly finer than that of location M. Likewise, the number of particles (Figure 4.3b) in location M filtrate were greater than location A which agrees with TSS results.

Although initial solids (0.3 %) of sediments from both locations A and M were the same and an identical procedure was used to mix sediments with polymer, testing determined that 73.8 ppm polymer was not as effective for the dewatering of the location M sediment compared to location A sediment. Differences in properties found in the water from both locations used to dilute samples led to differences in dewatering performance. As mentioned in Table 4.1 and discussed in the introduction, location A water has a lower salinity (0.3 ppt), compared to that of the location M water (0.68 ppt). Although this difference in salinity does not appear to be significant, it appears to be enough to impact the behavior of the chosen polymer. It also was observed that, although location M and location A sediments have a similar zeta-potential of about -28 mV, the zeta-potential of water from location M is -24 mV compared with -14 mV for location A water. For location M sediments diluted with location M water, a polymer dose of 73.8 ppm was found to be insufficient to diminish the surface charge and encourage the formation of larger flocs. Further jar tests would be needed to establish the proper polymer and dose for these location M sediments. However, for the purposes of comparisons with the other dewatering methods, this same polymer and dose was used for location M sediments as well.

4.3.3 Laboratory Centrifuge Testing

As shown in Table 4.4, the TSS of the supernatant water decreased as the time and speed of centrifuging increased for all cases (untreated/treated samples, both coves, both speeds). For samples without polymer, at 2500 rpm, time generally played a more significant role in the removal of the suspended solids from the supernatant. However, for the optimum polymer dose, increasing the centrifuge speed did not have any major effect on the TSS values at the end of the test. In addition, there was very little difference in TSS values over time for treated sediment from location A, suggesting that proper dose of polymer with minimal centrifuge effort can control the dewatering efficiency.

For location M, treated and untreated sediment showed similar behavior over time, at different speeds. TSS decreased as speed and time of centrifuging increased. However, the TSS values were much higher than that of location A due to the inadequacy of the polymer. Although conditioning the sample with polymer improved the removal of TSS from the

filtrate at location M, it could not overcome the effect of time and speed on TSS removal by centrifuging.

Table 4.4 Centrifuge tests supernatant and filter cake results for BH sediment.

Location	Centrifuge speed (rpm)	Polymer dose (ppm)	Supernatant TSS (mg/L)			Solids content (%)
			5 min	30 min	60 min	
Location A	2500	0	105	45	33	12.5
		73.8	13	4	3	14.1
Location M	2500	0	498	282	164	8.3
		73.8	328	162	115	8.8
Location A	4500	0	59	25	18	13.4
		73.8	8	2	2	17.1
Location M	4500	0	319	261	178	8.4
		73.8	226	123	67	10.0

A maximum solids content of 17.1% was obtained after 60 min at 4500 rpm for treated location A sediment (Table 4.4). This value decreased to 14.1% when centrifuge speed was reduced to 2500 rpm. A minimum solids content of 8.3% was obtained at the end of centrifuge dewatering at 2500 rpm for location M sediments without any polymer. Although centrifuging did not reduce TSS of location M sediments as much as that from location A, it did increase solids content by a relatively similar amount with and without polymer.

Figure 4.4 shows the particle count and size distribution of the supernatant after centrifugation of both locations' sediments at varying speeds and polymer doses. Particle sizes as well as counts of the untreated samples originating in both locations reveal the similarity between the two sample locations. The original samples both contain approximately 80% of the solids (5×10^4 particles) finer than 10 μm. When observing the material following centrifuge (at either speed), or the addition of the optimum polymer dose combined with centrifuging, both resulted in lower number of particles, as well as smaller particles. Location A samples rotated at both 2500 and 4500 rpm, without the addition of polymer, both resulted in 85% of material being finer than ~2 to 3 μm.

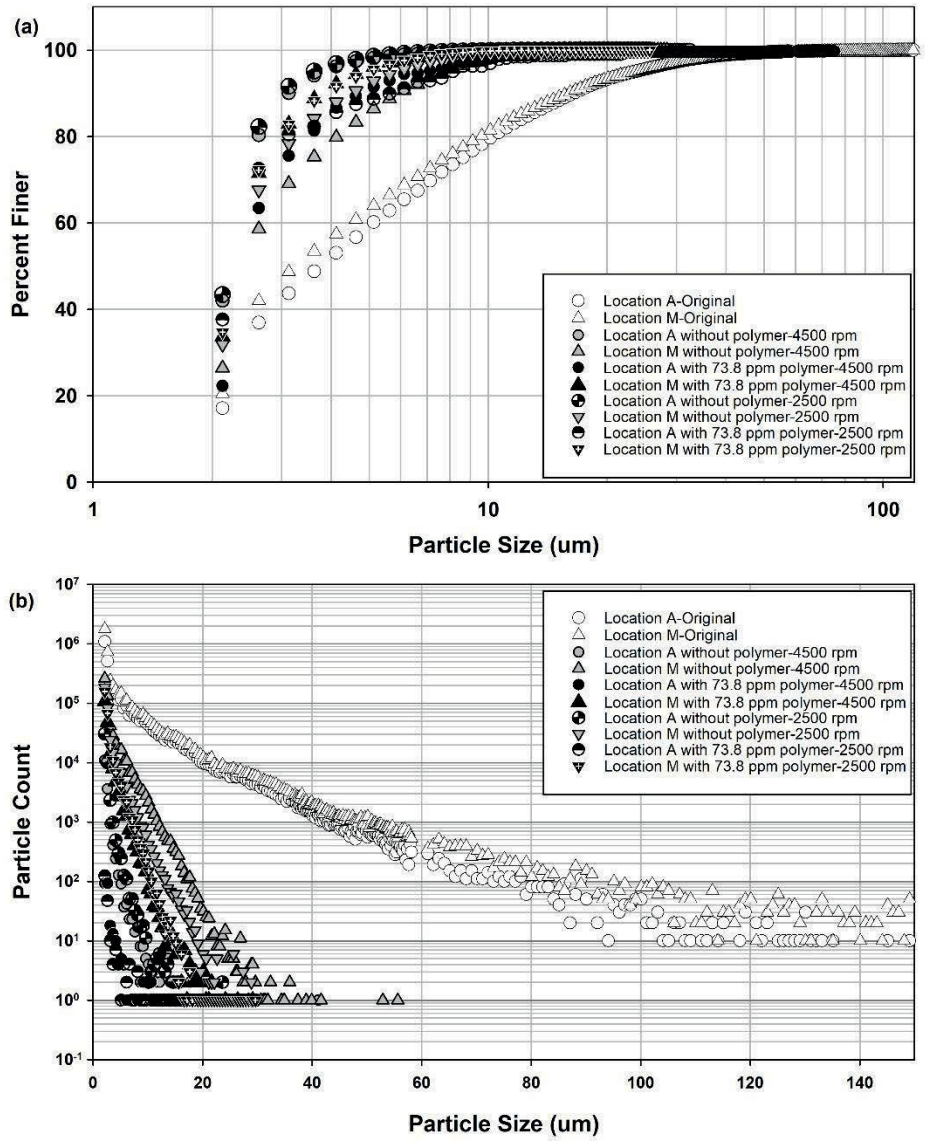

Figure 4.4 Centrifuge supernatant (a) particle size distribution, (b) particle count for BH sediments.

In comparison, when polymer was added, these sediments had similar particle size distributions at both speeds but with 85% of material being finer than ~3 to 4 µm. This suggests the supernatant contains finer particles without adding polymer. Supernatant after centrifuging location A sediments without polymer, contains approximately 100 times more 3 µm size particles than supernatant containing polymer (Figure 4.4b). Dewatering of sediments taken from the location M, however, were only slightly improved with addition of polymer. Without addition of polymer, approximately 85% of the material was

finer than 3-5 μm, while with polymer, values were between 3-4 μm. Treatment of sediment by centrifuge is an effective method of producing a filtrate with low particulate matter. However, it is evident that the optimum dose of polymer, as well as an appropriate speed of rotation, is required to ensure low particulate matter in the effluent.

4.3.4 Sedimentation Testing

A total of four sedimentation tests were conducted on sediments from both locations at the same solids content of 0.3 %. These tests were completed without polymer and with polymer (73.8 ppm) to determine the supernatant clarity (TSS, particle size) and the final proportion of solids (solids content) due to gravity sedimentation. Figure 4.5 shows the levels of TSS variation with depth from surface (from nozzle 4 to 2). For location A sediment with polymer, the supernatant became visually clear after the first hour of settling and the TSS dropped to 17 mg/L at the upper nozzle (4). For the same sediment location without polymer, TSS was 640 mg/L after one hour. Sedimentation of the location A sediment at the optimum polymer dose was almost completed in the first hour. As shown in Figure 4.5, unlike the treated sample, the TSS of supernatant of the untreated sediment in the location A trial decreased as time increased. Similarly, location M sediment with and without polymer showed a decrease of TSS over time, albeit not nearly as effective as location A.

Particle size distribution graphs for sediment supernatant at both locations (with polymer) at the upper nozzle (4) (Figure 4.6) show that particle sizes in suspension decreases as the test progressed, due to settling of larger particles. MFI analysis at other nozzles also showed a similar trend. The finest (D_{85}=3 μm) particles were obtained at the end of sedimentation (240 h) at the shallowest depth (i.e. nozzle 4).

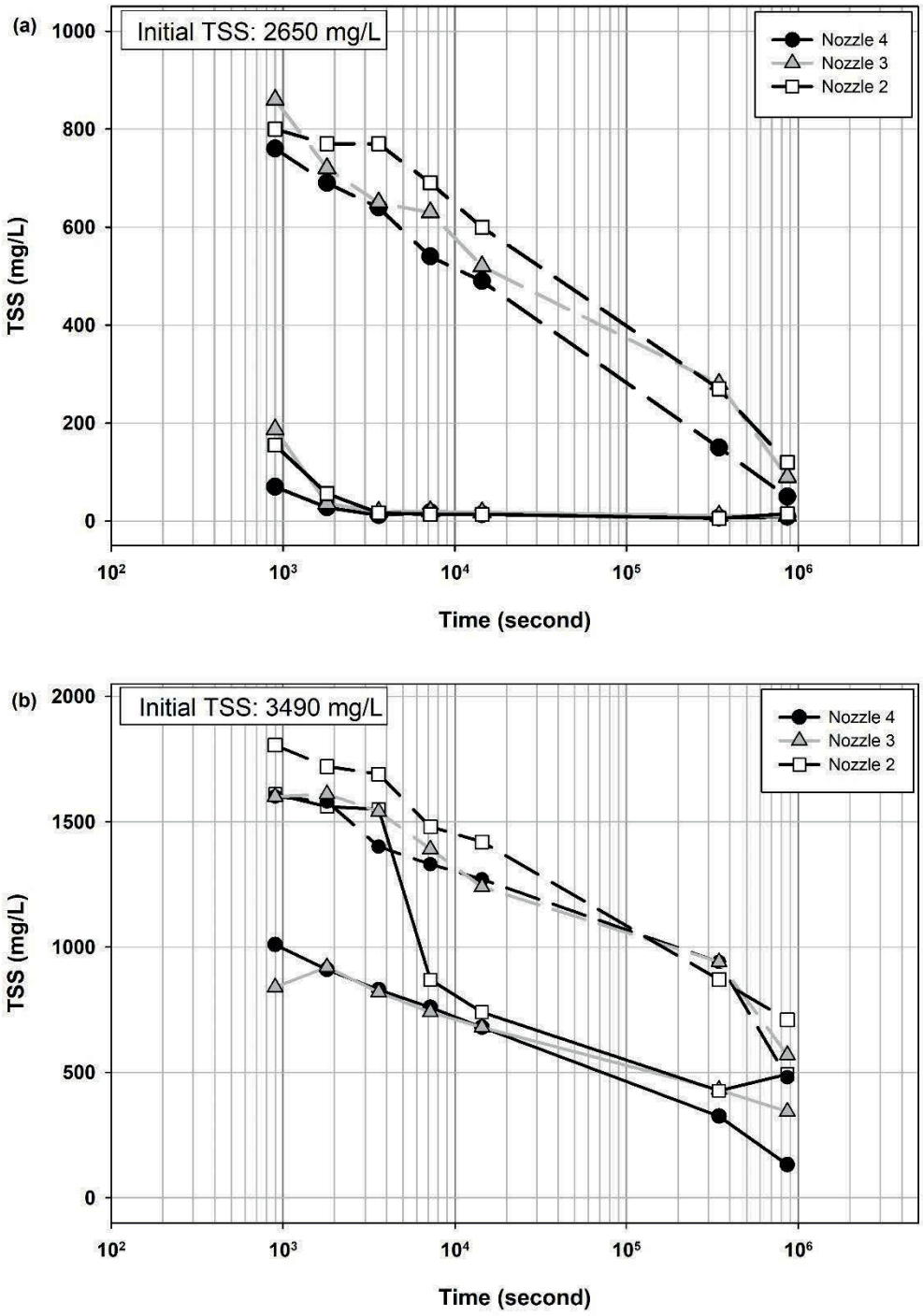

Figure 4.5 TSS results of sedimentation supernatant for (a) Location A (b) Location M sediments, dashed and solid lines show untreated and treated samples, respectively.

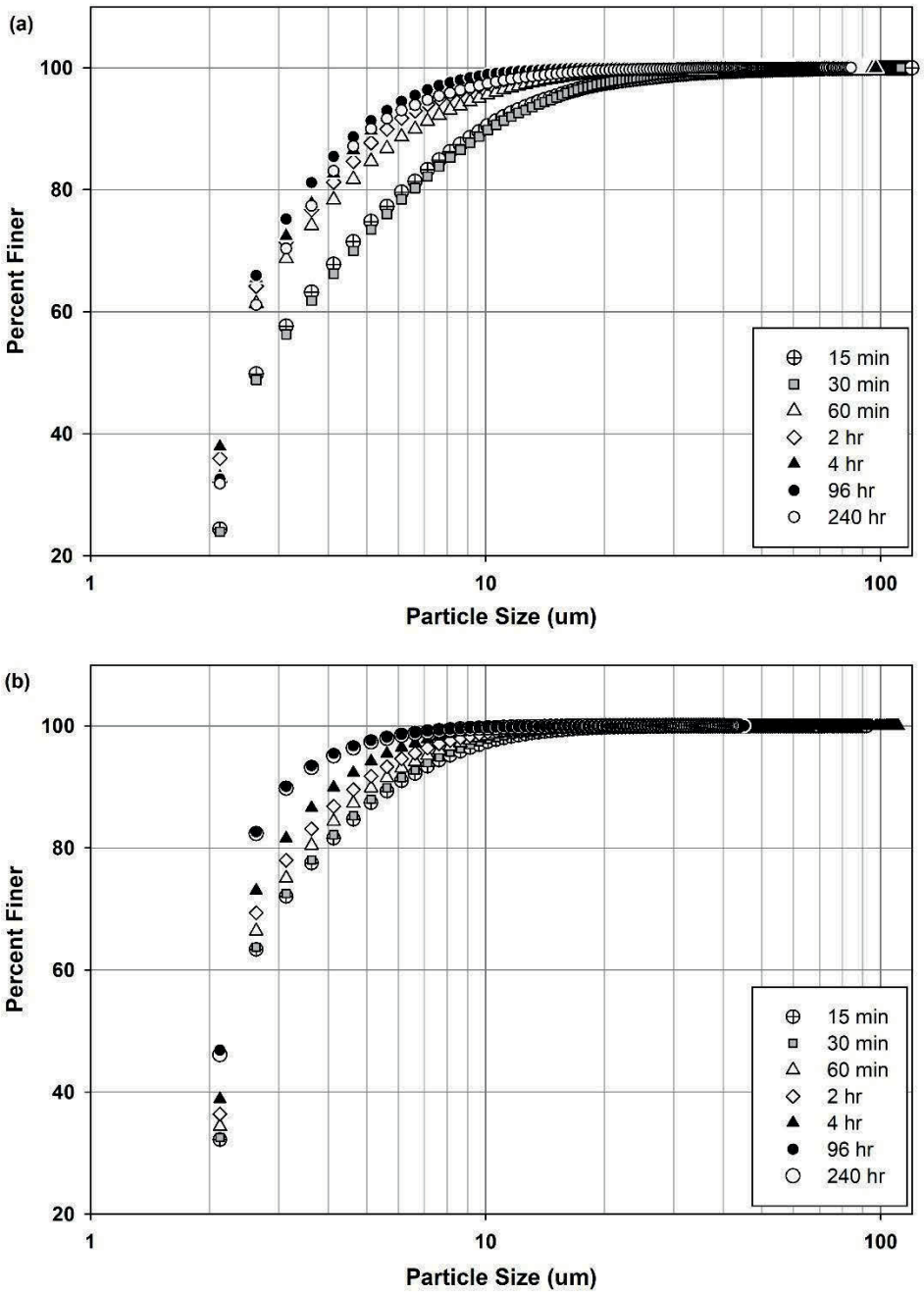

Figure 4.6 Particle size distribution of sedimentation supernatant at nozzle 4 for (a) Location A (b) Location M sediments, with polymer over time.

4.3.5 Comparison of different dewatering techniques

Various dewatering methods (i.e. geotextile filtering, centrifuge and sedimentation) for BH sediments have examined, at the laboratory scale, the influence of these techniques and polymers on resulting particles in the water resulting from the given dewatering technique. Given that some of the key contaminants present in BH sediments are associated with these particles, it is useful to understand their fate during each of the different dewatering methods. Each of these dewatering techniques represents different levels of cost, time and performance. Filtrate quality in terms of amount and size of TSS was studied for each method individually. It is useful to compare the results of these different techniques at the optimum polymer dosage (73.8 mm) and same times of dewatering in terms of TSS and particle size.

Centrifuging at 4500 rpm was able to remove 99.9% of TSS after 1 h. Results were calculated using equation 1, where $TSS_{initial}$ and TSS_{final} are the initial and final volumes of TSS present.

$$\frac{TSS_{initial} - TSS_{final}}{TSS_{initial}} \quad \text{Eq. [1]}$$

Geotextile filtering, sedimentation and 2500 rpm centrifuging were able to remove 98.8 %, 99.4% and 99.9%, respectively. Geotextile filtering obtained slightly lower efficiency amongst the methods for dewatering location A sediments with polymer, however, all worked quite similar. Although, considering power requirements and cost for centrifugation, time requiring for sedimentation, geotextile filtration methods may be an economical alternative when considering large volumes of sediments (577,000 m^3). It should be noted that minimal filter cake formed during these short-term tests (i.e. longer test times would likely increase removal rates). As was shown in Figure 4.3 and discussed previously, 73.8 ppm is not an optimum dose for location M sediments. Although, dewatering by 4500 rpm centrifuge removed 98% of TSS for the location M sediments, 67 mg/L remains almost three times the standard limit (~25 mg/L) (Government of Canada 2019) allowed for wastewater discharge to open water without further treatment. In the case of dewatering without polymer for location M, minimum and maximum TSS amounts were obtained using centrifuge and geotextile filtering, showing how geotextile

performance depends on the use of polymer to improve particle retention. Due to the stability of location M sediments (higher zeta potential), the time required for settling was much greater than that of samples taken from Location A.

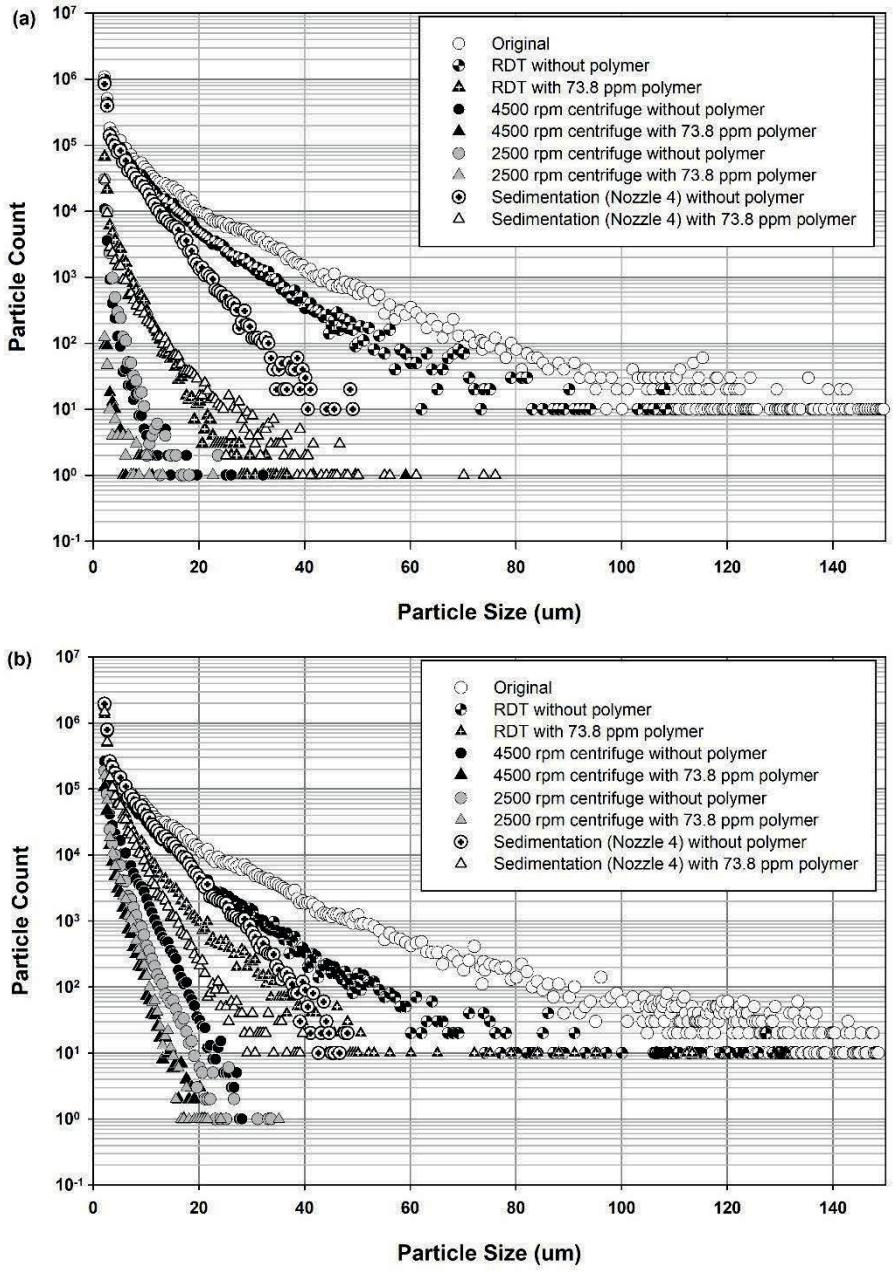

Figure 4.7 Particle count of filtrate after an hour dewatering by different methods for a) location A and b) location M sediments.

Figure 4.7 represents the particle counts of filtrate after dewatering by the three different methods, as well as original samples for comparison purposes. As shown in this figure, flocculation of location A sediments with 73.8 ppm followed by geotextile filtering reduced the amount of particulate by three orders of magnitude. For example, based on MFI results, original location A sediment contain approximately 10^4 particles at 20 μm diameter, which decreased to 10 particles after the RDT test. However, as 73.8 ppm polymer for location M was not an optimum dose, flocculation did not adequately take place, and therefore RDT could not improve filtrate quality as much as location A sediment.

For location A sediments, RDT with 73.8 ppm polymer resulted in particle counts slightly more than sedimentation. Filtrate resulting after centrifuging at different speeds with polymer had similar counts of particles sized between 2 and 10 μm, which shows that at optimum polymer dose, centrifuge improves filtrate quality even at low speeds (2500 rpm). For location M sediments, the number of particles was not reduced by centrifuge with or without using as much polymer as location A. For example, the number of particles with a 20 μm diameter decreased from 2×10^4 in the original sample to, at most, 100 for location M, while there are not many particles with a 20 μm diameter after centrifuging of location A sediments.

The study by Mori et al. (2002) is one of the few that investigated dioxin and furan fate in geotextile dewatering. Sediments used in that study had dioxin and furan levels as high as 71,500 pg-TEQ/g and showed that over 99% of dioxins and furans were removed by dewatering in the effluent. However, Mori also highlighted that the limit of dioxins and furans in effluent allowed by Japanese regulators was exceeded because of the low regulatory level. Mean dioxin and furan concentrations in BH sediments has been reported by Hoffman et al (2019) and GHD (2018b) to be lower than 100 pg-TEQ/g and 500 pg-TEQ/g, accordingly, for the human/mammal as a receptor according to WHO and CCME (van den Berg et al. 1998, CCME 2002). Although further work would have to be performed to assess actual dioxin and furan levels in the effluent during geotextile dewatering (the current choice for dewatering for the project (GHD 2018a)), it appears that

these lower dioxin and furan levels would result in low levels in the effluent based on the amount of particulate matter present.

It is acknowledged that as with any study of this nature, there are limitations to application of the results. Firstly, these tests were performed under controlled conditions in the laboratory and may vary from large scale field testing (although it should be noted that pilot testing for geotextile dewatering was being performed at the time of this study). Secondly, the testing was performed from one sampling location in the stabilization basin. Alimohammadi et al. (2019) showed that the sediment in the basin is relatively consistent in terms of physical characteristics but nonetheless this is limitation of this, and other, bench scale studies. As was discussed in the paper, the water chemistry plays an important role in polymer effectiveness and hence any variation in water quality during actual dredging operations would likely influence the applicability of these findings to full scale.

4.4 Summary and Conclusion

A series of bench scale dewatering tests have been performed on a fine-grained sediment material obtained from field sampling of a future remediation project. Characterization tests on this sediment showed similarity in most properties except for the water column above the sediments that will ultimately be entrained during dredging operations. It was shown during the development of polymer doses for the bench scale testing that this water quality variation resulted in differing performances of the polymer from the two sediment locations. This highlights the need for field specific water for bench scale dewatering testing.

Three types of dewatering tests were examined in this bench scale study; geotextile filtration via rapid filtration testing, centrifuge testing and sedimentation testing. The main purpose of the study was to examine the ability of the various methods to remove particulate matter when undergoing the same polymer treatment. Given that contamination is associated with the particulate matter, it was deemed important to understand particulate removal from the various dewatering tests. It was shown that all methods resulted in greater than 98.8% of removal (based on TSS measurements) when polymer doses could be

optimized (i.e. location A). Geotextile filtration removed 98.8% of solids which was lower than that obtained from sedimentation and centrifuge methods. Effluent particle numbers and sizes were reduced for all three methods relative to the original sediments. From a practical perspective, when considering time and space required (Segré 2013) for sedimentation ponds (also considering dewatering that would be required after) and the energy requirements and mechanical upkeep to run the machine (Newman et al. 2004) for centrifuging, geotextile filtration could be a preferred alternative. This is especially true when considering the large volume of sediments associated with the project under study. It is likely that filter cake formation during large scale trials will improve solids removal efficiency. Geotextile filtration is currently the option of choice for dewatering of the large volume of sediments in the BH remediation document (GHD 2018a).

CHAPTER 5: MIGRATION OF PARTICLES THROUGH GEOTEXTILE TUBE DEWATERING IN A FIELD SCALE TEST

5.1 Introduction

The objective of this chapter is to evaluate the filtrate quality and particle transport during a pilot scale geotextile tube dewatering of the BH sediment as the basis for fate and transport testing to be presented in Chapter 6. As previously discussed in Chapter 4, a filtration efficiency of 98.8% was obtained from the laboratory-based rapid dewatering tests (RDT) using the GT-500. However, it is likely that filter cake formation during large scale trials will be different than the laboratory tests performed in Chapter 4 for reasons of scale and time. Hence a demonstration of a geotextile tube dewatering test (GDT) was undertaken to dewater a larger volume sediment sample taken from BH; with the objective to observe the filtering efficiency. The Geotextile tube Dewatering Test (GDT) was first developed by TenCate in order to adequately simulate actual geotextile tube dewatering process (TenCate, 2016). Since 2013 GDT is recognized as a standard testing method (ASTM D7880) by ASTM.

5.2 Materials and Methods

5.2.1 Sediment

Sediment samples were obtained from BH (Cove A), and its physical properties were previously studied as described in Chapter 3 and 4. The BH sediment is rich in organic matter (TOC~30%), has a small particle size (D_{85}=11μm), a specific gravity of 1.71 and a bulk density of (1.07 ± 0.05) g/cm^3. The average in-situ water and solids content of (957±71)% and (9±1)% was found using the composite gravity core sampling described in Chapter 3. Sediment was diluted to approximately 0.3% solids content to simulate dredging conditions for the current study. Chemical Solve 9244 was found to provide adequate dewatering capabilities for the BH sediment at 1.5% of the total volume of sediment slurry, as described in Chapter 4.

5.2.2 Geotextile

The geotextile used in the experiments was GT-500, the same as used in previous chapters, produced by the TenCate Corporation. Water flow rate of this woven geotextile made of "polypropylene multifilament and monofilament yarns" is reported as 813 l/min/m^2 by the manufacturer. The GT-500's apparent opening size (AOS) is 430 μm and the thickness averages 1.8 mm. The pore size distribution values for O_{50} and O_{95} are 80 μm and 195 μm, respectively (GT 500 technical data sheet, TenCate Corporation, 2015).

5.2.3 Demonstration of Geotube Dewatering Test (GDT)

A pillow-shaped standard geotextile bags made of GT-500 textile were obtained from Bishop Water Technologies (Renfrew, Ontario, Canada). The purpose of this large-scale test was to empirically observe the behavior of the BH sediment particle's transport as larger volumes of the conditioned sediment was being filtered by the geotextile (i.e. with filter cake). The geotextile bags (50cm × 50cm) were stitched along three sides, with the fourth side folded. The bags came pre-fitted with a 5 cm ABS threaded pipe fitting located in the center of the largest side. As shown in Figure 5.1, the geobag dewatering setup was designed and constructed to allow filtration of up to 140 L of conditioned BH sediments at one time. The assembly consisted of a large plastic drum to which a series of ABS pipes and flanges were attached. The apparatus was fastened to a steel frame with a height of 75 cm, allowing for increased accessibility to the filtrate. The dimensions and materials were chosen to coincide with the fitting which came standard on the geotextile bags. The ABS tubing was designed to be easily removable in order to allow for the relatively easy exchange of new and used bags. The rate of flow was controlled by a limiting valve which was placed directly adjacent to the opening on the bottom of the drum. The geotextile was suspended beneath the drum by a PVC mesh, which allowed the filtrate to pass unabated while still offering support.

Figure 5.1 Geotube Dewatering Test (GDT) Setup (Photograph taken on December 6, 2018)

Sediment samples were taken from Cove A of BH at the time of conducting the GDT. The solids content of the sampled sediment was measured using a portable turbidimeter in the field. The relationship between turbidity (NTU) and solids content (%) of BH sediment was determined in the laboratory before starting the field experiment. The test was designed to be run multiple times in succession, in an attempt to fill the entire geotextile bag. Prior to filtering, the plastic drum was filled with 100 L of sediments at 0.3% solids content, then 1.5 L of Solve 9244 was added to the drum and mixed at varying speeds using an electric mixing drill. As mentioned in Chapter 4, due to the difference in water quality of Cove A, only Solve 9244 (1.5% of total volume of the slurry) was needed to enhance the dewatering capabilities of sediments (Alimohammadi et al., 2019). After approximately 30 seconds of mixing, large flocs began to form and settle out of the solution. At this point the control valve was opened and the solution was allowed to drain into the geotextile bag.

Filtrate was collected for TSS, particle size, and particle concentration analysis at several selected time intervals (i.e. 10 s, 20 s, 30 s, 60 s, 120 s, 300 s, 600 s, 600 s, 1200 s, 1800 s) as it was secreted from the geobag. Also, at each time interval, the volume of retained solution in the drum was determined. Upon filtering 100 L of slurry through the bag, the drum was refilled, and the experiment repeated 4 additional times (with the final test consisting of 50 L of slurry) using the same bag. Following the fifth addition of sediment, the filtrate ceased from the bag and the test was terminated. The bag was then transported back to Dalhousie University for analysis, where it was allowed to dewater for 7 days before being analyzed for total mass and solids content of filter cake formed inside of the geotextile bag.

5.3 Results and Discussion

The geotube demonstration large-scale field test consisted of four 100 L and one 50 L trials, which were filtered into a single geotextile bag. As each subsequent volume of sediment passed through the bag (i.e. as each new trial was performed), the filtering performance of the geotextile bag increased due to the formation of a filter cake inside of the bag. This was immediately evident by the clarity of the filtrate visually observed in the field (see Figure 5.2) and also confirmed in the laboratory through the analysis of particle concentration.

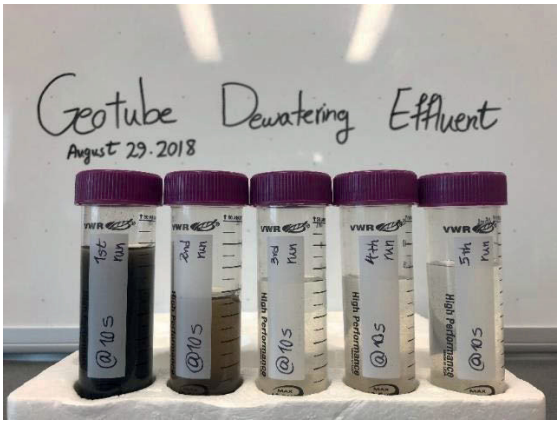

Figure 5.2 Visual filtrate quality after 10 second of the beginning of each trial

Figure 5.3a illustrates particle concentration results throughout the five trials as well as the length of time required to complete each trial. For the 1st trial, it only took approximately

60 seconds to pass the entire 100L of conditioned sediment through the bag, while for the remaining trials, as the filter cake formed, the filtration process became much slower (e.g. 4th trial took 1850 sec). Figure 5a shows that particle concentrations decreased over the time of filtration for each trial, as the filter cake formed inside of the geotextile bag and the filtration efficiency improved. The particle concentration in the sampled filtrate 10 seconds after the beginning of first trial was found to be 9.2 million/ mL which quickly reduced to 163,521 (#/mL) after 50 sec. Despite the decreasing trend in particle concentration over time (due to the increasing the filter cake thickness) within each trial, an initial spike was observed in particle concentration at the beginning of each trial. This is likely due to a higher total head present above the geotextile bag, pushing the sediment through the geotextile bag at the initial moments of each trial, since more sediment slurry existed inside the drum. As discussed by Tackley et al. (2020), this is also likely due to some liquid being expelled from the top surface area of the bag (due to these higher initial pressures) in areas without significant filter cake formation. As presented in Figure 5a, particle concentrations in the 10 sec sampled filtrate of each trial is higher than previous measured concentrations. However, particle concentration continued to reduce further as the test proceeded and maintained the constant range between 40,000 and 60,000 (#/mL). Considering the initial particle concentration of sediment (at 0.3% solids content) which was 20 million per mL, an average filtration efficiency of 99.7% was achieved. Figure 5b shows the total suspended solids (TSS) results for five trials. As with particle concentrations, the overall decrease in TSS can be seen over time. Results revealed that the TSS of releasing filtrate after 30s after the initiation of the second trial is below the limit of 25 mg/L (standard limit for wastewater discharge to open water without further treatment - Government of Canada, 2019), except for the TSS values of 33, 80, and 41 mg/L, which are related to the sampled filtrate at 10 s of the third, fourth, and fifth trial respectively. This agrees with increasing particle concentration at the beginning of each trial because of the applying pressure. Hence, it can be concluded that TSS in the filtrate may only be an issue at the initial time of geotube filling/refilling for small volumes but likely not an issue when averaged over the cumulative volume of the trial, as a result of the improvement of filtering efficiency due to the presence of filter cake formation inside the geotextile bag. The average size of

the filtrate particles remained consistent in the range of 3.5µm to 5.5µm throughout the 5 trials, while the mean size of input sediment was found to be approximately 9µm. Tackley et al. (2019) conducted the same demonstration of geotube dewatering test (GDT) with BH sediment at 1% solids content. Due to the higher initial solids content and therefore faster forming of filter cake inside of geobag, filtration process (discharge rate) was slower than this study; two trials (200 L in total) were performed in two hours, while in this study 450L of sediments were filtered in approximately 2 hours. Even though initial solids content was higher, they found less particle concentrations in the range between 9,000 and 14,000 (#/mL) in the later samples of filtrate of second trial showing the role of thicker filter cake in retaining particles inside.

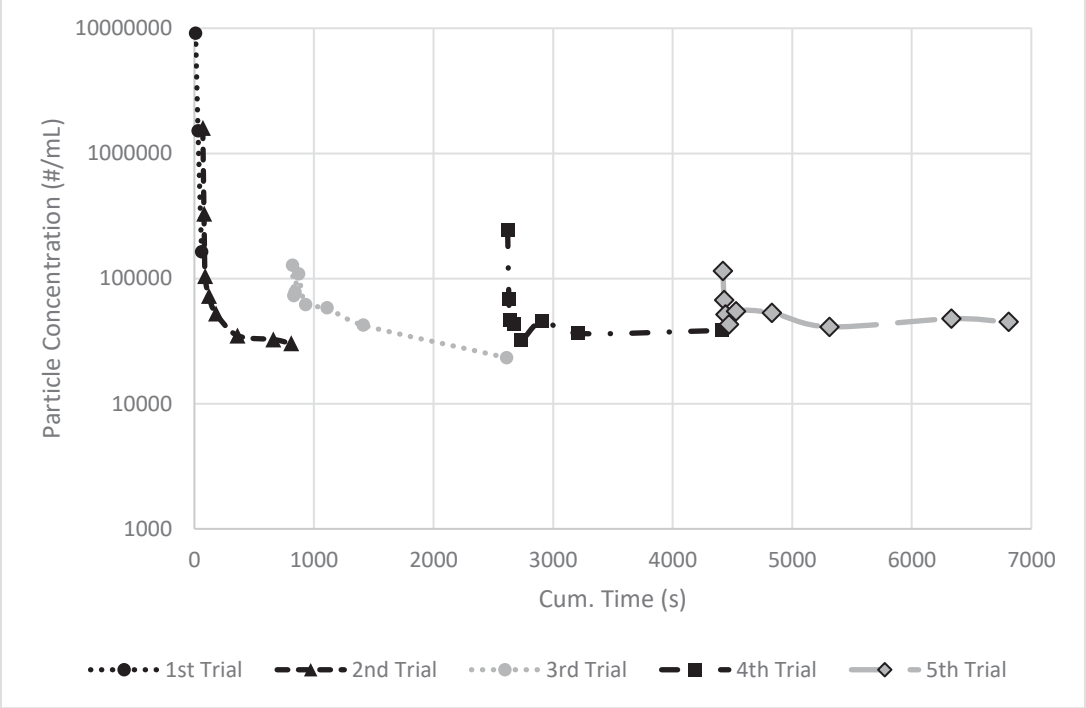

a

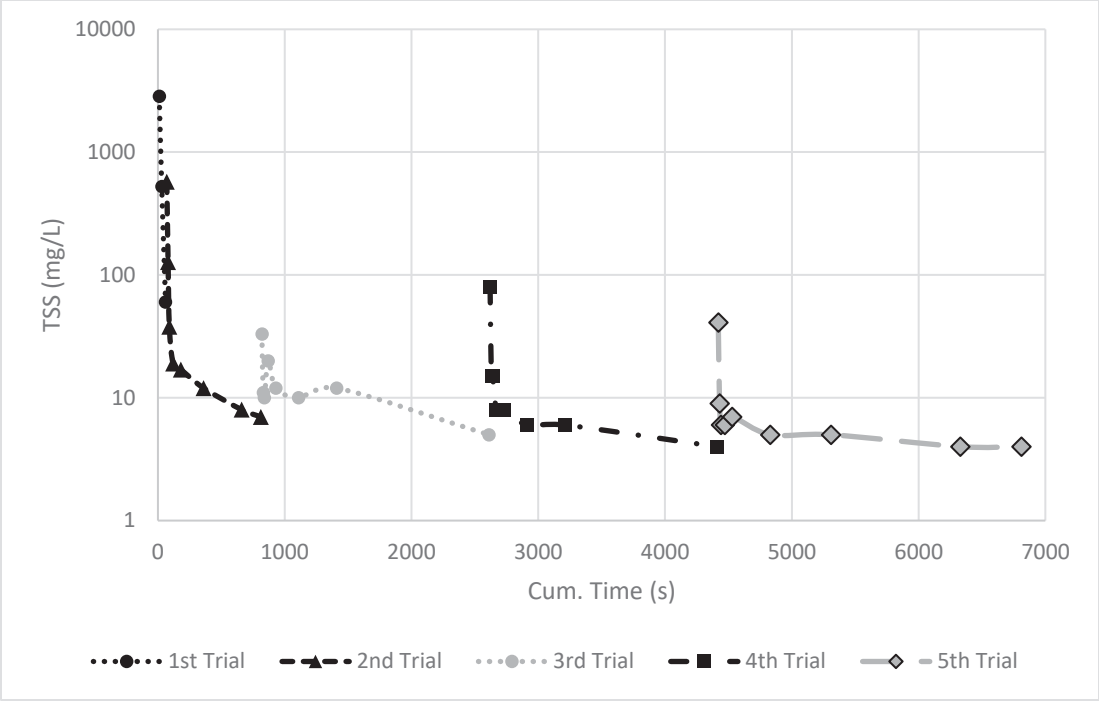

b

Figure 5.3 a) Particle concentration, and b) TSS results of the GDT filtrate

The solids content of filter cake inside of geobag was measured after 7 days of further dewatering in Dalhousie laboratories. A solids content of 13.3% was obtained at the middle of the bag while 14.3%, 13.4%, 14.5%, and 14.2% were found at the four edges of the bag for an average of 14.0% compared to the starting solids content of 0.3%. The thickness of the formed filter cake at the middle of bag was greater than edges, however consolidation happened at a slower rate due to a greater drainage height. Therefore, sediments at the middle of the bag had a higher water and lower solids content. It should be noted the average solids content obtained by geobag dewatering after 7 days would likely increase if allowed to consolidate longer.

5.4 Summary and Conclusion

In this chapter, a geotextile tube dewatering test was conducted to study the geotextile filtering performance in larger scale. Filtrate quality in terms of particle concentration was

analyzed and results revealed that approximately 99.7% of the initial concentration was removed during the geotextile dewatering process. However, 98.8% removal efficiency had been obtained in laboratory scale test of RDT, as described in Chapter 4. It is likely that filter cake formation during large scale trials improves the solids removal efficiency. Hence, as each trial was performed, more filter cake deposited inside the geotextile bag and particle concentration in the filtrate decreased.

Moreover, filtrate analysis showed that particle concentration maintained a consistent concentration range, except perhaps at beginning of each trial (i.e. when the plastic drum is full) due to the higher pressure. It can be concluded that when the geotextile dewatering system is at stable condition, filtrate particle concentration does not change considerably. However, what mechanisms control this particle transport during the geotextile dewatering is currently unknown. For this purpose, laboratory scale tests were developed (as will be discussed in next chapter) to investigate the transport of particles during the controlled conditions.

CHAPTER 6: FATE AND TRANSPORT OF PARTICLE MATTER DURING GEOTUBE DEWATERING OF A DIOXIN AND FURAN (PCDD/F) CONTAMINATED SEDIMENT

Abstract

Geotextile tube dewatering is a pre-treatment method which has been utilized in the remediation of high-water content materials (i.e. sediments and slurries). However, given the association some contaminants (e.g. dioxins and furans) have with the particulate matter in contaminated sediments, understanding the fate and transport of this particle matter in the effluent is essential. In this paper, pressure filtration tests (PFTs) were conducted to investigate the effect of pressure and filter cake formation on both geotextile filtration efficiency and effluent quality. Transport tests were then performed to evaluate the particle transport through the developed filter cake, as well as the hydraulic characteristics of the medium during dewatering. HYDRUS, a one-dimensional model contaminant transport model was then employed to simulate the experimental particle transport test results. Three different mechanisms of particle transport (i.e. attachment, detachment, attachment and detachment) through saturated porous media were examined to identify the ideal simulation of observed effluent particle concentration. HYDRUS modeling outputs suggest that both attachment and detachment mechanisms are involved in a given particles fate and transport during geotextile dewatering. In addition, different parameters such as confining pressure and filter cake properties effect the particle concentration in the effluent. Furthermore, HYDRUS modeling was used to predict the transport of particles during the geotextile tube dewatering under different practical circumstances, the findings of which are presented in this paper.

6.1 Introduction

The disposal and storage of dredged sediment/sludge has become a critical issue, due to economic and environmental challenges (Yu, 2014; Saadet and Begüm, 2016; Louchouarn et al., 2018; CBC News, 2020). To manage large volumes of contaminated, high water content dredged sediments, viable dewatering techniques are required to efficiently decrease the total volume of material for practical and economical disposal considerations (Kutay and Aydilek, 2005; Shin and Oh, 2007; Lawson, 2008; Yan and Chu, 2010; Cantre´ and Saathoff, 2011; Chu et al., 2011; Malik and Sysala, 2011; Chu et al., 2012; Yee et al., 2012; Yee and Lawson, 2012; Saadet and Begüm, 2016). Geotube dewatering has been shown to be a proven method that can effectively separate the solids and liquid fractions in a high water content sediment using geotextile fabric as the filter media (Aydilek and Edil, 2002; Kutay and Aydilek, 2004; Liao and Bhatia, 2005;). In practical applications, a liquid slurry is pumped into a geotube under pressure, with the liquid in the sediment being expelled through the pores of the geotextile and the majority of the sediment solids being retained inside the geotextile tube. The geotextile tube is then refilled, repeating the cycle several times until the amount of filtrate passing through the textile is insignificant (Lawson, 2008).

Characteristics such as dewatering efficiency (i.e. how much the solids content can be increased) and dewatering rate (i.e. how long it will take), have been evaluated by numerous researchers using small and large scale laboratory tests (i.e. pressure filtration test [PFT], falling head test [FHT], hanging bag test [HBT]) (Gaffney et al., 1999; Moo-Young and Ochola, 1999a, Young and Ochola, 1999b; Moo-Young et al., 2002; Mori et al., 2002; Bhatia and Liao, 2004; Gaffney et al., 2004; Kutay and Aydilek, 2004; Huang and Koerner, 2005; Koerner and Koerner, 2006; Liao and Bhatia, 2005; Liao and Bhatia, 2006; Muthukumaran and Ilamparuthi, 2006; Liao, 2008; Huang and Luo, 2007; Satyamurthy, 2008; Segre, 2013; Bhatia et al., 2013; Khachan et al., 2014). It has been found that as the filtration proceeds in geotextile tube dewatering, a layer of solids (filter cake) is deposited on the surface of the geotextile, promoting retention and dominating subsequent filtration behavior. The filtration process generally becomes controlled by the

filter cake properties, more so than the geotextile properties. Its formation and stability are affected by the particle size distribution of the solids in the sediments, the concentration of particles, the flow rate, the applied pressure on the geotextile and the structure of the geotextile (Teoh et al., 2006; Tien et al., 2011; Weggel and Ward, 2012). Tackley et al. (2020) showed through bench and field scale filtration results that dewatering efficiency was improved with respect to metal contaminant migration as a growing filter cake was deposited on the surface of the geotextile; suggesting filtration efficiency of contaminants within a sediment may be largely dependent on the presence of the filter cake.

Many successful applications of geotextile tube dewatering of contaminated sediments have been reported (e.g. Wangensteen et al., 2001; Lawson, 2008; Mastin et al., 2008, Yee et al., 2012), providing site-specific information. However, few detailed observations of filtrate quality have been identified in the literature. Specifically, there is little information about the fate and transport of small levels of particle transport that could prove significant when dealing with PCDD/Fs which have very low criteria for environmental exceedances.

The purpose of this chapter is to investigate the fate and transport of a sediment known to be contaminated with PCDD/Fs from Boat Harbour, Nova Scotia, Canada. Specifically, the objectives of this study are: 1) to investigate the role of filter cake and pressure in particle matter concentration in the effluent after geotextile dewatering; and 2) to study the possible mechanisms responsible for particle matter transport through the filter cake during geotextile dewatering using a commercially available transport model (i.e. HYDRUS). Pressure filtration tests (PFT) at three different pressures (21, 35, and 49 kPa) were conducted to assess these objectives. Experimentation was also performed to investigate the role of a developed filter cake in particle transport. In these experiments, a solution of conservative tracer (Br^-) was passed through the filter cake under constant pressure. Filtrate volume, and its quality in terms of particle concentration were measured for all conducted tests. Numerical model using the HYDRUS-3D software package was performed to simulate particulate transport through a saturated filter cake, based on experimental results, with the ultimate goal of delineating particle transport mechanisms through the geotextile and developed filter cake.

6.1.1 Background

The sediment used to perform the laboratory testing in this chapter was obtained from Boat Harbour, Nova Scotia. The Boat Harbour (BH) remediation project in Nova Scotia, Canada is a ongoing project at the time of this thesis and is anticipated to involve dredging, geotube dewatering, and subsequent storage of contaminated material in a secure containment cell (GHD, 2018; Alimohammadi et al., 2019). Details on Boat Harbour and the fine grained sediment contaminated with PCDD/Fs have been discussed in previous chapters and will not be repeated here. In summary, dioxin and furan (PCDD/F) concentrations in the sediment consistently exceeded highest effect thresholds for CCME SQGs, posing an ecological risk, and making them the main contaminant of concern in the remediation of the site (Hoffman et al. 2017b; Hoffmann et al. 2019).

It is well documented that PCDD/F compounds have a strong affinity for sediment particles, particularly absorption and adsorption onto high surface area (i.e. particle matter), organic rich sediments (Fiedler et al., 1990; Mackay et al., 1992; Tyler et al., 1994; Lyytikainen et al., 2003; Louchouarn et al., 2018). Chalmers et al. (2019) examined the partitioning of PCDD/Fs in sediments adjacent to the Woodfibre Pulp and Paper Mill (British Columbia, Canada), identified in a core retrieved from an area exposed to effluent discharged by the mill. Results showed that both dioxin and furan concentrations were related to organic matter concentration, molecular chlorination, and sediment surface area. Another study by Louchouarn et al. (2018) which looked at sediments derived from the Houston Ship Channel (HSC) San Jacinto Superfund site (i.e waste pit), showed that diffusive transport of dioxins were unlikely from these sediments, and that the only potentially significant export mechanism from the waste pit was advective transport of particulate or colloid-sorbed dioxins. This is similar to observations from the 50+ years of deposition of PCDD/Fs in BH (i.e. little to no movement of the PCDD/Fs outside the stabilization basin) (GHD Limited 2018a, Chaudhary et al., 2020).

As discussed in Chapter 2, the BH sediment is known to contain elevated levels of PCCD/Fs. The small size of the particles (D_{85}=11μm) and its highly organic nature (total organic carbon ~ 30%) (i.e. Chapters 3 and 4) present a potential risk during geotextile

dewatering operations. This sediment provides an opportunity to study the transport of particle matter during the dewatering due to their association with PCCD/Fs. If excessive levels of PCCD/Fs were to be present in the filtrate, further treatment may be required before being discharged. In the literature, there are limited works related to dewatering of PCDD/F contaminated sediments and examining the particle matter migration during geotube dewatering. Mori et al. (2002) studied the applicability of geotubes as a containment method for dioxin-contaminated sediment. Results indicated the strong correlation (R^2=0.98-0.99) between measured suspended solids and dioxin concentration in the filtrate. Also, dioxins in the geotube filtrate were scarcely observed showing that when particulate matter was sufficiently removed during geotextile dewatering, the dioxins were essentially contained with the solids retained by the geotextile. Another study by Moo-Young et al. (1999) investigated the effluent quality from geotextile dewatering in terms of dioxin and furan concentrations, albeit at field scale and for limited conditions. However, mechanisms controlling particle matter migration during geotube dewatering process have not been investigated in these studies. The literature also includes very few works on the effect of geotextiles on particle transport under high infiltration rates. Lamy et al. (2008) and Lamy et al. (2013) carried out column experiments to investigate the effect of a geotextile on flow and colloid transport within homogenous sand and heterogeneous gravel under both saturated and unsaturated conditions. They concluded that the geotextile impacted flow homogeneity and colloid removal. However, the influence of the geotextile may also depend on the saturation degree of the soil-geotextile system. The ability to understand the mechanisms responsible for this transport could be potentially assessed in numerous ways but a combination of physical experimentation and modelling represent a robust manner to understand the mechanisms that dominate the fate and transport of fine grained particle matter during geotextile tube dewatering operations.

HYDRUS is a general software package for simulating water flow by solving the Richards equation, heat, solute movement, and microbial transport process by the convection-dispersion equation in two and three dimensional variably saturated porous media (Simunek, 2012; Šejna et al., 2014). Several studies have simulated the transport of bacteria, viruses, and colloids with HYDRUS including, but not limited to, Hayward

(2020), Morales et al. (2014) Morales et al. (2015), Balkhair (2017), Zhang et al. (2018) Zhang et al. (2018b), Jiang et al. (2010), Lamy et al. (2013), Pang et al. (2006), Bradford et al. (2003) and Gargiulo et al. (2008). Colloids represent a group of small size particles in solution that have effective diameters ranging from 1 nm to 10 μm (Chrysikopoulos and Sim, 1996; Sirivithayapakorn and Keller, 2003). In this thesis, sediment particles are considered as colloids due to their small size (D_{85}=11μm). Hence the approach for modeling colloidal transport, as described in many of the studies listed above, was used in this thesis. The terms of "particle" and "colloid" are used interchangeably in this thesis in all related experiments and HYDRUS modeling.

Transient, one-dimensional variably saturated water flow in porous media can be described using the Richards equation (Richards, 1931):

$$\frac{\partial \theta}{\partial t} = \frac{\partial}{\partial x}\left[K\left(\frac{\partial h}{\partial x} + \cos\alpha\right)\right] - S \qquad \text{Eq. [1]}$$

Where h is the water pressure head [L], θ is the volumetric water content [L^3 L^{-3}], t is time [T], x is the spatial coordinate [L] (positive upward), S is the sink term [L^3 L^{-3} T^{-1}], α is the angle between the flow direction and the vertical axis, and K(h) is the unsaturated hydraulic conductivity function [L T^{-1}].

Colloid fate and transport models are commonly based on the advection–dispersion equation but modified to account for colloid filtration (Harvey and Garabedian, 1991; Hornberger et al., 1992; Corapcioglu and Choi, 1996; Bradford et al., 2003). A general equation for colloid transport describing colloid/matrix mass partitioning in multi-dimensional form is given by (Šimůnek et al., 2012):

$$\frac{\partial \theta_c C_c}{\partial t} + \rho\frac{\partial S_{c1}}{\partial t} + \rho\frac{\partial S_{c2}}{\partial t} + \frac{\partial A_{aw}\Gamma_c}{\partial t} = \frac{\partial}{\partial_{x_i}}\left(\theta D_{ij}^c \frac{\partial C_c}{\partial x_i}\right) - \frac{\partial q_{ic} C_c}{\partial x_i} - \mu_{cw}\theta C_c - \mu_{cs}\rho S_c \qquad \text{Eq. [2]}$$

Where:

C_c: colloid concentration in the liquid phase (mobile colloids) [nL^{-3}]

S_c: colloid concentration in the solid phase (attached, immobilized, immobile colloids; two sites are considered, and they may have different interpretation; for example, S_{c1} may be represented as colloids attached to the solid phase, and S_{c2} may be represented as strained colloids) [nM^{-1}].

θ_c: volumetric water content accessible to colloids [L^3L^{-3}] (due to ion or size exclusion, θ_c may be smaller than the total volumetric water content θ)

ρ: bulk density [ML^{-3}]

A_{aw}: air-water interfacial area per unit volume [$L^2\ L^{-3}$]

Γ_c: colloid concentrations adsorbed to the air–water interface [$n\ L^{-2}$],

q_{ic}: Darcy's flux for colloids [LT^{-1}]

D_{ij}: dispersion coefficient for colloids [L^2T^{-1}]

T: time [T]

x_i: spatial coordinate [L]

μ_{cw}: colloid decay in the liquid phase [T^{-1}]

μ_{cs}: colloid decay in the solid phase [T^{-1}]

The value of θ_c is defined as:

$$\theta_c = \theta - \theta_{im} \qquad \text{Eq. [3]}$$

Where θ is the total water content [L^3L^{-3}] and θ_{im} is the water content that is not accessible to mobile colloids [-] due to size exclusion (Bradford et al., 2006).

Colloid mass transfer between the aqueous and solid phases is traditionally described using attachment-detachment models of the form (Šimůnek et al., 2012):

$$\rho \frac{\partial S_{c1}}{\partial t} = \theta_c \psi_c K_{ac} C_c - \rho K_{dc} S_{c1} - \mu_{cs} \rho S_{c1} \qquad \text{Eq. [4]}$$

Where:

k_{ac}: colloid attachment coefficient [T^{-1}]

k_{dc}: colloid detachment coefficient [T^{-1}]

ψ_c: dimensionless colloid retention function or blocking coefficient

To simulate reductions in the attachment coefficient due to filling of favorable sorption sites, ψ_c is sometimes assumed to decrease with increasing colloid mass retention.

$$\psi_c = 1 - \frac{S_{c1}}{S_{c1}^{max}} \qquad \text{Eq. [5]}$$

Which S_{c1}^{max} is the maximum solid-phase colloid concentration [nM^{-1}].

Straining involves the entrapment of colloids in downgradient pores that are too small to allow particle passage (Simunek et al., 2006) and is calculated using Equation 6. The magnitude of colloid retention by straining depends on both colloid and porous medium properties (McDowell-Boyer et al., 1986; Bradford et al., 2002; Bradford et al., 2003). Carsel and Parrish (1988) calculated that a 2 μm colloid, which is the size of a clay particle, will be excluded or strained in 10 to 86% of the soil pore space for the various soil textures (Bradford et al., 2006). These percentages should significantly increase if the soils become unsaturated. Bradford et al. (2003) also found that straining tends to increase with decreasing porous media median grain size and increasing the colloid size.

$$\rho \frac{\partial S_{c2}}{\partial t} = \theta_c \psi_{str} K_{str} C_c \qquad \text{Eq. [6]}$$

Where:

k_{str}: colloid straining coefficient [T^{-1}]

ψ_{str}: dimensionless straining blocking coefficient

$$\psi_{str} = (\frac{d_{50} + x}{d_{50}})^{-\beta} \quad \text{Eq. [7]}$$

Where d_{50} is the median grain size of the porous media [L], β is a fitting parameter [-], and x is distance from the porous-medium inlet [L]. Hence, straining is greatest at the column inlet and is expected to decrease with increasing distance. These governing flow and transport equations are solved numerically in HYDRUS using standard Galerkin-type linear finite element schemes which are solved with various matrix algebra methods (Šimůnek et al., 2012).

6.2 Material and Methods

6.2.1 Sediment

BH sediment was used for the laboratory testing in this chapter. The physical properties of the material were identified in Chapter 3. In summary, the BH sediment is rich in organic matter (TOC~30%), has a small particle size (D_{85}=11μm), a specific gravity of 1.71, and a bulk density of 1.07 ± 0.05 g/cm^3. The sediment's average in-situ water and solids content of 957±71 % and 9±1 % were found using the composite gravity core sampling described in Chapter 3. For the testing in this chapter, sediment was diluted to approximately 5% solids content to simulate dredging conditions. Although this solids content is largely unknown, pilot scale work at BH at the time of this work suggests that solids contents could be as high as 5% and hence it was adopted for this study. The two chemical additives (Solve 7118 and Solve 9244) were added at concentrations of 13% and 10% of the total volume of sediment slurry, respectively, to improve dewatering capabilities for the BH sediment. These optimum additive dosages were found as described in Chapter 4 and Tackley et al. (2020).

6.2.2 Geotextile

The GT-500 geotextile was used in the experiments. Water flow rate through this woven geotextile is reported by the manufacturer to be 813 L/min/m^2. The apparent opening size

(AOS) is 430 μm and the thickness averages 1.8 mm. The values for O_{50} and O_{95} are 80 μm and 195 μm, respectively (GT 500 technical data sheet, TenCate Corporation, 2015).

6.2.3 Experimental Testing Program

Table 6.1 summarizes each of the experiments performed for this chapter. The various subsections below provide more details on the procedures and objectives for each test type.

Table 6.1 Summary of tests performed in this study

Test Type	Pressure	Test Label	Objective
Pressure Filtration Testing (PFT)	21 kPa	Trial 1	- Observe the behavior of the particle transport under laboratory controlled conditions - Investigate the role of filter cake and pressure on the particle transport during the dewatering - Develop a filter cake for the transport tests
		Trial 2	
		Trial 3	
	35 kPa	Trial 1	
		Trial 2	
		Trial 3	
	49 kPa	Trial 1	
		Trial 2	
		Trial 3	
Transport Testing	21 kPa	Phase 1-BH water	- Observe the behavior of particle transport through the developed filter cake, under pressure - Investigate particle transport mechanisms
		Phase 2-BH water	
		Phase 3-MQ water	
		Phase 4-MQ water-no pressure	
	35 kPa	Phase 1-BH water	
		Phase 2-BH water	
		Phase 3-MQ water	
		Phase 4-MQ water-no pressure	
	49 kPa	Phase 1-BH water	
		Phase 2-BH water	
		Phase 3-MQ water	
		Phase 4-MQ water-no pressure	

6.2.3.1 Pressure Filtration Testing (PFT)

To examine particle migration during geotextile dewatering of the BH sediment, laboratory pressure filtration testing (PFT) was performed to evaluate the flow rate, filtration efficiency, and particle migration during the dewatering process. PFT was also conducted

to investigate the influence of pressure on the sediment dewatering process as well as particle migration through a developed filter cake. The increase in solids content to 5% compared to that discussed in Chapter 4 (0.3 %) caused the filter cake to develop at an increased rate. Three confining pressures of 21, 35, and 49 kPa (3, 5, and 7 psi) were applied and each test was repeated three times (i.e. a "trial" in Table 6.1).

As shown in Figure 6.1a, the PFT apparatus consisted of an upper aluminum lid with a pressure inlet, a translucent acrylic chamber (middle chamber) with an inner diameter of 7.5 cm and a height of 17 cm, and a lower acrylic chamber with an outlet to collect the filtrate.

For testing, a circular geotextile specimen (8.5 cm diameter) saturated in Milli-Q water (meeting ASTM Type 1 guidelines) (ASTM International, 1999) was placed on the lower chamber beneath the O-ring (shown in orange in Figure 6.1). The middle chamber was fixed at the top by several screws.

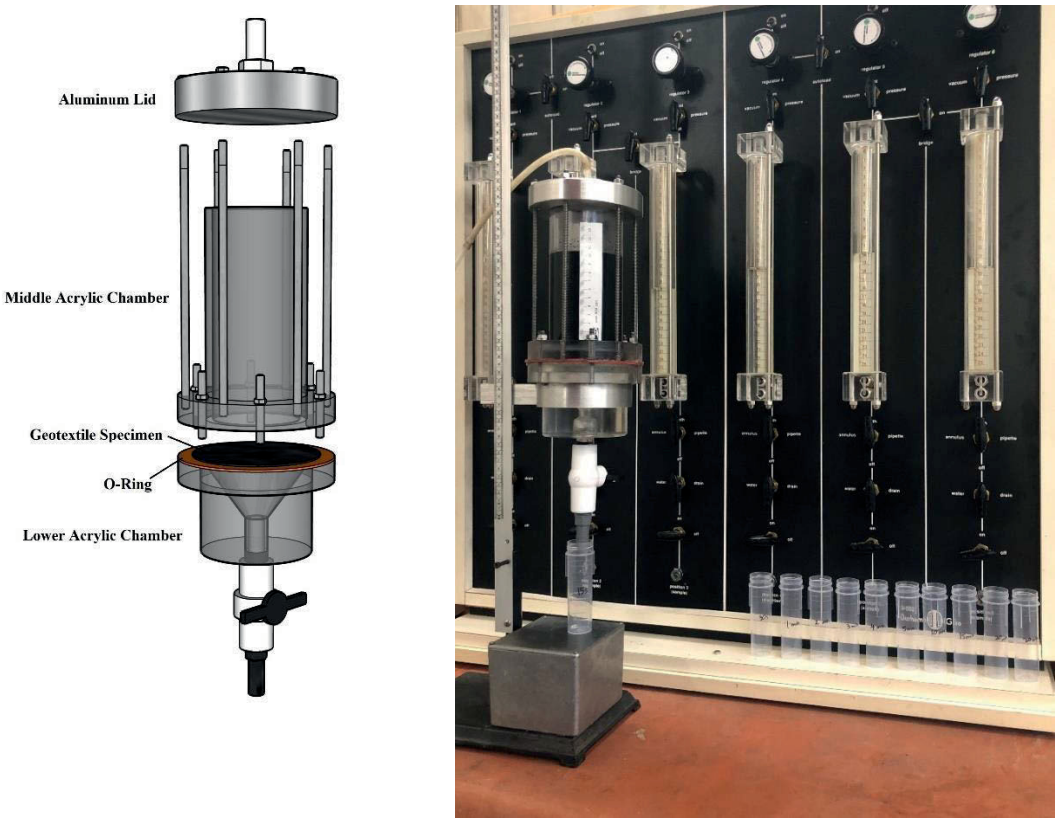

a b

Figure 6.1 Pressure Filtration Test (PFT) (a) cell, (b) setup

A volume of 700 mL of Milli-Q water was poured into the reservoir (middle chamber) and passed through the geotextile three consecutive times to remove any trapped air, as well as to ensure a watertight condition. For each test, 65 mL of Solve 7118 and 50 mL of Solve 9244 were added to 500 mL of BH sediment at 5% solids content in a separate container. With the outflow valve closed, the prepared slurry was then poured into the testing reservoir with a graduated vial placed under the outlet to collect the filtrate. The initial height of slurry was measured, and the top cover was placed to apply the pressure. Upon creating an airtight condition by fastening of the cover, the outflow valve was then opened, allowing the slurry to pass through the geotextile.

For each PFT trial, filtrate volume was recorded, and the corresponding particle concentrations were measured using a flow imaging machine (FIM) (Alimohammadi et al., 2019). Filtrate was sampled at different time intervals measured from the beginning of each

dewatering test (15 s, 30 s, 60 s, 1 min, 2 min, 3 min, 4 min, 5 min, 10 min, 15 min, 20 min, 30 min). The change in the slurry's height was also recorded at the same time intervals. The solid content of filter cake was measured after each test.

6.2.3.2 Transport Testing

Transport testing experiments were conducted to assess the role of a developed filter cake on particle transport, as well as possible mechanisms controlling particle transport during the dewatering process. To conduct these transport tests, the development of a filter cake was first required. A volume 500 mL of conditioned BH sediment was filtered using the normal (aforementioned) PFT procedure at the desire pressure (i.e. 21, 35, and 49 kPa) and as a result, a filter cake was deposited on the geotextile. Each individual transport test was performed for the first three phases at the same pressure that the filter cake was developed at; while phase 4 was conducted under atmospheric pressure (see Table 6.1). Phase one and two of these tests consisted of filtering of BH water (containing particle matter) through the filter cake, while Milli-Q water was filtered through the filter cake in phases three and four. To characterize the conservative transport parameters (such as dispersity of the filter cake) a tracer experiment was performed in conjunction with the two first phases. During phases 1 and 2, 3 ml of Br^- (1000 mg/L) was added to 500 mL of BH water; 480 mL of this water was then poured into the reservoir of the PFT apparatus as shown in Figure 6.2 (on top of the filter cake) with the outlet valve closed. The remainder (i.e. 20mL) was used to confirm the initial concentration of the tracer and particles in BH water. Following preparation of the apparatus (sealing of the containment cell), the desired pressure was applied (e.g. 21 or 35 or 49 kPa) and the outlet valve was opened. Effluent was collected during filtration until the water level reached that of the filter cake height. Water samples were taken at different time intervals from the beginning of the test (15s, 30s, 1min, 2min, 3min, 4 min, 5 min, 10 min, etc.). However, time intervals were longer (30min, 1hr, 2hr, etc.) in phase four due to testing at atmospheric pressure conditions. The volume of effluent as well as particle concentration at above mentioned time intervals were measured. The effluent concentrations of bromide were determined using inductively coupled plasma-mass spectrometry (ICP-MS) at the Centre for Water Resources at Dalhousie University.

In the third phase of each transport test, 500 mL of Milli-Q water was used instead of BH water, without any Br^- tracer (at the specified pressure). The fourth phase was conducted using the falling head test (FHT) procedure, where 500 mL of Milli-Q water was filtered through the filter cake-geotextile system without applying any pressure beyond that supplied by the height of the water. The height of the water on top of the filter cake was monitored during the FHT (~ 4 h). As with the previous three tests, volume of filtrate, Br^- and particle concentrations were measured in all effluent samples. At the end of the experiment, the filter cake was completely removed from the geotextile and placed into the oven to determine the solids content and total porosity. Table 6.2 presents the initial conditions of the transport tests. It should be noted that phases one and two of the transport experiments were conducted to make a stable condition in the filter cake/geotextile system, while particle transport mechanisms and factors affecting the mechanism parameters were studied using the third and fourth phase results.

a b

Figure 6.2 Transport experiment setup: a) under pressure, b) FHT – without pressure

Table 6.2 Initial conditions of transport experiments

Phase	Applied pressure (kPa)	Water in reservoir	Filter cake height (cm)	Initial concentration in reservoir water	
				Bromide (ppm)	Particles (#/mL)
1	21	BH water	5.5	5.85	40145
2	21	BH water	5.5	5.75	41325
3	21	MQ water	5.5	n.a	755
4	Atmospheric	MQ water	5.5	n.a	705
1	35	BH water	5.3	5.78	42500
2	35	BH water	5.3	5.69	41320
3	35	MQ water	5.3	n.a	740
4	Atmospheric	MQ water	5.3	n.a	810
1	49	BH water	4.8	5.74	39929
2	49	BH water	4.8	5.57	36676
3	49	MQ water	4.8	n.a	789
4	Atmospheric	MQ water	4.8	n.a	755

6.2.4 HYDRUS modeling

The C-Ride module of HYDRUS 1-D (Šimůnek et al., 2012) was used to simulate the one-dimensional transport of particles through the filter cake during the aforementioned transport experiments.

In this research, the modeling of flow rate and particle transport through the filter cake during the dewatering process involved the following assumptions:

- The filter cake and geotextile act as one integrated matrix (system).
- The matrix of geotextile/filter cake is fully saturated.
- Since the filtration process is mostly controlled by filter cake properties (Soo-Khean Teoh et al., 2006; Chi Tien et al., 2011; Weggel and Ward, 2012; Tackley et al., 2019), the hydraulic and advection-dispersion parameters of the filter cake (i.e. volumetric water content, saturated hydraulic conductivity, dispersity coefficient, etc.) were considered for the whole matrix.
- Due to the short duration of the experiments, degradation and transformation of colloids were neglected (Zhang et al. 2017). Hence, μ_{cw} and μ_{cs} coefficients in equation [2] were taken as zero.

- Since the matrix is considered to be fully saturated, it was assumed that there was no air-water interfacial area (A_{aw}=0) and no colloid deposit on the air-water interface ($\Gamma_c = 0$).
- Due to the short duration of the transport experiments and also relatively low solids content in water, ψ_c (blocking coefficient) is considered to be 1, which means no decreasing of attachment coefficient with time (Bradford et al. 2003).
- Straining, which is a depth dependent mechanism, was not considered here due to several reasons: First, the height of the matrix was only 5 cm. Second, the spatial distribution of retained colloids in the matrix would need to be observed in addition of effluent concentration to find the straining rate coefficient.

In order to simulate the particle transport through the geotextile/filter cake system using the HYDRUS model, the following steps were conducted:

1. Model set up: to define physical characteristics of geotextile/filter cake system (e.g. dimensions), initial conditions, and boundary conditions;
2. Model calibration: to calibrate the hydraulic characteristics of geotextile/filter cake system (e.g. longitudinal dispersivity, hydraulic conductivity, saturated water content) based on the observed tracer (bromide) response curve;
3. Simulation of the colloid transport through the geotextile/filter cake system considering three different mechanisms:
    a. M_1: attachment
    b. M_2: detachment
    c. M_3: attachment and detachment
    d. M_4: attachment and detachment under atmospheric pressure

    (M_1, M_2, M_3 and M_4 are used throughout this chapter to quickly describe the mechanisms modelled).
4. Parametric study: to investigate the effects of different parameters (e.g. pressure, filter cake thickness and properties) on simulated results (i.e. attachment and detachment coefficient).

6.2.4.1 Model Set-Up

The one-dimensional model was established in HYDRUS 2D/3D version 2 (PC-Progress, Prague, Czech Republic). The filter cake and geotextile were set as one integrated matrix. Saturated hydraulic conductivity of the filter cake was calculated based on the measured effluent volume over time, considering the constant total head during the transport tests. Porosity (i.e. volumetric water content) was also calculated by measuring the amount of water inside of a known volume of filter cake (height of 5.5, 5.3, and 4.8 cm at pressure of 21, 35, and 49 kPa respectively; diameter of 7.5 cm). Boundary conditions of constant head, no flux and seepage face were defined for the top, sides, and bottom of the filter cake/geotextile matrix respectively. The applied pressure during transport experiments was converted to equivalent water head for simulation. The C-Ride module was activated by selecting the solute transport check box and the colloid-facilitated solute transport "radio button". Crank-Nicholson time weighting scheme and the Galerkin finite element space weighting scheme was specified. Reaction parameters for the particles (i.e. colloids in the model) were fitted considering three scenarios: only attachment (M_1), only detachment (M_2), and both attachment/detachment (M_3). A third type solute flux boundary condition was applied to the flux boundaries to ensure conservation of mass for the simulations. To simulate water flow through the filter cake/geotextile matrix, the single porosity model with the modified van Genuchten hydraulic model, assuming no hysteresis, was specified. A finite element (FE) mesh size of equal 0.25 cm was specified for the matrix. The FE mesh generator function built into HYDRUS was used to generate each of the FE meshes.

6.2.4.2 Calibration

The hydraulic characteristics of model were initially calibrated by simulating the bromide (Br^-) tracer (i.e. K_d of zero) through the matrix. At each pressure, the first three transport phases were simulated as one single test; considering an injection pulse (s) of tracer equal to the time of first two phases (i.e. when the reservoir water had particles and bromide present). For example, at 35 kPa, a pulse of 5.7 ppm of Br^- was applied to the filter cake over 550 seconds. Longitudinal dispersivity and porosity of the filter cake were calibrated with porosity being slightly different from that measured volumetrically. Porosity was calculated in the laboratory by measuring the water weight inside the known volume of

filter cake after each transport test. Porosity of 0.91, 0.85, and 0.85 were calculated at pressure of 21, 35, and 49 kPa, respectively. Calibrated parameters that produced a simulated tracer response curve, which most closely matched the observed tracer response curve in lab experiments, were selected as base parameters for all subsequent modeling.

Other flow parameters such as residual water content (Θ_r), pore connectivity (l), empirical coefficients of α and n (see Table 6.3) were chosen from HYDRUS database according to the texture similarity of BH fine grained sediment to silt.

Table 6.3 Assumed and calibrated hydraulic and advection dispersion parameterization values for the geotextile/filter cake matrix. Values in the square brackets were calibrated to enable matching of the simulated data to the laboratory observed data.

Parameter	**Unit**	Transport test at		
		21 kPa	35 kPa	49 kPa
Residual water content, Θ_r,	cm^3/cm^3	0.0501	0.0501	0.0501
Saturated water content, Θ_s,	cm^3/cm^3	[0.95]	[0.87]	[0.87]
Fitted parameter, α,	1/cm	0.0066	0.0066	0.0066
Fitted parameter, *n,*	-	1.6769	1.6769	1.6769
Saturated hydraulic conductivity, K_s,	cm/s	[0.00055]	[0.00042]	[0.00034]
Pore connectivity, *l*, (dimensionless)	-	0.5	0.5	0.5
Bulk media density, p_b	gr/cm^3	1	1	1
Longitudinal dispersivity, D_L	Cm	[0.5]	[0.5]	[0.5]
Transverse dispersivity, D_T	Cm	0.1	0.1	0.1

6.3 Results and Discussion

6.3.1 Pressure Filtration Testing (PFT)

Figures 6.3a, b, and c present the filtrate volume and height of sediment slurry inside the chamber of the PFT apparatus at pressures of 21, 35, and 49 kPa, respectively. The x-axis presents cumulative time of the test over which samples were taken, while the y-axis displays filtrate volume (left) and sediment height (right). As these three figures show, at each pressure, the triplicate trial results mostly overlapped indicating that results were generally reproducible. The small disparity in results observed was likely due to slight variations of the pore size distribution of the geotextile sample, differences in floc size distribution in each trial, and/or the accuracy of controlling the applied pressure (±3 kPa).

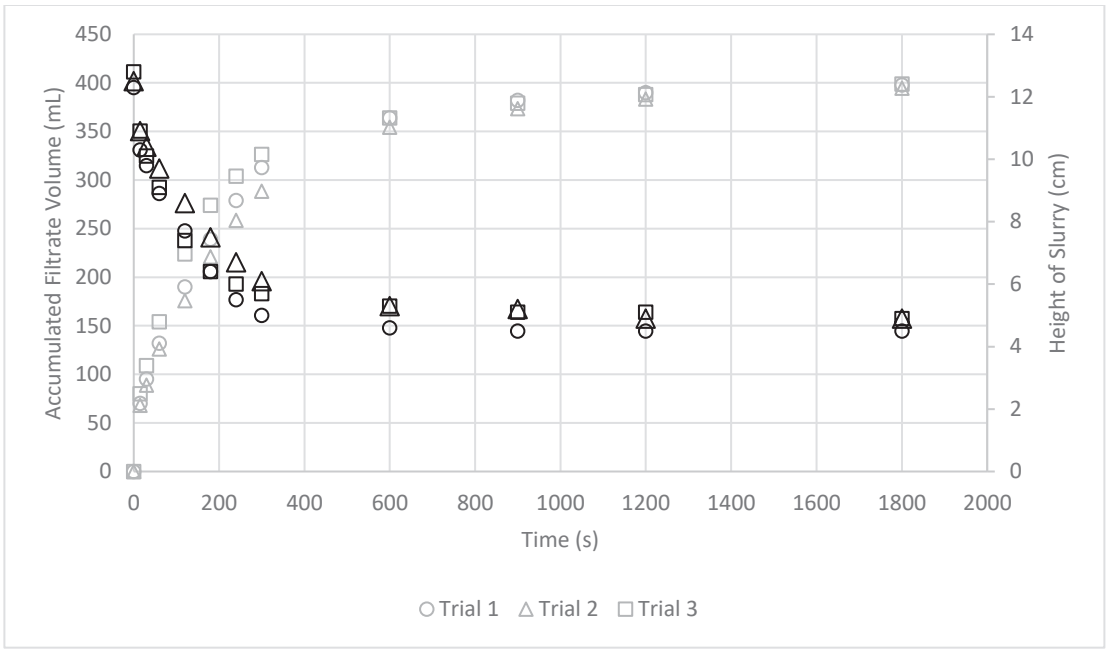
Accumulated Filtrate Volume (mL)
Height of Slurry (cm)
Time (s)
Trial 1
Trial 2
Trial 3

a

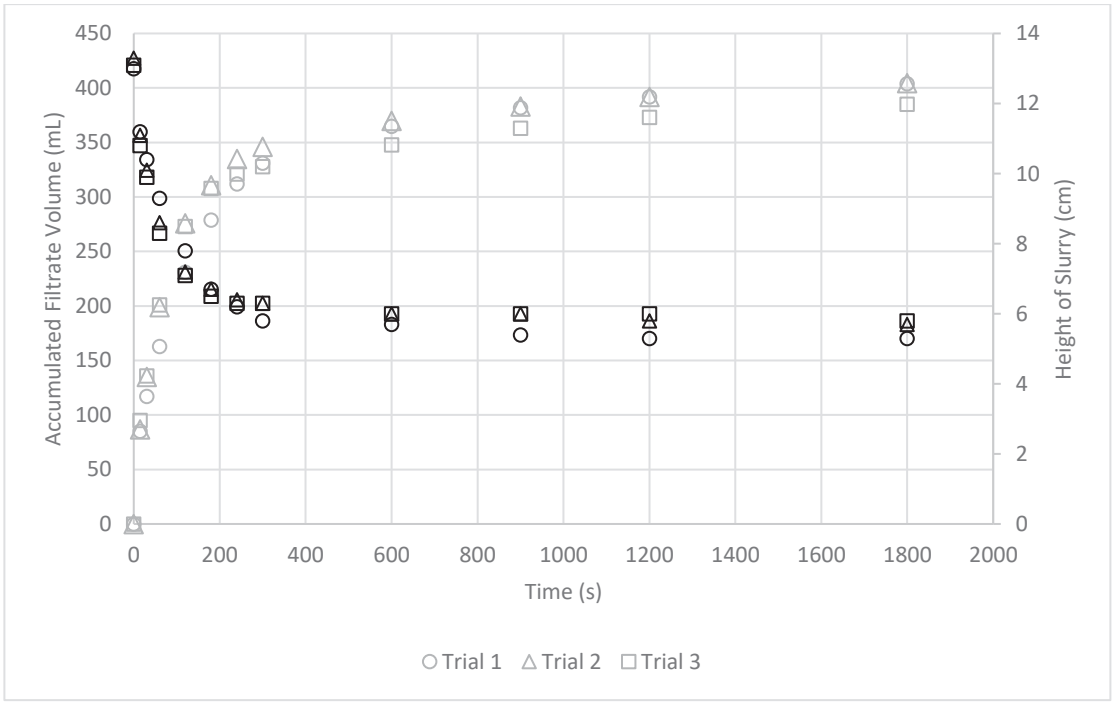
Accumulated Filtrate Volume (mL)
Height of Slurry (cm)
Time (s)
Trial 1
Trial 2
Trial 3

b

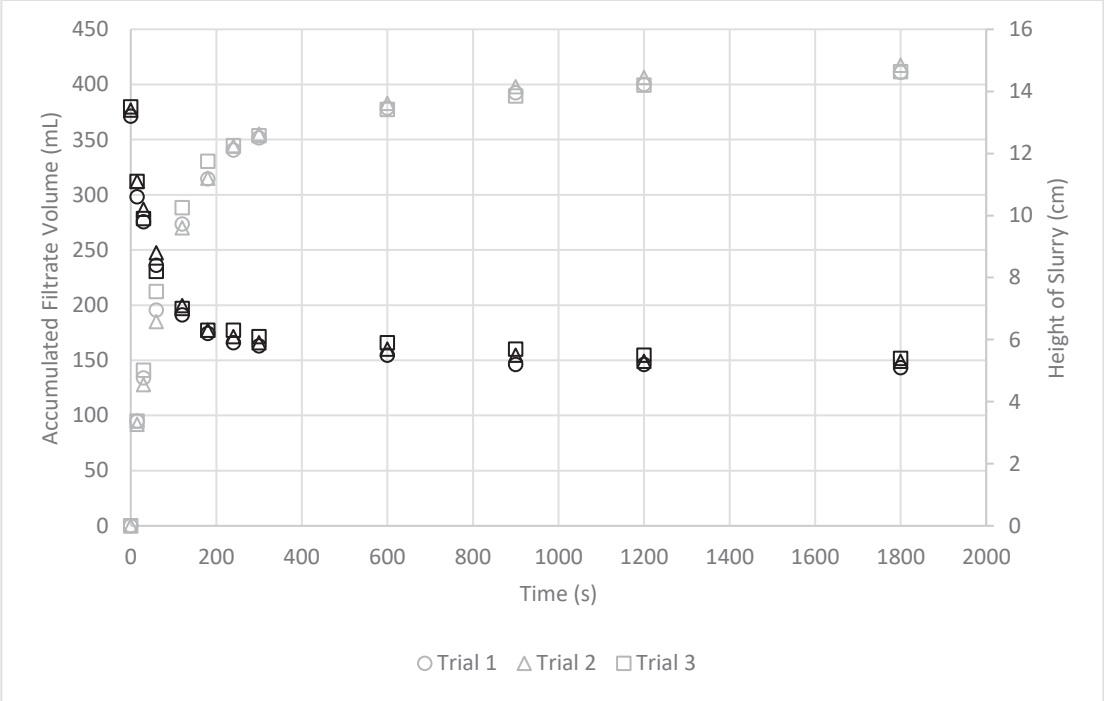

c

Figure 6.3 Filtrate volume and height of sediment for PFT at (a) 21, (b) 35 and (c) 49 kPa. (Curves in grey and black present the accumulated volume and height of slurry, respectively)

The average values of filtrate volume and height of sediment for each of the three different pressures are presented in Figure 6.4 where the influence of pressure on dewatering rate and filter cake formation can be observed. During 30 minutes of PFT, maximum filtrate volumes of 394, 398, and 413 mL were obtained at pressures of 21, 35, 49 and kPa respectively, indicating that as the pressure increased, the amount of water expelled increased. Also, by increasing the confining pressure, the sediment compressed to a greater extent, and the final height (at 30 min) of the filter cake decreased. Final filter cake heights of 5.9, 5.7, and 5.3 cm were obtained at the pressures of 21, 35, and 49 kPa respectively from the initial sediment slurry height of 13.4 cm.

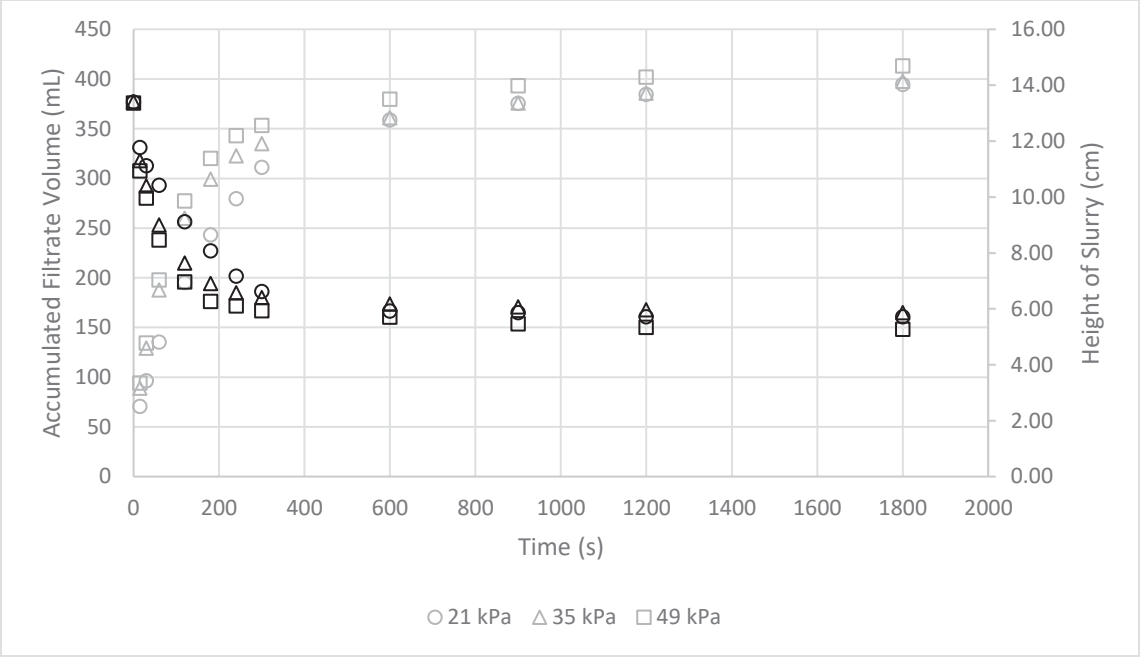

Figure 6.4 Average filtrate volume and sediment height for PFT at different pressure. (Curves in grey and black present the accumulated volume and height of slurry, respectively)

The instantaneous flow rate from these tests was calculated using the following equation:

$$\emptyset = \frac{V_{filtrate}}{A \times t} \qquad \text{Eq. [8]}$$

Where $\emptyset$ is the instantaneous flow rate of water passing through the geotextile (cm/s), $V_{filtrate}$ is the volume of collected filtrate passing through the geotextile (cm^3), t is the time to collect the corresponding volume of filtrate (second), and A is the area of geotextile involved in filtration (cm^2).

As shown in Figure 6.5, at each of the different pressures, the flow rate decreased with time. Because the sediment particles settled and compressed with time, the height of filter cake depositing on the geotextile increased, and the hydraulic conductivity of the system decreased to a stable value. The flow rate maintained a constant value of 0.005 cm/s after about 300s. As the test continued, the flow rate decreased to approximately zero.

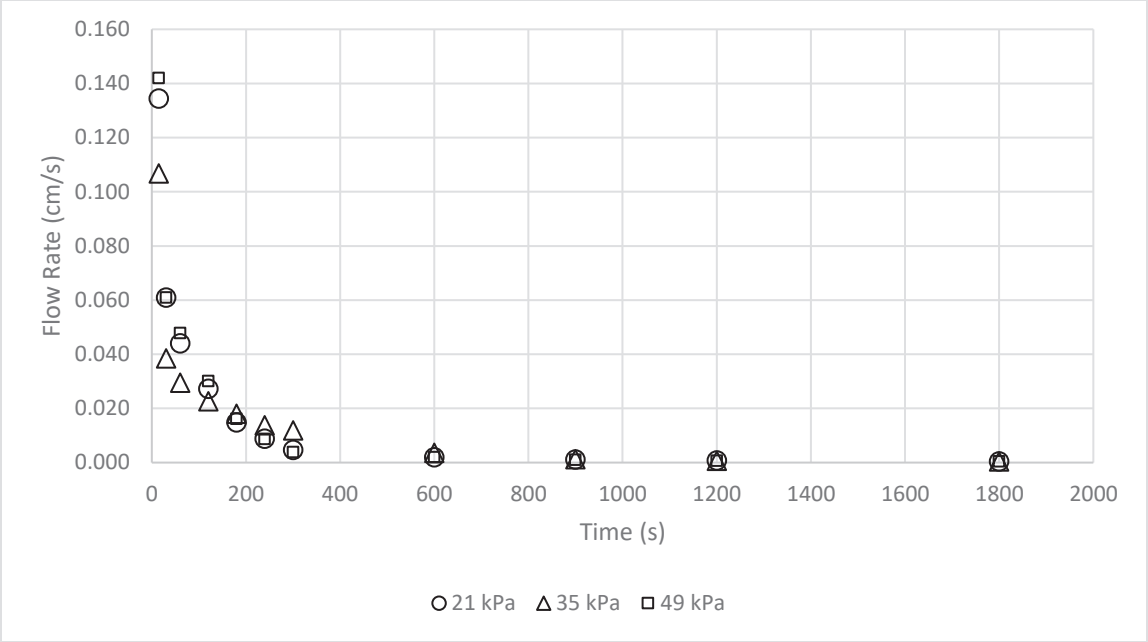

Figure 6.5 Average flow rate for PFT at different pressure

Table 6.4 presents the solids content (SC) of the filter cake at the end of each trial of PFT. By increasing the confining pressure from 21 to 35 kPa, to 49 kPa, the solids content increased from 12.4% to 12.9% and 13.2%, respectively. Generally, it can be said that by increasing pressure in a geotextile dewatering process, flow rate and solids content increase.

Table 6.4 PFT filter cake solids content (note: starting solids content of 5%)

Pressure (kPa)		Solids Content (%)	Average Solids Content at the End of Test (%)
21	Trial 1	12.4	12.4
	Trial 2	12.5	
	Trial 3	12.2	
35	Trial 1	13.2	12.9
	Trial 2	12.7	
	Trial 3	12.9	
49	Trial 1	12.7	13.2
	Trial 2	13.3	
	Trial 3	13.5	

Figure 6.6 presents the collected filtrate particle concentration at each of the conducted trials. Unlike previously discussed results of filtrate volume and sediment height (i.e. Figure 6.3), larger variations were observed in particle concentration for the different trials, at similar pressures. Again, these differences may be due to variation in pore size distribution of the geotextile sample, accuracy of applied pressure and particle size distribution of the conditioned sediment slurry. As shown in Figure 6.6, particle concentration is highest at the early stages of dewatering, decreasing as the filtration process proceeds, indicating that by depositing the filter cake on the geotextile, the filtration efficiency improves and more particles can be retained by geotextile/filter cake system.

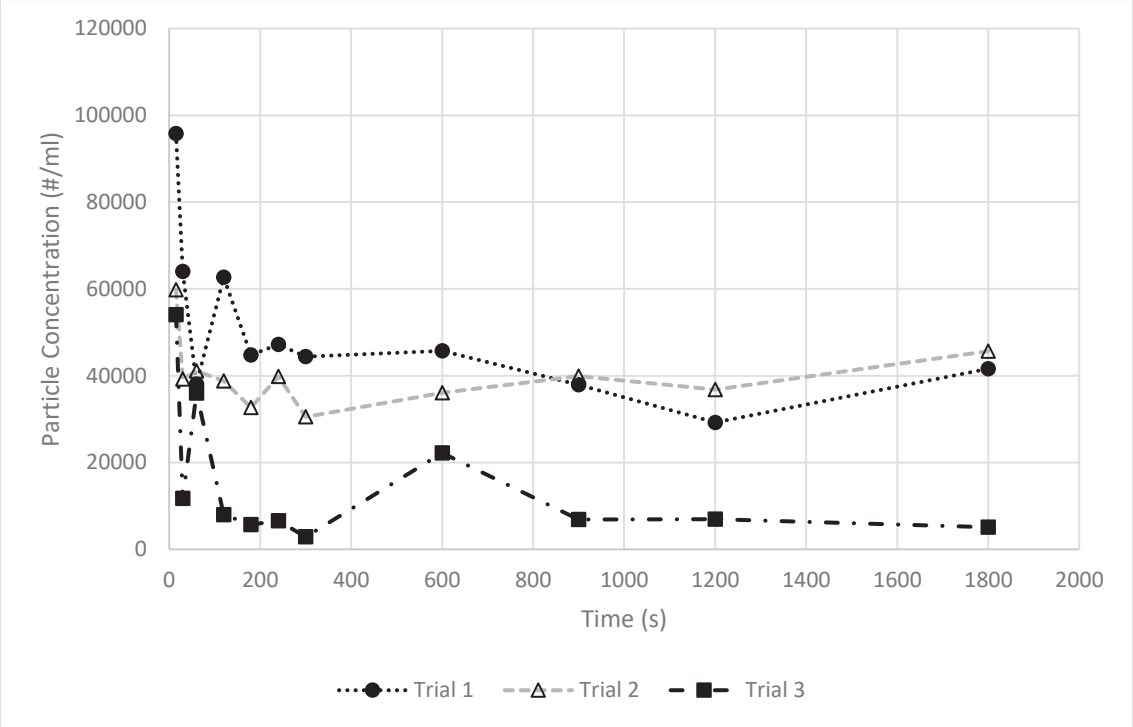

a

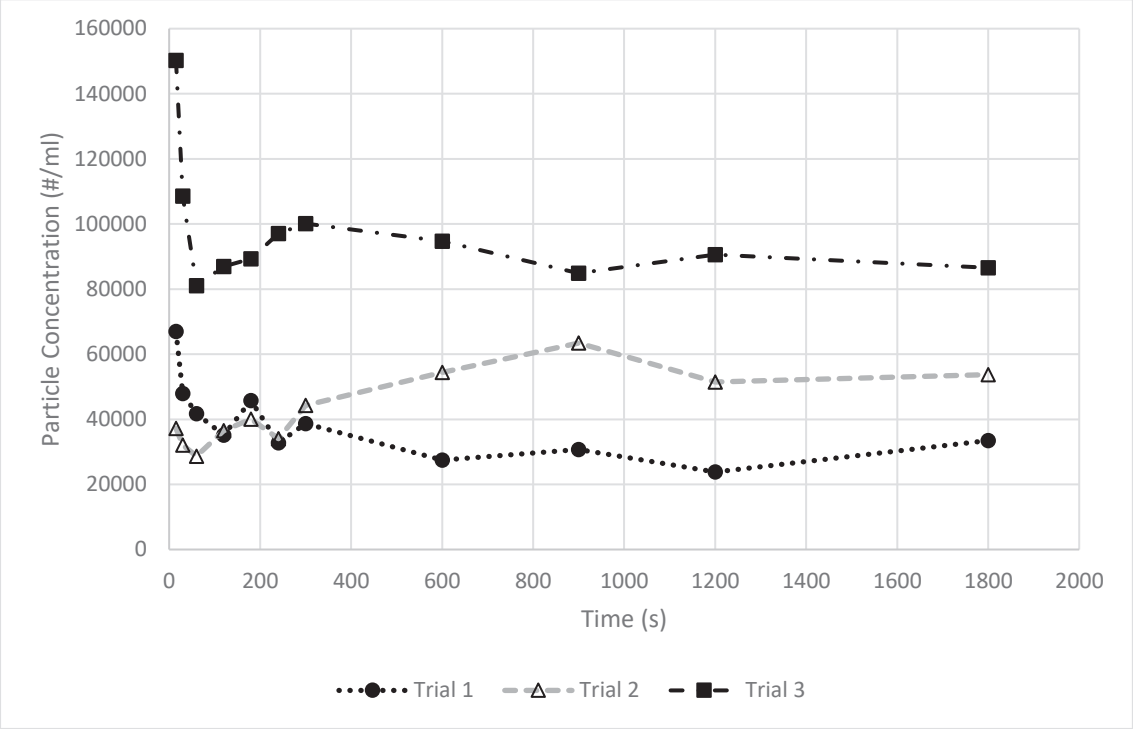

b

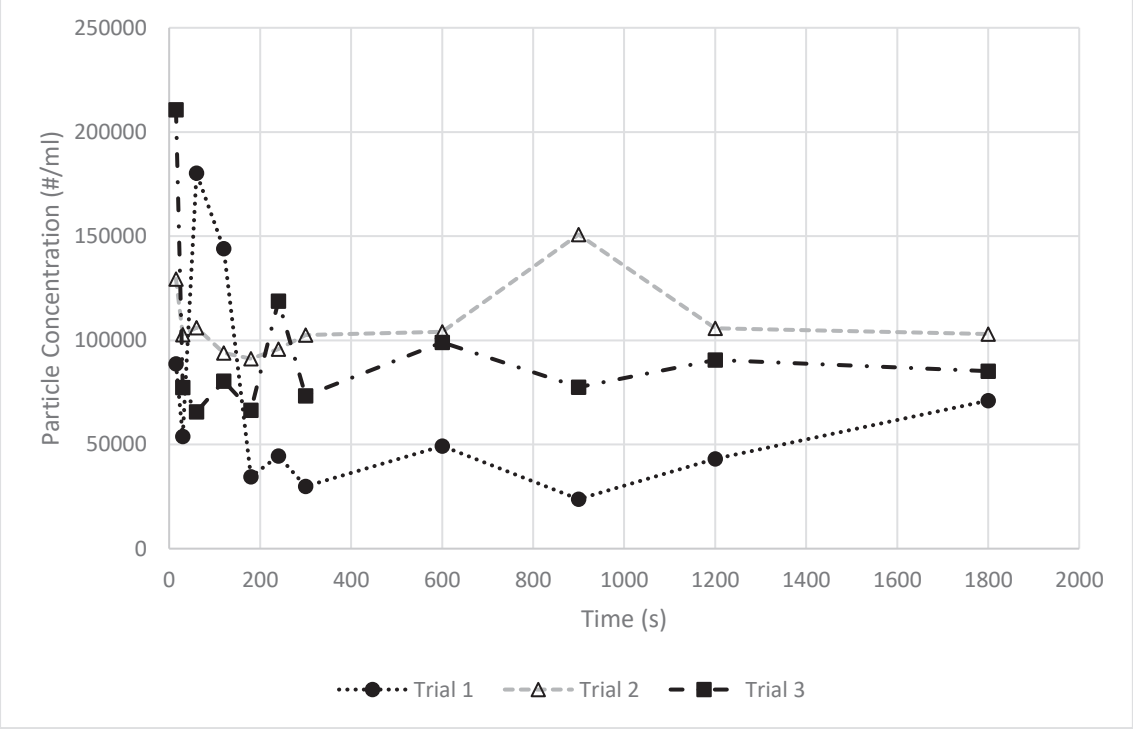

c

Figure 6.6 Particle concentration in collected filtrate for PFT at (a) 21 (b) 35, and (c) 49 kPa confining pressure

The average particle concentrations of three trials, at the different pressures are presented in Figure 6.7. There were 142,000 #/mL particles measured in the collected filtrate after 15 s at a pressure of 49 kPa, which reduced to a constant amount of approximately 80,000 #/mL after 600 s. When the PFT was conducted at 35 kPa, the particle concentration in collected filtrate decreased from 85,000 #/mL to 60,000 #/mL between 15 s and 600 s. Moreover, particle concentration values of 70,000 and 30,000 #/mL were obtained at 15 s and 600 s when 21 kPa was applied. These results indicate that the number of particles passing through the filter cake/geotextile system increases as the confining pressure increases, especially at the beginning of the experiment when the filter cake has not yet formed. However, when the system reaches a stable condition, with less variation in filter cake height (~ 600 s), particle concentrations maintain a constant range, showing the role of filter cake in promoting the retention performance (Kutay and Aydilek, 2004).

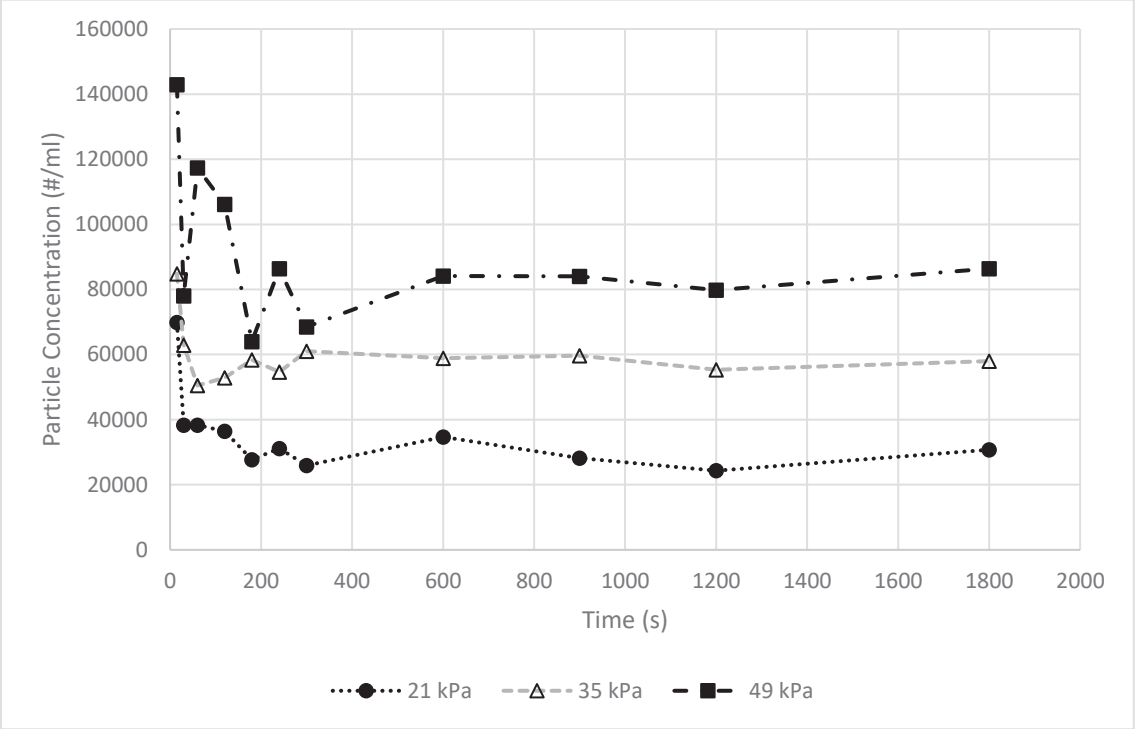

Figure 6.7 Average particle concentration in collected filtrate for PFT at different pressure

6.3.2 Transport Experiments

For each series of transport tests, at each of the desired pressures (i.e. 21 or 35 or 49 kPa), the filter cake was first developed using the PFT procedure at the desired pressure. Since no solids were added to the column during the transport experiments and it was assumed that no additional compression of the filter cake took place, the solids content of the filter cake did not change throughout the transport test. A filter cake volumetric water content (equivalent to porosity under saturated conditions) was found by measuring the volume of water in the known volume of filter cake at the end of test.

Figure 6.8 shows the volume of collected filtrate during the transport experiments at different pressures. It should be noted that each phase was ceased when the water level in the cell reached the top of the filter cake. It can be observed that the first three phases (under pressure) were completed in approximately 1200 s, while the fourth phase took approximately 14,400 s (4 hr). The saturated hydraulic conductivity (K_s) of the filter cake/geotextile matrix was determined by considering each transport experiment at the given pressure as a constant head pressure test. Experimental results found the hydraulic conductivity to range between 0.0005-0.0006 cm/s, 0.0004-0.0005 cm/s, and 0.00025-0.0004 cm/s for the first three phases at pressures of 21, 35, and 49 kPa, respectively. These results showed that the hydraulic conductivity of the system was reduced slightly as the pressure increased. HYDRUS modeling was also used to find the hydraulic conductivity, which could be considered constant during the transport experiments. As presented in Figure 6.9, K_s equal to 0.00055, 0.00042, and 0.00034 cm/s matched best with experimental results at pressure of 21, 35, and 49 respectively. These values were selected for subsequent modeling.

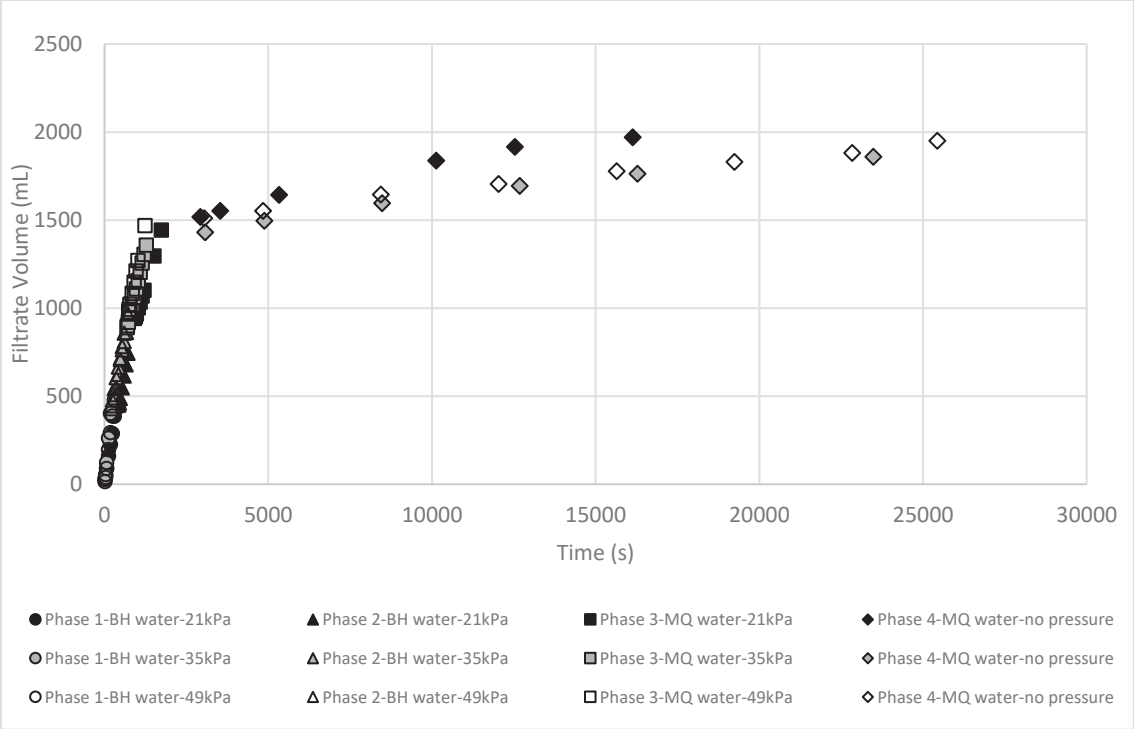

Figure 6.8 Filtrate volume at each individual transport experiment phases

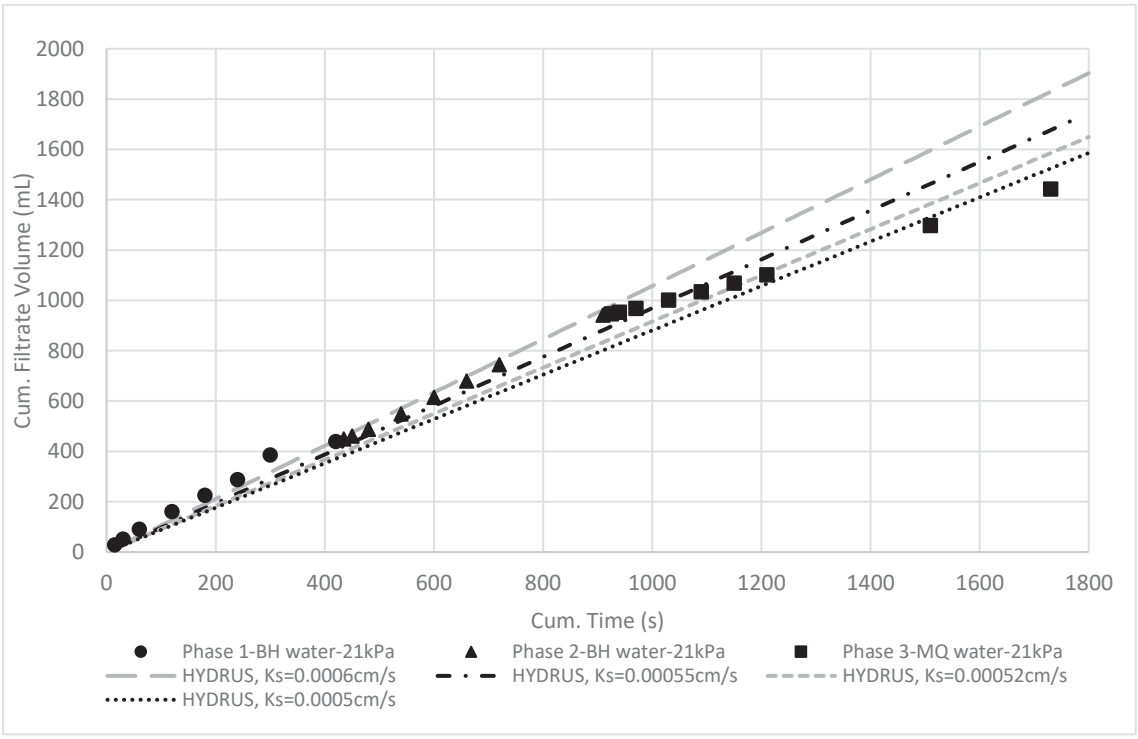

a

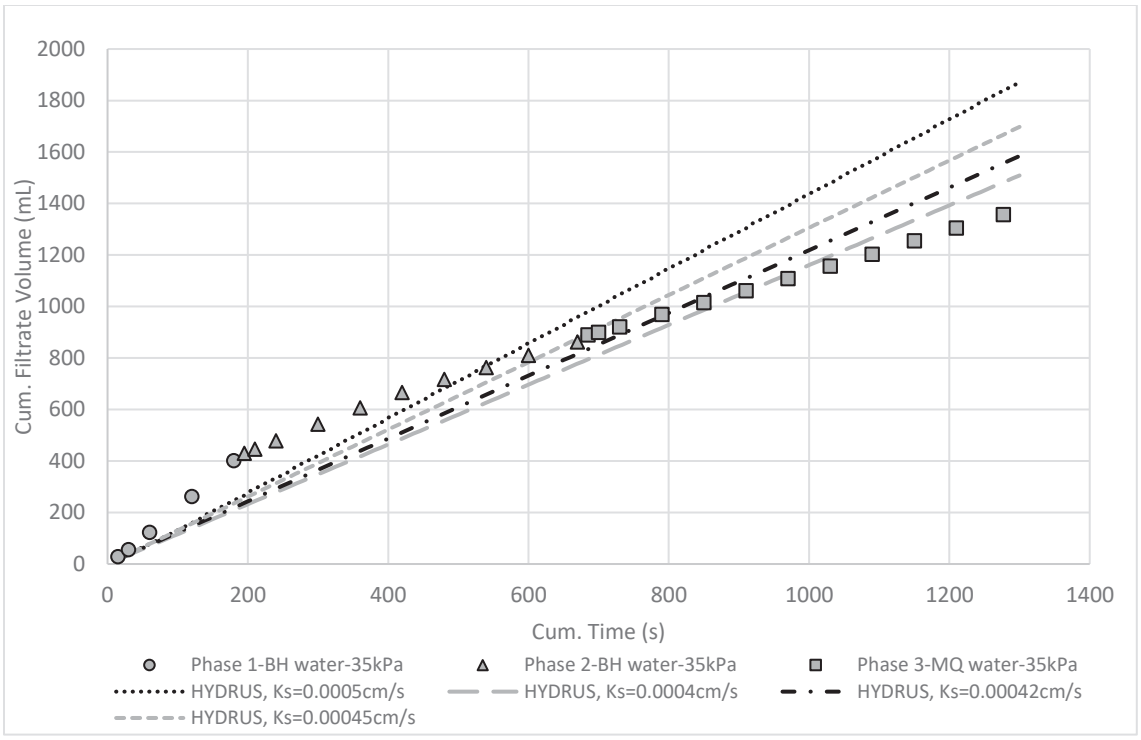

b

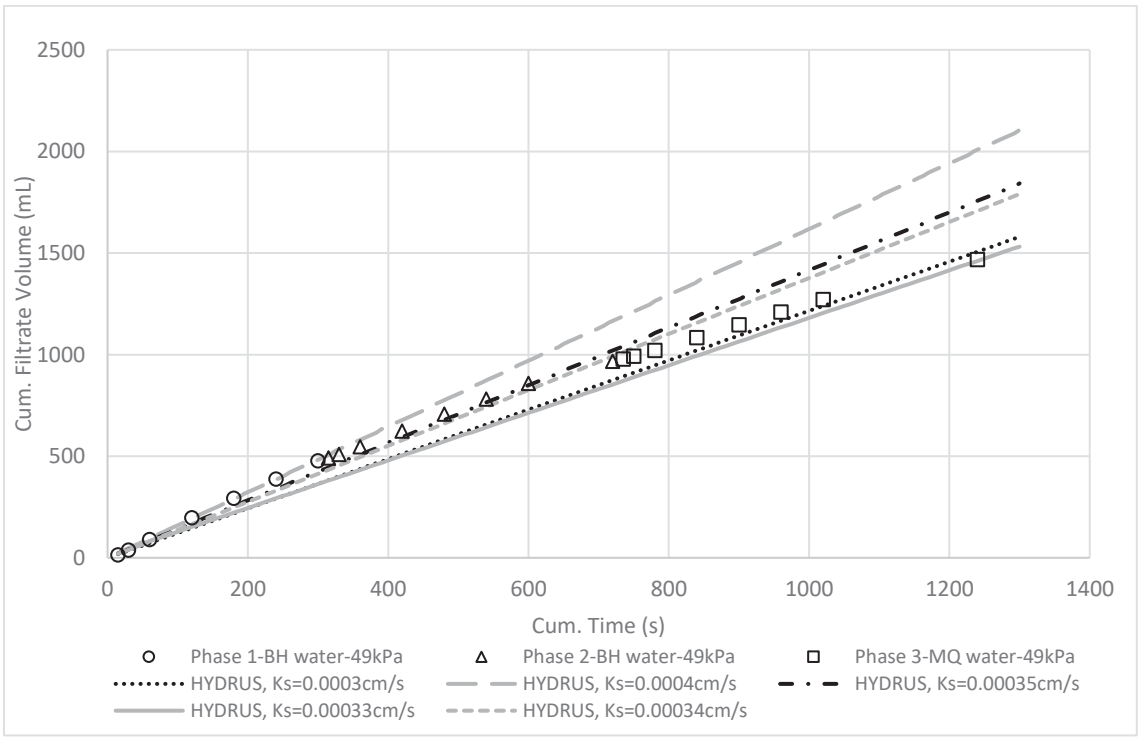

c

Figure 6.9 Observed and HYDRUS modeling results of cumulative filtrate volume for transport test under pressure of (a)21, (b)35, and (c)49 kPa

Phase 4 was performed under atmospheric pressure conditions and hence hydraulic conductivity also needed to be established for this phase. Phase 4 results (filtrate volume) from each transport test series were used to find the hydraulic conductivity of the filter cake/geotextile system using HYDRUS modeling. Figure 6.10 shows the observed and HYDRUS results of the filtrate volume when no constant pressure (i.e. beyond the head pressure felt by the height of water in the reservoir) was applied during the transport test. For modeling purposes, the height of water in phase 4 was considered to be constant (~5cm). Hydraulic conductivity values of 0.0005, 0.00035, 0.00025 cm/s resulted in a best match to the collected filtrate volume during phase 4 of transport experiment when a filter cake was developed at pressures of 21, 35, and 49 kPa, respectively. These values, which were close to the K_s of the system when pressure was applied, indicate that hydraulic characteristics of filter cake remained approximately consistent during the four trails of each transport test.

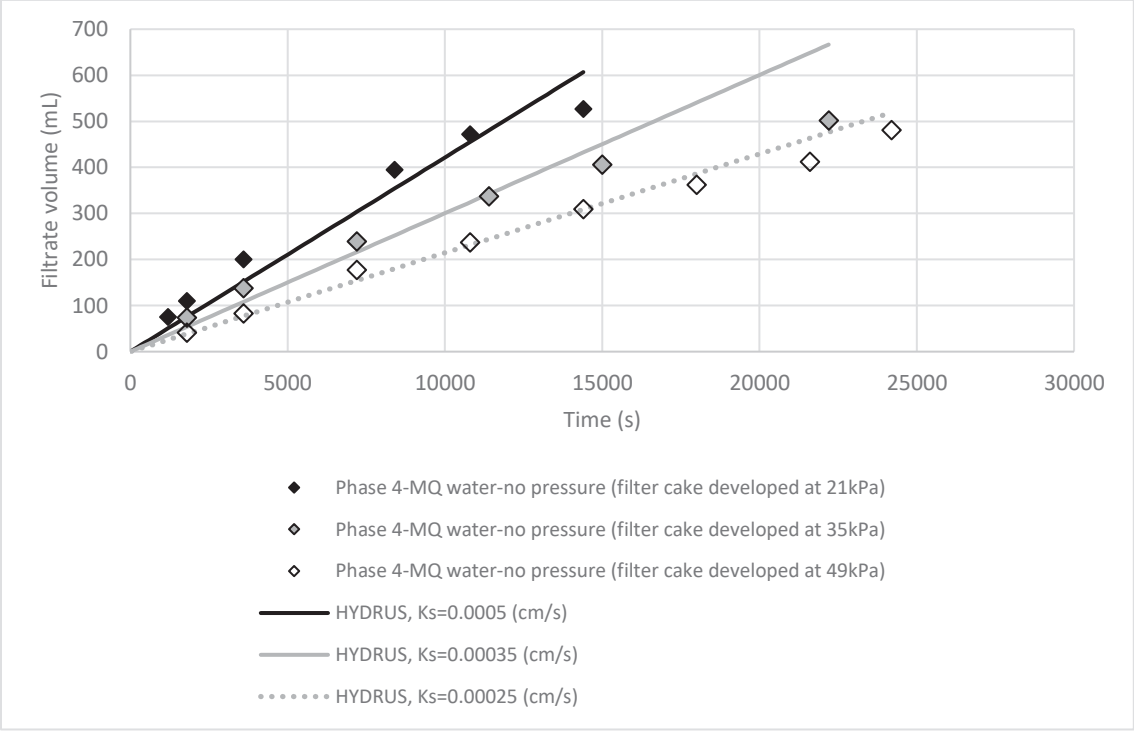

Figure 6.10 Observed and HYDRUS modeling results of cumulative filtrate volume for phases 4 of transport test under atmospheric pressure

Figure 6.11a shows the observed bromide concentrations in the collected filtrate from the transport experiments at a pressure of 21 kPa. As previously discussed, in phases 1 and 2, bromide was added to the reservoir containing BH water, while in phases 3 and 4, only Milli-Q water was added above the filter cake and geotextile. As shown in this figure, since bromide is non-reactive, its concentration in the collected filtrate was measured to be similar to the initial concentration measured in the inflow water (see Table 6.2 for the initial concentration). When Milli-Q water was added to the chamber (phase 3), bromide concentrations in collected filtrate reduced as the phase progressed. The decrease in Br^- in phase 3 is due to the presence of bromide in the pore spaces of the filter cake/geotextile matrix from the previous phases. As Milli-Q water filtered through the system, the bromide moved through the system and its concentration in the filtrate decreased. Bromide concentration curves for the first three phases were used to optimize the saturated volumetric water content (θ_s), and longitudinal dispersivity (D_L). HYDRUS modelling of the filtrate bromide concentrations is shown in Figure 6.11b. The best fit of simulated models to the observed bromide concentration is related to the D_L, which was determined to be 0.5 cm (as shown in black dotted line). Longitudinal dispersivity of a one-direction filtration column has previously been found to be approximately one tenth of the length of a column (i.e. filter cake/geotextile system) length (Bennacer et al. 2013).

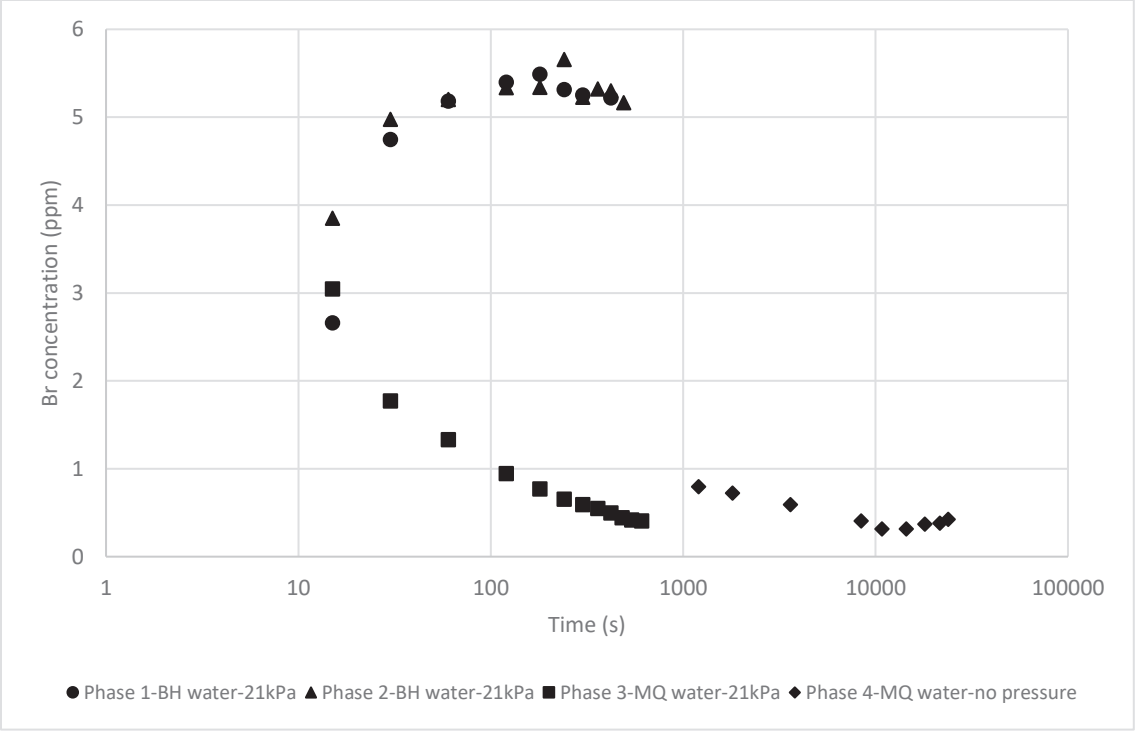

a

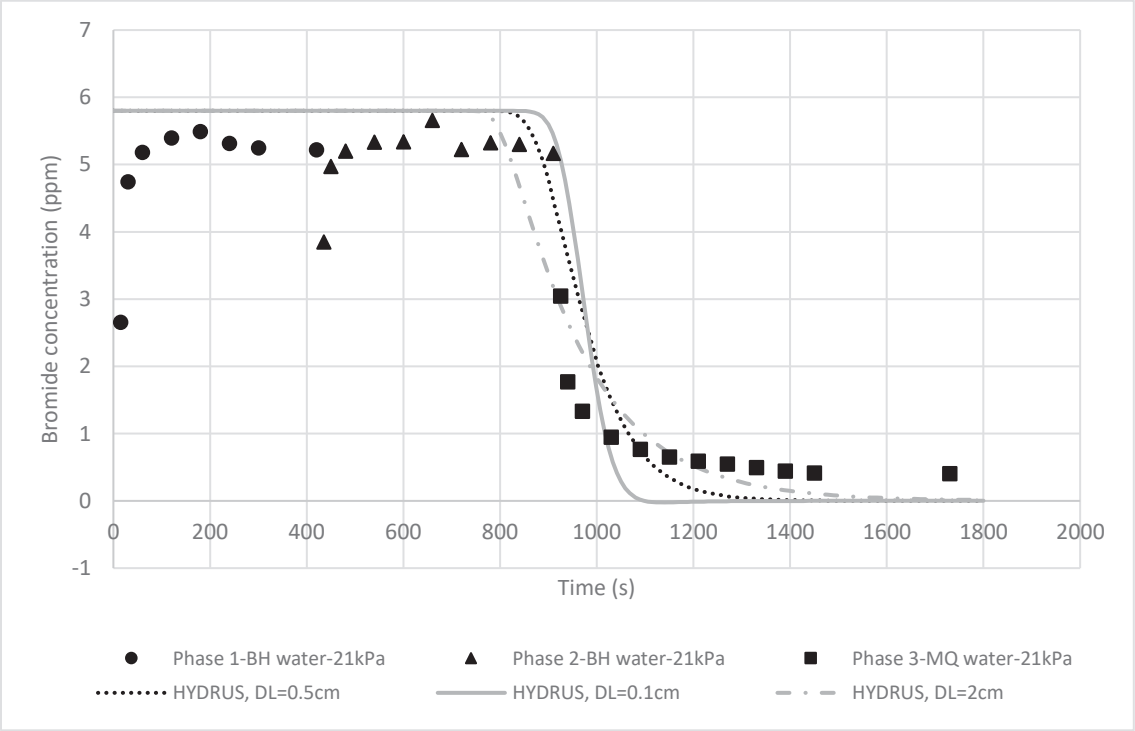

b

Figure 6.11 (a) Observed bromide concentration in the collected filtrate of transport test at 21 kPa pressure (b) HYDRUS simulated bromide concentration

Bromide concentrations in the collected filtrate sampled from transport tests at pressures of 35 and 49 kPa, as well as related HYDRUS simulated bromide results are presented in Figure 6.12 and Figure 6.13, respectively. A similar trend was observed at different pressures (i.e. close to the initial concentration in first two phases, reducing to near zero in the next two phases). Furthermore, HYDRUS modeling revealed the same D_L for the filter cake/geotextile system under 35 and 49 kPa showing that the longitudinal dispersivity (D_L) did not change significantly with these higher pressures.

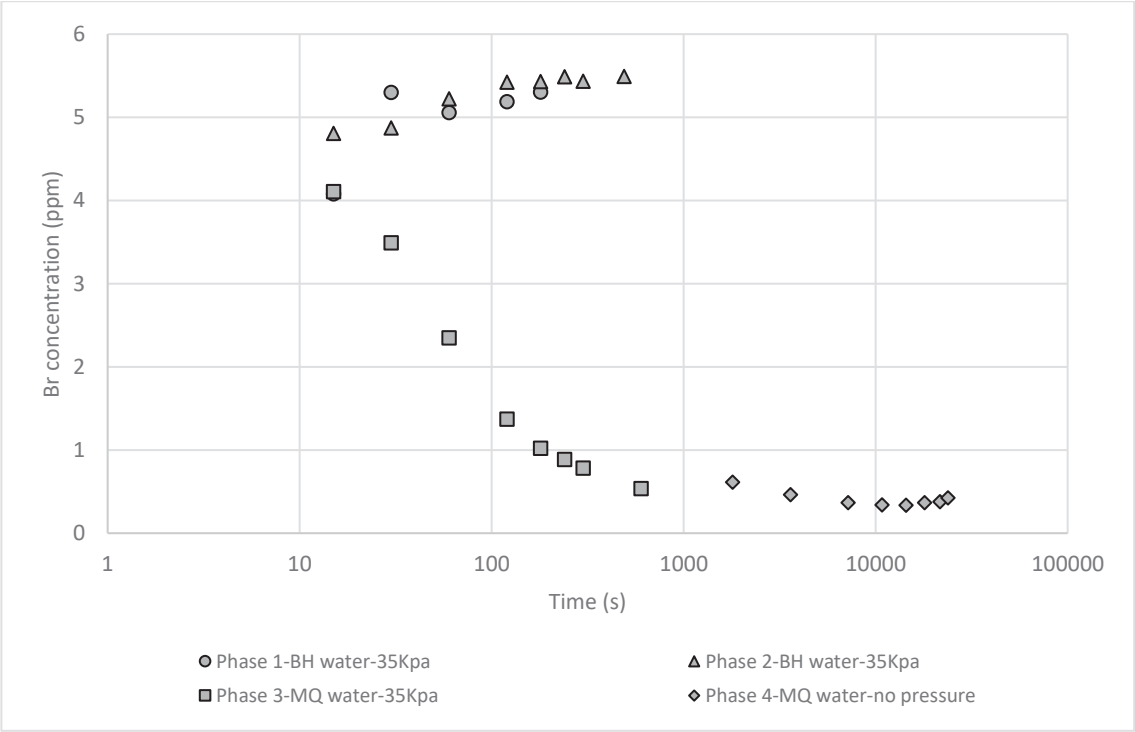

a

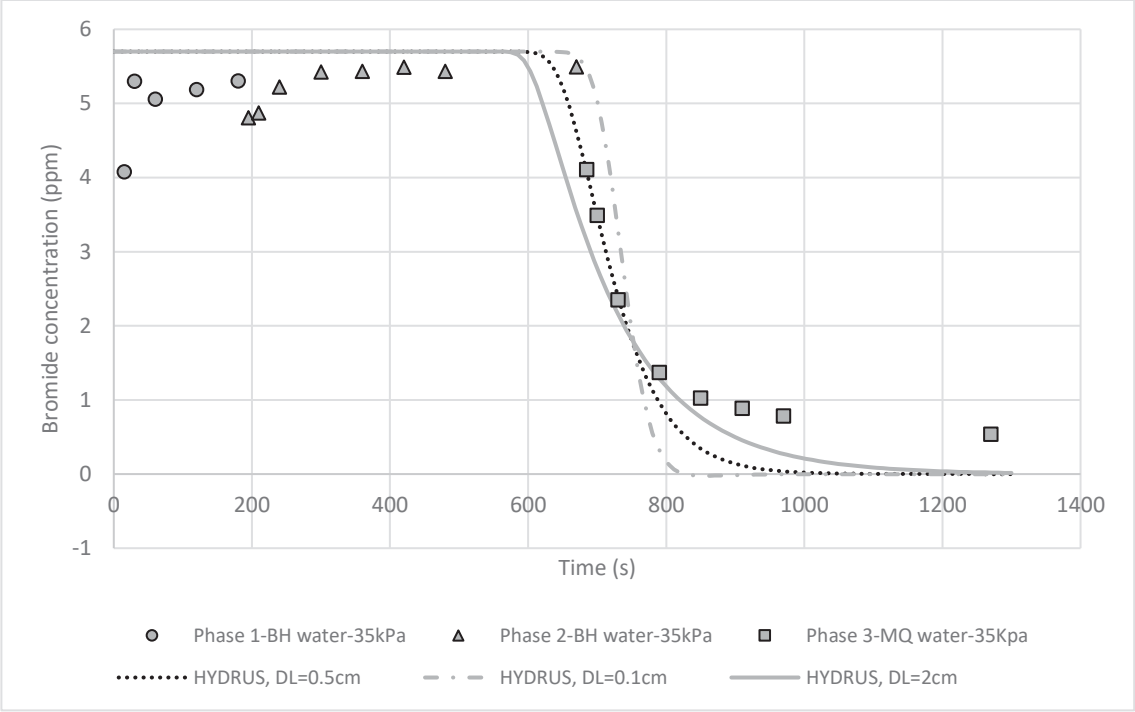

b

Figure 6.12 (a) Observed bromide concentration in the collected filtrate of transport test at 35 kPa pressure (b) HYDRUS simulated bromide concentration

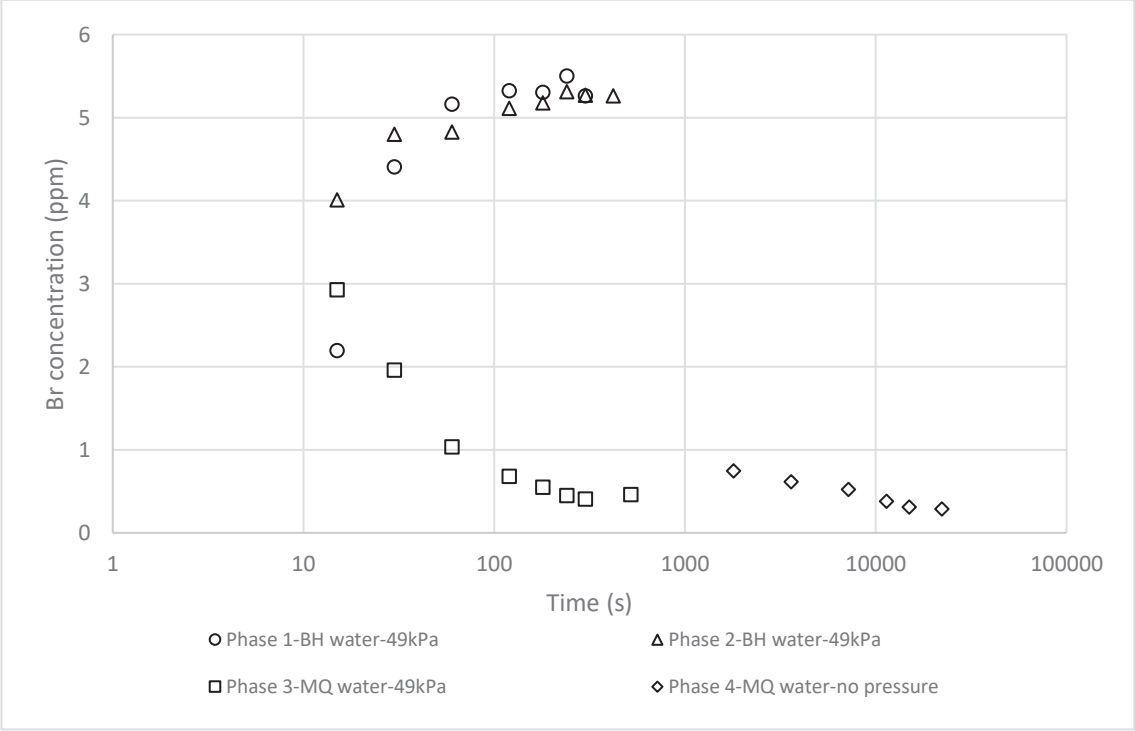

a

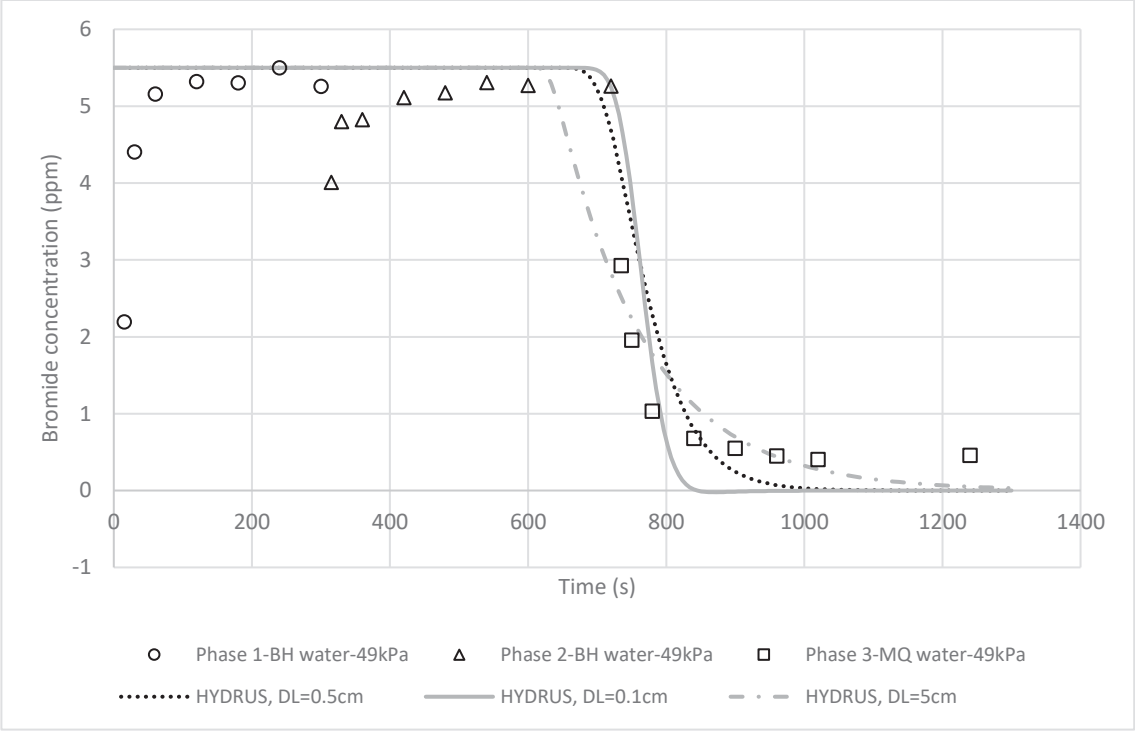

b

Figure 6.13 (a) Observed bromide concentration in the collected filtrate of transport test at 49 kPa pressure (b) HYDRUS simulated bromide concentration

Particle concentrations in the collected filtrate of the transport experiments at the three different pressures are presented in Figure 6.14. It is shown that when the applied pressure increased, additional particles passed through the filter cake/geotextile system, even though a similar initial particle concentration was injected into the system at the beginning of each phase (Table 6.2). This finding agrees with the PFT findings shown in the Figure 6.7; when increasing the applied pressure from 21 to 49 kPa, an increase in the filtrate particle concentration resulted.

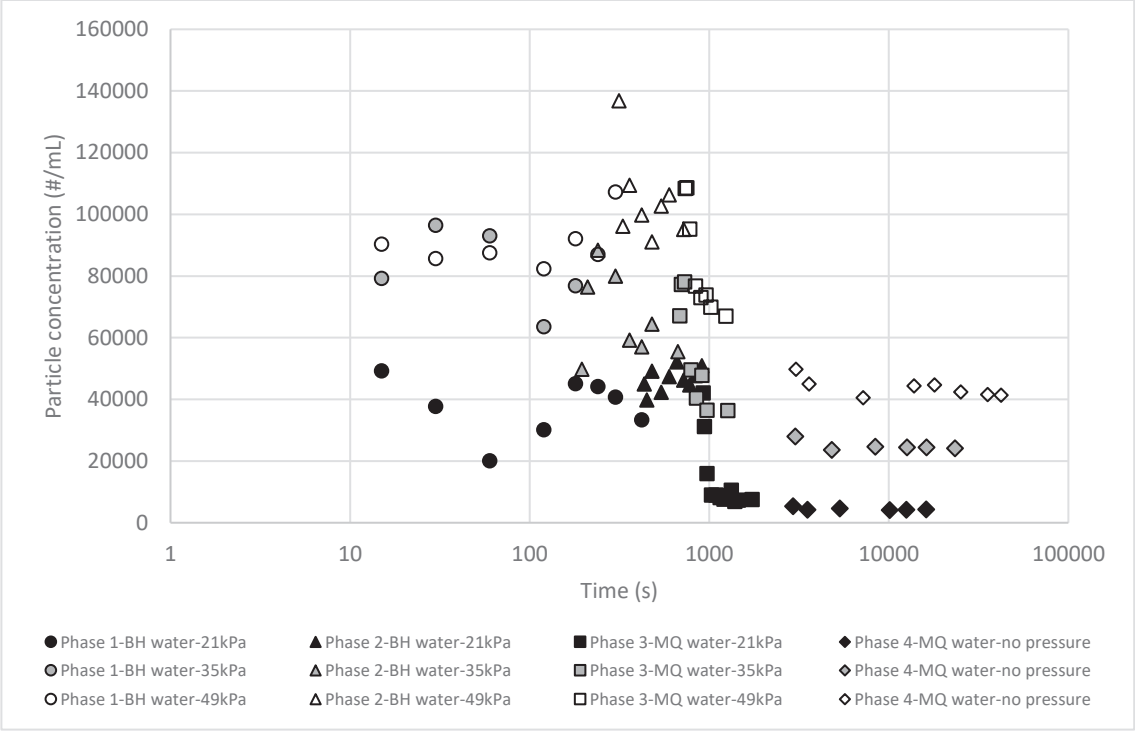

a

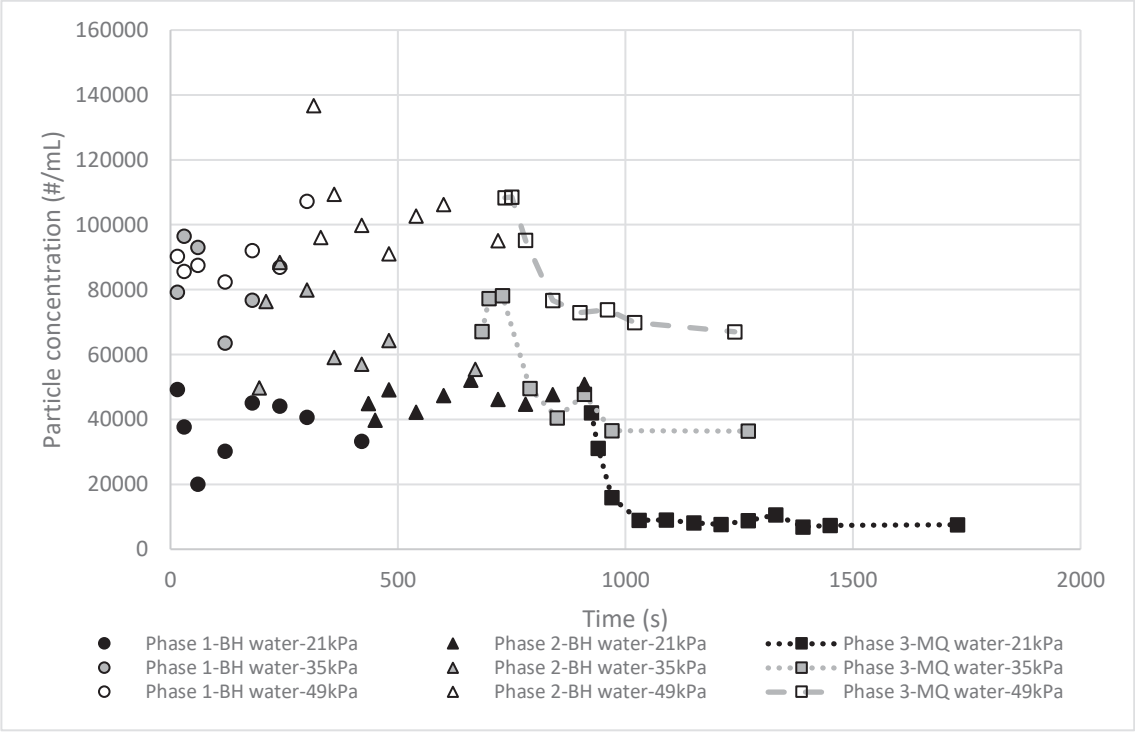

b

Figure 6.14 Particle concentrations of collected filtrate from (a) all the phases of transport experiments, (b) only under pressure

6.3.3 HYDRUS Modeling

To further investigate potential mechanisms for this particle transport, HYDRUS simulations were performed with results for phase 3. Particle concentrations were simulated using the experimental results to: 1) identify best-fit values of the particles (colloid) reaction parameters (i.e. attachment, detachment) using the HYDRUS model, and, 2) observe how these reaction parameters matched the shape of the particle concentrations in the effluent. To accomplish this, the initial concentration of mobile particles (colloids) in the liquid phase (C_c) and immobile particles (attached to the solid phase, which is the filter cake/geotextile system in this research - S_c) needed to be defined. In relation to C_c, as Figure 6.14b illustrates, particle concentrations in the filtrate of the first two phases can be considered to be about 40,000 #/mL at 21 kPa. Likewise, particle concentrations of approximately 80,000 and 110,000 #/mL were observed in the filtrate collected from first two phases of 35 and 49 kPa, respectively. Hence, phase 3 results were simulated with the assumption of an initial mobile concentration of 40,000, 80,000, and 110,000 #/mL at 21, 35, and 49 kPa (i.e. to reflect that observed in the experiments).

With respect to S_c, given the observed stability of the filter cake, the number of immobile particles should be significantly higher than the mobile particles. This parameter is difficult to measure experimentally and hence the range of immobile particles was assumed to be 500,000 to 1,000,000 #/mg (approximately 5 to 10 times more than mobile concentration). The influence of this unknown parameter on simulated particles will be shown in a future section.

Given the unknown mechanism for particle migration through the filter cake, three different assumptions in the model formulations (i.e. Table 6.5) were considered to simulate the particle concentration in the filtrate collected from phase 3 under pressure: M_1-attachment; M_2-detachment; and M_3-attachment and detachment. In all models, the same longitudinal dispersivity (D_L) which was found using the tracer concentration curve (D_L=0.5cm) was employed. The attachment and detachment rate coefficients used in these models were obtained by fitting the particle concentration curve. The fitted coefficients which most closely matched the observed results were selected to simulate the phase 4

results (atmospheric pressure) and investigate the effect of pressure on the reaction parameters (M_4).

Table 6.5 HYDRUS models initial conditions

	Dominant Transport Mechanism	Confining Pressure (kPa)		C_c: Initial Mobile Colloids Concentration (#/mL)	S_c: Initial Immobile Colloids Concentration (#/mg)
M_1	Attachment	Phase 3	21	40,000	500,000
					1,000,000
			35	80,000	500,000
					1,000,000
			49	110,000	500,000
					1,000,000
M_2	Detachment	Phase 3	21	40,000	500,000
					1,000,000
			35	80,000	500,000
					1,000,000
			49	110,000	500,000
					1,000,000
M_3	Attachment and Detachment	Phase 3	21	40,000	500,000
					1,000,000
			35	80,000	500,000
					1,000,000
			49	110,000	500,000
					1,000,000
M_4	Attachment and Detachment Without Confining Pressure	Phase 4	atmospheric	10,000	500,000
					1,000,000
				40,000	500,000
					1,000,000
				60,000	500,000
					1,000,000

6.3.3.1 Model M_1: Attachment

Figure 6.15a presents the experimental and M_1 model filtrate concentrations at a confining pressure of 21 kPa. Initial mobile and immobile particles were set at 40,000 #/mL and 500,000 #/mg, respectively. Different attachment rate coefficients (K_{ac}) were employed in an attempt to find a suitable theoretical match to the experimental results, but as can be seen in Figure 6.15a, none of the theoretical curves appear to represent the mechanism of the particle movement behavior through the filter cake. As is shown in this figure, by

increasing the level of particle attachment, via an increase in K_{ac}, the filtrate particle concentration decreases due to more of the mobile particles being retained on the porous media (filter cake/geotextile system). None of the K_{ac} curves properly simulated the filtrate particle concentrations (i.e. shape of the particle effluent curve) and all of the attachment coefficient (K_{ac}) curves resulted in poor fits to the experimental data.

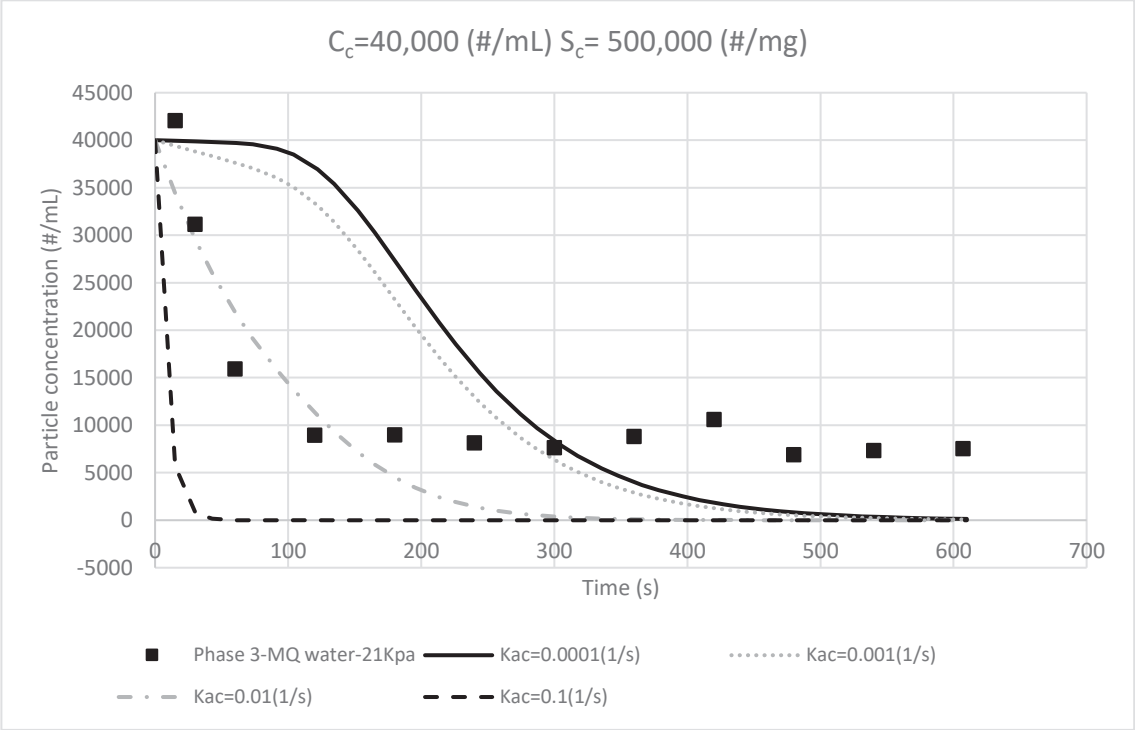

a

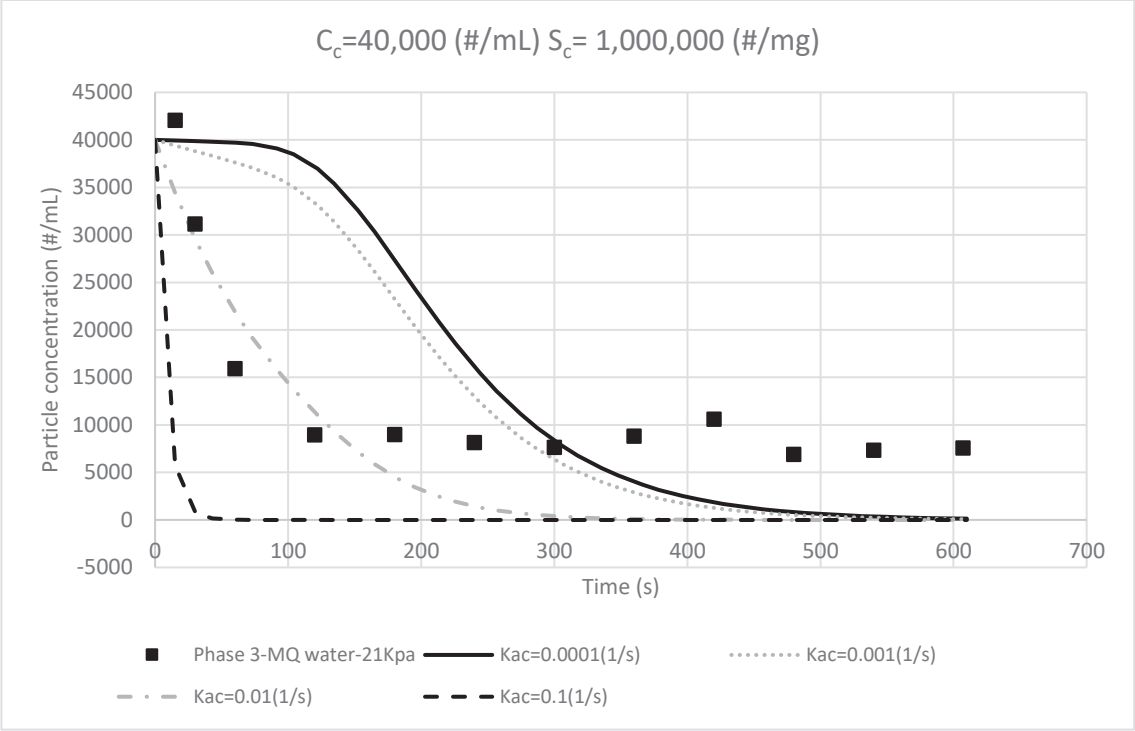

b

Figure 6.15 Observed and model M_1 fitted filtrate concentration curves at pressure of 21 kPa considering the C_c=40,000 (#/mL) and different S_c of a) 50,000 and b) 1,000,000 (#/mg)

To examine the impact of the uncertainty of the initial number of immobile particles (S_c) on the solid phase at this 21 kPa pressure, the initial number of immobile particles was increased to 1,000,000 #/mg, as shown in Figure 6.15b. This increase was found to have little effect on the model output, suggesting that this parameter has little influence on the model outcome when only attachment is considered as a mechanism. In summary, the shape of the particle effluent curve was not represented correctly by the M_1 model and hence it was concluded that attachment is most likely not the only mechanism controlling the particle transport in this system. Phase 3 observed results at the other two pressures (35 and 49 kPa) were also simulated using the same attachment coefficient to investigate the effect of pressure on particle transport behavior. The mobile particle concentration was set at 80,000 and 110,000 #/mL respectively for 35 and 49 kPa. Since the 21 kPa results showed that the concentration of immobile particles had no effect on the attachment modeling outputs, a single concentration of 1,000,000 #/mg was considered for the 35 and 49 kPa pressures (see Figure 6.16).

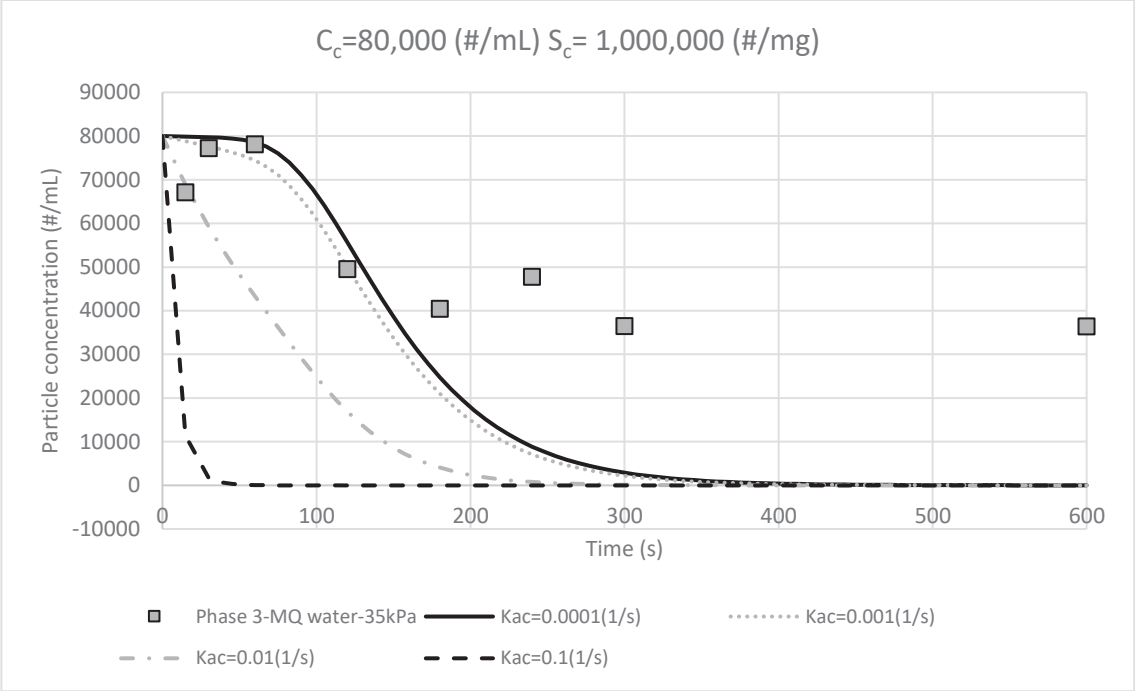

a

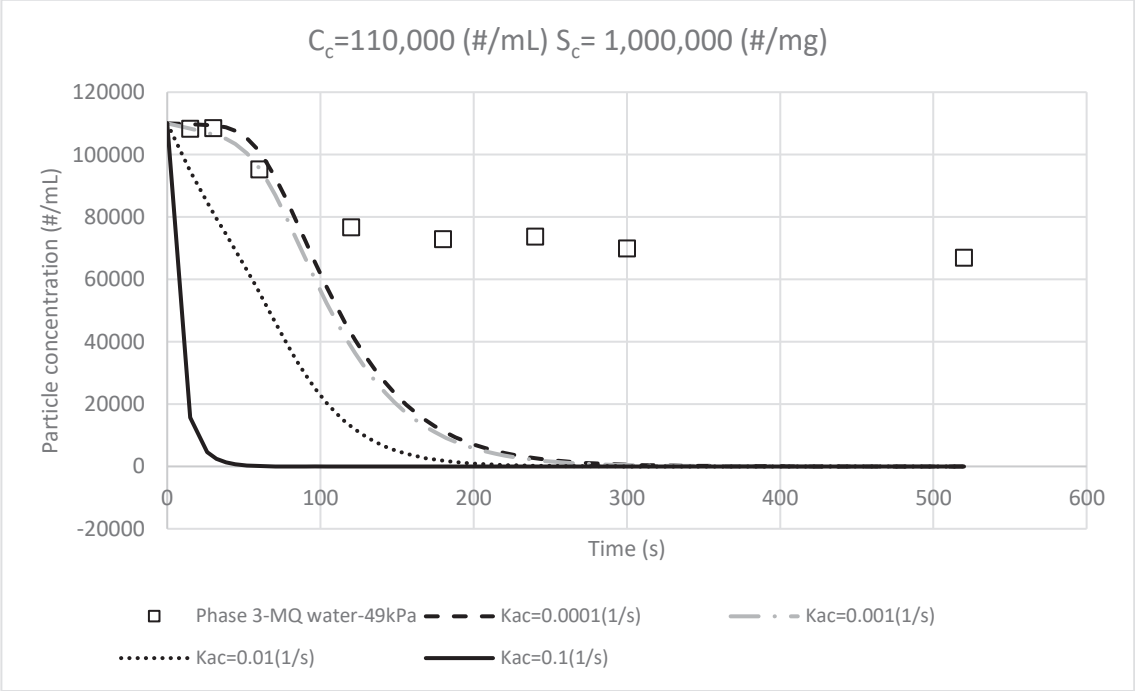

b

Figure 6.16 Observed and model M_1 fitted filtrate concentration curves considering the S_c=1,000,000 (#/mg) and different C_c of (a) 80,000 (#/mL) at 35 kPa and (b) 110,000 (#/mL) at 49 kPa

As can be seen in Figure 6.16, experimentally measured particle concentrations at both the 35 and 49 kPa pressures also did not match well with the simulated M_1 model. If the attachment mechanism was the only process controlling the particle concentration in the filtrate, no particles would be migrating through the system after approximately 300 s.

6.3.3.2 Model M_2: Detachment

Figures 6.17a and b show the experimental phase 3 filtrate particle concentrations at 21 kPa and the M_2 simulated model concentrations when considering only the detachment mechanism of particle transport. Mobile particle concentrations (C_c) were set at 40,000 #/mL for these models. To again investigate the influence of S_c, two different immobile concentrations (S_c) of 500,000 and 1,000,000 #/mg were considered. The detachment mechanism was evaluated by running the M_2 model with several different detachment rate coefficients (K_{dc}), as shown in Figures 6.17a and b. As shown in these figures, by increasing the detachment coefficient, particle concentration in the filtrate also increased. Moreover, unlike the M_1 model in which immobile concentrations (i.e. S_c) did not impact the particle concentrations in the filtrate, the M_2 model considering only detachment as a transport mechanism shows that the assumption of more immobile particle concentrations (i.e. S_c of 1,000,000 #/mg) resulted in higher filtrate particle concentrations, particularly at a higher detachment coefficient value (i.e. K_{dc}=0.001 (1/s)). This is likely due to the greater availability of immobile particles on the solid phase and their ability to detach and migrate through the filter cake. Most of the simulated M_2 results were found to be greater than the observed values, suggesting that a higher concentration would have been achieved in the filtrate during the experimentation if detachment was the primary responsible transfer mechanism. Hence, the inability of the M_2 model to accurately depict the shape of the particle concentration curve in the filtrate suggests that detachment cannot be a stand-alone mechanism in the transport of particles through the filter cake/geotextile system at the 21 kPa pressure.

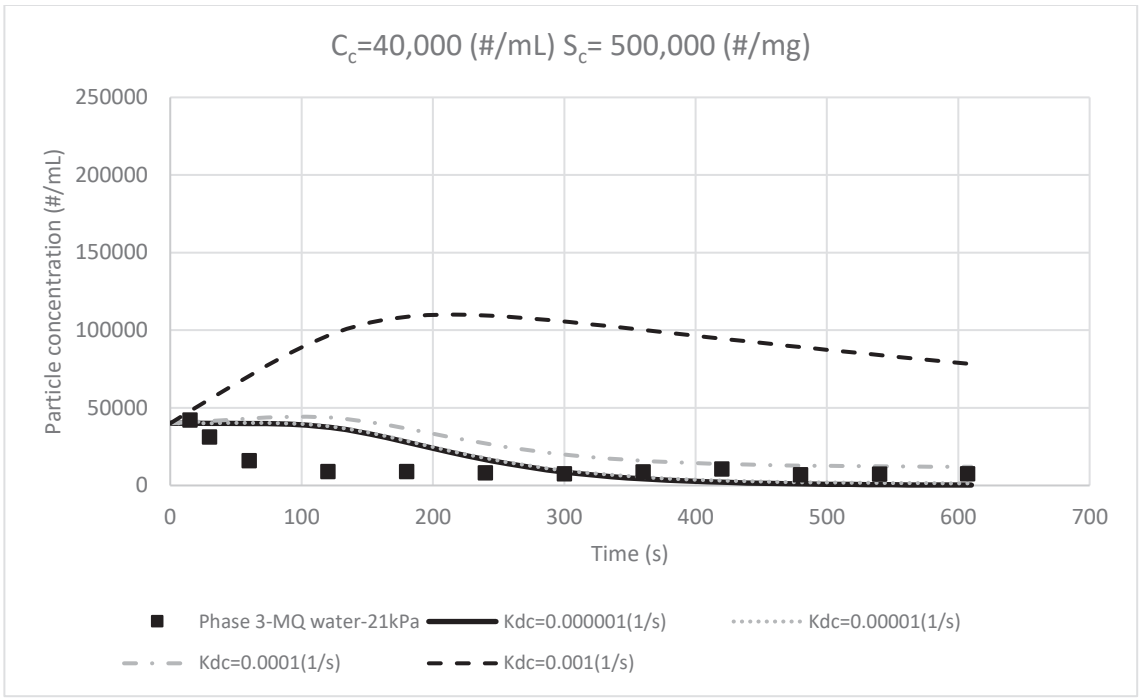

a

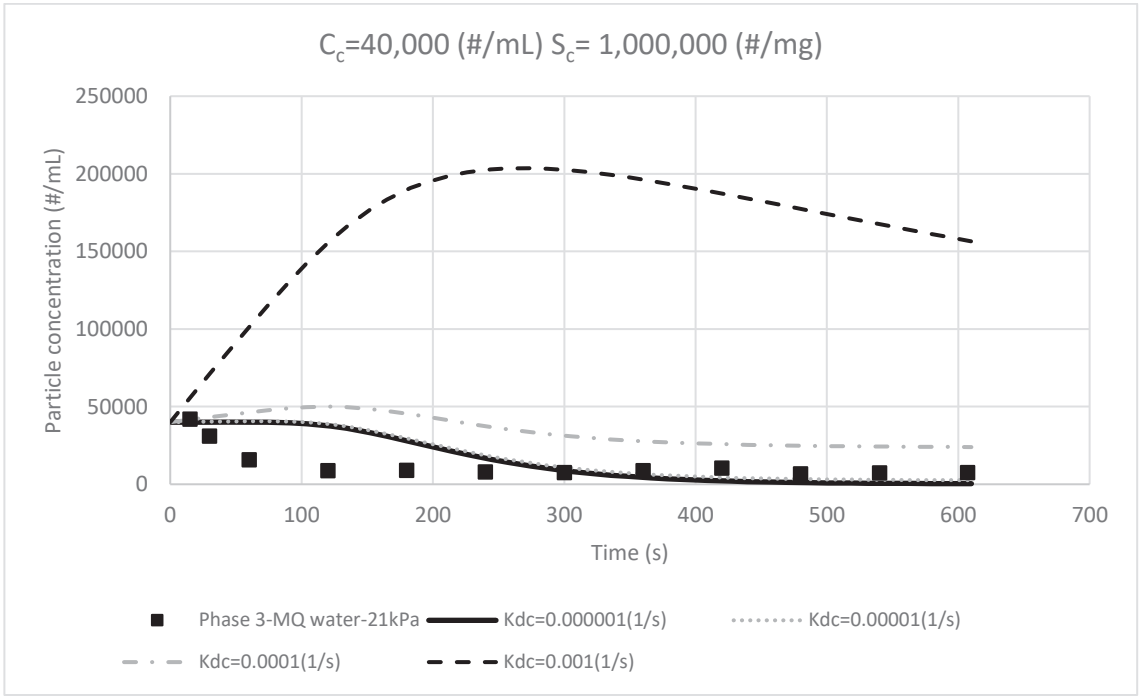

b

Figure 6.17 Observed and model M_2 fitted filtrate concentration curves at pressure of 21 kPa considering the C_c=40,000 (#/mL) and different S_c of (a) 500,000 and (b) 1,000,000 (#/mg)

At the two higher pressures, the M_2 model appeared to perform slightly better than at 21 kPa. However, using only the detachment coefficient did not appear to match all times of the effluent data. As can be seen in Figure 6.18a and b for 35 kPa, detachment coefficients of 0.0005 and 0.0002 (1/s) resulted in the best fit to experimental observed particle concentrations in the filtrate when S_c was considered to be 500,000 and 1,000,000 #/mg. This result suggests that when particle availability limits detachment from the solid phase (S_c=500,000 #/mg), a higher detachment rate (k_{dc}=0.0005 1/s) is required to match the data. Comparatively, for the higher S_c value (1,000,000 #/mg) as shown in Figure 16.8b, a lower detachment rate (k_{dc}=0.0002 1/s) is required to match the data. Regardless of the combination of parameters when only considering the detachment mechanism, the model fails to sufficiently capture particle concentrations. However, the detachment coefficient of 0.0005 (1/s) and 0.0002 (1/s) resulted in best match for S_c values of 500,000 and 1,000,000 #/mg, respectively.

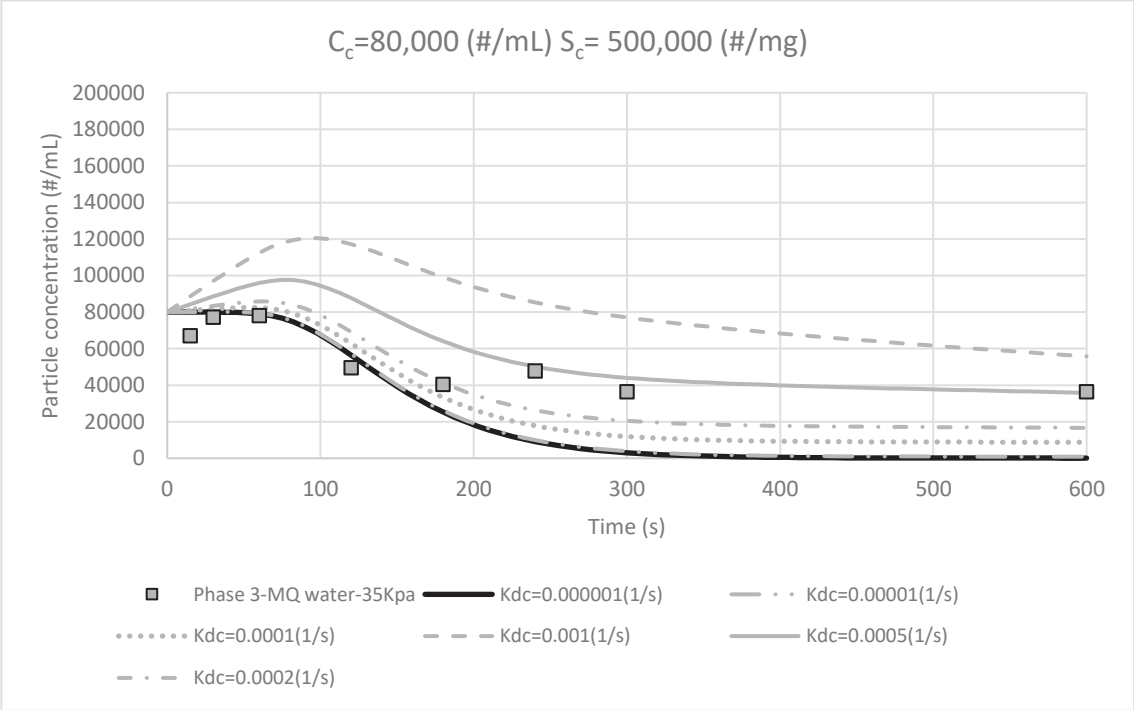

a

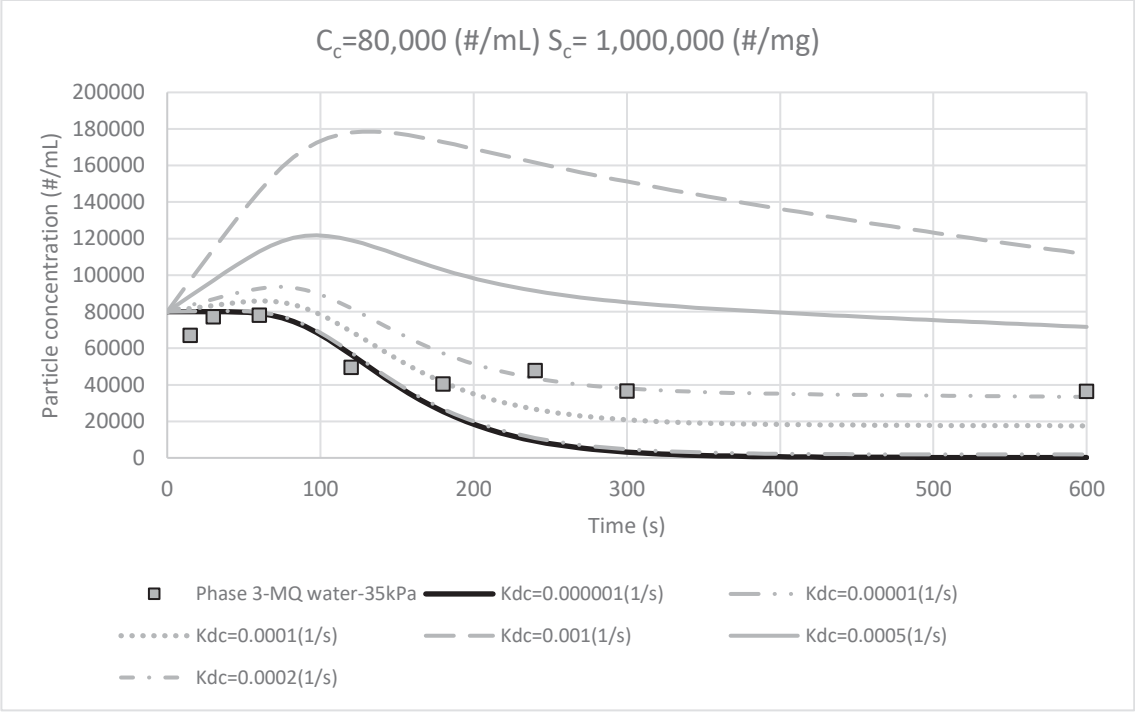

b

Figure 6.18 Observed and model M_2 fitted filtrate concentration curves at pressure of 35 kPa considering the C_c=80,000 (#/mL) and different S_c of (a) 500,000 and (b) 1,000,000 (#/mg)

At the 49 kPa confining pressure, higher detachment coefficients relative to the 35 kPa pressure were required to obtain reasonable fits to the observed filtrate concentration. For example, K_{dc} of 0.001 and 0.0006 (1/s) moderately depicts the shape of the particle effluent curve when immobile concentrations are 500,000 and 1,000,000 (#/mg), respectively. However, as Figure 6.19 illustrates, none of the simulated curves completely depicts the particle transport using the M_2 model (i.e. some match the initial observed values and others simulate the final results better). It can be concluded that although the M_2 model explains the particle transfer better than the M_1 model, it is not likely the only mechanism influencing the system.

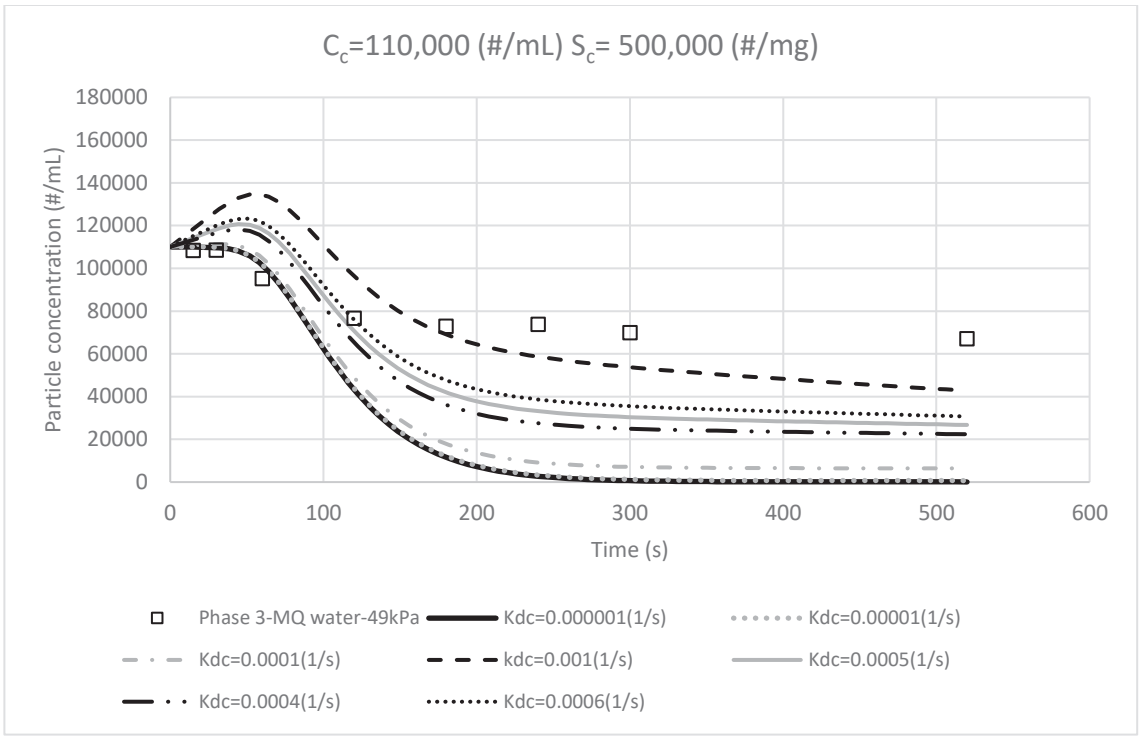

a

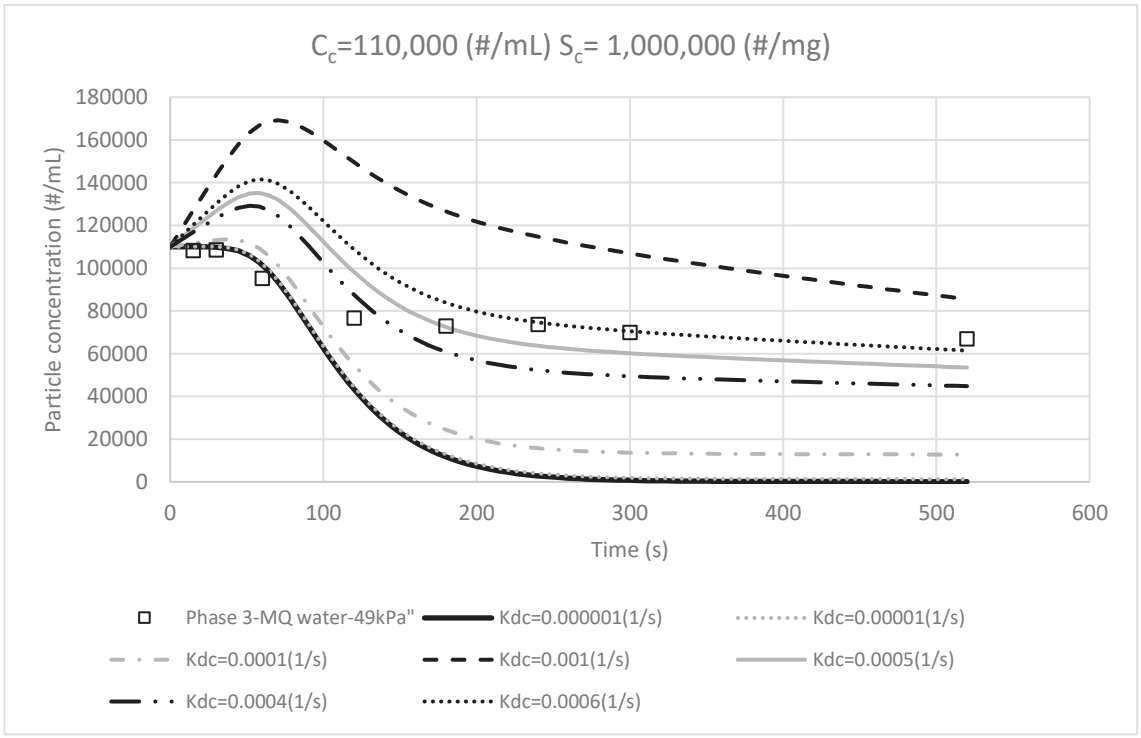

b

Figure 6.19 Observed and model M2 fitted filtrate concentration curves at pressure of 49 kPa considering the C_c=110,000 (#/mL) and different S_c of (a) 500,000 and (b) 1,000,000 (#/mg)

6.3.3.3 Model M_3: Attachment and Detachment

Figures 6.20 to 6.22 present the observed and M_3 model filtrate concentration curves at the three different pressures (21, 35, 49 kPa). As Figure 6.20 shows for the 21 kPa pressure, when HYDRUS simulates the particle transfer considering both attachment and detachment mechanisms (M_3), model outputs depict the trend of experimental results better compared to previous models (i.e. M_1 and M_2). K_{ac} of 0.02 (1/s) and K_{dc} of 0.0003 (1/s) give the best fit to the observed filtrate concentration in phase 3 at 21 kPa when mobile and immobile particle concentrations are set at 40,000 #/mL and 500,000 #/mg, respectively. Examining the sensitivity of S_c on model results, when S_c increases from 500,000 #/mg to 1,000,000 #/mg, the best fit for K_{dc} decreases to 0.00015 (1/s) (Figure 6.20b). It should be noted that since both K_{ac} and K_{dc} coefficients control the transport of particles in the model M_3, there are many possible combinations which could match with experimental values. For example, in Figure 6.20b, with K_{ac} and K_{dc} equal to 0.02 and 0.0002 (1/s), M_3 curves are similar to when 0.02 and 0.0003 (1/s) were considered as a K_{ac} and K_{dc}, respectively. Since the objective of this was investigating the transport mechanisms, the exact value of K_{ac} and K_{dc} is less important than the observation that the combination of attachment and detachment are required to reproduce the desired shape of the effluent curve. However, given the influence both K_{ac} and K_{dc} have on model output, if the true values of these parameters were desired, then an alternative set of experiments would have to be incorporated.

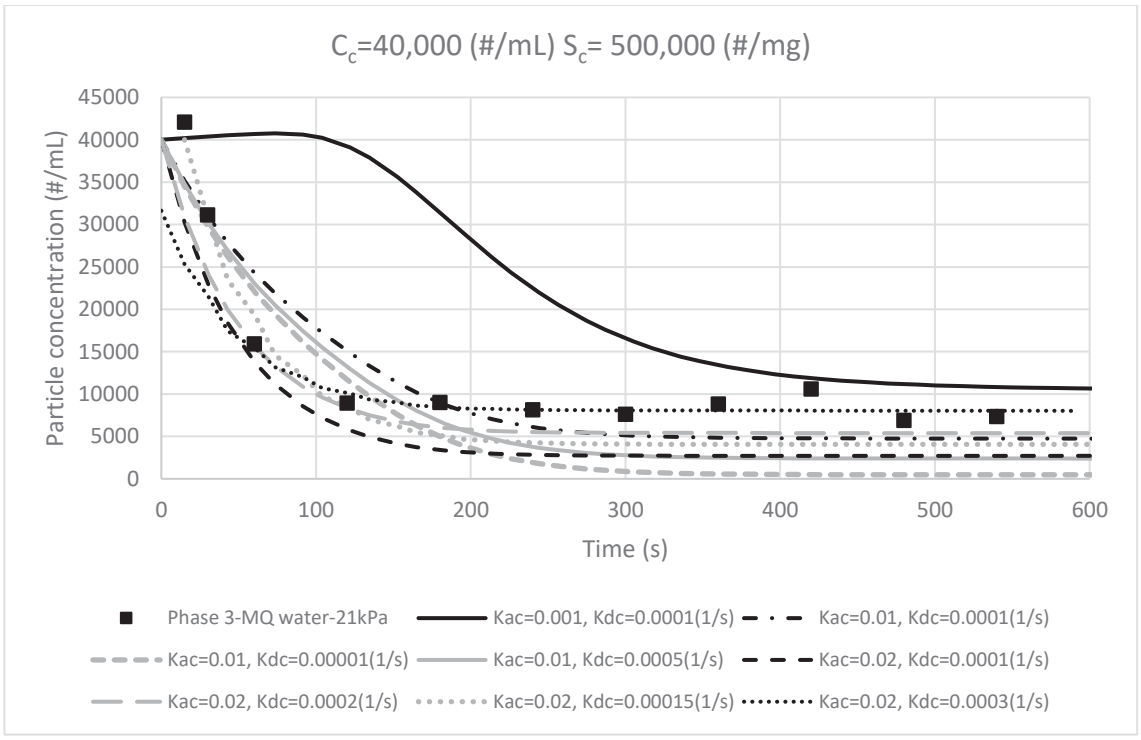

a

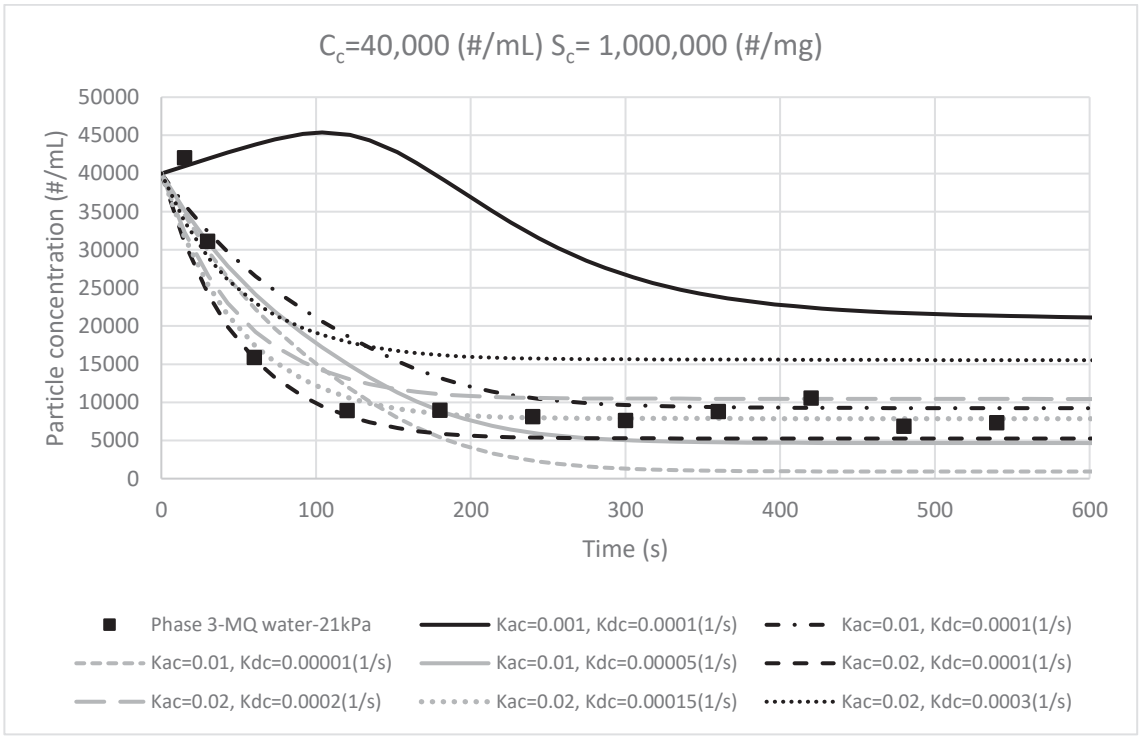

b

Figure 6.20 Observed and model M_3 fitted filtrate concentration curves at pressure of 21 kPa considering the C_c=40,000 (#/mL) and different S_c of (a) 500,000 and (b) 1,000,000 (#/mg)

Best fitted coefficients (K_{ac} = 0.02, K_{dc} of 0.00015 (1/s)) at 21 kPa were selected as initial estimates for the transport test at 35 kPa. As Figure 6.21 shows, a K_{ac} of 0.02 (1/s) and K_{dc} of 0.00015 (1/s) result in particle concentrations less than were observed experimentally in phase 3, when the confining pressure was set to 35 kPa and an initial mobile concentration of 80,000 #/mL was used. A simulated M_3 curve related to K_{ac} and K_{dc} of 0.012 and 0.0005 (1/s) can be considered a suitable match to phase 3 results when immobile concentration is set at a higher level of 1,000,000 #/mg. By decreasing the assumed immobile particle concentration to 500,000 #/mg, a fitted K_{dc} value of 0.001 (1/s) showed the dependence of detachment coefficient to immobile concentration. For the 49 kPa pressure, when mobile particles were set at 110,000 #/mL, the best fit K_{ac} decreased to 0.01 (1/s) and K_{dc} increased to 0.001 (1/s) (see Figure 6.22b). Table 6.6 summarizes the best fit coefficients found at each confining pressure. As shown in this table, the confining pressure influences the attachment and detachment rates in a consistent manner. In other words, when less pressure is applied to the geotextile/filter cake system, less particles are able to transport out of the system due to the detachment, while higher pressures (i.e. 49 kPa) resulted in a greater detachment from the system (K_{dc}=0.001 (1/s)). It can be concluded that when confining pressure was 21 kPa, the attachment mechanism controls particle transport to a greater extent (i.e. K_{ac}=0.02 (1/s)).

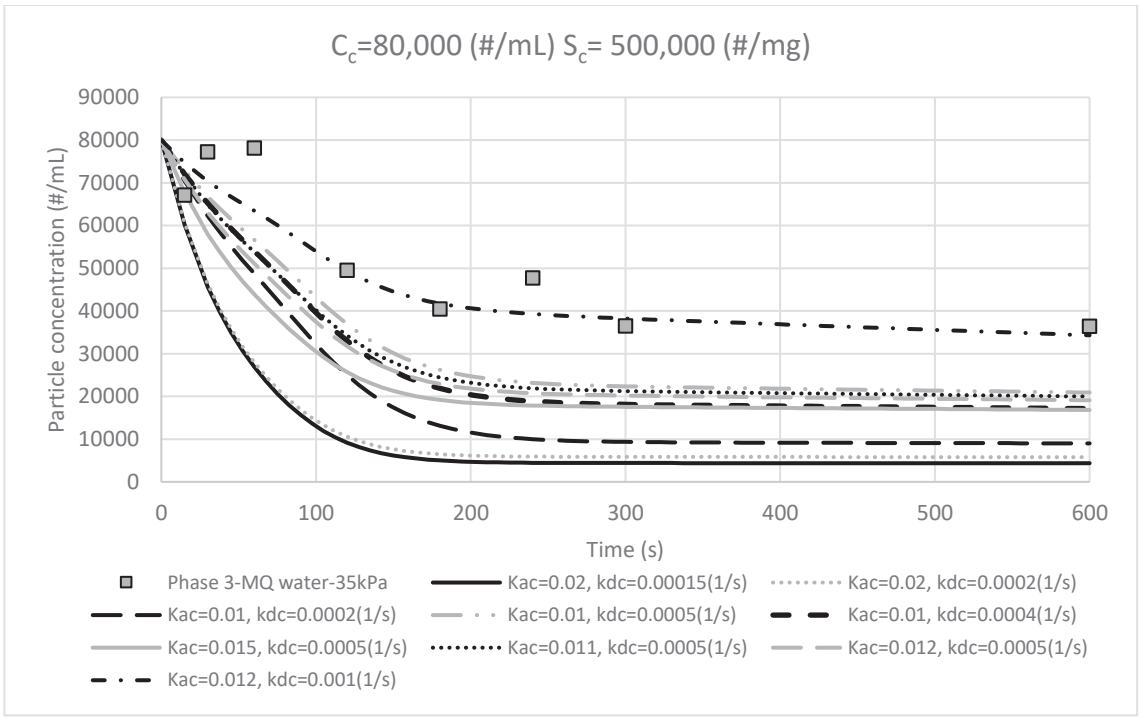

a

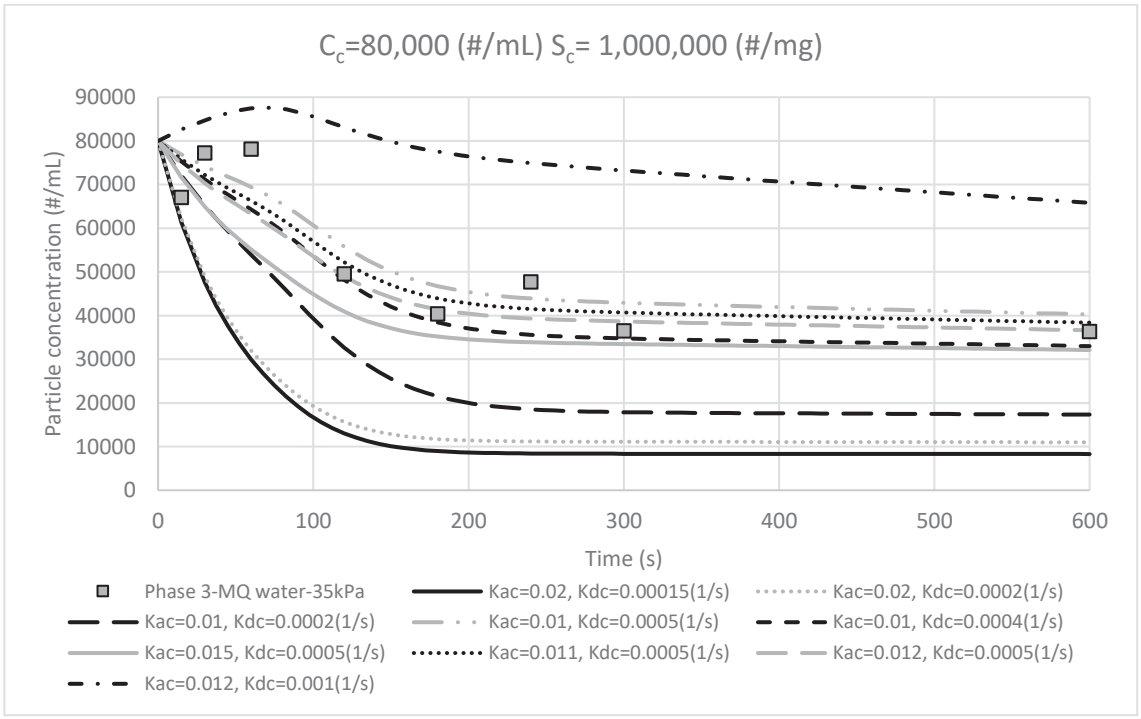

b

Figure 6.21 Observed and model M_3 fitted filtrate concentration curves at pressure of 35k Pa considering the C_c=80,000 (#/mL) and different S_c of (a) 500,000 and (b) 1,000,000 (#/mg)

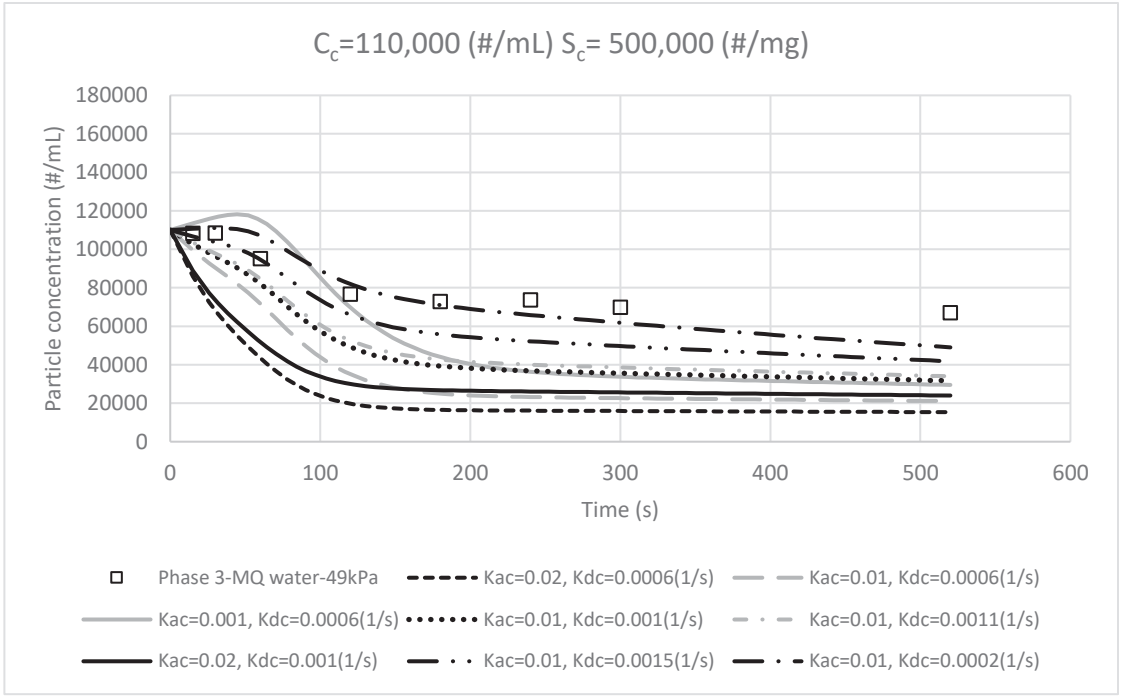

a

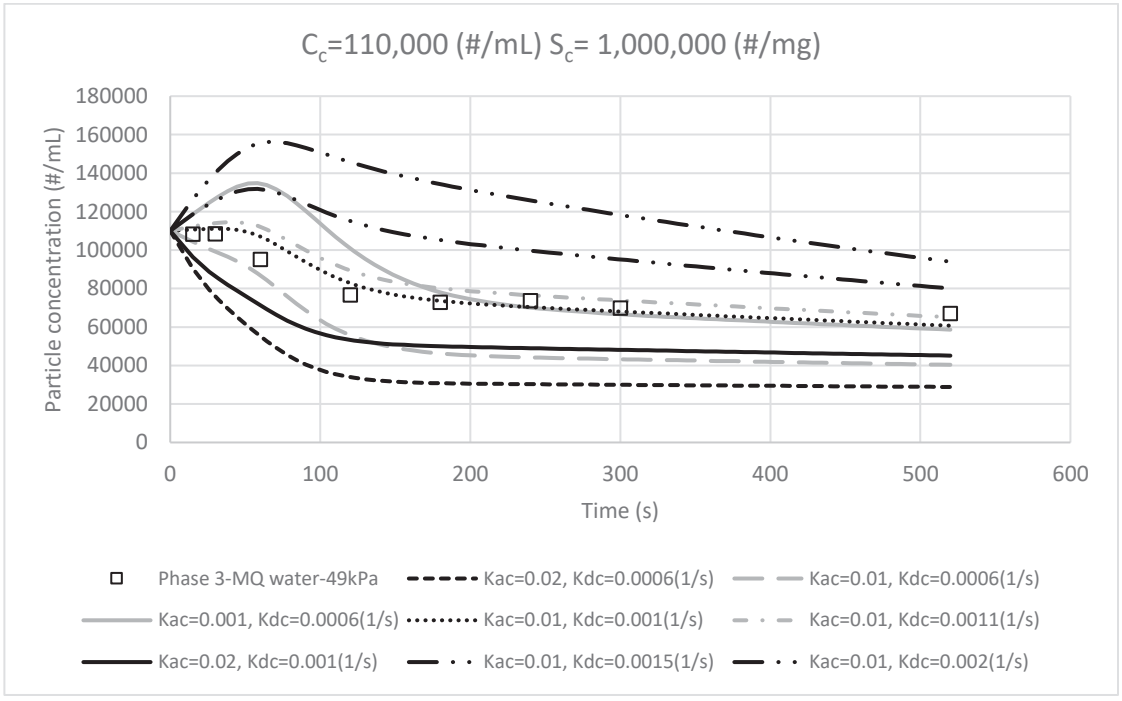

b

Figure 6.22 Observed and model M_3 fitted filtrate concentration curves at pressure of 49 kPa considering the C_c=110,000 (#/mL) and different S_c of (a) 500,000 and (b) 1,000,000 (#/mg)

Table 6.6 HYDRUS M_3 models fitted values of attachment and detachment coefficient

HYDRUS	Confining pressure (kPa)	C_c: Initial Mobile Colloids Concentration (#/mL)	S_c: Initial Immobile Colloids Concentration (#/mL)	K_{ac} (1/s)	K_{dc} (1/s)
M_3	21	40,000	500,000	0.02	0.0003
			1,000,000	0.02	0.00015
	35	80,000	500,000	0.012	0.001
			1,000,000	0.012	0.0005
	49	110,000	500,000	0.01	0.002
			1,000,000	0.01	0.001

6.3.3.4 Model M_4: Attachment and Detachment at Atmospheric Pressure

The previous section where different attachment and/or detachments scenarios were investigated suggested that both attachment and detachment mechanisms are likely present in particle transport during the dewatering experiments conducted in this study. Moreover, model outputs (i.e. Table 6.6) showed the impacts of confining pressure on attachment and detachment rates. To further investigate the effect of pressure on attachment and detachment rates and hence filtrate particle concentrations, the M_4 model was utilized to simulate particle transport through phase 4 of the transport experiments. As previously noted, these experiments were conducted at atmospheric pressure. Hydraulic characteristics of the filter cake/geotextile system were assumed to be the same as previous models related to applied pressure, with the exception of the hydraulic conductivity, which was calculated separately based on the observed filtrate volume. The initial mobile colloids in each of the phase 4 model runs were assumed to be the approximate final filtrate particle concentration of phase 3 (i.e. 10,000, 40,000, and 60,000 #/mL; see figure 6.14). Because an immobile concentration of 1,000,000 #/mg was shown in previous models to yield more accurate data when compared to 500,000 #/mL, this concentration was considered as the only immobile particle input used in the M_4 model.

As Table 6.6 shows, when the filter cake was developed at 21 kPa, coefficients for K_{ac} of 0.02 and K_{dc} of 0.00015 (1/s) matched observed concentrations reasonably well. These same coefficients were selected to be initial input for the M_4 simulation of phase 4 results when a filter cake developed at 21 kPa but performed under atmospheric pressure

conditions. Similarly, fitted values at the other two pressures were considered as the initial presumed coefficients for their M_4 model. In M_3 models, the boundary condition on top of the system was constant head (e.g. 214 cm equals to 21 kPa), while in the M_4 model, a constant head equal to the average height of the water (5 cm) on top of the filter cake during the 4th phase was considered as the top boundary condition.

Figure 6.23 shows the experimental and M_4 simulated filtrate concentrations for the three filter cakes at the three different pressures. In Figure 6.23a the solid black line represents the simulation related to K_{ac} and K_{dc} at 0.02 and 0.00015 (1/s) respectively (i.e. 21 kPa values). These coefficients most accurately fitted the phase 3 results, however, were not able to describe the filtrate concentration for phase 4 with atmospheric pressure. As discussed in previous sections, the particle reaction parameters (K_{ac} and K_{dc}) appear to change as the pressure changes. Phase 3 values for K_{ac} and K_{dc} of 0.012 and 0.0005 (1/s) (Figure 6.23b) (i.e. 35 kPa values) and K_{ac} and K_{dc} of 0.01 and 0.001 (1/s) (in Figure 6.23c) (i.e. 49 kPa values) overestimate the particle transport under the phase 4 conditions. Adjusting the detachment and attachment coefficients provides more reasonable matches to the filtrate concentration at atmospheric pressure. For example, setting the coefficient values K_{ac} to 0.02 (1/s) and K_{dc} to 0.0007 (1/s) (Figure 6.23c) best simulate the observed phase 4 results. It is probable that the higher pressure (i.e. phase 3) causes the immobile particles to detach from the solid phase and encourages the mobile particles in the liquid phase to attach to the porous media. For this reason, the M_4 curve related to different coefficients of (K_{ac} of 0.001 and K_{dc} of 0.00004 (1/s)) in Figure 6.23c, also provides a good match to the observed curve. However, as it was discussed earlier, as it is the combination of the two coefficients controlling the transport process; more than one suitable set of parameters can match the experimental concentrations.

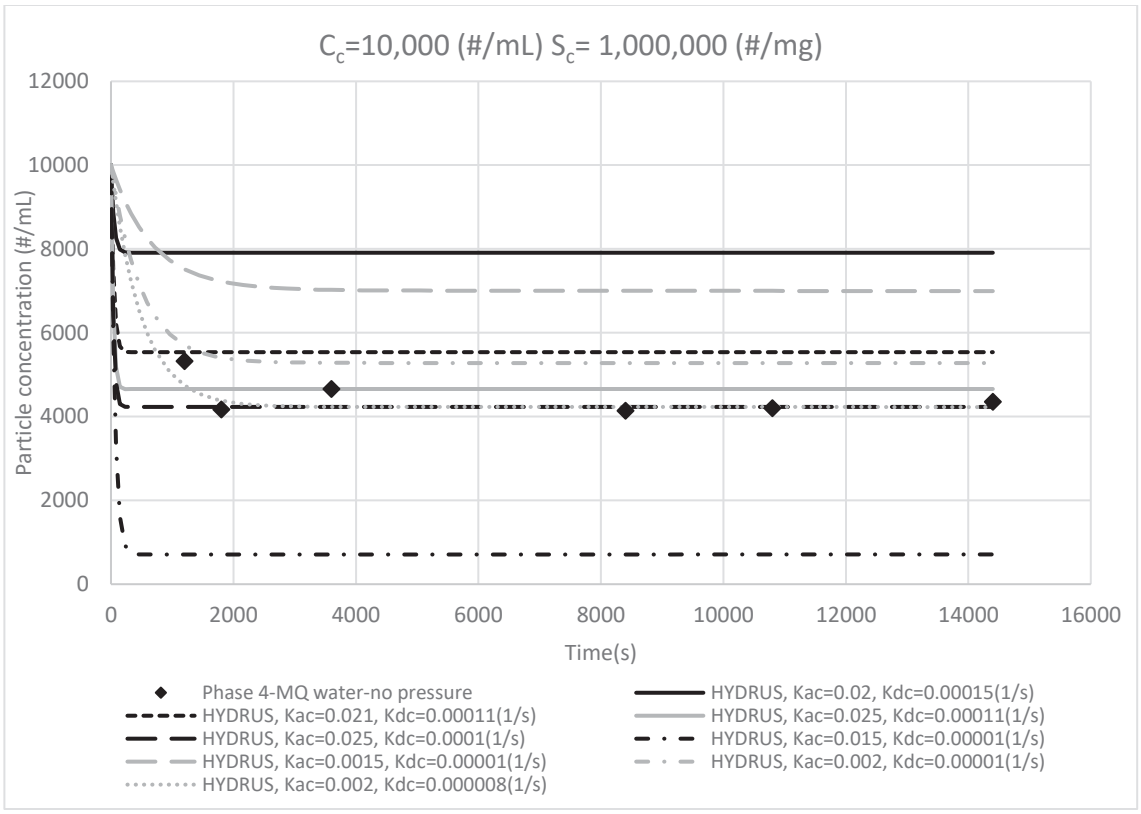
C_c=10,000 (#/mL) S_c= 1,000,000 (#/mg)
Particle concentration (#/mL)
Time(s)
Phase 4-MQ water-no pressure
HYDRUS, Kac=0.021, Kdc=0.00011(1/s)
HYDRUS, Kac=0.025, Kdc=0.0001(1/s)
HYDRUS, Kac=0.0015, Kdc=0.00001(1/s)
HYDRUS, Kac=0.002, Kdc=0.000008(1/s)
HYDRUS, Kac=0.02, Kdc=0.00015(1/s)
HYDRUS, Kac=0.025, Kdc=0.00011(1/s)
HYDRUS, Kac=0.015, Kdc=0.00001(1/s)
HYDRUS, Kac=0.002, Kdc=0.00001(1/s)

a

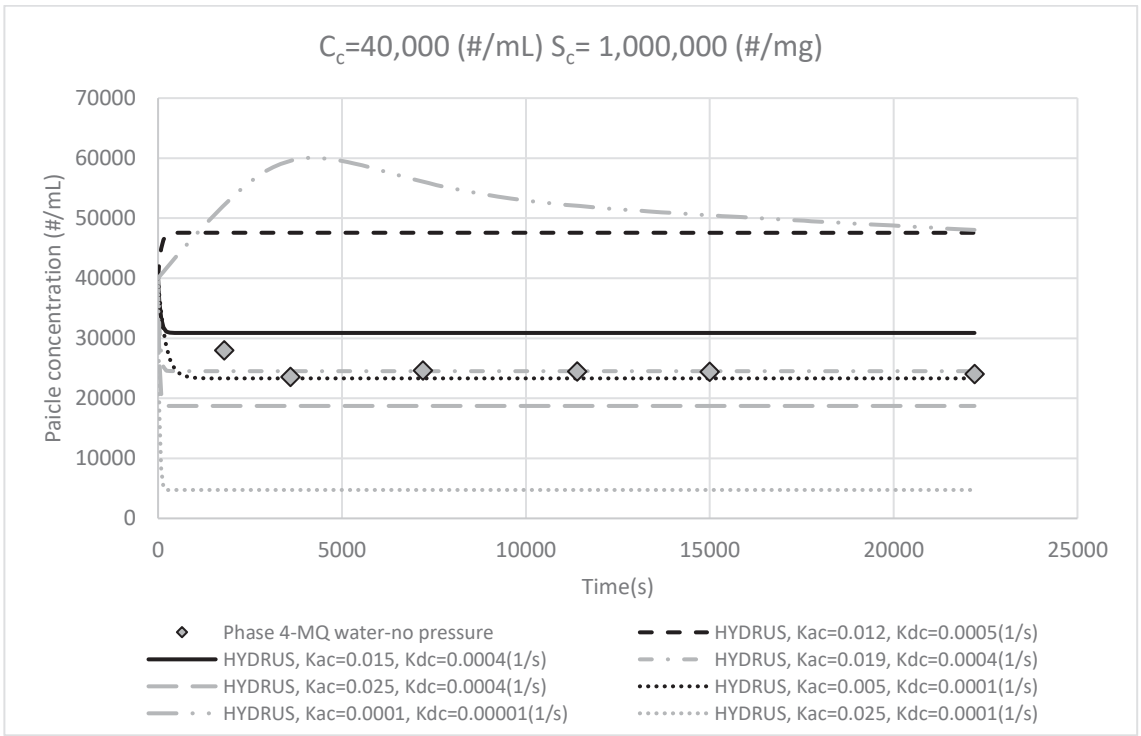
C_c=40,000 (#/mL) S_c= 1,000,000 (#/mg)
Paicle concentration (#/mL)
Time(s)
Phase 4-MQ water-no pressure
HYDRUS, Kac=0.015, Kdc=0.0004(1/s)
HYDRUS, Kac=0.025, Kdc=0.0004(1/s)
HYDRUS, Kac=0.0001, Kdc=0.00001(1/s)
HYDRUS, Kac=0.012, Kdc=0.0005(1/s)
HYDRUS, Kac=0.019, Kdc=0.0004(1/s)
HYDRUS, Kac=0.005, Kdc=0.0001(1/s)
HYDRUS, Kac=0.025, Kdc=0.0001(1/s)

b

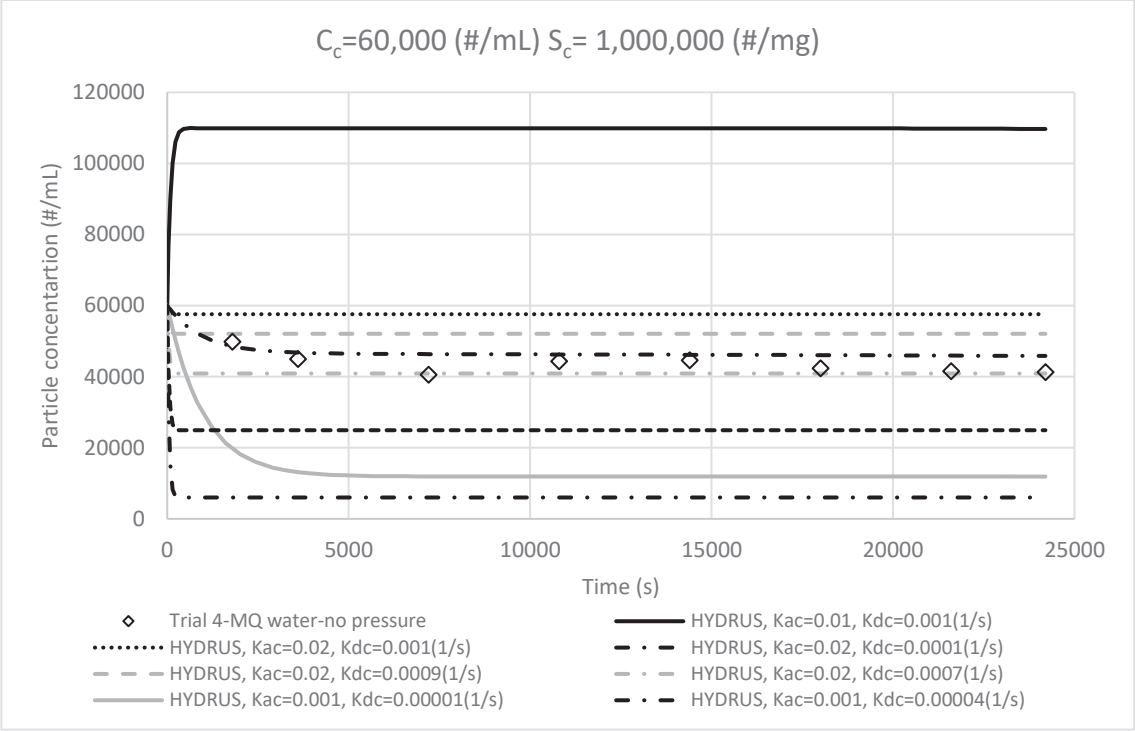

c

Figure 6.23 Observed and model M4 fitted filtrate concentration curves considering filter cake developed at (a) 21, (b) 35 and (c) 49 kPa

6.3.4 Application of Findings: Geotextile Tube Dewatering Scenario

In this section, to investigate some practical application of the findings in this chapter, some hypothetical scenarios were examined. For these scenarios, it was assumed that conditioned BH sediment (solids content of 5%) has been dewatered similarly to that using the PFT apparatus (at pressure of 35 kPa) in the laboratory condition. Therefore, a 5.3 cm filter cake with hydraulic conductivity of 0.00042 cm/s was developed. A slurry with a particle concentration of 80,000 #/mL was filtered through the geotextile/filter cake system over a period of 10 minutes at 35 kPa. This is unlike the M_3 experiments performed where Milli-Q water was used. HYDRUS was utilized in this scenario to predict the filtrate concentration with the same initial and boundary conditions as the M_3 model at 35 kPa (i.e. C_c = 80,000 #/mL, S_c = 1,000,000 #/mg). Also, it was assumed that both attachment and detachment mechanisms occur in the system at the rates of 0.012 and 0.0005 (1/s) respectively, similar to the model findings explained in a previous section. Shown on Figure 6.24a is the observed particle concentrations at the end of the Milli-Q water test (this thesis) for comparison to the predicted BH water particle concentrations predicted by the model. The filtrate

concentration decreases with time, and modelled concentrations are higher than that observed from the Milli-Q water results. Also shown on this same figure are model results for different filter cake thicknesses (H = 10 and 2 cm) to investigate the role of filter cake thickness in retaining the slurry particles during the geotextile dewatering. When the height of filter cake is 2 cm, more particles from the beginning of the dewatering procedure are released to the filtrate, when compared to a 10 cm filter cake; indicating that when a thicker filter cake is deposited on the geotextile, filtration efficiency as well as filtrate quality (in terms of particle concentration) is improved.

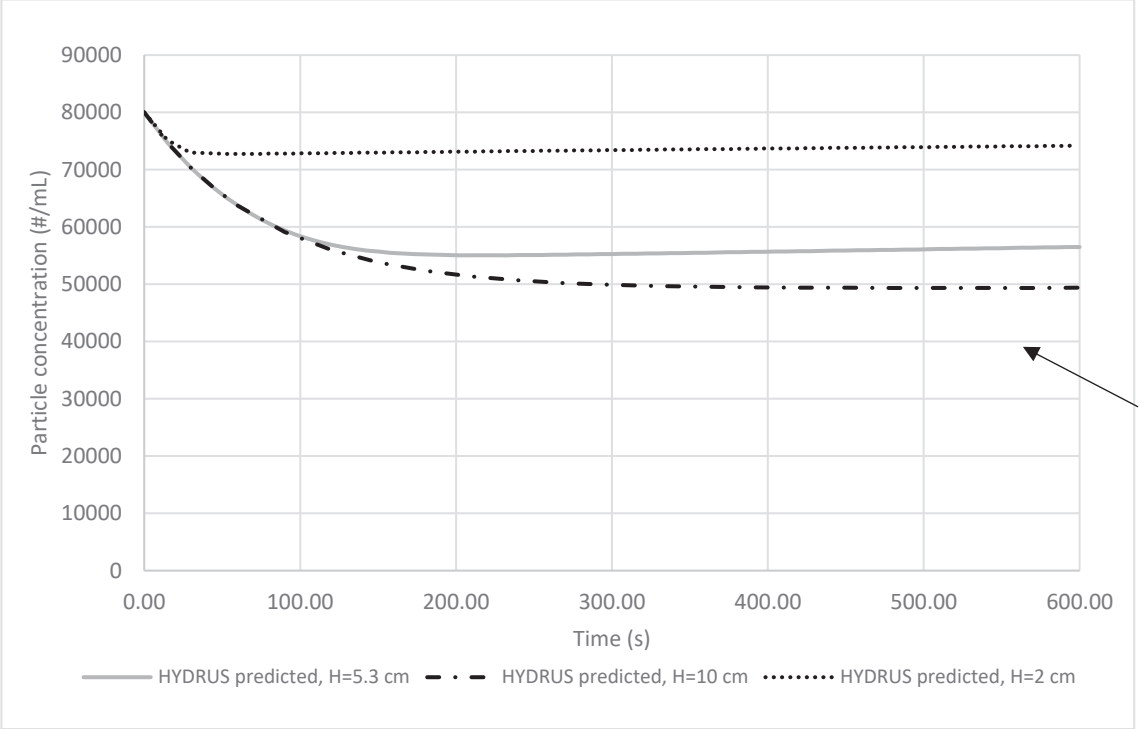

a

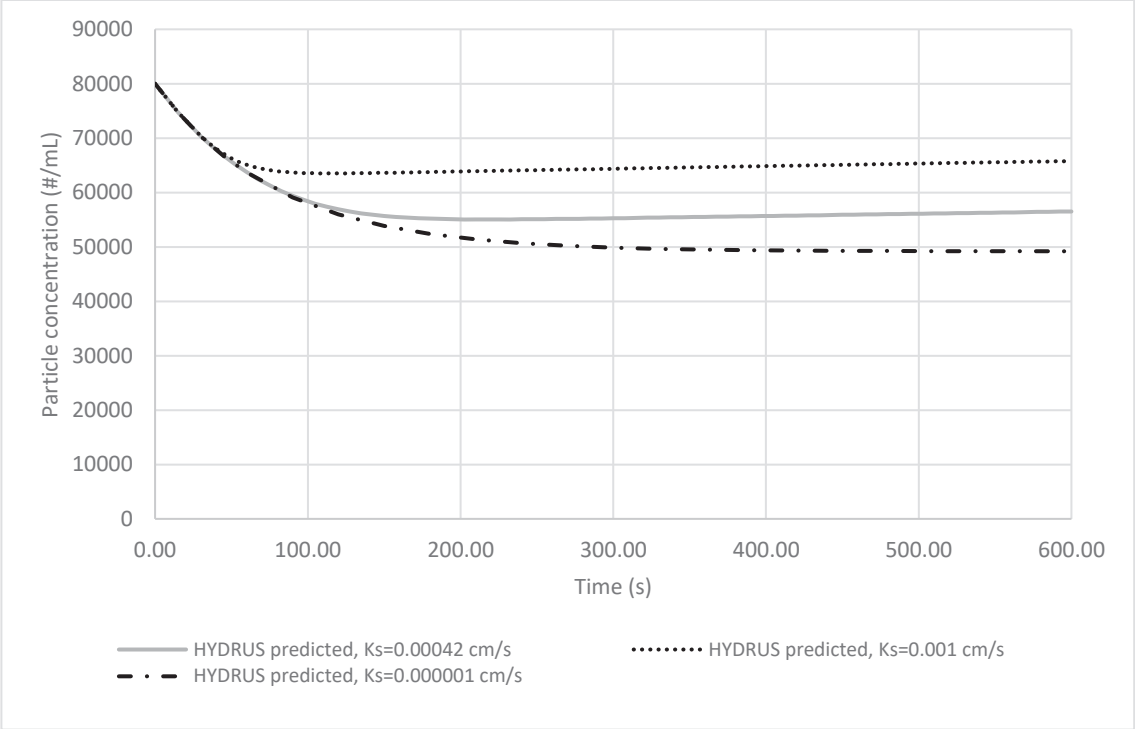

b

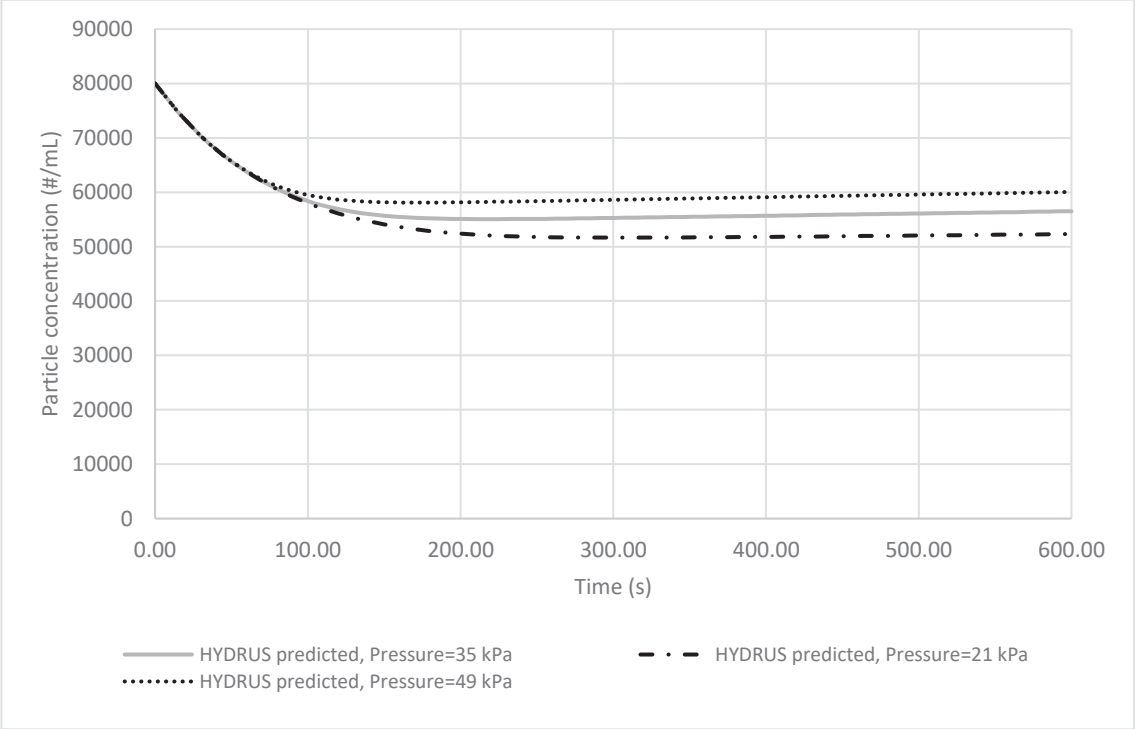

c

Figure 6.24 HYDRUS predicted filtrate particles concentration at different (a) filter cake thickness, (b) hydraulic conductivity, (c) pressure. C_c=80,000 (#/mL) S_c= 1,000,000 (#/mg)

Figure 6.24b illustrates this same scenario (i.e. same initial parameters as the experiment but this time with an examination of the effect of filter cake hydraulic conductivity on filtrate quality. As expected, a greater hydraulic conductivity resulted in greater water flux and more particles exiting the filter cake/geotextile system. In other words, if filter cake (i.e. lower K_s) compress more, filtering performance would enhance.

In the field, confining pressure may also be variable during geotextile tube dewatering applications. In Figure 6.24c it is assumed that slurry of 80,000 #/mL is filtered through same filter cake/geotextile system but at a different pressure for 10 minutes. It was previously found that pressure can change hydraulic characteristics as well as attachment detachment rates. When only considering the impacts of pressure, all the others parameter are considered to remain constant during the modeling. HYDRUS predicted that by applying more pressure on the system, filtrate concentration increases. However, this change in concentration due to the pressure is not as much as observed in PFT experiments in this study. This result may be explained by the fact that during real world implementation, properties such as porosity, hydraulic conductivity, attachment, and detachment rates change with changing the boundary condition (i.e. pressure). Therefore, the assumption of keeping them constant is not quantitatively accurate but may yield approximate results.

HYDRUS outputs in these scenarios show that particle concentrations remain constant over time, however initial particle concentrations (first seconds at small scale and hours or days in the large scale) are critical especially when contaminants associated with particle (i.e. dioxins and furans in BH sediment) exist inside the geotextile tube. To understand the practical implications of these experimental observations and modelled results, consider if filtrate particle concentrations were 60,000 #/mL under pressure of 35 kPa (See Figure 6.7). If one assumed these particles are spherical in shape with a diameter of 5 μm (average particle size of the filtrate) and density of 1.71 gr/cm^3, this particle concentration would correspond to 672×10^{-5} mg/mL in terms of mass. Given that the total PCDD/F TEQ in Boat Harbour sediment is approximately 400 pg/g (calculated for fish as a receptor as discussed in Chapter 2), a PCDD/Fs concentration associated with 672×10^{-5} mg of

particle in 1 mL of filtrate is approximately 2.69×10^{-3} pg/mL (2.69 pg/L) which is much less than standard limit for drinking water (15 pg/L) (Canadian Environmental Protection Act 1990). This suggest that as long as particle concentrations are controlled to the levels shown in this thesis for the majority of the dewatering operations, the amount of PCDD/F in the effluent will not be an issue with environmental compliance. However, it should be noted that in a geotextile tube dewatering project, boundary conditions do not remain constant over both the operating and the monitoring period. As noted in the experiments in this and previous chapters, the particle counts can be high in the initial establishment of the filter cake and therefore it is likely that initial effluent may have to be collected and reintroduced into the geotextile bag under these initial conditions until the filter cake is established.

6.4 Summary and Conclusions

In this chapter, a series of laboratory scale experiments were conducted to evaluate the geotextile dewatering performance under different pressures, with an established filter cake. The migration of particles through the geotextile/filter cake medium was monitored. Numerical modeling using the HYDRUS software was employed to simulate this particle migration during the geotextile dewatering with the intent of trying to establish the mechanisms responsible for this particle migration.

Examining filtrate quality in terms of particle concentration using the PFT at different pressures showed higher pressure (i.e. 49 kPa) results in more particles through the filter cake (i.e. increasing the particle concentration of the filtrate). However, when the system reached a stable condition, with less change in the filter cake thickness, particle concentration maintained a constant range, showing the role of filter cake in improving retention efficiency.

Particle fate and transport during the geotextile dewatering was assessed by several transport experimental tests and results were analyzed using HYDRUS modeling to identify the potential mechanisms responsible for the particle migration. Simulated results

with HYDRUS revealed that when both attachment and detachment mechanism appear to be involved in order to achieve the best match to experimental results. In addition, confining pressure during dewatering influences these attachment/detachment rates. The parametric study showed that filter cake characteristics such as thickness and hydraulic conductivity can influence particle migration during geotextile dewatering.

From a practical perspective, it was also shown that geotextile dewatering reduced the filtrate particle concentration to an acceptable level considering a typical PCDD/F standard limit for water quality. This suggests that geotextile dewatering is not only an effective method of increasing the solids content of fine-grained unconsolidated sediments (i.e. BH sediment) but can also provide an economical approach to meet the regulatory limits in terms of filtrate quality.

CHAPTER 7: CONCLUSIONS AND RECOMMENDATIONS

7.1 Conclusions

The thesis was established to answer specific research questions related to the fate and transport of particle matter during the geotextile tube dewatering of PCDD/Fs contaminated sediment. In this study Boat Harbour Stabilization Lagoon (BHSL) located in Pictou County, Nova Scotia, Canada was used as a "field lab" to investigate the geotextile tube dewatering technique for fine grained contaminated sediments. This research involved field scale experimental studies, complementary laboratory bench scale experiments and numerical modeling. The following section reviews the major contributions of the research.

7.1.1 Research Question 1: Characterization of Boat Harbour Sediment Contaminants (i.e. PDCC/Fs)

Previous pulp mill (from 1967 to present) and chlor-alkali (from 1971 to 1992) effluent discharge into Boat Harbour has deposited large quantities of unconsolidated sediment requiring remediation. Spatiotemporal characterization of contaminants (i.e. PCDD/Fs) in BH sediments was investigated using secondary monitoring data between 1992-2015. Review of secondary monitoring data discovered that PCDD/F sediment concentrations consistently exceeded highest effect thresholds for CCME SQGs, posing ecological risk, making them the main contaminant of concern. High sediment PCDD/F concentrations have persisted in Boat Harbour over the entire period (25 years). This is despite implementation of the Pulp and Paper Mill Effluent Chlorinated Dioxins and Furans Regulations in 1992, which prohibits the release of measurable PCDD/Fs in effluent wastewater (EC 2013, 2014). High PCDD/Fs concentrations measured in Boat Harbour sediments after 1992, reflect highly persistent properties of these bioaccumulative, acutely toxic organic compounds, which were presumably present before sediments were collected and reported in studies reviewed herein. Temporal georeference analysis of sampling locations revealed that overall spatial coverage was lacking. Half of (54%) Boat Harbour sediment samples analyzed for PCDD/F concentrations (from 60 samples and 49 locations) were from shallow horizons (0-15 cm), leaving deeper horizons under characterized.

Twenty-five years of monitoring data revealed large data gaps in our understanding of sediment characteristics in Boat Harbour. Gaps included spatial (vertical and horizontal) and temporal variation, presenting challenges for remediation to accurately delineate sediment contaminants.

7.1.2 Research Question 2: Variability of Physical Properties of Boat Harbour Sediment

The impact of various sampling methods (i.e. discrete versus composite versus vacuum) on the physical characteristics of contaminated sediments obtained from a large effluent stabilization lagoon of BH was assessed. A time-consuming discrete sampling technique was compared to a more time-efficient composite sample technique as well as vacuum sampling technique. The distribution of sediment thickness measured throughout the lagoon by gravity core sampling was shown to vary substantially throughout the 160 ha site. Extrusions of these gravity core samples to obtain discrete and composite samples indicate that there was no significant difference between physical characteristics (water / solids content, density, particle size) of composite samples taken from different areas within the BHSL when compared to discrete samples. For this particular site, it appears that composite sampling would provide reasonable physical parameters when compared to more time-consuming discrete sampling methods (i.e. should reflect the overall physical characteristics of the black sediment throughout the basin for practical purposes). The physical characteristics of vacuum-obtained samples were compared to gravity core samples (both discrete and composite). This sampling method resulted in more water entrained in the samples, lower solids content (~0.5–2.8%) and slightly finer particles in the samples. However, the mean particle size for the vacuum sampling was not statistically different than that of discrete and composite samples.

7.1.3 Research Question 3: Filtrate Quality (in Terms of Particle Concentration) in Different Dewatering Techniques

A series of bench scale dewatering tests were performed on a fine-grained sediment material obtained from the BHSL to examine the ability of these methods to remove particulate matter when undergoing the same polymer treatment. Three types of dewatering

tests in this bench scale study included geotextile filtration via rapid filtration testing, centrifuge testing and sedimentation testing. Given that contamination is associated with the particulate matter, it was deemed important to understand particulate removal from the various dewatering tests. It was shown that all methods resulted in greater than 98.8% of removal (based on TSS measurements) when polymer doses could be optimized (i.e. location A). Geotextile filtration removed 98.8% of solids which was lower than that obtained from sedimentation and centrifuge methods. Effluent particle numbers and sizes were reduced for all three methods relative to the original sediments. From a practical perspective, when considering time and space required (Segré, 2013) for sedimentation ponds (also considering dewatering that would be required after) and the energy requirements and mechanical upkeep to run the machine (Newman et al., 2004) for centrifuging, geotextile filtration could be a preferred alternative. This is especially true when considering the large volume of sediments (577,000 m^3) associated with the project under study. It is likely that filter cake formation during large scale trials will improve solids removal efficiency.

7.1.4 Research Question 4: Effect of Filter Cake and Confining Pressure on Geotextile Tube Dewatering Filtrate Quality

A Geotextile tube Dewatering Test (GDT) was conducted to study the geotextile filtering performance in large scale. Filtrate quality in terms of particle concentration was analyzed and results revealed that approximately 99.7% of initial concentration was removed during the geotextile dewatering process. Given the higher removal efficiency of large scale GDT comparing to that of bench scale (98.8%), it concluded that filter cake formation during large scale trials improves the solids removal efficiency. Moreover, examining the filtrate quality (in terms of particle concentration) using the laboratory scale PFT at different pressures showed that when the system reaches a stable condition (i.e. with less variation in the filter cake thickness) particle concentration maintained a constant range. This finding confirmed the role of the filter cake in improving contaminant retention efficiency.

In addition, PFT results indicated that the number of particles passing through the filter cake/geotextile system increased as confining pressure increased (i.e. 49 kPa), especially

at the beginning of the experiment when the filter cake had not yet formed. Likewise, at the beginning of each field scale GDT trail (i.e. when the plastic drum was full) the number of particles measured in the filtrate was greater, owing to the higher pressure experience at the bottom of the tank.

7.1.5 Research Question 5: Possible Mechanisms of Particle Migration During Geotextile Dewatering and Simulation of Particle Transport under Different Scenarios

The simulation of particle transport in the geotextile dewatering process was conducted with HYDRUS software. The model was parameterized and calibrated with data collected from conducted transport tests (as described in Chapter 6). The simulated model results revealed that attachment and detachment mechanisms are both responsible in fate and transport of particles through the filter cake/geotextile system during the dewatering. The HYDRUS parametric study was capable of predicting effluent concentrations that were similar to laboratory-observed results (PFT). However, due to the changing of hydraulic characteristics and geometric properties (i.e. thickness of filter cake) of the system under different conditions, identifying the exact values of attachment and detachment rates was not possible.

7.2 Recommendations

Based on the findings of this research, several recommendations for future work in this field are suggested:

- establishment of local baseline concentrations for a suite of organic and inorganic contaminants, which should also be complimented by discussions with local knowledge holders to elucidate pre-1967 conditions within Boat Harbour;
- analysis of filtrate PCDD/Fs concentration of the laboratory scale PFT as well as field scale GDT to further investigate the fate and transport of these congeners during the geotextile dewatering operation;
- long term monitoring of geotextile dewatering filtrate in terms of particle concentration (i.e. consolidation);
- develop and conduct additional transport tests and employ HYDRUS modelling to isolate accurate attachment and detachment rate coefficients during dewatering;
- compare the particle concentrations found in this study with field dewatering monitoring data in the Boat Harbour dewatering project.

References

Ali, M., Sreekrishnan, T.R. (2001). Aquatic toxicity from pulp and paper mill effluents: a review. *Advances in Environmental Research* 5(2), 175-196. https://doi.org/10.1016/S1093-0191(00)00055-1

Alimohammadi, M. Hoffman, E., Lyons, J.A., Walker, T.R., Lake, C.B. (2017). Historical sampling of dioxin and furan contaminated sediment from pulp and paper effluent. Retrieved from: GeoOttawa2017 Conference. http://www.geoottawa2017.ca/ [September 20, 2018].

Alimohammadi, M., Tackley, H., Holmes, B., Davidson, K., Lake, C.B. Spooner, I.S., Jamieson, R.C. Walker, T.R. (2019). Laboratory and field physical property characterization for a contaminated sediment for bench scale dewatering purposes. Geo-Environmental Engineering Conference, Concordia University, Montreal, Canada, May 30-31, 2019

Alimohammadi, M., Tackley, A. H., Lake, C. B., Spooner, I. S., Walker, T. R., Jamieson, R. C., Gan, C., Bossy, K. (2019). Effect of different sediment dewatering techniques on subsequent particle sizes in industrial derived effluent. *Canadian Journal of Civil Engineering,* 191(9):590. https://doi.org/10.1139/cjce-2019-0269

Alimohammadi, M., Tackley, H. A., Holmes, B., Davidson, K., Lake, C. B., Spooner, I. S., Jamieson, R. C., & Walker, T. R. (2020). Characterizing sediment physical property variability for bench scale dewatering purposes. *Environmental Geotechnics.* https://doi.org/10.1680/jenge.19.00214

Atlantic RBCA (Risk-Based Corrective Action) (2012). Ecological Screening Protocol for Petroleum Impacted Sites in Atlantic Canada Scientific Rationale Scientific Rationale to support the Adoption/Development of Tier 1 Ecological Screening Levels for Soil, Surface Water, Groundwater and Sediment, Version 3, July 2012.

APHA, AWWA, WEF. (2005). Standard methods for the examination of water and wastewater. 21st Edition. Published jointly by the American Public Health Association, American Water Works Association, and Water Environment Federation. New York.

Arnold, D., Plank, C., Erickson, E., Pike, F. (1958). Solubility of Benzene in Water. *Industrial & Engineering Chemistry Chemical & Engineering Data Series*. 3 (2): 253–256. https://doi:10.1021/i460004a016

ASTM (2007) D 4972-01: Standard Test Method for pH of Soils. West Conshohocken, PA, USA.

ASTM (2010) D7503-18: Standard Test Method for Measuring the Exchange Complex and Cation Exchange Capacity of Inorganic Fine-Grained Soils. West Conshohocken, PA, USA.

ASTM (2013) D2035-13: Standard Practice for Coagulation-Flocculation Jar Test of Water. West Conshohocken, PA, USA.

ASTM (2014) D 2974-14: Standard Test Methods for Moisture, Ash, and Organic Matter of Peat and Other Organic Soils. ASTM International, West Conshohocken, PA, USA.

ASTM (2019) D 2216-19: Standard Test Methods for Laboratory Determination of Water (Moisture) Content of Soil and Rock by Mass. ASTM International, West Conshohocken, PA, USA.

ASTM (2014) D 854-14: Standard Test Methods for Specific Gravity of Soil Solids by Water Pycnometer. ASTM International, West Conshohocken, PA, USA.

ATSDR - Agency for Toxic Substances and Disease Registry (1995). Toxicological Profile for Polycyclic Aromatic Hydrocarbons (PAHs). U.S. Department of Health and Human Services, Public Health Service, Georgia, USA. Retrieved from: https://www.atsdr.cdc.gov/toxprofiles/tp.asp?id=122&tid=25 [August 10, 2020]

ATSDR - Agency for Toxic Substances and Disease Registry (1998). Toxicological Profile for Chlorinated Dibenzo-p-Dioxins. U.S. Department of Health and Human Services, Public Health Service, Georgia, USA. Retrieved from: https://www.atsdr.cdc.gov/toxprofiles/tp.asp?id=366&tid=63 [August 10, 2020]

ATSDR - Agency for Toxic Substances and Disease Registry (2007). Toxicological Profile for Benzene. U.S. Department of Health and Human Services, Public Health Service, Georgia, USA. Retrieved from: https://www.atsdr.cdc.gov/toxprofiles/tp.asp?id=40&tid=14 [August 10, 2020]

ATSDR - Agency for Toxic Substances and Disease Registry. (2009). Case Studies in Environmental Medicine Toxicity of Polycyclic Aromatic Hydrocarbons (PAHs). Retrieved from: https://www.atsdr.cdc.gov/ [February 2, 2017].

Aydilek, A. H., Edil, T. B. (2002). Filtration performance of woven geotextiles with wastewater treatment sludge. *Geosynthetics International*, 9(1), 41–69. https://doi.org/10.1680/gein.9.0210

Bennett, E., (2013). *We Had Something Good and Sacred Here': ReStorying A'se'k with Pictou Landing First Nation*. Master of Applied Science Thesis dissertation. Dalhousie University, Halifax, Nova Scotia, Canada.

Balkhair, K. S. (2017). Modeling fecal bacteria transport and retention in agricultural and urban soils under saturated and unsaturated flow conditions. *Water Research*, 110, 313-320. https://doi.org/10.1016/j.watres.2016.12.023

Bhatia, S.K., Liao, K. (2004). Overview of Geotextile Tube Applications & Research. ICGGE-2004, IIT Bombay, Mumbai, India.

Bhatia, S. K., Maurer, W. B., Khachan, M. M., Grzelak, D. M., Pullen, S. T. (2013). Performance Indices for Unidirectional Flow Conditions Considering Woven Geotextiles and Sediment Slurries. *Sound Geotechnical Research to Practice*, 318–332. https://doi.org/10.1061/9780784412770.021

Boat Harbour Act. (2015). An Act Respecting the Cessation of the Use of the Boat Harbour Effluent Treatment Facility for the Reception and Treatment of Effluent from the Northern Pulp Mill. Bill 89, c. 4, s. 1. Government of Nova Scotia. Retrieved from: http://nslegislature.ca/legc/ [September 20, 2016].

Bradford, A. S., Bettahar, M., Simunek, J., Genuchten, M.Th. (2003). Straining and attachment of colloids in physically heterogeneous porous media. *Vadose Zone Journal*, 3(2), 384-394. https://doi.org/10.2113/3.2.384

Canadian Environmental Protection Act (1990). Polychlorinated dibenzodioxins and polychlorinated dibenzofurans. Ontario

Canadian Environmental Protection Act. (1999). Pulp and Paper Mill Effluent Chlorinated Dioxins and Furans Regulations. Retrieved from: http://laws-lois.justice.gc.ca/ [January 21, 2017]

Cantre´, S., Saathoff, F. (2011). Design method for geotextile tubes considering strain – Formulation and verification by laboratory tests using photogrammetry. *Geotextiles and Geomembranes*, 29(3), 201–210. https://doi.org/10.1016/j.geotexmem.2010.10.009

CBC News. Withers, P. (2019). Citing online sources: Province says it's not budging on Boat Harbour deadline. Retrieved from: https://www.cbc.ca/news/canada/nova-scotia/northern-pulp-boat-harbour-pictou-county-1.4981174 [March 19, 2019].

CBC News. Smith, E. (2020). Citing online source: Pictou Landing chief 'shocked' by look of Boat Harbour months after mill shutdown. Retrieved form: https://www.cbc.ca/news/canada/nova-scotia/chief-andrea-paul-boat-harbour-northern-pulp-treatment-facility-1.5532999 [September 20, 2020]

CCME - Canadian Council of Ministers of the Environment. (2001a). Canadian sediment quality guidelines for the protection of aquatic life: Polychlorinated dioxins and furans (PCDD/Fs). Retrieved from: http://st-ts.ccme.ca/ [June 16, 2017].

CCME. (2001b). Canadian Tissue Residue Guidelines for the Protection of Wildllife Consumers of Aquatic Biota: polychlorinated dibenzo-p-dioxins and polychlorinated dibenzofurans (PCDD/Fs). Retrieved from: http://st-ts.ccme.ca/ [June 16, 2017].

CCME. (2002). Canadian soil quality guidelines for the protection of environmental and human health: Dioxins and Furans. Retrieved from: http://st-ts.ccme.ca/ [June 16, 2017].

CCME. (2008). Canadian Sediment Quality Guidelines: carcinogenic and other polycyclic aromatic hydrocarbons (PAHs). Retrieved from: http://st-ts.ccme.ca/ [January 24, 2017].

CCME. (2016). Canadian Sediment Quality Guidelines for the Protection of Aquatic Life. Canadian Environmental Quality Guidelines. Retrieved from: http://st-ts.ccme.ca/ [June 25, 2016].

Chalmers, G., Adams, R., Bustin, A., Bustin, M. (2019). The environmental significance of sediment surface area as a controlling factor in the preservation of Polychlorinated Dibenzo-P-Dioxins and Dibenzofurans (PCDD/PCDF) in sediments adjacent to woodfibre pulp mill, Howe Sound, British Columbia. *Minerals*, 9(11), 711. https://doi.org/10.3390/min9110711

Chapman, P.M. (2011). Framework for Addressing and Managing Aquatic Contaminated Sites Under the Federal Contaminated Sites Action Plan (FCSAP), Taylor & Francis, Burnaby (BC), Canada.

Chaudhary, M., Walker, T. R., Willis, R., Oakes, K. (2020). Baseline characterization of sediments and marine biota near industrial effluent discharge in Northumberland Strait, Nova Scotia, Canada. *Marine Pollution Bulletin, 157*. https://doi.org/10.1016/j.marpolbul.2020.111372

Chu, J., Guo, W., Yan, S. W. (2011). Geosynthetic tubes and geosynthetic mats: Analyses and applications. *Geotechnical Engineering*, 42(1), 56–65.

Chu, J., Yan, S. W., Li, W. (2012). Innovative methods for dike construction – An overview. *Geotextiles and Geomembranes*, 30, 35–42. https://doi.org/10.1016/j.geotexmem.2011.01.008

Colodey, A.G., Wells, P.G. (1992). Effects of pulp and paper mill effluents on estuarine and marine ecosystems in Canada: a review. *Journal of Aquatic Ecosystem Health* 1, 201-226.

Contaminated Sites Regulations. (2013). Environment Act. S.N.S. 1994-95, c. 1 O.I.C. 2012-60.

Corapcioglu, M. Y., Choi, H. (1996). Modeling colloid transport in unsaturated porous media and validation with laboratory column data. *Water Resource Research*, 32, 3437-3449.

Davis, E., Walker, T.R., Adams, M., Willis, R. (2018). Characterization of polycyclic aromatic hydrocarbons (PAHs) in small craft harbour (SCH) sediments in Nova Scotia, Canada. *Marine Pollution Bulletin*. 137, 285-294. https://doi.org/10.1016/j.marpolbul.2018.10.043

Davis, E., Walker, T.R., Adams, M., Willis, R. (2019). Estimating PAH sources in harbor sediments using diagnostic ratios. *Remediation Journal*, 29(3), 51-62. https://doi.org/10.1002/rem.21600

Dunnington, D. W., White, H., Spooner, I. S., Mallory, L. M., White, C., O'Driscoll, J. N., McLellan, R. N. (2017). A paleolimnological archive of metal sequestration and release in the Cumberland Basin Marshes, Atlantic Canada. *Journal of FACETS*, 2, 440-460. https://doi.org/10.1139/facets-2017-0004

El-Shahawi, M.S., Hamza, A., Bashammakh, A.S., Al-Saggaf, W.T. (2010). An overview on the accumulation, distribution, transformations, toxicity and analytical methods for the monitoring of persistent organic pollutants. *Talanta*, 80(5), 1587-1597. https://doi.org/10.1016/j.talanta.2009.09.055

Environment Canada (EC). (1992). The development of Canadian marine environmental quality guidelines. Ecosystems science and evaluate directorate; Marine Environmental Quality Series No. 1. Ottawa, Ontario.

EC. (2013). Science solutions for improved pulp and paper mill effluents. Retrieved from: http://www.ec.gc.ca/ [March 23, 2015].

EC. (2014). Pulp and paper mill effluent chlorinated dioxins and furans regulations. Retrieved from: http://www.ec.gc.ca/ [March 23, 2015].

EC. (2016). Historical substance reports. Retrieved from: http://www.ec.gc.ca/ [April 4, 2017].

EC. (2017). National Pollutant Release Inventory. Retrieved from: http://www.ec.gc.ca/ [August 8, 2017].

Esri (2019). How Topo to Raster Works. Retrieved from: https://pro.arcgis.com/en/pro-app/tool-reference/3d-analyst/how-topo-to-raster-works.htm [September 10, 2019]

Fisheries Act. (1985). R.S., c. F-14, s. 1.

Fowler, J., Bagby, R.M., Trainer, E. (1997). Dewatering sewage sludge with geotextile tubes. Geotechnical Fabrics Report, pp. 26–30. Retrieved from: https://www.arieng.com/dosyalar/sayfa/sludge.pdf

Gaffney, D.A., Martin, S.M., Maher, M.H., Bennert, T.A. (1999). Dewatering Contaminated, fine-grained Material Using Geotextiles. Geosynthetics'99, Boston, MA, pp1016-1031.

Gaffney, D.A. (2001a). Geotextile Tube Dewatering-Part 1: Design Parameters. Geotechnical Fabrics Report, September, 2001, pp12-15.

Gaffney, D.A. (2001b). Geotextile Tube Dewatering-Part 2: Successful Project Implementation. Geotechnical Fabrics Report, October/November, 2001, vol. 19, no. 18.

Gargiulo, G., Bradford, S. A., Simunek, J., Ustohal, P., Vereecken, H., & Klumpp, E. (2008). Bacteria transport and deposition under unsaturated flow conditions: The role of water content and bacteria surface hydrophobicity. *Vadose Zone Journal*, 7(2), 406-419. https://doi.org/10.2136/vzj2007.0068

GHD Limited (2018a) Phase 2 Environmental Site Assessment, Boat Harbour Remediation Planning and Design, Pictou County, Nova Scotia, Nova Scotia Land Inc., Project No. 11148275, Report No. 6.

GHD Limited. (2018b). Remedial Option Decision Document, Project No. 11148275.

Glew, J. R., Smol, J. P., Last, W. M. (2002). Sediment Core Collection and Extrusion. In: Last W.M., Smol J.P. (eds) Tracking Environmental Change Using Lake Sediments. Developments in Paleoenvironmental Research, vol 1. Springer, Dordrecht. https://doi.org/10.1007/0-306-47669-X_5

Government of Canada. (2019). Wastewater Systems Effluent Regulations (SOR/2012-139), Fisheries Act of Canada, Government of Canada.

Hach Company/Hach Lange GmbH, (2014). Method 8006: Suspended Solids, Photometric Method (750 mg/L). DOC316.53.01139

Harvey, R. W., Garabedian, S. P. (1991). Use of colloid filtration theory in modeling movement of bacteria through a contaminated sandy aquifer. *Environmental Science and Technology*, 25, 178-185.

Hayward, J. L. (2020). Fate and transport of determinants of antimicrobial resistance in variably saturated terrestrial environments. PhD thesis in civil engineering in Dalhousie university.

Hewitt, M.L., Parrott, J.L., McMaster, M.E. (2006). A decade of research on the environmental impacts of pulp and paper mill effluents in Canada: sources and characteristics of bioactive substances. *Journal of Toxicology and Environmental Health, Part B: Critical Reviews*, 9(4), 341–356. https://doi.org/10.1080/15287390500195976

Hites, R.A. (2011). Dioxins: An Overview and History. *Environmental Science & Technology,* 45(1), 16-20. https://doi.org/10.1021/es1013664

Hoffman, E., Bernier, M., Blotnicky, B., Golden, P.G., Janes, J., Kader, A., Kovacs-Da Costa, R., Pettipas, S., Vermeulen, S., Walker, T.R. (2015). Assessment of public perception and environmental compliance at a pulp and paper facility: A Canadian case study. *Environmental Monitoring Assessment*. 187(12), 766. https://doi.org/10.1007/s10661-015-4985-5

Hoffman, E., Lyons, J., Boxall, J., Robertson, C., Lake, C.B., Walker, T.R. (2017a). Spatiotemporal assessment (quarter century) of pulp mill metal(loid) contaminated sediment to inform remediation decisions. *Environmental Monitoring Assessment*. 189(6), 257. https://doi.org/10.1007/s10661-017-5952-0

Hoffman, E., Guernsey, J.R., Walker, T.R. Kim, J.S., Sherren, K., Andreou, P. (2017b). Pilot study investigating ambient air toxics emissions near a Canadian kraft pulp and paper facility in Pictou County, Nova Scotia. *Environmental Science and Pollution Research*. 249250, 20685–20698. https://doi.org/10.1007/s11356-017-9719-5

Hoffman, E., Alimohammadi, M., Lyons, J., Davis, E., Walker, R. T., Lake, B. C. (2019). Characterization and spatial distribution of organic contaminated sediment derived from historical industrial effluents. *Environmental Monitoring and Assessment*, 191(9):590. https://doi.org/10.1007/s10661-019-7763-y

Hope, B.K. (2006). An examination of ecological risk assessment and management practices. *Environment International*. 32(8), 983–995. https://doi.org/10.1016/j.envint.2006.06.005

Hornberger G. M., Mills, L. A., Herman, S. J. (1992). Bacterial transport in porous media: Evaluation of a model using laboratory observations. *Water Resource Research*, 28, 915-938.

Huang, W., Koerner, R.M. (2005). An Amendment Strategy for Enhancing the Performance of Geotextile Tubes Used in Decontamination of Polluted Sediments and Sludges, Proceedings of the Sessions of the Geo-Frontiers 2005 Congress, Robert M. Koerner, George R. Koerner, Y. Grace Hsuan, Marilyn V. Ashley - Editors, January 24–26, 2005, Austin, Texas, USA

Huang, C. C., Luo, S. Y. (2007). Dewatering of reservoir sediment slurry using woven geotextiles. Part I: Experimental results. *Geosynthetics International*, 14(5), 253–263. https://doi.org/10.1680/gein.2007.14.5.253

Jiang, S., Pang, L., Buchan, G. D., Šimůnek, J., Noonan, M. J., & Close, M. E. (2010). Modeling water flow and bacterial transport in undisturbed lysimeters under irrigations of dairy shed effluent and water using HYDRUS-1D. *Water Research*, 44(4), 1050-1061. https://doi.org/10.1016/j.watres.2009.08.039

JWEL - Jacques Whitford Environment Limited (1994). Nova Scotia Department of Supply and Services: initial environmental assessment of a pipeline and diffuser proposal for the Boat Harbour Treatment Facility. Report No. 9768.

JWEL. (1997). Shoreline Remediation, Boat Harbour Stabilization Lagoon. Draft report to NSTPW. Report No. 11412.

JWEL. (1999). Sediment Chemistry and Biotoxicity at the BHTF Stabilization Lagoon. Report to NSTPW. Report No. 13248.

JWEL. (2001). 2000 Sediment Sampling BHTF Stabilization Lagoon. Report to NSTPW, Project No. NSD 15200.

JWEL. (2005). 2003/2004 sediment sampling BHTF stabilization lagoon. Report to NSTPW. Project No. NSD 17324–7.

JWEL and Beak Consultants. (1992). An investigation of sediment characteristics at Boat Harbour Treatment Facility. Report to Nova Scotia Department of Supply and Services, NSDSS Project. No. 8109.

JWEL and Beak Consultants. (1993). A supplementary study to assess the sediment characteristics of the estuary at the Boat Harbour Treatment Facility.

Kannan, K., Watanabe, I., Giesy, J.P. (1998). Congener profile of polychlorinated/brominated dibenzo-p-dioxins and dibenzofurans in soil and sediments collected at a former chlor-alkali plant: Communicated by Toxicological and Environmental Chemistry. *Toxicological & Environmental Chemistry*. 67, 135-146. https://doi.org/10.1080/02772249809358608

Khachan, M. M., Bhatia, K. S., Maurer, B. W., Gustafson, C. A. (2012). Dewatering and utilization of fly ash slurries using geotextile tubes. *Indian Geotechnical Journal*, 42(3),194–205. https://doi.org/10.1007/s40098-012-0019-1

Khachan, M.M., Bhatia, S.K. (2017). The efficacy and use of small centrifuge for evaluating geotextile tube dewatering performance. *Geotextiles and Geomembranes*, 45(4), 280-293. https://doi.org/10.1016/j.geotexmem.2017.04.001

King, T.L., Chou, C.L. (2003). Anthropogenic organic contaminants in American lobsters (Homarus americanus) procured from harbours, bays, and inlets of eastern Canada. Canadian Technical Reports Fisheries and Aquatic Sciences 2456, vi-24 pp.

Koerner, G.R., Koerner., R.M. (2006). Geotextile Tube Assessment Using a Hanging Bag Test. *Geotextiles and Geomembranes*, 24 (2), 129-137. https://doi.org/10.1016/j.geotexmem.2005.02.006

Kulkarni, P. S., Crespo, J. G., Afonso, C. A. M. (2008). Dioxins sources and current remediation technologies — A review. *Environment International*, 34 (1), 139–153. https://doi.org/10.1016/j.envint.2007.07.009

Kutay, M. E., Aydilek, A. H. (2004). Retention performance of geotextile containers confining geomaterials. *Geosynthetics International*, 11(2), 100–113. https://doi.org/10.1680/gein.2004.11.2.100

Kutay, M. E., Aydilek, A. H. (2005). Filtration performance of two-layer geotextile systems. *Geotechnical Testing Journal*, 28(1), 79-91. https://doi.org/10.1520/GTJ12580

Lamy, E., Lassabatere, L. Bechet, B., Andrieu, H. (2013). Effect of a nonwoven geotextile on solute and colloid transport in porous media under both saturated and unsaturated conditions. *Geotextiles and Geomembranes*, 36, 55-65. http://dx.doi.org/10.1016/j.geotexmem.2012.10.009

Lamy, E., Lassabatere, L., Béchet, B. (2008). Influence of porous media heterogeneity on flow and pollutant transfer in infiltration basin sub-soils. In: Proceeding of the 11th International Conference on Urban Drainage, Edinburgh, Scotland, UK.

Lawson, C. R. (2008). Geotextile containment for hydraulic and environmental engineering. *Geosynthetics International*, 15(6), 384–427. https://doi.org/10.1680/gein.2008.15.6.384

Liao, K., Bhatia, S. K. (2005). Geotextile tube: Filtration performance of woven geotextiles under pressure. Proceedings of NAGS 2005/GRI – 19 Cooperative Conference, Las Vegas, NV, December.

Liao, K., Bhatia, S.K. (2006). Evaluation on filtration performance of woven geotextiles by falling head, pressure filtration test, and hanging bag tests, Proceedings of 8th International Conferenence on Geosynthetics, Sep 18-22, Yokohama, Japan., Kuwani & Koseki, J (eds), Millpress, Rotterdam, ISBN 90 5966 0447

Liao, K. (2008). *Dewatering of natural sediments using geotextile tubes*. PhD thesis in civil and environmental engineering in L.C Smith College of Engineering & Computer Science of Syracuse University.

Lodge, K. B., Cook, P. M. (1989). Partitioning studies of dioxin between sediment & water: The measurement of K_{oc} for Lake Ontario sediment. Chemosphere. 19(1), 439-444. https://doi.org/10.1016/0045-6535(89)90349-4

Long, E.R., Field, L.J., MacDonald, D.D. (1998). Predicting toxicity in marine sediments with numerical sediment quality guidelines. *Environmental Toxicology and Chemistry*. 17(4), 714-727. https://doi.org/10.1002/etc.5620170428

Louchouarn, P., Seward, M. S., Cornelissen, G., Arp, H. P., Yeager, K. M., Brinkmeyer, R., Santschi, H. P. (2018). Limited mobility of dioxins near San Jacinto super fund site (waste pit) in the Houston Ship Channel, Texas due to strong sediment sorption. *Environmental Pollution*, 238, 988-998. https://doi.org/10.1016/j.envpol.2018.02.003

MacAskill, N.D., Walker, T.R., Oakes, K., Walsh, M. (2016). Forensic assessment of polycyclic aromatic hydrocarbons at the former Sydney tar ponds and surrounding environment using fingerprint techniques. *Environmental Pollution*. 212, 166-177. https://doi.org/10.1016/j.envpol.2016.01.060

Mackay, D., Shiu, W.Y., Ma, K.C. (1992). Illustrated Handbook of Physical-chemical Properties and Environmental Fate for Organic Chemicals, vol II. Lewis Publishers, Boca Raton, FL, USA.

Mackie, A.L. (2010). *Feasibility study of using cement kiln dust as a chemical conditioner in the treatment of acid mine effluent*. Master of Applied Science Thesis dissertation. Dalhousie University, Halifax, Nova Scotia, Canada.

Malik, J., Sysala, S. (2011). Analysis of geosynthetic tubes filled with several liquids with different densities. *Geotextiles and Geomembranes*, 29(3), 249–56. https://doi.org/10.1016=j.geotexmem.2010.11.004

Mao, S. (1997). *High water content sludge dewatering via freeze-thaw*. Master thesis, Department of Civil and Environmental Engineering, University of Alberta, Edmonton, Canada.

Mastin, B., Lebster, E. G., Salley, R. J. (2008). Use of Geotube dewatering containers in environmental dredging. Proceedings of GeoAmericas 2008 (CD-ROM), Cancun Mexico.

Maxxam. (2016). PAHs-Chemistry, Sources and Forensic Tools [Technical Education Webinar]. Retrieved from: http://sciencesummit.wpengine.com/ [May 10, 2017].

McLeay, D.J. (1987). Aquatic toxicity of pulp and paper mill effluent: a review. Environment Canada. Ottawa, Report EPS 4/PF/1,191.

Minitab (2019). Retrieved from: https://support.minitab.com/en-us/minitab-express/1/help-and-how-to/modeling-statistics/anova/how-to/one-way-anova/before-you-start/overview/ [September 10, 2019].

Moo-Young, H.K & Ochola, C. (1999 a). Laboratory evaluation of geosynthetic fabric containers for contaminant migration. In: G.C. Schafran, Editor, Environmental Engineering ’99, American Society of Civil Engineers, Reston, VA (1999), pp. 141–151.

Moo-Young & Ochola, C. (1999 b). Strain effects on the filtration properties of geotextiles. Geosynthetics ’99. Boston, MA, Industrial Fabrics Association International, Roseville, MN, pp. 757–768.

Moo-Young, H., Myers, T.E., Townsend, D., Ochola, C. (1999). The migration of contaminants through geosynthetic fabric containers utilized in dredging operations. *Engineering Geology*, 53(2), 167–176. https://doi.org/10.1016/S0013-7952(99)00030-7

Moo-Young, H.K., Douglas, A.G., Xinghua, Mo. (2002). Testing Procedures to Assess the Viability of Dewatering with Geotextile Tubes. *Geotextiles and Geomemebranes*, 20 (5). 289-303. https://doi.org/10.1016/S0266-1144(02)00028-6

Morales, I., Amador, J. A., & Boving, T. (2015). Bacteria transport in a soil-based wastewater treatment system under simulated operational and climate change conditions. *Journal of Environmental Quality*, 44(5), 1459-1472. https://doi.org/10.2134/jeq2014.12.0547

Morales, I., Atoyan, J. A., Amador, J. A., & Boving, T. (2014). Transport of pathogen surrogates in soil treatment units: Numerical modeling. *Water*, 6(4), 818-838. https://doi.org/10.3390/w6040818

Mori, H., Miki, H., Tsuneoka, N. (2002). The geo-tube method for dioxin-contaminated soil. *Geotextiles and Geomembranes*, 20(5), 281–288. https://doi.org/10.1016/S0266-1144(02)00027-4

Muthukumaran, A. E., Ilamparuthi, K. (2006). Laboratory studies on geotextile filters as used in geotextile tube dewatering. *Geotextiles and Geomembranes*, 24 (4), 210–219. https://doi.org/10.1016/j.geotexmem.2006.03.002

Munkittrick, K.R., McMaster, M.E., Servos, M.R. (2013). Detection of reproductive impacts of effluents from pulp and paper mills: shifts in issues and potential causes. *Environmental Toxicology and Chemistry*. 32(4), 729-731. https://doi.org/10.1002/etc.2143

Nedwell, D.B., Walker, T.R. (1995). Sediment-water fluxes of nutrients in an Antarctic coastal environment: influence of bioturbation. *Polar Biology*. 15(1), 57-64. https://doi.org/10.1007/BF00236125

Newman, P., Hodgson, M., Rosselot, E. (2004). The disposal of tailings and mine water sludge using geotextile dewatering techniques. *Minerals Engineering*, 17(2), 115–121. https://doi.org/10.1016/j.mineng.2003.10.020

NIOSH – National Institute of Occupational Safety and Health (1984). 2,3,7,8 - Tetrachlorodibenzo-p-dioxin (TCDD, "dioxin"). Retrieved from: https://www.cdc.gov/niosh/docs/84-104/default.html [August 10, 2020].

NOAA. (1999). Sediment Quality Guidelines developed for the National Status and Trends Program. Available at: http://archive.orr.noaa.gov/

Norstrom, R.J. (2006). Polychlorinated dibenzo-p-dioxins and dibenzofurans in the Great Lakes. *Persistent Organic Pollutants in the Great Lakes* (pp. 71-150). Springer Berlin Heidelberg.

Northern Pulp. (2017). Personal communication with Northern Pulp technical staff, Pictou Nova Scotia, July 2017.

Nova Scotia Environment (NSE). (2014). Air Quality 964 Health Index (AQHI). Retrieved from: http://novascotia.ca/nse/ [August 18, 2016].

NSE. (2015). 2015 industrial approval for Northern Pulp Nova Scotia. Province of Nova Scotia. Environment Act, S.N.S. 1994–95, c.1.

Oakes, K. (2016). Fish surveys at Boat Harbour. Report to Nova Scotia Lands Inc. p 7.

Ogden, J.G., III. 1(972). Oxygen demand of effluent from a bleached k raft pulp mill. *Water Air and Soil Pollution*, 1(4), 365-374. https://doi.org/10.1007/BF00250655

Pang, L., Šimůnek, J. (2006). Evaluation of bacteria-facilitated cadmium transport in gravel columns using the HYDRUS colloid-facilitated solute transport model. *Water Resource Research*. 42 (12), W12S10, https://doi.org/10.1029/2006WR004896

Parsons and Geosyntec. (2010). Draft Onondaga Lake SCA Civil and Geotechnical Final Design. Prepared for Honeywell. January 2010.

Persson, Y., Lundstedt, S., Oberg, L., Tysklind, M. (2007). Levels of chlorinated compounds (CPs, PCPPs, PCDEs, PCDFs and PCDDs) in soils at contaminated sawmill sites in Sweden. *Chemosphere*, 66 (2), 234–242. https://doi.org/10.1016/j.chemosphere.2006.05.052

Pinto, P. X., Al-Abed, S. R., Barth, E., Loftspring, C., Voit, J., Clark, P., Ioannides, A. M. (2011). Environmental impact of the use of contaminated sediments as partial replacement of the aggregate used in road construction. *Journal of Hazardous Materials*, 189, 546–555, https://doi.org/10.1016/j.jhazmat.2011.02.074

Pictou Landing Native Women's Group, Castleden, H., Lewis, D., Jamieson, R., Gibson, M., Rainham, D., Russell, R., Martin, D., Hart, C. (2016). Our Ancestors Are in Our Land, Water, and Air: A Two-Eyed Seeing Approach to Researching Environmental Health Concerns with Pictou Landing First Nation – Final Report. p. 117.

Pokhrel, D., Viraraghavan, T. (2004). Treatment of pulp and paper mill wastewater-a review. *Science of The Total Environment*. 333, 37-58. https://doi.org/10.1016/j.scitotenv.2004.05.017

Pulp and paper effluent regulations (PPER). (1992). Pulp and paper effluent regulations. Fisheries Act SQR/92–69. P.C. 1992–961.

Reis, E., Lodolo, A., Miertus, S. (2007). Survey of sediment remediation technologies. International center for science and high technology. Retrieved from: https://clu-in.org/download/contaminantfocus/sediments/Survey-of-sediment-remediation-tech.pdf [August 15, 2019].

Richards, L. A. (1931). Capillary conduction of fluid through porous mediums. *Physics*, (1), 318-333.

Richman, L., Haimovici, L., Kolic, T., Besevic, S., Reiner, E. (2016). Monitoring Re-Suspension and Transport of Dioxin Contaminated Sediment to Evaluate the Recovery of a Shallow Urban Creek Post Sediment Remediation. *Journal of Environmental Protection*. 7, 453-466.

Roach, B., Walker, T.R. (2017). Aquatic monitoring programs conducted during environmental impact assessments in Canada: Preliminary assessment before and after weakened environmental regulation. *Environmental Monitoring Assessment*. 189(3), 109. https://doi.org/10.1007/s10661-017-5823-8

Romo, J., Chaudhary, M., Walker, T.R. (2019). Baseline assessment of contaminants in marine biota prior to remediation of industrial effluent impacted sediments in a former tidal estuary in Nova Scotia, Canada. *Marine Pollution Bulletin.* 145, 641-648. https://doi.org/10.1016/j.marpolbul.2019.06.055

Rupakheti, P. (2016). *Containment and dewatering of heavy metal contaminated slurries using reactive soil mineral and cellulose materials*. Master of Science Thesis, Department of Civil Engineering, Syracuse University, New York, US.

Saadet, A. B., Begüm, T. B. (2016). Laboratory Investigations for Dewatering of Golden Horn Dredged Sludge with Geotextile Tubes. Marine *Georesources & Geotechnology*, 34(7), 638-647. https://doi.org/10.1080/1064119X.2015.1068894

Satyamurthy, R. (2008). Experimental investigations of geotextile tube dewatering. PhD. Thesis, Department of Civil Engineering, Syracuse University, New York, US.

Segré, G. (2013). A physicochemical evaluation of the compressibility and dewatering behavior of dredged sediments. MSc. Thesis, Department of Civil Engineering, Syracuse University, New York, US.

Šejna, M., Šimůnek, J., & van Genuchten, M.T. (2014) The HYDRUS software package for simulating the two- and three-dimensional movement of water, heat, and multiple solutes in variably-saturated porous media. HYDRUS user manual. Version 2.04. PC Progress, Czech Republic. Retrieved from: https://www.pc-progress.com/downloads/Pgm_Hydrus3D2/HYDRUS3D%20User%20Manual.pdf [January 2, 2020].

Sharma, D. K., King, D., Oma, P., Merchant, C. (2010). Micro-Flow Imaging: Flow microscopy applied to sub-visible particulate analysis in protein formulations. *AAPS Journal*. 12(3), 455-464. https://doi.org/10.1208/s12248-010-9205-1

Shin, E. C., Oh, I. Y. (2007). Coastal erosion prevention by geotextile tube technology. *Geotextiles and Geomembranes*, 25(4–5), 264–277. https://doi.org/10.1016/j.geotexmem.2007.02.003

Šimůnek, J., Šejna, M., & van Genuchten, M.T. (2012). The C-Ride Module for HYDRUS (2D/3D). Version 1.0. PC Progress, Ltd., Prague, Czech Republic. Retrieved from:

Šimůnek, J., Šejna, M., & van Genuchten, M.T. (2006). The HYDRUS software package for simulating the two- and three-dimensional movement of water, heat, and multiple solutes in variably-saturated porous media. Version 1.0. PC Progress, Czech Republic, 241 pp. Retrieved from: https://www.ars.usda.gov/arsuserfiles/20360500/pdf_pubs/P2165.pdf [January 2, 2020].

Šimůnek, J., van Genuchten, M.T., & Šejna, M. (2012). The HYDRUS software package for simulating two- and three-dimensional movement of water, heat, and multiple solutes in variably-saturated porous media, Technical Manual, Version 2.0, PC Progress, Prague, Czech Republic, 258 pp.

Sirivithayapakorn, S., Keller, A. (2003). Transport of colloids in saturated porous media: a pore-scale observation of the size exclusion effect and colloid acceleration. *Water Resources Research*, 39, 1109-1120. https://doi.org/10.1029/2002WR001583

Soskolne, C.L., Sieswerda, L.E. (2010). Cancer risk associated with pulp and paper mills: a review of occupational and community epidemiology. *Chronic diseases in Canada*. 29, 86-100.

Spooner, I., Dunnington, D. (2016). Boat Harbour gravity core sediment survey. Draft report to Nova Scotia Lands Inc. pp. 15.

Stantec. (2013). Sediment metals chemistry. (Unpublished raw data). Project No: 121410566.

Stantec. (2016). Final Report: Geotechnical and Contaminant Assessment. Report to Nova Scotia Lands Inc. File No: 121413919.

Stephens, T., Melo L. C., de Castro, N. P. B., and Marques, A. C. M. (2011). Canal Do Fundão contaminated sediments GDT analysis versus actual full scale project results. *Geo-Frontiers Congress*. https://doi.org/10.1061/41165(397)218.

St-Jean, S.D., Courtenay, S.C., Parker, R.W. (2003). Immunomodulation in blue mussels (Mytilus edulis) exposed to a pulp and paper mill effluent in eastern Canada. *Water Quality Research Journal*. 38(4), 647-666. https://doi.org/10.2166/wqrj.2003.041

Sunito, L.R., Shiu, W.Y., Mackay, D. (1988). A review of the nature and properties of chemicals present in pulp mill effluents. *Chemosphere*, 17(7), 1249-1290.

Svensson, B.G., Nilsson, A., Hansson, M., Rappe, C., Åkesson, B., Skerfving, S. (1991). Exposure to dioxins and dibenzofurans through the consumption of fish. *The New*

England Journal of Medicine. 324(1), 8-12. https://doi.org/10.1056/nejm199101033240102

Svensson, B.G., Barregård, L., Sällsten, G., Nilsson, A., Hasson, M., Rappe, C. (1993). Exposure to polychlorinated dioxins (PCDD) and dibenzofurans (PCDF) from graphite electrodes in a chloralkali plant. *Chemosphere*, 27, 259-262.

Tackley, H. (2019). *The behavior and migratory fate of select heavy metals during the dewatering of an effluent derived sediment*. Master of Science thesis, Dalhousie University, Halifax, Canada. Available from http://hdl.handle.net/10222/76263.

Tackley, H.A., Lake, C.B., Alimohammadi, M. (2020). Examining metal migration through geotextiles during dewatering. Accepted for publication, *Geotextiles and Geomembranes*.

Tencate. (2011). Geotube GT500 technical data sheet. Retrieved from: https://www.rhmooreassociates.com/images/pdf/Geotube-GT500-TDS2011.pdf

Tencate. (2015). Geotube® dewatering container (Standard Dewatering Specification). Version 15.

Tencate. (2016). Geotube® GDT Field Test. Retrieved from: https://bishopwater.ca/case-studies/ [September 21, 2020].

Tencate. (2017). Geotube RDT Test. Retrieved from: https://www.tencategeo.us/en-us/products/geotube-systems/geotube-dewatering [February 14, 2019].

Teoh, S., Tan, R.B.H., Tien, C. (2006). Analysis of cake filtration data - a critical assessment of conventional filtration theory. *AIChE Journal*. 52 (10), 3427–3442. https://doi.org/10.1002/aic.10952

Tien, C., Ramarao, V. B. (2011). Revisiting the laws of filtration: an assessment of their use in identifying particle retention mechanisms in filtration. *Journal of Membrane Science*. 383(1-2), 17–25. https://doi.org/10.1016/j.memsci.2011.07.019

Tobiszewski, M., Namieśnik, J. (2012). PAH diagnostic ratios for the identification of pollution emission sources. *Environmental Pollution*. 162, 110-119. https://doi.org/10.1016/j.envpol.2011.10.025

Trudel, L. (1991). Dioxins and Furans in Bottom Sediments Near the 47 Canadian Pulp and Paper Mills Using Chlorine Bleaching. Prepared for the Water Quality Branch of Environment Canada; Ottawa, Ontario.

USEPA. 1994a. Health assessment document for 2, 3, 7, 8-tertachlorodibenzo-p-dioxin (TCDD) and related compounds. EPA/600/Bp-92/001c estimating exposure to dioxin-like compounds, epa/600/6-88/005cb. Washington, DC: Office of research and development.

USEPA. (1994b). Combustion emission technical resource document (CETRED), Report No. EPA 530-R-94-014.Washington, DC: Office of Solid Waste Emergency Response.

van den Berg, M., Birnbaum, L., Bosveld, A.T., Brunström, B., Cook, P., Feeley, M., Giesy, J.P., Hanberg, A., Hasegawa, R., Kennedy, S.W., Kubiak, T. (1998). Toxic equivalency factors (TEFs) for PCBs, PCDDs, PCDFs for humans and wildlife. *Environmental Health Perspective*. 106(12), 775-792. https://doi.org/10.1289/ehp.98106775

Walker, T.R. (2014). Environmental effects monitoring in Sydney Harbor during remediation of one of Canada's most polluted sites: a review and lessons learned. *Remediation Journal*. 24(3), 103-117. https://doi.org/10.1002/rem.21397

Walker, T.R. (2016). Mercury concentrations in marine sediments near a former mercury cell chlor-alkali plant in eastern Canada. *Marine Pollution Bulletin*. 107(1), 398-401. https://doi.org/10.1016/j.marpolbul.2016.03.033

Walker, T.R., MacLean, B., Appleton, R., McMillan, S., Miles, M. (2013a). Cost-effective sediment dredge disposal options for small craft harbors in Canada. *Remediation*. 23(4), 123-140. https://doi.org/10.1002/rem.21371

Walker, T.R., MacAskill, D., Rushton, T., Thalheimer, A., Weaver, P. (2013b). Monitoring effects of remediation on natural sediment recovery in Sydney Harbour, Nova Scotia. *Environmental Monitoring and Assessment*. 185, 8089-8107. https://doi.org/10.1007/s10661-013-3157-8

Walker, T.R., MacAskill, D., Weaver, P. (2013c). Environmental recovery in Sydney Harbour, Nova Scotia: Evidence of natural and anthropogenic sediment capping. *Marine Pollution Bulletin*. 74(1), 446-452. https://doi.org/10.1016/j.marpolbul.2013.06.013

Walker, T.R., MacAskill, D., Weaver, P. (2013d). Legacy contaminant bioaccumulation in rock crabs in Sydney Harbour during remediation of the Sydney Tar Ponds, Nova Scotia, Canada. *Marine Pollution Bulletin*. 77, 412-417. https://doi.org/10.1016/j.marpolbul.2013.09.036

Walker, T.R., MacAskill, D. (2014). Monitoring water quality in Sydney Harbour using blue mussels during remediation of the Sydney Tar Ponds, Nova Scotia, Canada. *Environmental Monitoring Assessment*. 186, 1623-1638. https://doi.org/10.1007/s10661-013-3479-6

Walker, T.R., Willis, R., Leroy, M., MacLean, B., Appleton, R., McMillan, S., Wambolt, N., Gray, T., Smith, M. (2015a). Ecological Risk Assessment of Sediments in Sydney Harbour, Nova Scotia, Canada. *Soil and Sediment Contamination: An International Journal*. 24(5), 471-493. https://doi.org/10.1080/15320383.2015.982244

Walker, T.R., Bernier, M., Blotnicky, B., Golden, P.G., Hoffman, E., Janes, J., Kader, A., Kovacs-Da Costa, R., Pettipas, S., Vermeulen, S. (2015b). Harbour divestiture in Canada: Implications of changing governance. *Marine Policy*. 62, 1-8. https://doi.org/10.1016/j.marpol.2015.08.018

Walker, T.R., MacAskill, N.D., Thalheimer, A., Zhao, L. (2017). Contaminant mass flux and forensic assessment of polycyclic aromatic hydrocarbons: Tools to inform remediation decision making at a contaminated site in Canada. *Remediation Journal*. 27(4), 9-17. https://doi.org/10.1002/rem.21525

Wangensteen, M., Lafferty, P., Kobler, D. J. (2001). Innovative dewatering and water treatment techniques for hydraulically dredged sediments. The First International Conference on Remediation of Contaminated Sediments, Venice, October, 10–11, 361–69.

Weggel, R., Ward, D. (2012). A model for filter cake formation on geotextiles: Theory. *Geotextile and Geomembranes*, 31, 51–61. https://doi.org/10.1016/j.geotexmem.2011.10.002

Wente, M. M. (1991). Mobility of dioxins and furans from stabilized incineration residue in seawater. Marine science research center, Stony Brook university, Stony Brook, New York. Wilson DC. URI: http://hdl.handle.net/1951/61688

Williamson, D. F., Parker, R. A., Kendrick, J. S. (1989). The box plot: a simple visual method to interpret data. *Annals of Internal Medicine*, 110(11), 916-921. https://doi.org/10.7326/0003-4819-110-11-916

Ya, J. (2017). *Electro-dewatering Treatment of Pulp and Paper Mill Biosludge: The Effects of Conditioners*. Master of Science thesis, Department of Chemical Engineering and Applied Chemistry University of Toronto, Canada.

Yamamoto, T., Higashino, K., Abe, T., Takasuga, T., Takemori, H., Weber, R., Sasaki, Y. (2018). PCDD/PCDF formation in the chlor-alkali process—laboratory study and comparison with patterns from contaminated sites. *Environmental Science and Pollution Research volume*. 25, 31874-31884. https://doi.org/10.1007/s11356-017-0777-5

Yan, S. W., Chu, J. (2010). Construction of an offshore dike using slurry filled geotextile mats. *Geotextiles and Geomembranes*, 28, 422–33. https://doi.org/10.1016/j.geotexmem.2009.12.004

Yee, W. T., Lawson, R. C. (2012). Modelling the geotextile tube dewatering process. *Geosynthetics International*, 19(6), 339–53.

Yee, W. T., Lawson, R. C., Wang, Y. Z., Ding, L., Liu, Y. (2012). Geotextile tube dewatering of contaminated sediments, Tianjin Eco-City, China. *Geotextiles and Geomembranes*, 31, 39–50. https://doi.org/10.1016=j.geotexmem.2011.07.005

Yunker, M.B., MacDonald, R.W., Vingarzan, R., Mitchell, R.H., Goyette, D., Sylvestre, S. (2002). PAHs in the Fraser River basin: a critical appraisal of PAH ratios as indicators of PAH source and composition. *Organic Geochemistry*. 33(4), 489-515. https://doi.org/10.1016/S0146-6380(02)00002-5

Yunker, M.B., Lachmuth, C.L., Cretney, W.J., Fowler, B.R., Dangerfield, N., White, L., Ross, P.S. (2011). Biota – Sediment partitioning of aluminium smelter related PAHs and pulp mill related diterpenes by intertidal clams at Kitimat, British Columbia. *Marine Environmental Research*. 72(3), 105-126. https://doi.org/10.1016/j.marenvres.2011.06.004

Zhang, S., Yang, G., Hou, S., Zhang, T., Li, Z., & Liang, F. (2018a). Distribution of ARGs and MGEs among glacial soil, permafrost, and sediment using metagenomic analysis. *Environmental Pollution*, 234, 339-346. https://doi.org/10.1016/j.envpol.2017.11.031

Zhang, Y., Li, A., Dai, T., Li, F. Xie, H., Chen, L., & Wen, D. (2018b). Cell-free DNA: A neglected source for antibiotic resistance genes spreading from WWTPs. *Environmental Science & Technology*, 52, 248-257. https://doi.org/10.1021/acs.est.7b04283

APPENDIX A — Supplemental Figures

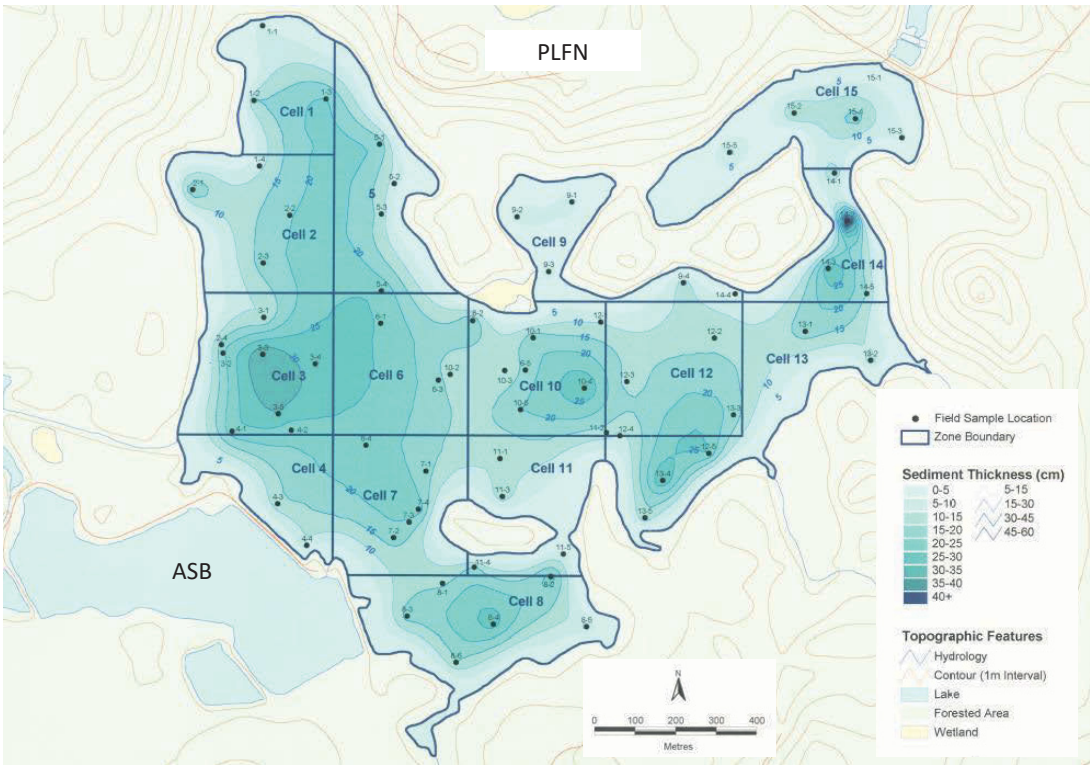

Figure A.1 Mean sediment thickness (cm) in BH adapted from JWEL (2005) and Hoffman et al. (2017a).

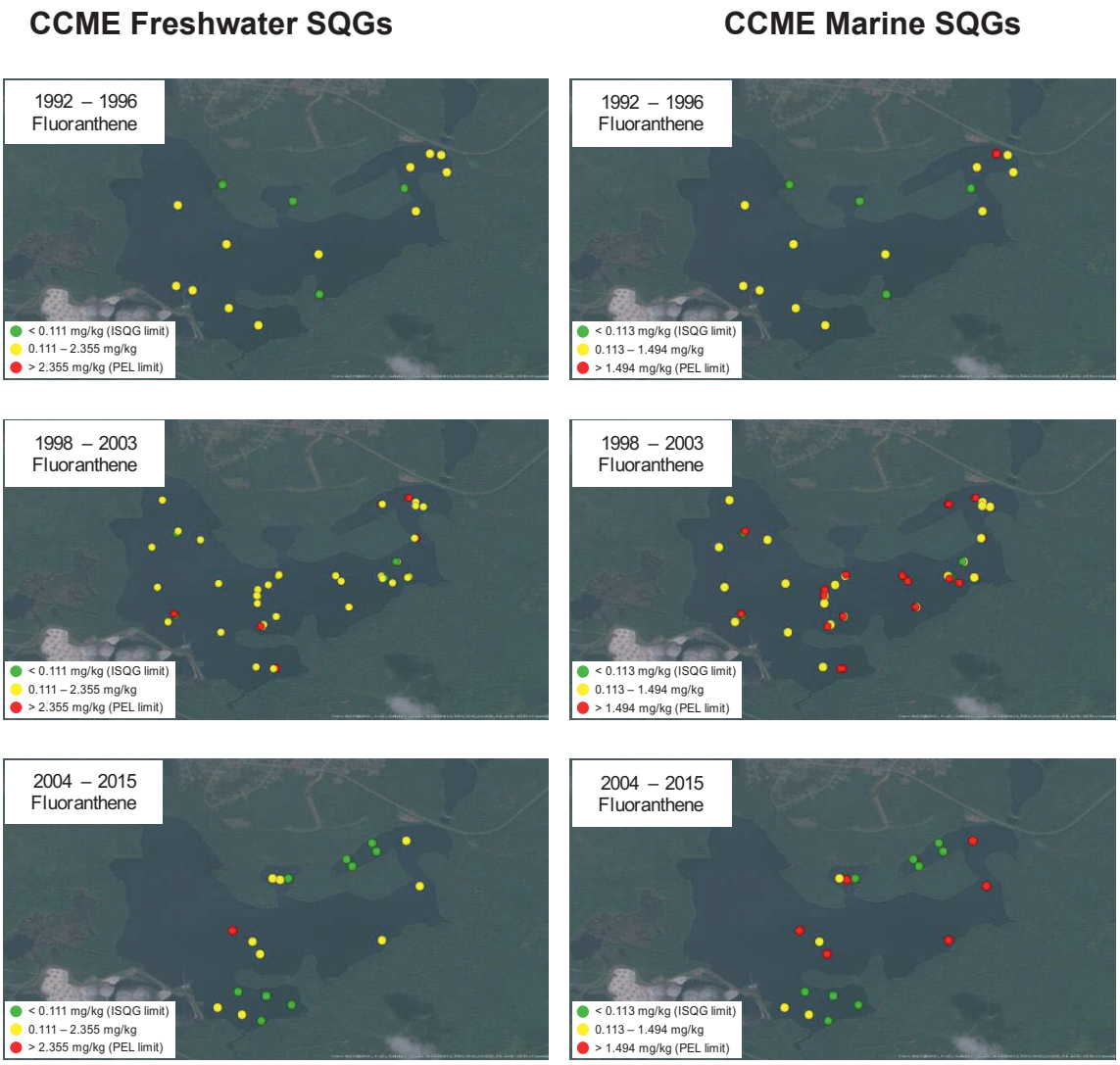

Figure A.2 Spatiotemporal variation of fluoranthene compared to CCME freshwater (green, <0.111 [ISQG]; yellow, 0.111-2.355; red, >2.355 [PEL] mg/kg) and marine (green, <0.113 [ISQG]; yellow, 0.113-1.494; red, >1.494 [PEL] mg/kg) SQGs in Boat Harbour sediment over three periods: top 1992-1996; middle 1998-2003; bottom 2004-2015.

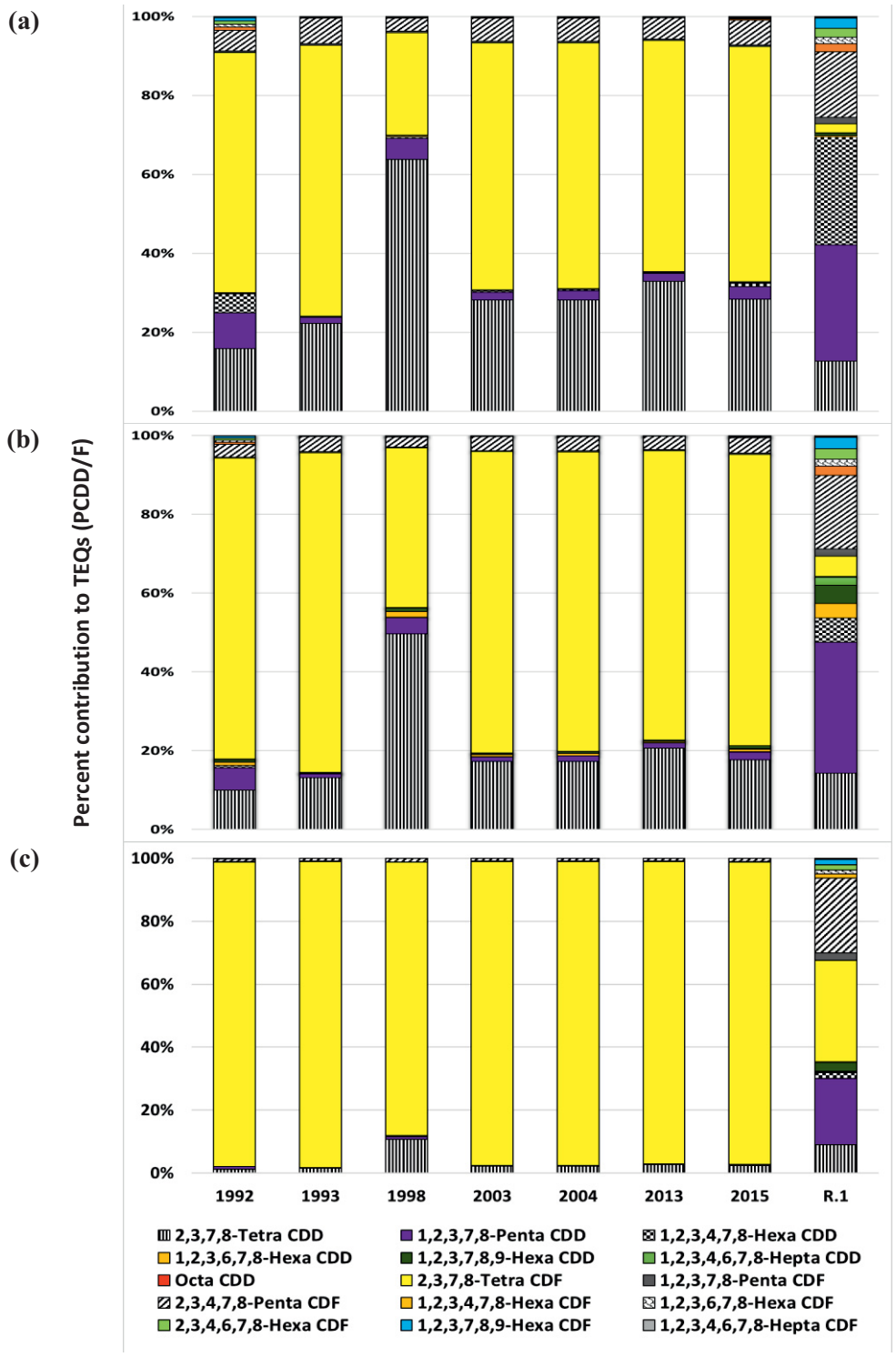

Figure A.3 PCDD/F congener patterns in Boat Harbour sediments compared with congener patterns in sediment collected at the R.1 reference station (JWEL 1994). Data reflect percent contributions of each congener to the ∑17PCDD/Fs.

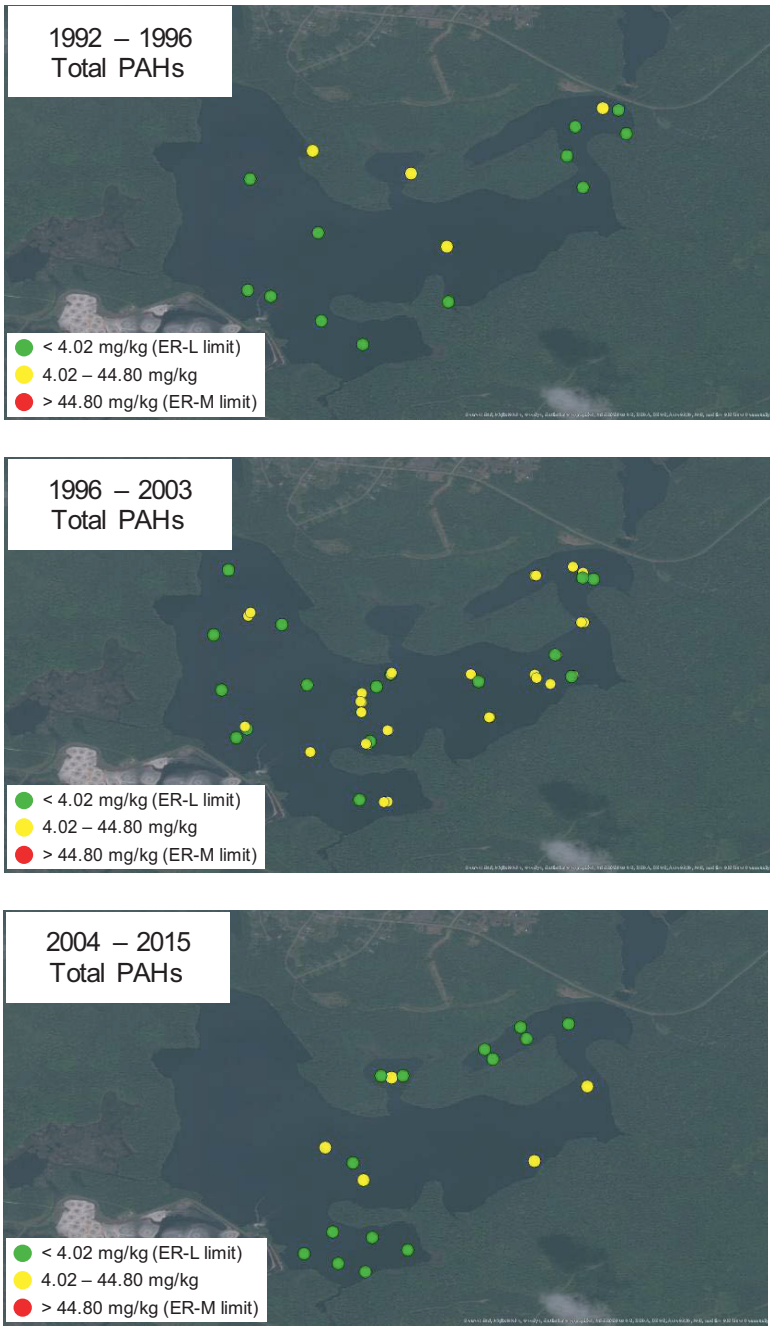

Figure A.4 Spatiotemporal variation of total PAHs compared effects range low (ER-L) and effects range median (ER-M) (green, <4.02 [ER-L]; yellow, 4.02-44.80; red, >44.80 [ER-M] mg/kg) measures of toxicity in Boat Harbour over three periods: top 1992-1996; middle 1998-2003; bottom 2004-2015 (Long et al. 1998; NOAA 1999).

(a)

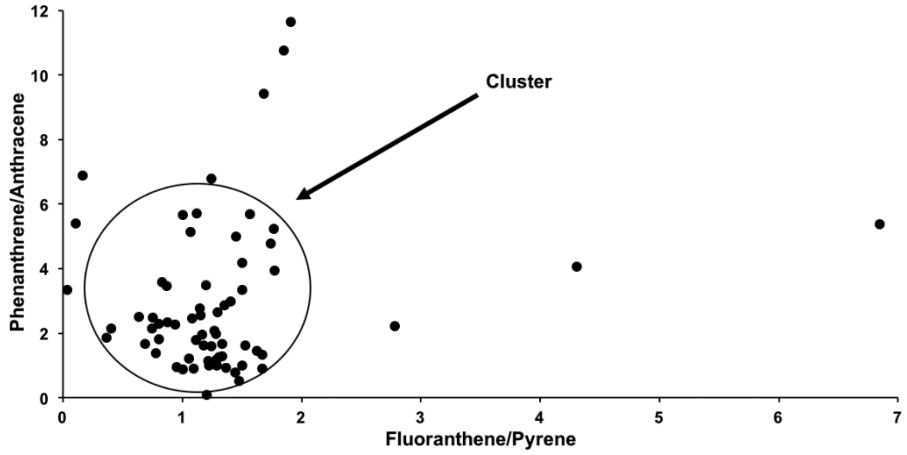

(b)

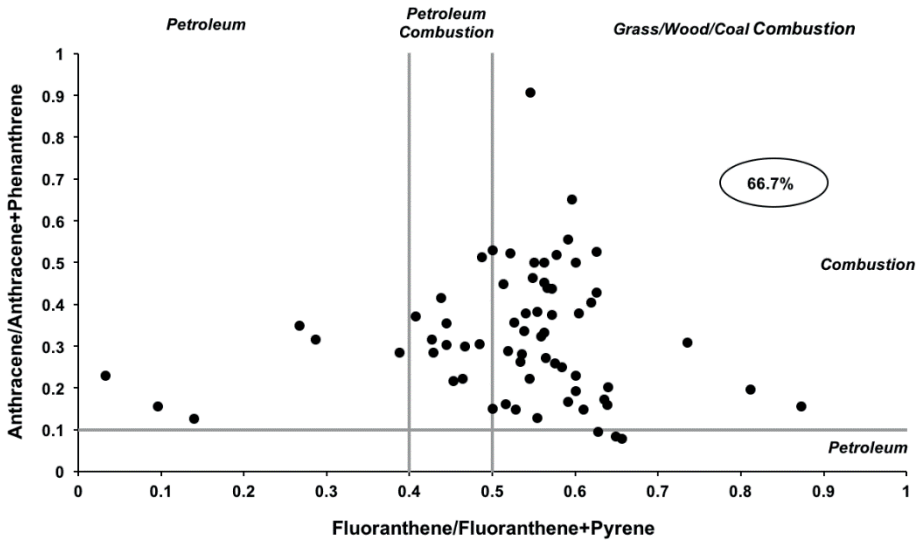

Figure A.5 PAH diagnostic ratios of fluoranthene to pyrene vs. phenanthrene to anthracene (a). PAH ratios plot were adopted from a technical webinar resource from Maxxam (2016). (b) PAH double ratio of fluoranthene/fluoranthene+pyrene vs. anthracene/anthracene+phenanthrene (n=66). Solid grey lines represent source transition points identified by Yunker et al. (2002).

Figure A.6 Gravity corer device (Photograph taken on May 17, 2018).

Figure A.7 Gravity core extruder apparatus (Photograph taken on July 7, 2017)

Figure A.8 Vacuum sampling method (Photograph taken on May 17, 2018)

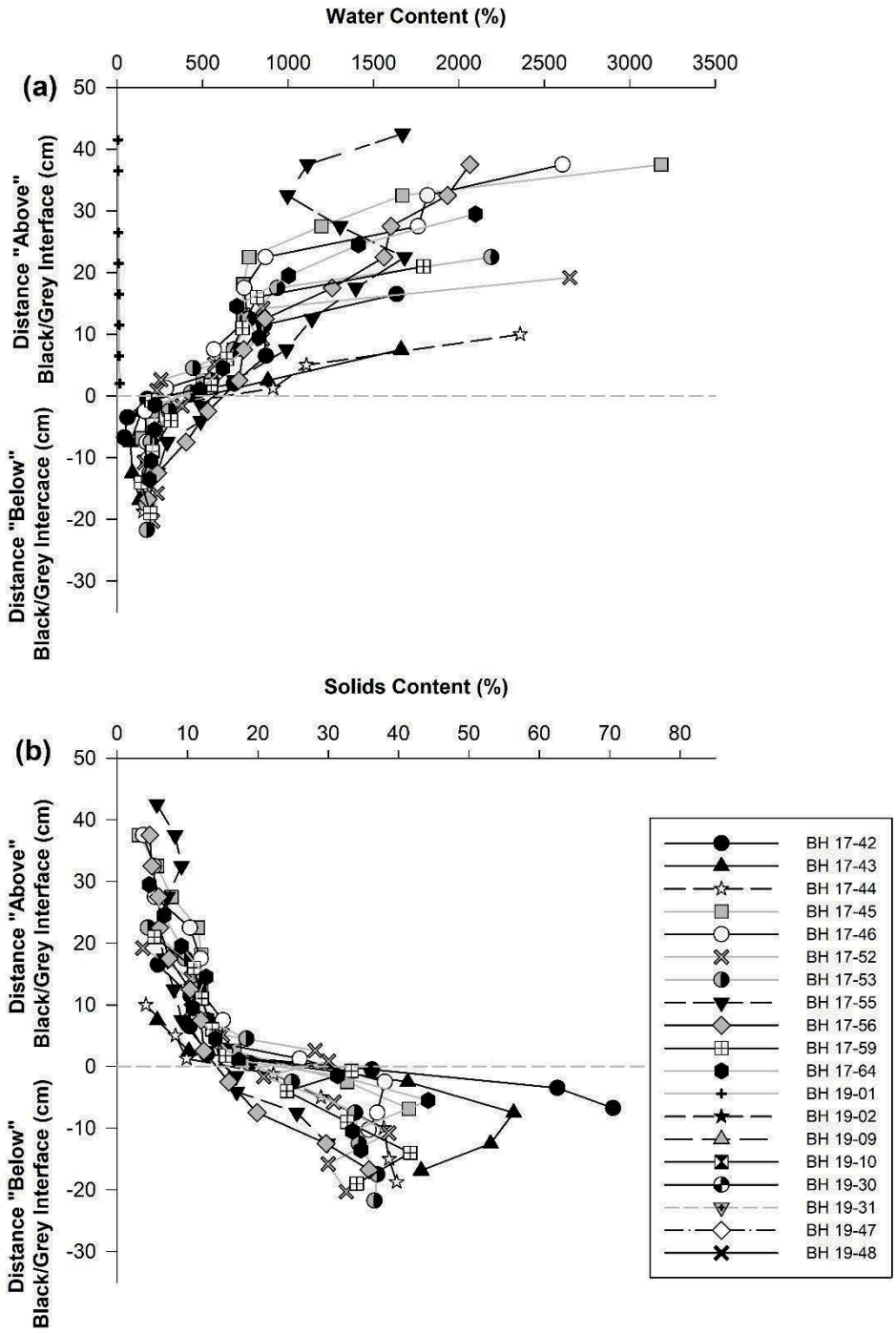

Figure A.9 (a) Water and (b) Solid contents at various depths taken via discrete sampling of selected cores (dashed grey line shows interface between black and grey sediments, distances expressed from this interface).

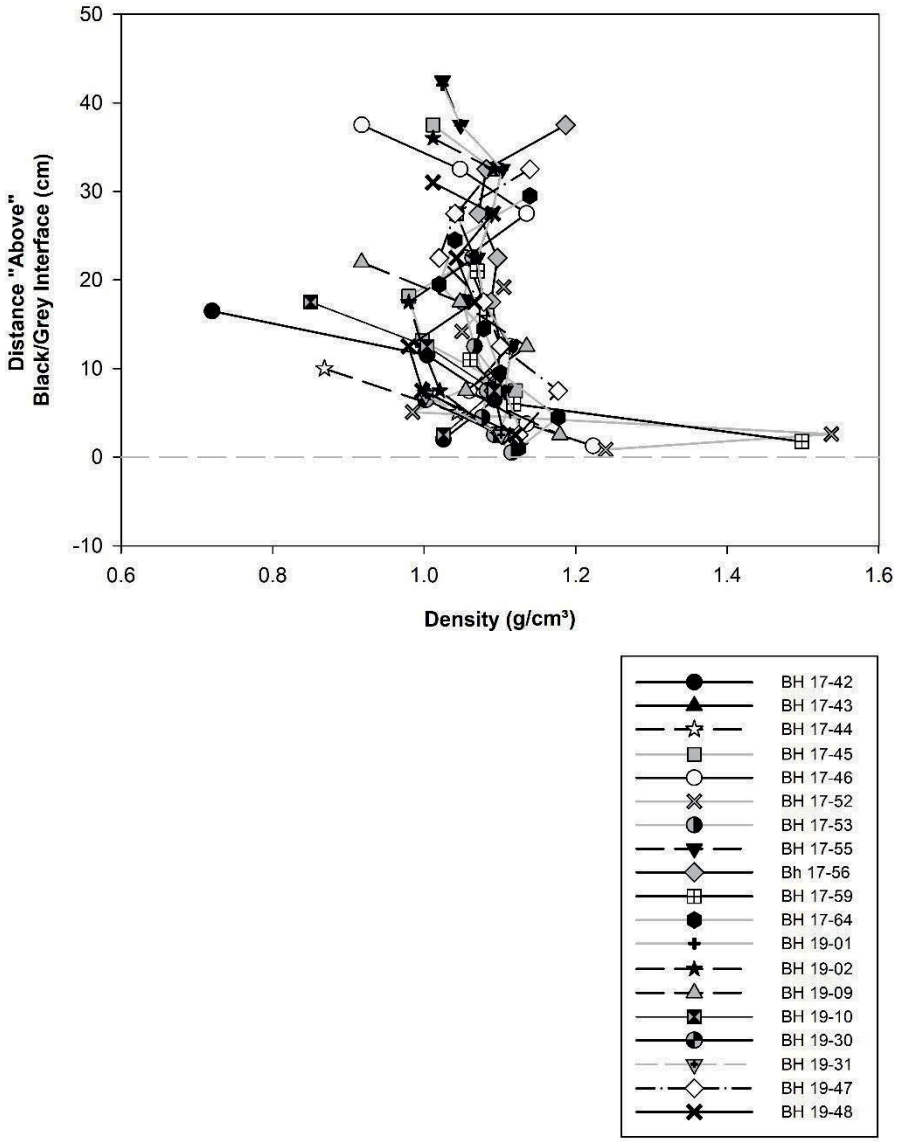

Figure A.10 Bulk density of black sediment at various depths taken via discrete sampling of selected cores (dashed grey line shows interface between black and grey sediments, distances expressed from this interface).

APPENDIX B — Supplemental Tables

Table B1. Boat Harbour sample depth (cm) categories from 1992–2015 (n=103) from Hoffman et al. (2017a).

Boat Harbour Stabilization Lagoon		
Depth (cm)	***n* (%)**	**Aggregate *n* (%)**
0-5	48 (46.6)	48 (46.6)
0-10	11 (10.7)	59 (57.3)
0-15	12 (11.7)	71 (68.9
0-20	7 (6.8)	78 (75.7)
0-25	2 (1.9)	80 (77.7)
0-30	1 (1.0)	81 (78.6)
0-50	16 (15.5)	97 (94.2)
50-100	3 (2.9)	3 (2.9)
100-150	3 (2.9)	3 (2.9)

Table B2. Number of sampling stations and sediment samples (n) in Boat Harbour collected and analyzed for PCDD/Fs and PAHs from 1992-2015.

Report	Number of sediment samples		Number of sampling stations	
	PCDD/F (*n*)	PAH (*n*)	PCDD/F (*n*)	PAH (*n*)
JWEL and Beak Consultants (1992)	8	9	8	9
JWEL and Beak Consultants (1993)	3	3	3	3
JWEL (1997)	5	10	5	5
JWEL (1999)	2	26	2	21
JWEL (2001)	0	14	0	14
JWEL (2005)	17	17	15	15
Stantec (2013)	3	3	3	3
Stantec (2016)	22	21	12	15
Total samples	**60**	**103**	**48**	**85**

APPENDIX C — Copyright Permissions

Chapter 2:

The following statement was retrieved from: https://www.springer.com/gp/rights-permissions/obtaining-permissions/882 on September 28, 2020.

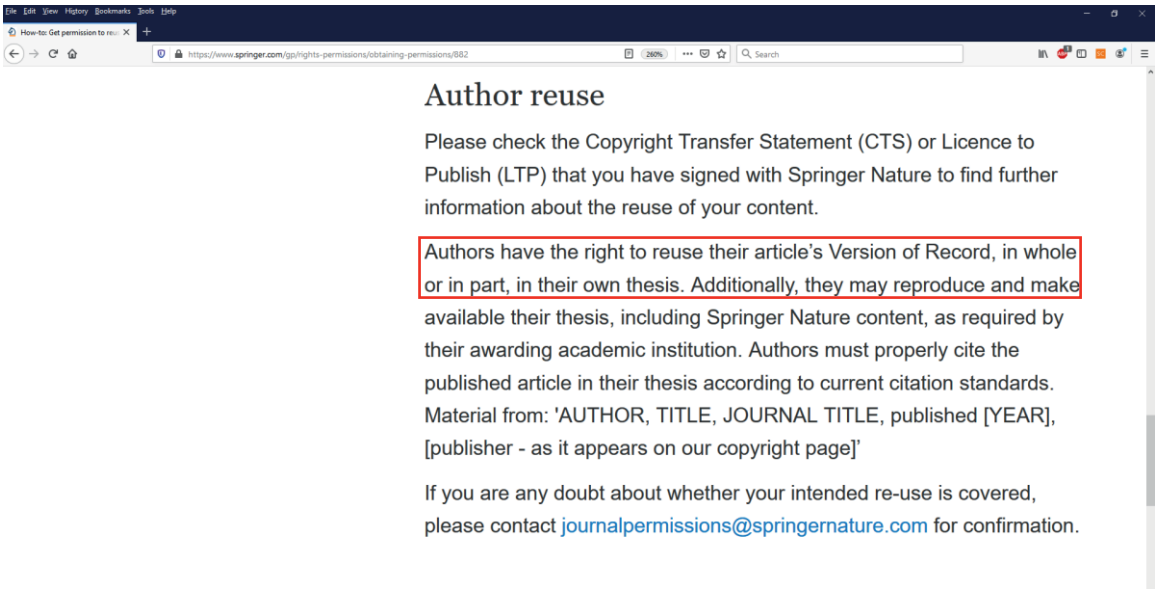

Author reuse

Please check the Copyright Transfer Statement (CTS) or Licence to Publish (LTP) that you have signed with Springer Nature to find further information about the reuse of your content.

Authors have the right to reuse their article's Version of Record, in whole or in part, in their own thesis. Additionally, they may reproduce and make available their thesis, including Springer Nature content, as required by their awarding academic institution. Authors must properly cite the published article in their thesis according to current citation standards. Material from: 'AUTHOR, TITLE, JOURNAL TITLE, published [YEAR], [publisher - as it appears on our copyright page]'

If you are any doubt about whether your intended re-use is covered, please contact journalpermissions@springernature.com for confirmation.

Chapter 3:

The following statement was retrieved from: https://www.icevirtuallibrary.com/page/authors/copyright-and-permissions on September 28, 2020.

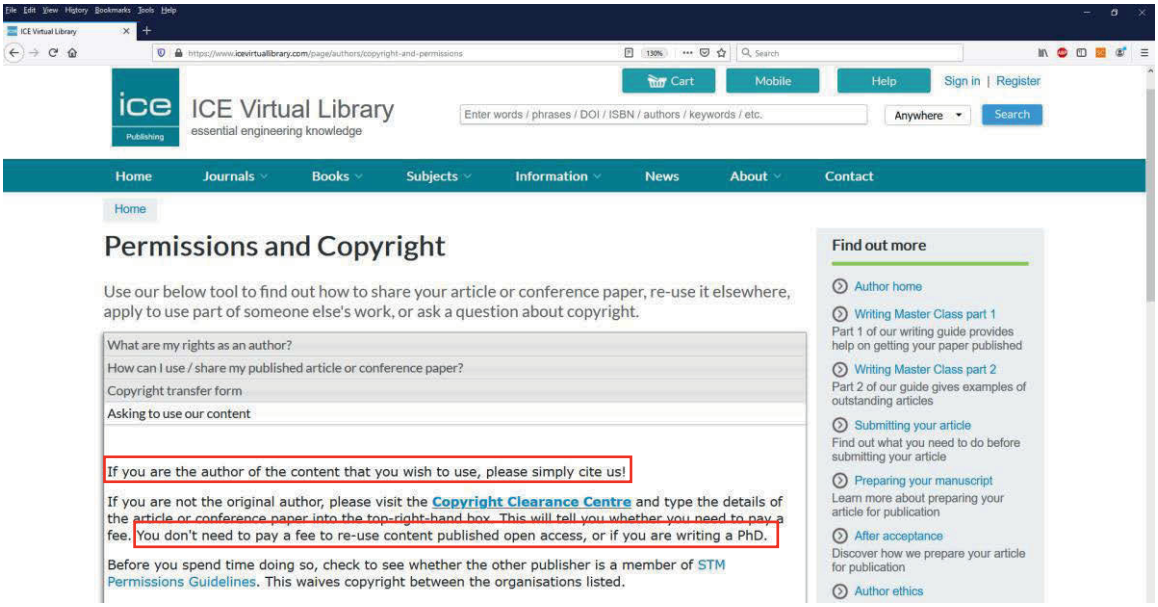

Chapter 4:

The following statement was retrieved from: https://www.nrcresearchpress.com/page/authors/information/rights on September 28, 2020.

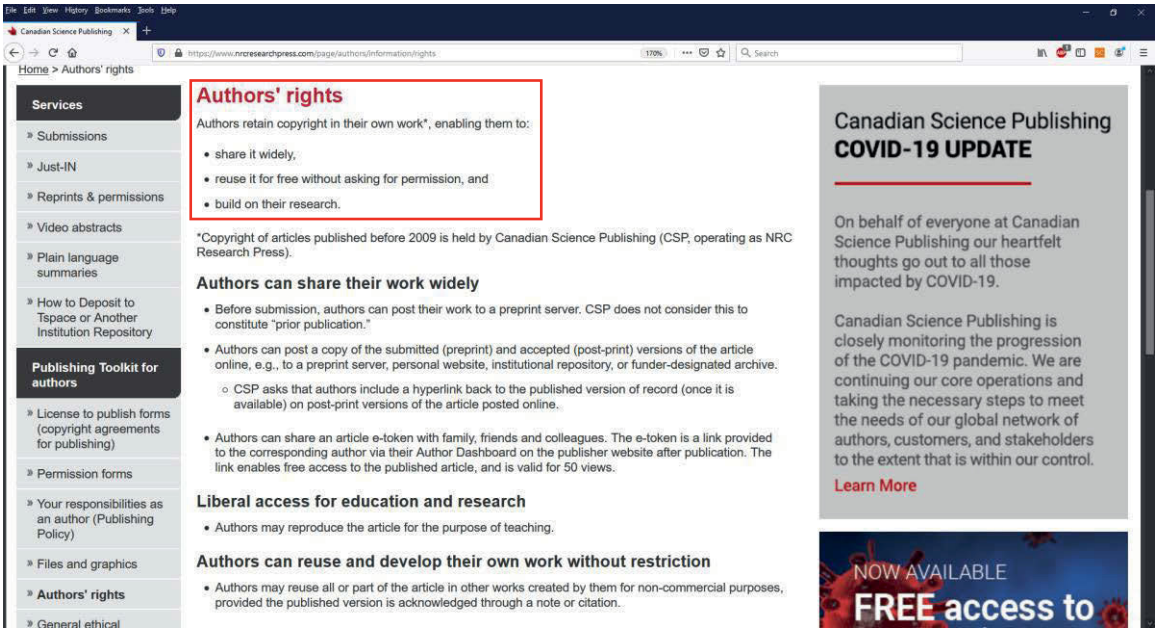

Table 2.1 Sediment quality guideline (SQG) exceedances for select PAH compounds, total PAHs and PCDD/F TEQs in Boat Harbour between 1992-2015. Total sediment samples (*n*) are indicated under each parameter and include sediment collected from all depth horizons.

Parameter	Freshwater				Marine			
	ISQG		PEL		ISQG		PEL	
	SQG Limit	Number of exceedances (%)	SQG Limit	Number of exceedances (%)	SQG Limit	Number of exceedances (%)	SQG Limit	Number of exceedances (%)
Anthracene mg/kg (*n* = 103)	0.047	52(50.5)	0.245	31(30.1)	0.047	52(50.5)	0.245	31(30.1)
Fluoranthene mg/kg (*n* = 103)	0.111	77(74.8)	2.355	8(7.8)	0.113	77(74.8)	1.494	29(28.2)
Fluorene mg/kg (*n* = 103)	0.021	76(73.8)	0.144	7(6.8)	0.021	76(73.8)	0.144	7(6.8)
Phenanthrene mg/kg (*n* = 103)	0.042	86(83.5)	0.515	60(58.3)	0.087	77(74.8)	0.544	59(57.3)
Pyrene mg/kg (*n* = 103)	0.053	81(78.6)	0.875	42(40.8)	0.153	72(69.9)	1.398	29(28.2)

Total PAHs mg/kg (n = 103)	ER-L		ER-M	
	SQG Limit	Number of exceedances (%)	SQG Limit	Number of exceedances (%)
	4.02	46(44.7)	44.80	0(0)

PCDD/Fs pg/g (n = 60)	Freshwater and Marine (Fish)				Canadian Tissue Residue Guidelines				Canadian Soil Quality Guidelines for the Protection of Environmental and Human Health	
	ISQG		PEL		Mammals		Birds		Human	
	0.85	60(100)	21.50	40(66.6)	0.71	60(100)	4.75	60(100)	4.00	56(93.3)

ISQG indicates CCME interim sediment quality guidelines and PEL indicates CCME probable effect levels (CCME 2016). There are no CCME guidelines for total PAHs, so these were compared to effects range low (ER-L) and effects range median (ER-M) (Long et al. 1998; NOAA 1999).

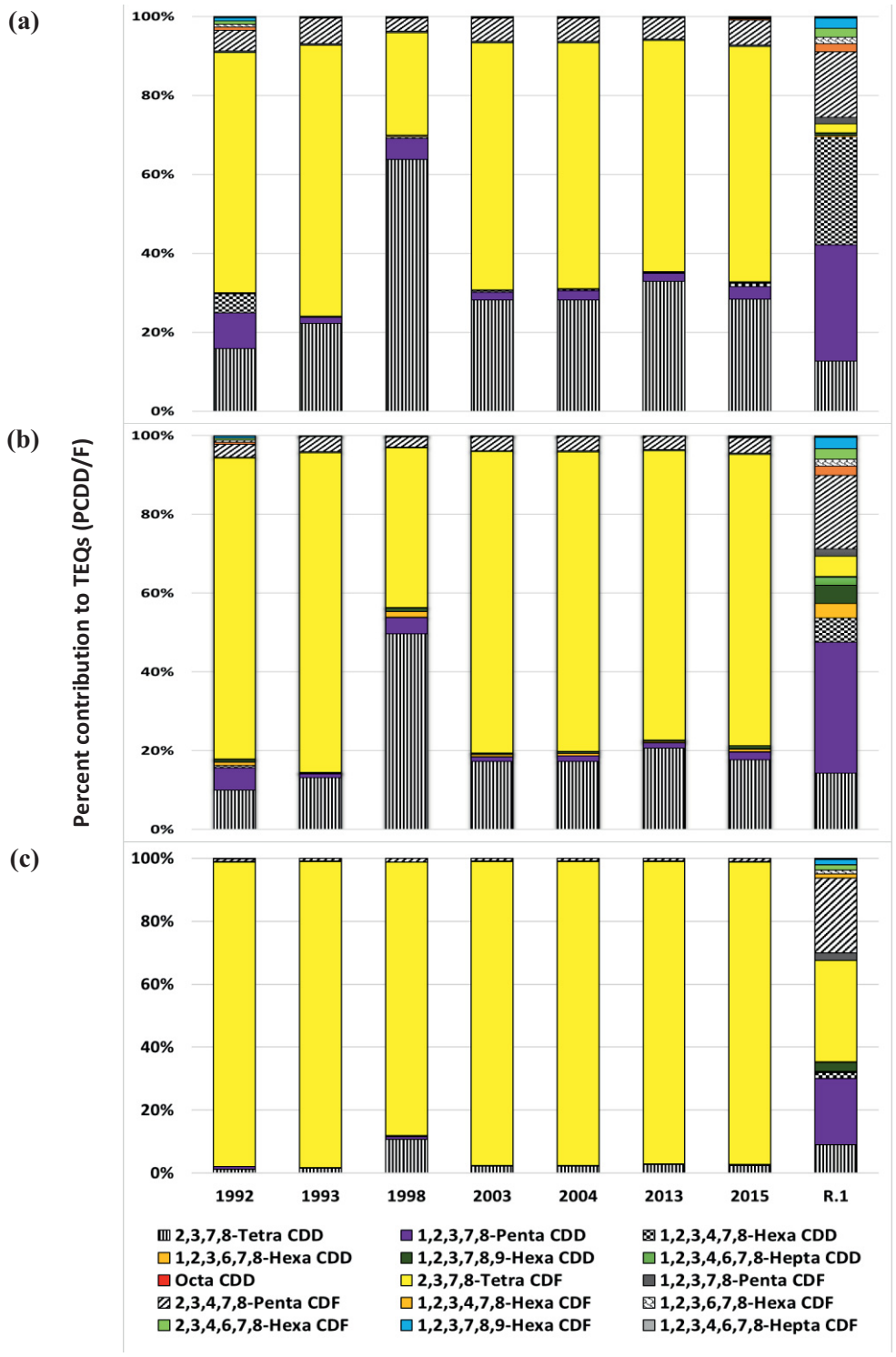

Figure A.3 PCDD/F congener patterns in Boat Harbour sediments compared with congener patterns in sediment collected at the R.1 reference station (JWEL 1994). Data reflect percent contributions of each congener to the ∑17PCDD/Fs.

Table 2.1 Sediment quality guideline (SQG) exceedances for select PAH compounds, total PAHs and PCDD/F TEQs in Boat Harbour between 1992-2015. Total sediment samples (*n*) are indicated under each parameter and include sediment collected from all depth horizons.

Parameter	Freshwater				Marine			
	ISQG		PEL		ISQG		PEL	
	SQG Limit	Number of exceedances (%)	SQG Limit	Number of exceedances (%)	SQG Limit	Number of exceedances (%)	SQG Limit	Number of exceedances (%)
Anthracene mg/kg (*n* = 103)	0.047	52(50.5)	0.245	31(30.1)	0.047	52(50.5)	0.245	31(30.1)
Fluoranthene mg/kg (*n* = 103)	0.111	77(74.8)	2.355	8(7.8)	0.113	77(74.8)	1.494	29(28.2)
Fluorene mg/kg (*n* = 103)	0.021	76(73.8)	0.144	7(6.8)	0.021	76(73.8)	0.144	7(6.8)
Phenanthrene mg/kg (*n* = 103)	0.042	86(83.5)	0.515	60(58.3)	0.087	77(74.8)	0.544	59(57.3)
Pyrene mg/kg (*n* = 103)	0.053	81(78.6)	0.875	42(40.8)	0.153	72(69.9)	1.398	29(28.2)

Total PAHs mg/kg (n = 103)	ER-L		ER-M	
	SQG Limit	Number of exceedances (%)	SQG Limit	Number of exceedances (%)
	4.02	46(44.7)	44.80	0(0)

PCDD/Fs pg/g (n = 60)	Freshwater and Marine (Fish)				Canadian Tissue Residue Guidelines				Canadian Soil Quality Guidelines for the Protection of Environmental and Human Health	
	ISQG		PEL		Mammals		Birds		Human	
	0.85	60(100)	21.50	40(66.6)	0.71	60(100)	4.75	60(100)	4.00	56(93.3)

ISQG indicates CCME interim sediment quality guidelines and PEL indicates CCME probable effect levels (CCME 2016). There are no CCME guidelines for total PAHs, so these were compared to effects range low (ER-L) and effects range median (ER-M) (Long et al. 1998; NOAA 1999).

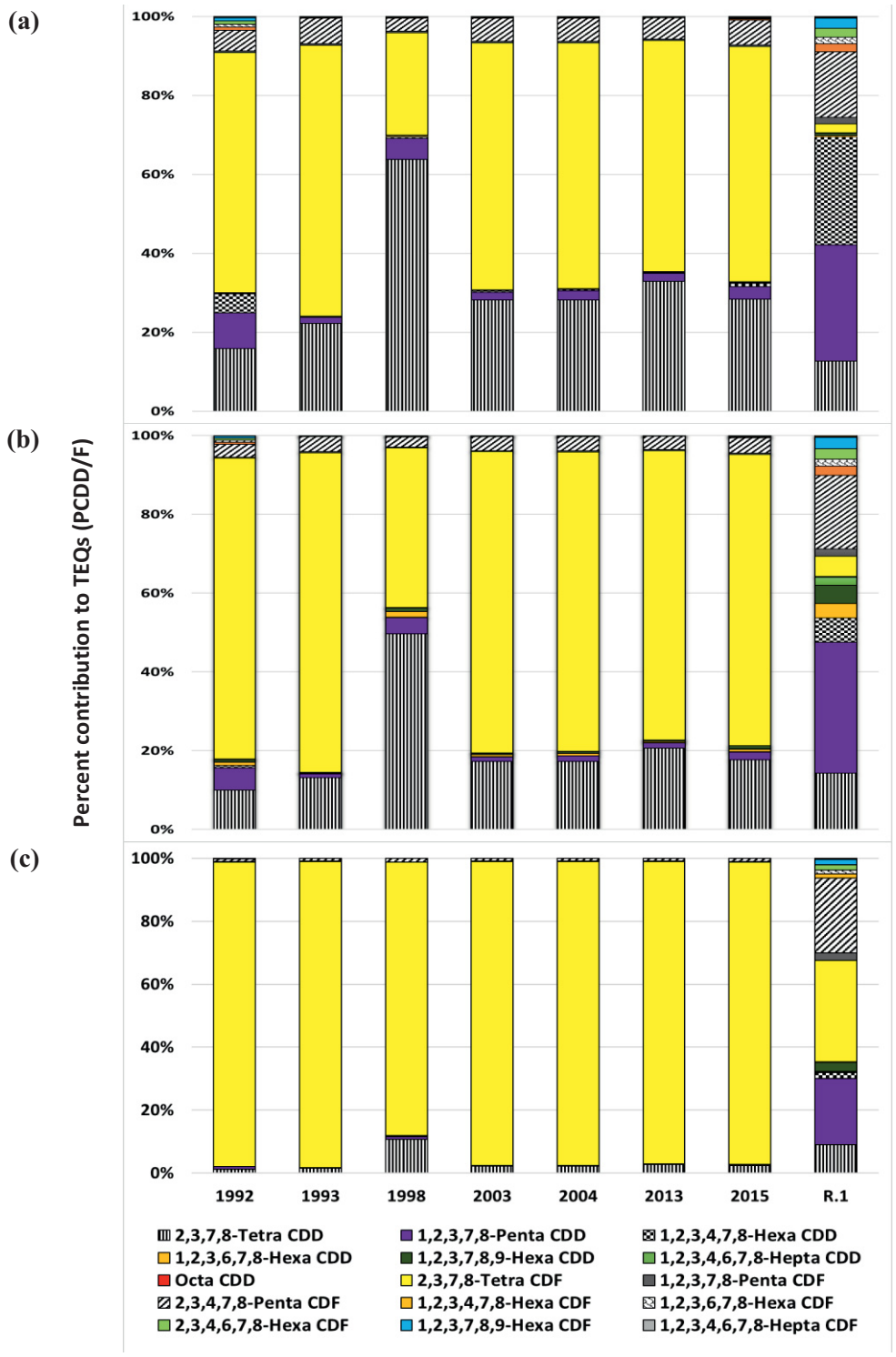

Figure A.3 PCDD/F congener patterns in Boat Harbour sediments compared with congener patterns in sediment collected at the R.1 reference station (JWEL 1994). Data reflect percent contributions of each congener to the ∑17PCDD/Fs.